Research Project Number TPF-5(193) Supplement #130

DEVELOPMENT OF A MASH TL-3 COMPLIANT PARAPET MOUNTED FENCE

Submitted by

Luis Rodriguez-Alvizo, M.S.M.E
Former Graduate Research Assistant

Robert W. Bielenberg, M.S.M.E.
Research Engineer

Cody S. Stolle, Ph.D.
Research Assistant Professor

Ronald K. Faller, Ph.D., P.E.
Research Professor & MwRSF Director

MIDWEST ROADSIDE SAFETY FACILITY
Nebraska Transportation Center
University of Nebraska-Lincoln

Main Office
Prem S. Paul Research Center at Whittier School
Room 130, 2200 Vine Street
Lincoln, Nebraska 68583-0853
(402)472-0965

Outdoor Test Site
4630 N.W. 36th Street
Lincoln, Nebraska 68524

Submitted to

IOWA DEPARTMENT OF TRANSPORTATION
800 Lincoln Way
Ames, IA 50010

MwRSF Research Report No. TRP-03-434-22

December 1, 2022

TECHNICAL REPORT DOCUMENTATION PAGE

1. Report No.	2. Government Accession No.	3. Recipient's Catalog No.
TRP-03-434-22		

4. Title and Subtitle Development of a MASH TL-3 Compliant Parapet Mounted Fence	**5. Report Date** December 1, 2022 **6. Performing Organization Code**
7. Author(s) Rodriguez-Alvizo, L., Bielenberg, R.W., Stolle, C.S., Faller, R.K.	**8. Performing Organization Report No.** TRP-03-434-22
9. Performing Organization Name and Address Midwest Roadside Safety Facility (MwRSF) Nebraska Transportation Center University of Nebraska-Lincoln Main Office: Prem S. Paul Research Center at Whittier School Room 130, 2200 Vine Street Lincoln, Nebraska 68583-0853 Outdoor Test Site: 4630 N.W. 36th Street Lincoln, Nebraska 68524	**10. Work Unit No.** **11. Contract** TPF-5(193) Supplement #130
12. Sponsoring Agency Name and Address Iowa Department of Transportation 800 Lincoln Way2 Ames, IA 50010	**13. Type of Report and Period Covered** Final Report: 2019–2022 **14. Sponsoring Agency Code**

15. Supplementary Notes

Prepared in cooperation with U.S. Department of Transportation, Federal Highway Administration

16. Abstract

When roadways pass over railway tracks, there is a risk that debris from the roadway or pedestrians may fall onto the tracks and interfere with railway operations. Because of this, state Departments of Transportation (DOTs) commonly install debris fences in conjunction with bridge rails over railway tracks. However, the safety performance of debris fence systems when impacted by an errant vehicle has not been demonstrated through full-scale crash testing. Thus, the objective of this research was to develop a new, parapet-mounted debris fence for the Iowa DOT according to safety performance guidelines included in the American Association of State Highway and Transportation Officials (AASHTO) Manual for Assessing Safety Hardware (MASH 2016) for Test Level 3 (TL-3). In this study, various state DOT fence designs were reviewed and ranked to select a baseline fence system that would be used as the groundwork for the design of the Iowa DOT fence. Furthermore, crash testing, zone of intrusion studies, and anecdotal real-world crashes were reviewed to understand the expected interaction between an errant vehicle impacting a parapet-mounted fence. The new debris fence was then designed to meet severe weather events inducing high winds and ice accumulation. Impact loading was also considered, primarily in the design of the fence-to-barrier connection. The new debris fence and fence terminations were designed and optimized based on crashworthiness, cost, constructability, and aesthetics. Finally, recommendations were provided to accommodate design modifications, such as adaptations to alternate barriers, changes in geographic location, and considerations for MASH TL-4 impact safety criteria

17. Key Words	18. Distribution Statement
Debris Fence, Pedestrian Fence, Railroad, Bridge Rail, Highway Safety, Roadside Appurtenances, MASH 2016	No restrictions. This document is available through the National Technical Information Service. 5285 Port Royal Road Springfield, VA 22161

19. Security Classification (of this report)	20. Security Classification (of this page)	21. No. of Pages	22. Price
Unclassified	Unclassified	276	

Form DOT F 1700.7 (8-72) Reproduction of completed page authorized

DISCLAIMER STATEMENT

ACKNOWLEDGEMENTS

The authors wish to acknowledge the Iowa Department of Transportation and MwRSF personnel for their contributions to this project.

Midwest Roadside Safety Facility
J.C. Holloway, M.S.C.E., Research Engineer & Assistant Director –Physical Testing Division
K.A. Lechtenberg, M.S.M.E., Research Engineer
S.K. Rosenbaugh, M.S.C.E., Research Engineer
J.S. Steelman, Ph.D., P.E., Associate Professor
M. Asadollahi Pajouh, Ph.D., P.E., Research Assistant Professor
A.T. Russell, B.S.B.A., Testing and Maintenance Technician II
E.W. Krier, B.S., Engineering Testing Technician II
D.S. Charroin, Engineering Testing Technician II
R.M. Novak, Engineering Testing Technician II
S.M. Tighe, Engineering Testing Technician I
T.C. Donahoo, Engineering Testing Technician I
J.T. Jones, Engineering Testing Technician I
E.L. Urbank, B.A., Research Communication Specialist
Z.Z. Jabr, Engineering Technician
Undergraduate and Graduate Research Assistants

Iowa Department of Transportation
Chris Poole, P.E., Roadside Safety Engineer
Daniel Harness, P.E., Transportation Engineer Specialist
Stuart Nielsen, P.E., Transportation Engineer Administrator, Design
Mike Thiel, P.E., Transportation Engineer Specialist

SI* (MODERN METRIC) CONVERSION FACTORS				
APPROXIMATE CONVERSIONS TO SI UNITS				
Symbol	**When You Know**	**Multiply By**	**To Find**	**Symbol**
		LENGTH		
in.	inches	25.4	millimeters	mm
ft	feet	0.305	meters	m
yd	yards	0.914	meters	m
mi	miles	1.61	kilometers	km
		AREA		
in^2	square inches	645.2	square millimeters	mm^2
ft^2	square feet	0.093	square meters	m^2
yd^2	square yard	0.836	square meters	m^2
ac	acres	0.405	hectares	ha
mi^2	square miles	2.59	square kilometers	km^2
		VOLUME		
fl oz	fluid ounces	29.57	milliliters	mL
gal	gallons	3.785	liters	L
ft^3	cubic feet	0.028	cubic meters	m^3
yd^3	cubic yards	0.765	cubic meters	m^3
		NOTE: volumes greater than 1,000 L shall be shown in m^3		
		MASS		
oz	ounces	28.35	grams	g
lb	pounds	0.454	kilograms	kg
T	short ton (2,000 lb)	0.907	megagrams (or "metric ton")	Mg (or "t")
		TEMPERATURE (exact degrees)		
°F	Fahrenheit	5(F-32)/9 or (F-32)/1.8	Celsius	°C
		ILLUMINATION		
fc	foot-candles	10.76	lux	lx
fl	foot-Lamberts	3.426	candela per square meter	cd/m^2
		FORCE & PRESSURE or STRESS		
lbf	poundforce	4.45	newtons	N
lbf/in^2	poundforce per square inch	6.89	kilopascals	kPa
APPROXIMATE CONVERSIONS FROM SI UNITS				
Symbol	**When You Know**	**Multiply By**	**To Find**	**Symbol**
		LENGTH		
mm	millimeters	0.039	inches	in.
m	meters	3.28	feet	ft
m	meters	1.09	yards	yd
km	kilometers	0.621	miles	mi
		AREA		
mm^2	square millimeters	0.0016	square inches	in^2
m^2	square meters	10.764	square feet	ft^2
m^2	square meters	1.195	square yard	yd^2
ha	hectares	2.47	acres	ac
km^2	square kilometers	0.386	square miles	mi^2
		VOLUME		
mL	milliliter	0.034	fluid ounces	fl oz
L	liters	0.264	gallons	gal
m^3	cubic meters	35.314	cubic feet	ft^3
m^3	cubic meters	1.307	cubic yards	yd^3
		MASS		
g	grams	0.035	ounces	oz
kg	kilograms	2.202	pounds	lb
Mg (or "t")	megagrams (or "metric ton")	1.103	short ton (2,000 lb)	T
		TEMPERATURE (exact degrees)		
°C	Celsius	1.8C+32	Fahrenheit	°F
		ILLUMINATION		
lx	lux	0.0929	foot-candles	fc
cd/m^2	candela per square meter	0.2919	foot-Lamberts	fl
		FORCE & PRESSURE or STRESS		
N	newtons	0.225	poundforce	lbf
kPa	kilopascals	0.145	poundforce per square inch	lbf/in^2

*SI is the symbol for the International System of Units. Appropriate rounding should be made to comply with Section 4 of ASTM E380.

TABLE OF CONTENTS

LIST OF FIGURES

LIST OF TABLES

1 INTRODUCTION

1.1 Problem Statement

When roadways pass over railway tracks, there is a risk that road debris may fall and damage tracks, clutter rail lines, or potentially cause concerns for train stability and safety. To prevent debris from interfering with railway operations, a debris fence may be installed in conjunction with bridge rails on overpasses over railway tracks. In many cases, there are limited space limitations on the bridge rail, and the fence may be located within the barrier's Zone of Intrusion (ZOI), which is the lateral extent that a vehicle extends over the top-front face or corner of a barrier during an impact scenario.

Debris fences attached to bridge rails are subject to two concerns. If the debris fence is located within the ZOI, it must not produce excessive occupant compartment deformations, vehicle snag, nor occupant risk due to the presence of stiff beam and post members. However, the fences must also be strong enough to withstand live, dead, and wind loads. It is desirable that, if an impact results in contact with the fence, the fence be retained on the overpass and not produce additional debris on the railroad tracks.

The Iowa Department of Transportation (DOT) Office of Rail recently requested that the Midwest Roadside Safety Facility (MwRSF) develop a new debris fence design, which could be attached to the top of a concrete bridge rail to prevent road debris from falling onto railroad tracks below. However, limited debris fence crash tests have been conducted according to the American Association of State Highways and Transportation Officials (AASHTO) *Manual for Assessing Safety Hardware* (MASH) Test Level 3 (TL-3) specifications [1]. These test conditions require that the roadside safety hardware be capable of safely containing and redirecting passenger vehicles, consisting of a 1100C small car and 2270P pickup truck, during impact events at 62 mph occurring at a 25-degree angle relative to the test article.

1.2 Objective

The objective of this research is to design a MASH TL-3 compliant debris fence system with attachment to a crashworthy concrete bridge parapet design. This design will be used along high-speed roadways and must satisfy MASH safety performance criteria for passenger vehicles during impact scenarios. In addition, this design must comply with current Iowa DOT Standards for the usage of chain-link fences near the travelled way.

1.3 Scope

The research objective was to complete Phase I of a two-phase research effort. Phase I of the research consisted of the background review and initial design of a debris fence system which was likely to satisfy MASH TL-3 evaluation criteria. First, a literature review was performed on previously crash-tested fences mounted on concrete parapets and ZOI details. Next, current fence designs used by states were reviewed to compile details regarding fence geometries, key components, and connection details. MwRSF also collected information on debris fence design standards to ensure the design met wind load, dead load, and ice load requirements. The results of the literature review and collection of state DOT standards were used to select a parapet shape and vertical post, design barrier mounting attachments for the debris fence, design fence retention features, and specify debris fence construction details.

Phase II of the research effort would consist of the crash testing and evaluation of the proposed debris fence design from Phase I. Prior to executing Phase II, the Iowa DOT and railroad industry will review the proposed design and provide comments and recommendations as well as determine if full-scale crash testing of the proposed system is desired.

2 LITERATURE REVIEW

2.1 Overview

A literature review was conducted to collect information necessary for the development of the parapet-mounted fence. Studies on the Zone of Intrusion (ZOI), which measures the extension of the vehicle beyond the top-front corner of a barrier during impact events, were reviewed to identify the effects of having elements within the barrier's ZOI. Crash test conducted with parapet-mounted fences along with crash test with vertical elements within the ZOI were collected and reviewed. To gain an understanding of the real-world performance of parapet-mounted fences, real world crashes were analyzed. State DOT standard fence plans were then gathered, designs were ranked, and a baseline design was selected to be used as the groundwork for the fence developed in this design effort. Examples of existing barrier-mounted fences were analyzed to gain further insight on fence designs and construction practices. Finally, Iowa DOT fence standards and Union Pacific-BNSF standards were studied to ensure the parapet-mounted fence was designed to comply their requirements.

2.2 Review of Concerns Related to Zone of Intrusion

The ZOI in roadside safety nomenclature is defined as the lateral extent that a vehicle extends beyond the top-front corner of a barrier during an impact scenario [2]. The ZOI is a very important parameter when attempting to mount items on top of both rigid and non-rigid parapets, because of the potential for the vehicle to extend over a barrier and snag on vertical elements. This snag event can lead to excessive occupant compartment deformation and/or penetration, disengaged hardware, and vehicle stability issues.

2.2.1 Guidelines for Attachments to Bridge Rails and Median Barriers

In February 2003, MwRSF researchers published a report titled *Guidelines for Attachments to Bridge Rails and Median Barriers* [3]. This research report quantified ZOI values for multiple parapet geometries from historical crash test data. To accomplish this, videos and pictures from previous tests were obtained and video analysis techniques were used to determine the lateral extent of vehicles behind the top-front corner of the test installations.

The research team initially hypothesized that the barrier height would relate best to the amount of intrusion, but the test data was too limited to confirm this assumption. Researchers observed that the bumper and bottom portion of the front fender of the pickup truck were typically crushed during rigid barrier impacts, while the engine hood and upper front fender panel generally extended over the top of the barrier. This behavior resulted in the greatest intrusion, generally occurring early in the impact event.

Researchers reviewed crash tests involving rigid barriers ranging from 27¾ in. to 42 in. tall, impacted with pickup trucks and cars. The ZOI for the pickup truck varied between 8 and 30 in., and the ZOI for the car varied between 0 and 8 in., depending on the parapet geometry and attachments. The report notes that if posts are mounted at least 7 in. behind the front face of a rigid barrier, the risk of vehicle snag is greatly reduced, but the authors also noted that offsetting posts to the back of the barrier will not eliminate all of the vehicle snag concerns for all barriers and impact conditions. ZOI values obtained for crash tests on small cars and pickup trucks are shown in Table 1.

Table 1. ZOI Values [3]

Barrier Class	**Barrier Name**	**Barrier Height (in.)**	**Vehicle**	**Maximum Intusion (in.)**	**Vehicle Component**
Concrete with Sloped Face	762-mm (30-in.) New Jersey Safety Shape	30	Small Car	6	Hood / Fender
			Pickup	8	Hood / Fender
	Single Slope Concrete Bridge Rail	32	Pickup	12	Hood / Fender
	813-mm (32-in.) F-Shape Bridge Rail	32	Small Car	2	Hood / Fender
			Pickup	8	Hood / Fender
	813-mm (32-in.) New Jersey Safety Shape Bridge Rail	32	Pickup	18	Hood / Fender
	813-mm (32-in.) New Jersey Rail	32	Pickup	9	Hood / Fender
Concrete with Vertical Face	Nebraska Open Concrete Bridge Railing (AASHTO Bridge Guide Specifications)	29	Pickup	16	Hood / Fender
			Pickup	14	Hood / Fender
	813-mm (32-in,) Vertical Wall	32	Small Car	8	Hood
		32	Pickup	15	Hood / Fender
	Texas Tyle T411 Bridge Rail	32	Pickup	24	Hood / Fender
Steel Tubular Rails	Illinois Side-Mounted Bridge Rail	32	Small Car	0	None
			Pickup	13	Hood / Fender
	Steel Bridge Rail with Tube Rail System for Transverse Decks	36	Pickup	21	Hood / Fender
	Texas Type T6 Bridge Rail	27.75	Pickup	30	Hood / Fender
	California Type 115 Bridge Rail	30	Pickup	30	Hood / Fender
Steel Tubular Rails on Curbs	Illinois 2399 Bridge Rail	32	Small Car	6	Hood
			Pickup	11	Fender
	NETC Bridge Rail, Curb Mounted	34	Small Car	3	Hood
			Pickup	12	Hood / Fender
Concrete / Steel Combination Bridge Rails	Minnesota Combination Bridge Rail	35	Small Car	0	None
			Pickup	24	Hood
	BR27C Bridge Railing on Deck	42	Small Car	0	None
			Pickup	10	Hood
Timber Bridge Rails	GC-8000 Bridge Rail for Longitudinal Decks	33	Pickup	24	Hood / Fender
	Wood Bridge Rail with Curb System for Transverse Decks	33	Pickup	21	Hood / Fender

2.2.2 Zone of Intrusion Study

In October 2010, MwRSF researchers published a research report titled *Zone of Intrusion Study* [4]. This report detailed the results of nonlinear finite element testing using LS DYNA simulations to investigate the ZOI for an NCHRP-350 2000P pickup truck [5]. This pickup truck simulation impacted a 40-in.tall, F-shape parapet at TL-2 and TL-3 testing conditions. The ZOI was determined to be 5 in. for the simulation with NCHRP Report 350 TL-3 test no. 3-11 conditions. It was observed that with a barrier height of 40 in., the vehicle protrusion over the barrier was limited to the front corner of the hood and a small section of the fender.

Under NCHRP Report 350 TL-2 test no. 2-11 conditions [5], 45 mph and at a 25-degree angle, a ZOI between 1.8 in. and 2.5 in. was predicted for the pickup truck. The authors attributed the variation in this ZOI value to the mesh quality of the simulation model and the overall system geometry.

2.2.3 ZOI for Permanent 9.1-Degree Single-Slope Concrete Barriers

In March 2014, MwRSF researcher published a research report that detailed efforts involving simulation analysis of the MASH TL-3 ZOI of a Wisconsin DOT single-slope concrete barrier. ZOI values were calculated for a pickup truck at three different single-slope parapet heights. The ZOI for 36-, 42-, and 56-in tall barriers were 12.2 in., 6.4 in., and 0 in., respectively. Additionally, during this simulation effort, the left fender always protruded the farthest behind the barrier, which was followed by the corner of the engine hood [6].

2.3 Full-Scale Crash Testing of Objects in Rigid Barrier Zone of Intrusion

2.3.1 Median Barrier-Mounted Fence: TTI Test Nos. CMB-1 Through CMB-4

In September of 1972, researchers from the TTI published a report titled *Vehicle Crash Test and Evaluation of Median Barriers for Texas Highways* [8]. This document reported the finding from four full-scale crash tests involving a concrete median barrier with a top-mounted chain link fence. The test vehicle used during full-scale crash testing consisted of a standard size 4,000-lb passenger car.

The barrier used in full-scale crash testing had a height of 32 in., an 8-in. thickness at the top and had a geometry similar to that of a New Jersey Median barrier. The barrier was reinforced with eight no. 5 longitudinal bars spaced at 9-in. vertical increments. The chain-link fence was attached near the centerline of the barrier and used 3-ft tall chain-link fabric with 1-in. mesh openings constructed using 9-gauge wires. The terminal end of the fence included large diameter round posts while the fence line posts consisted of ⅝-in. diameter eye bolts with a maximum spacing of 10 ft on center. System details are shown in Figure 1 and Figure 2.

In test no. CMB-1, a large diameter light pole was installed between two fence sections and was impacted at 60 mph at a 25-degree angle. The objective of this test was to determine if the vehicle would snag and detach the luminaire pole from the top of the barrier. Test no. CMB-2 was conducted to evaluate an un-anchored section of the median barrier with the attached chain-link fence, impacted at 60 mph at a 25-degree angle. The objective of this test was to determine if the un-anchored barrier section would slide or rotate during the redirection of the impacting vehicle. In test no. CMB-3, the crashworthiness of the system was evaluated during impact conditions with a target impact speed and angle of 60 mph and 7 degrees, respectively. Test no. CMB-4 consisted of impact conditions with a target impact speed and angle of 60 mph and 15 degrees, respectively. These tests were conducted to evaluate the barriers performance under in-service narrow median type collisions [8].

The authors of this report indicated that the barriers remained "intact" during the restraint and redirection of the impacting vehicle. Moreover, permanent deformation experienced by the chain-link fabric was evident in posttest barrier damage of test no CMB-2. Test vehicle damage from this test series varied from severe to minimal, as shown in Figure 4.The authors also reported that these barriers have performed adequate while in service [8].

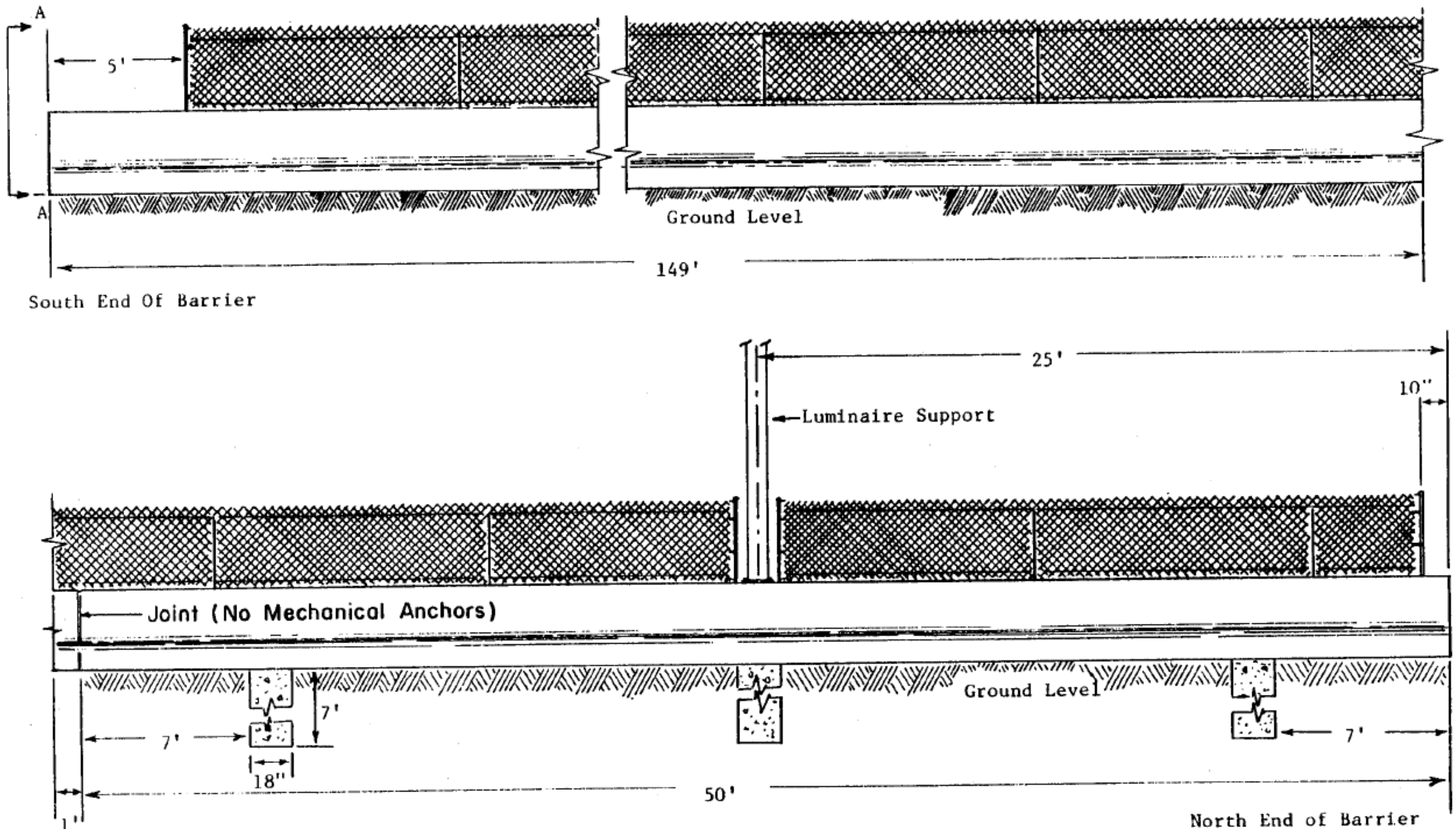

Figure 1. Chain-Link Fence and Concrete Median Barrier [8]

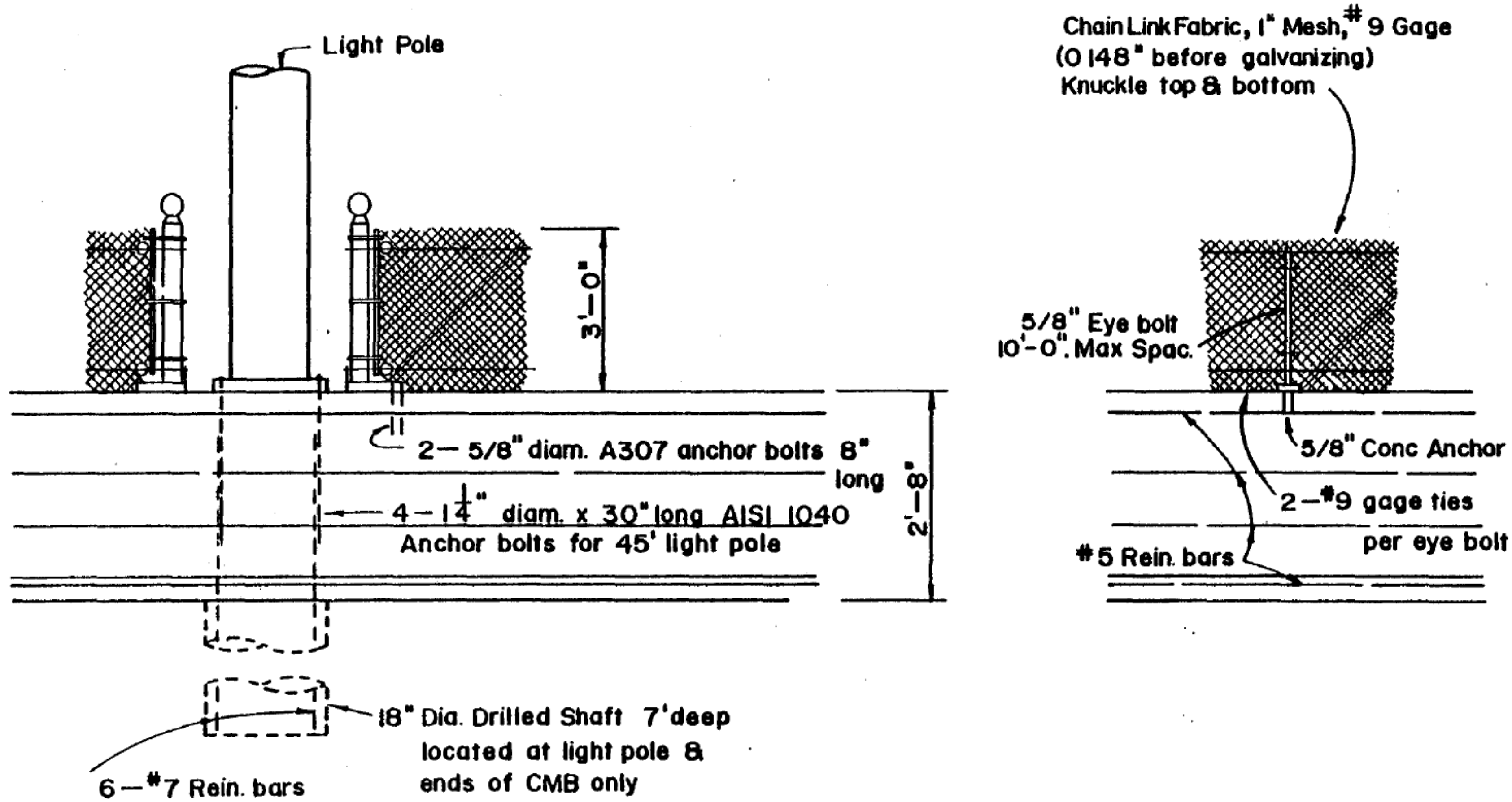

Figure 2. Chain-Link Fence and Concrete Median Barrier Details [8]

DATA	BARRIER TEST			
	CMB-1	CMB-2	CMB-3	CMB-4
VEHICLE				
Year	1963	1964	1963	1963
Make	Plymouth	Chevrolet	Chevrolet	Chevrolet
W, Weight (lbs)	4000	4230	4210	4210
θ, Impact Angle (deg)	25	25	7	15
FILM DATA				
V_I, Initial Impact Speed (mph)	62.4	55.7	60.9	60.7
V_P, Speed at Parallel (mph)	47.2	--	58.8	50.5
S_{long}, Longitudinal Distance to Parallel (ft)	15.3	--	17.6	23.0
D, Dynamic Barrier Deceleration (ft)	0.0	0.0	0.0	0.0
S_{lat}, Lateral Distance to Parallel (ft)	2.9	2.9	0.85	1.74
Δt, Time to Parallel (sec)	0.223	0.320	0.206	0.298
a. G_{long}, Average Longitudinal Deceleration (G's) (Parallel to Barrier)	2.0	--	0.4	1.3
b. G_{lat}, Average Lateral Deceleration (G's) (Normal to Barrier)	8.0	6.4	2.2	4.7
Departure Angle (deg)	7.3	6.0	6.5	11.5
ACCELEROMETER DATA				
Longitudinal Deceleration (G's) (parallel to long. axis of vehicle)				
Maximum	8.7	10.3	8.4	7.8
Average	3.2	1.8	0.5	1.4
Time (sec)	0.184	0.271	0.325	0.244
Transverse Deceleration (G's) (normal to long. axis of vehicle)				
Maximum	16.1	13.3	29.2	14.0
Average	4.4	2.8	1.8	3.0
Time (sec)	0.254	0.280	0.282	0.264

Figure 3. Test Data Summary, Test Nos. CMB-1 Through CMB-4 [8]

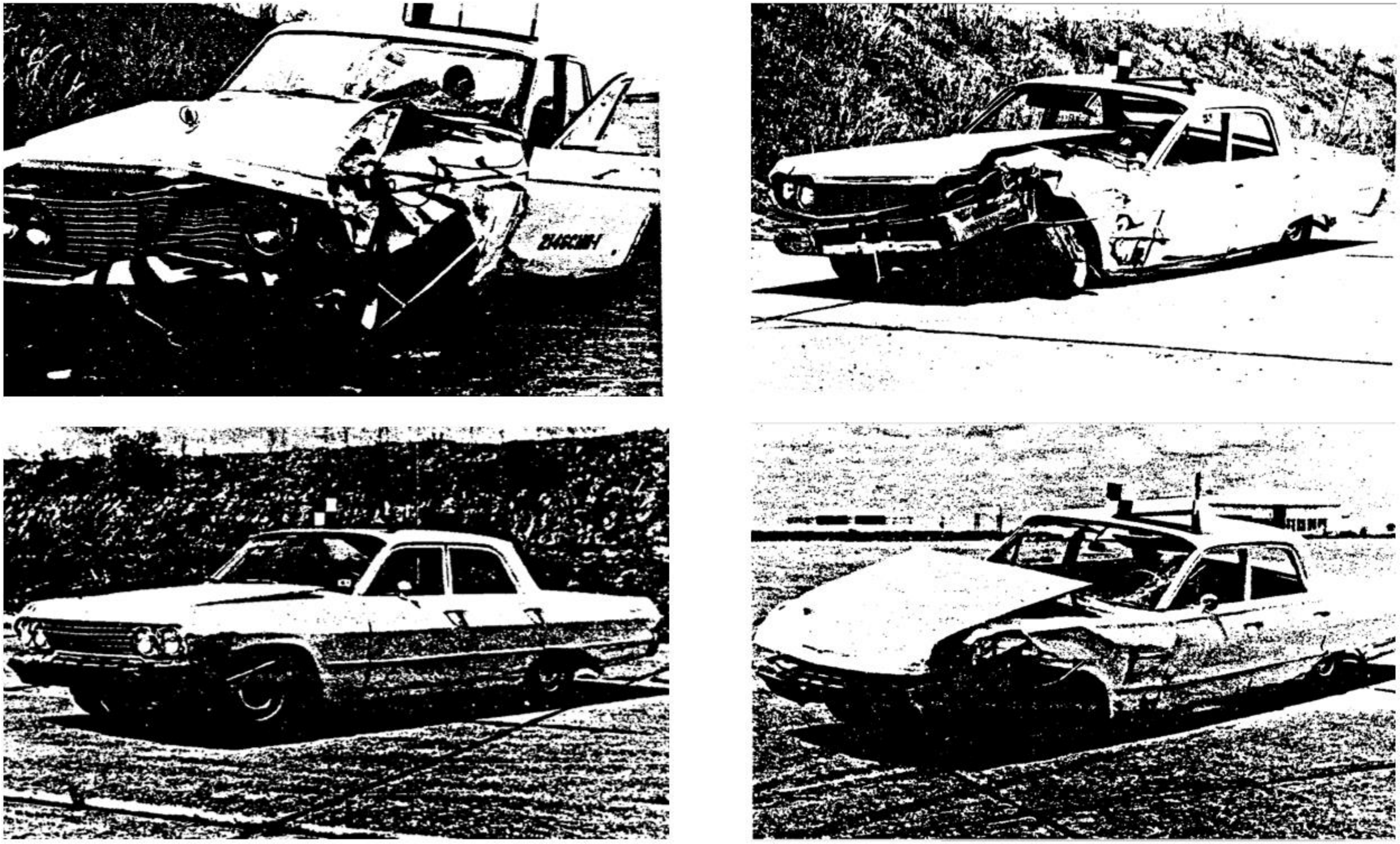

Figure 4. Vehicle Damage, Test Nos. CMB-1 (Top Left), CMB-2 (Top Right), CMB-3 (Bottom Left), CMB-4 (Bottom Right) [8]

2.3.2 Vandal Protection Fence: TTI Test No. 42070-6

In August of 1995, TTI researchers published a report titled *Crash Testing and Evaluation of Retrofit Bridge Railings and Transitions* [9]. This research report contained findings from the completion of full-scale crash tests completed at TTI. Test no. 42070-6 was conducted to determine the safety performance of a vandal protection fence mounted on top of a New Jersey concrete barrier [9].

The New Jersey barrier used in this full-scale crash test extended 100 ft in length. The parapet had a height of 32 in., a thickness of 15 in. at the base, and tapering up to a minimum of 6 in. at the top. The barrier was reinforced with eight no. 4 longitudinal bars and multiple no. 5 vertical stirrups, spaced at 8-in. increments.

A 6-ft tall vandal protection fence was connected onto the back of the New Jersey barrier. Vertical posts consisted of 2½-in. nominal diameter schedule 40 pipes measuring 7.3-ft long and were spaced 10 ft on center. Posts were connected to the back of the parapet with two saddle clamps and anchored with ⅝-in diameter bolts. Between the vertical posts, three horizontal stiffeners were used to provide shear continuity which had 1⅝-in. outside diameters. The horizontal stiffeners were connected to the 1-in. gap, diamond mesh with wire ties. CAD details and pretest photos of the system are shown in Figures 5 through 7 [9].

The full-scale crash test was conducted according to the AASHTO *Guide Specifications for Bridge Railings* Performance Level 2 (PL-2) criteria [10]. A 1991 Ford F250 pickup truck with a test inertial weight of 5,397 lb impacted the concrete barrier and vandal protection fence at 62.8 mph and at 20.2 degrees approximately 33 ft downstream from the beginning of the system.

All occupant safety risk values were within acceptable limits specified in the AASHTO PL-2 standards. The length of contact spanned 17 ft downstream from the point of impact, and the test vehicle exited the system at 49.5 mph and at an angle of 4.4 degrees. After the vehicle left the barrier, it came to rest 91 ft downstream from the initial impact point. Overall, the vehicle received moderate damage, which included bending of the stabilizer bar, floor pan, frame, and front axle on the right side of the vehicle. In addition to this localize damage, the windshield was cracked.

The system experienced minimal damage during the full-scale crash test. The lower edge of the chain-link wire was pushed behind the lower horizontal member between post nos. 5 and 6. Also, the middle horizontal member disconnected on the upstream side at post no. 5. An anchor used to attach post no. 5 to the barrier was also pulled out of the concrete. Researchers determined that the presence of the fence itself did not result in an adverse safety performance. Post-test damage photos are shown in Figure 8, and a summary of the test results is shown in Figure 9 [9].

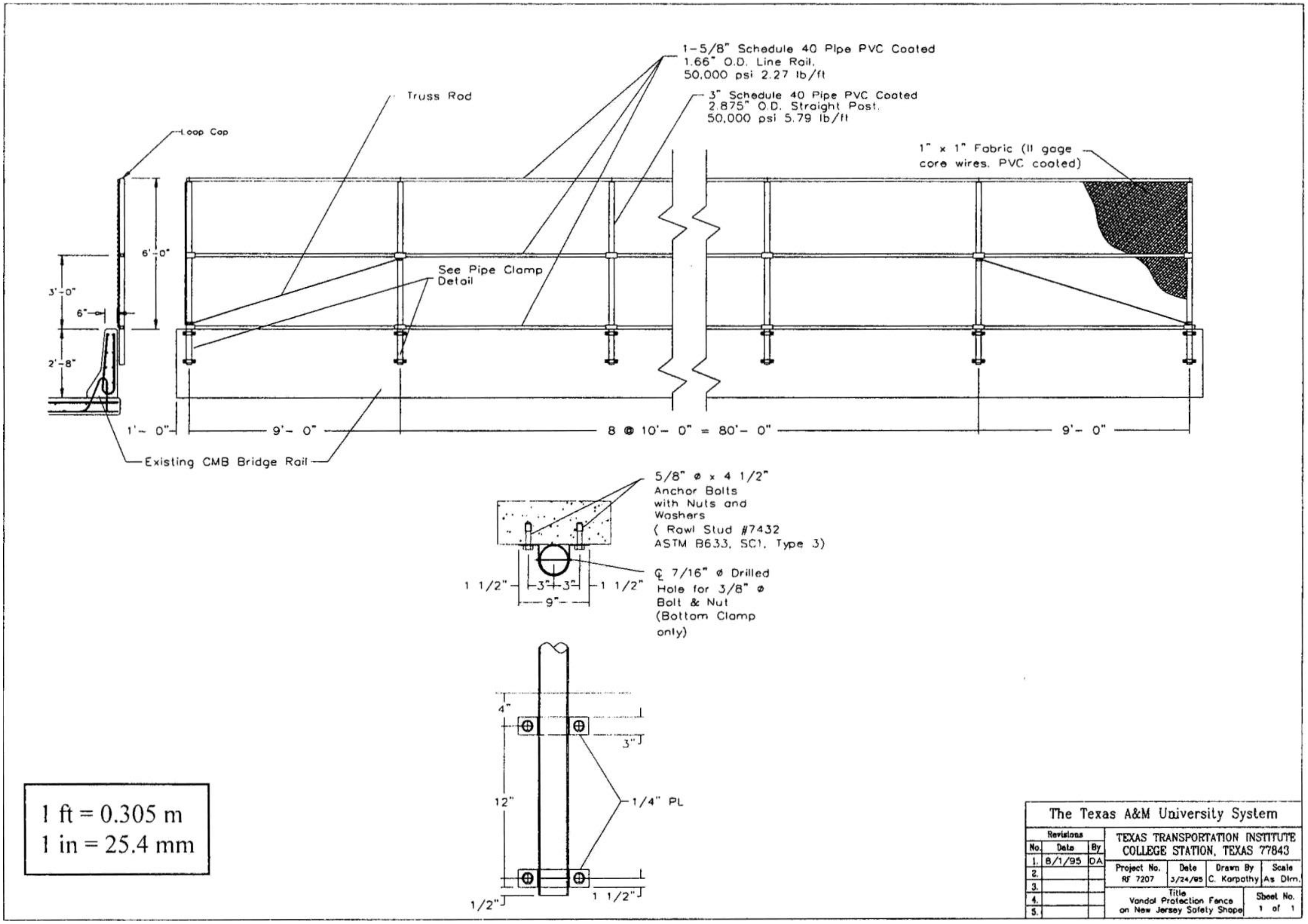

Figure 5. TTI Vandal Protection Fence Details [9]

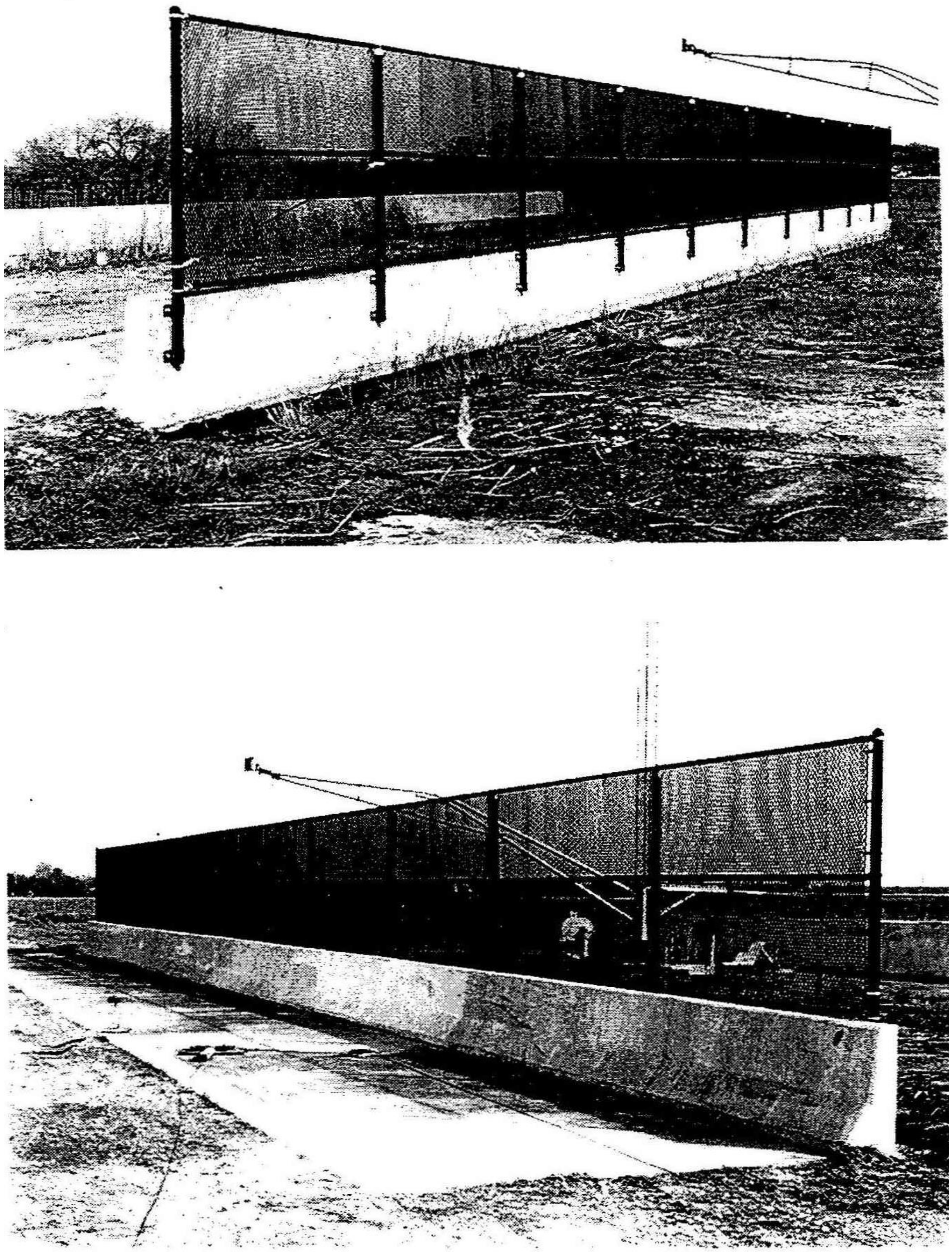

Figure 6. Pretest Parapet and Fence Details [9]

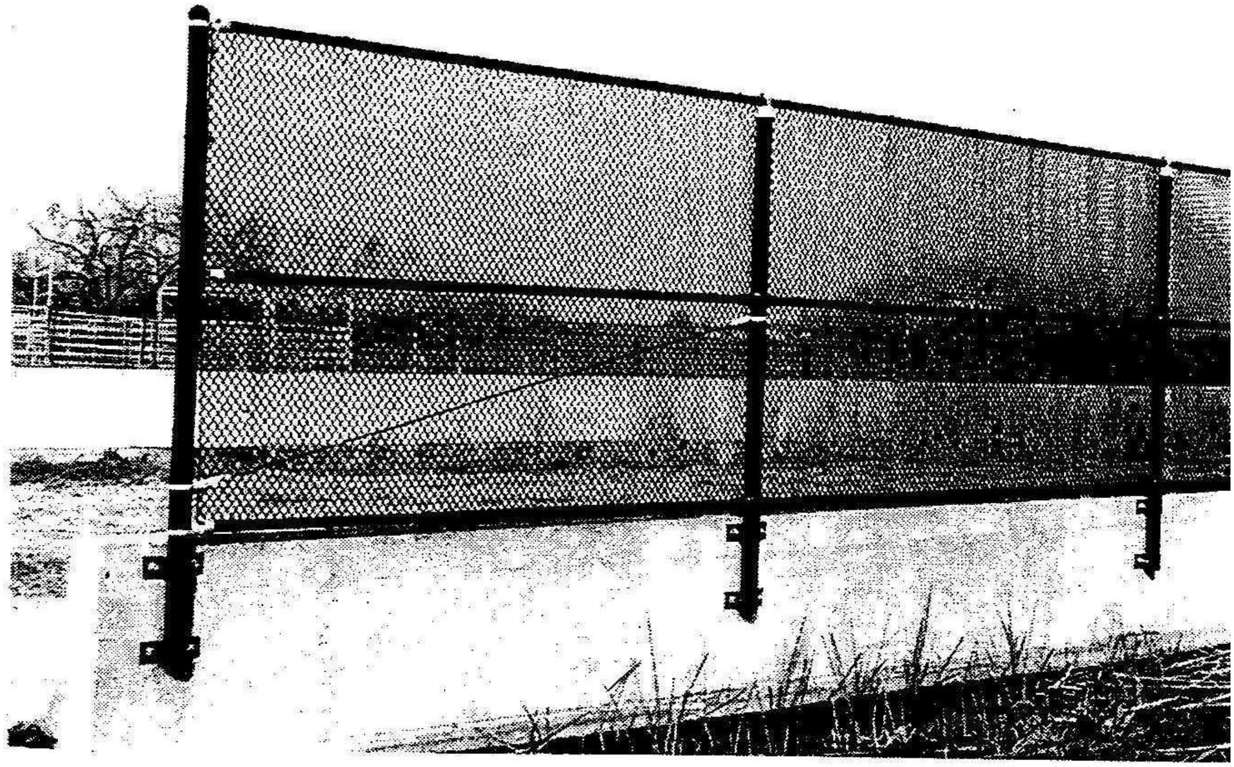

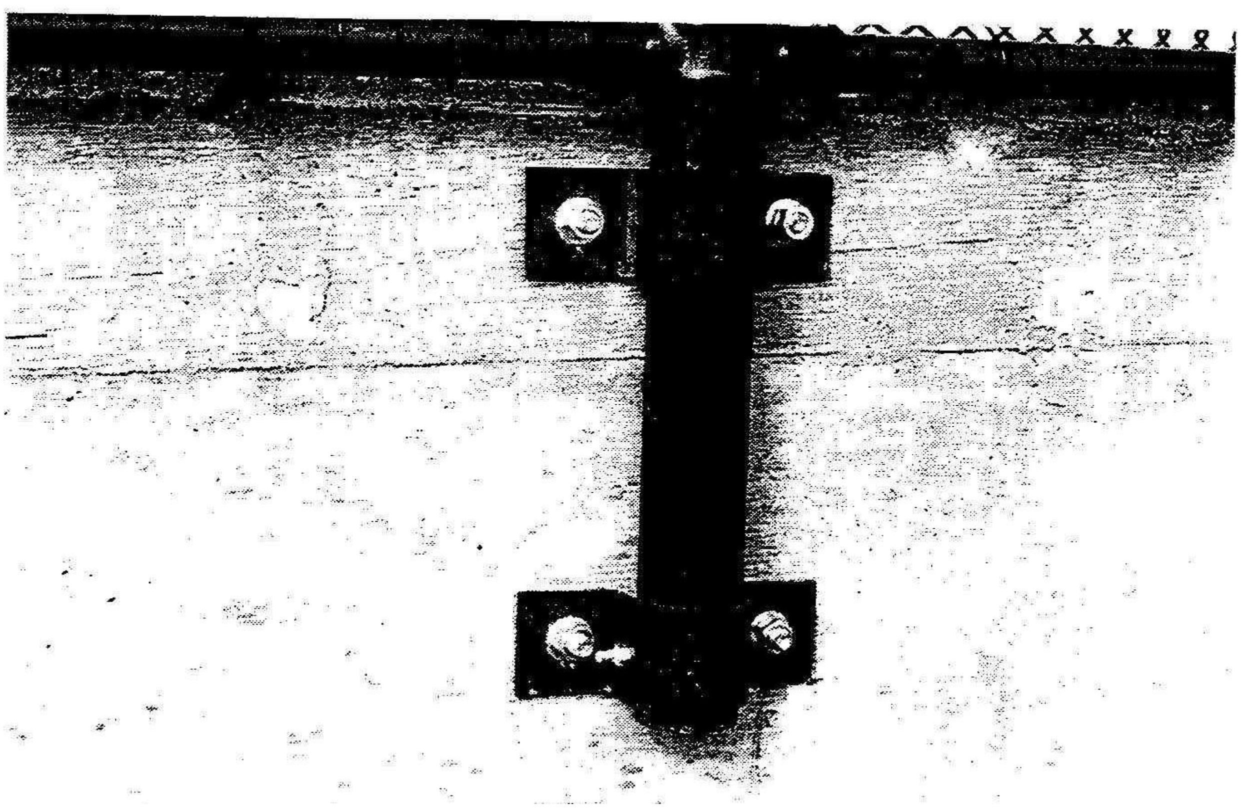

Figure 7. Pretest Fence and Connection Details [9]

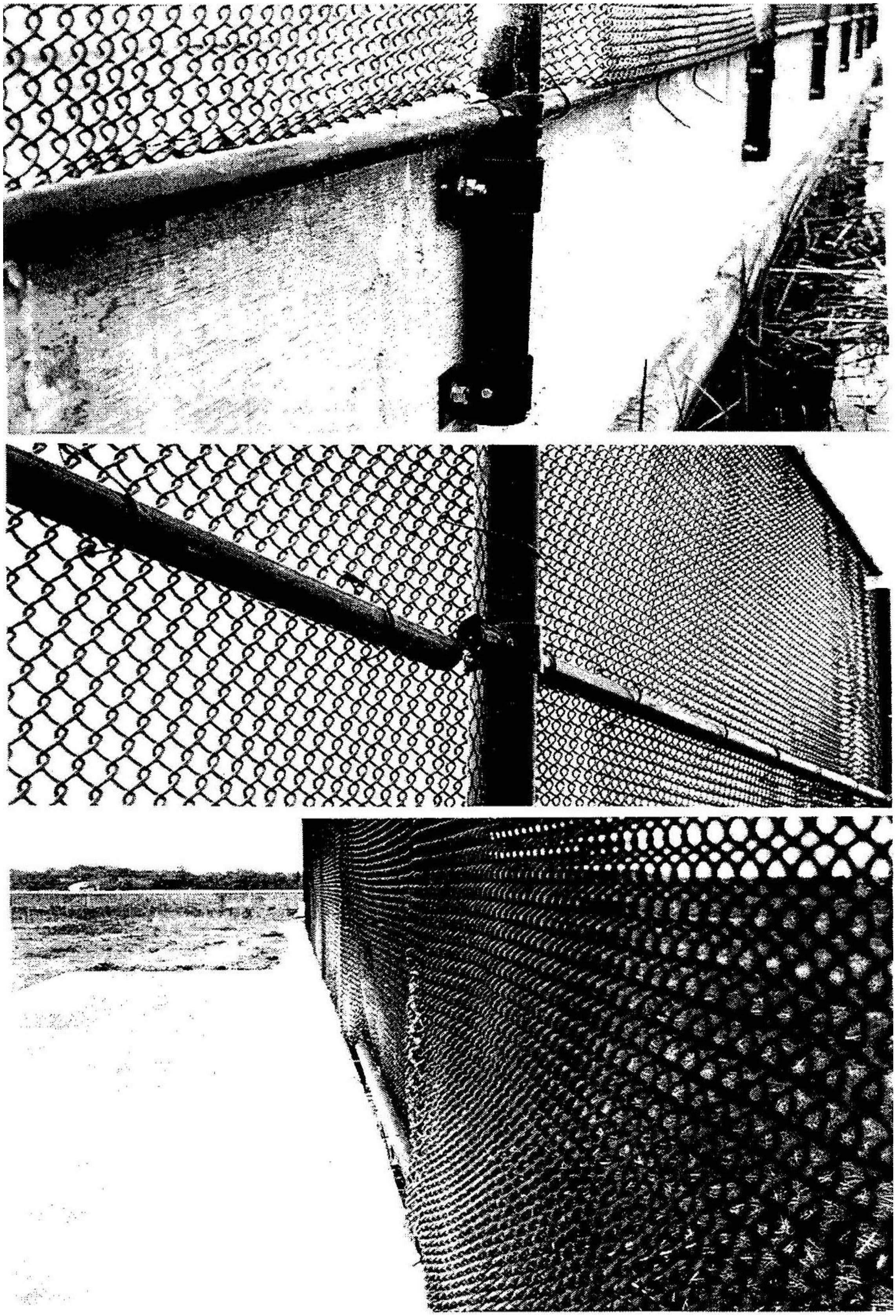

Figure 8. Post-test Fence Damage [9]

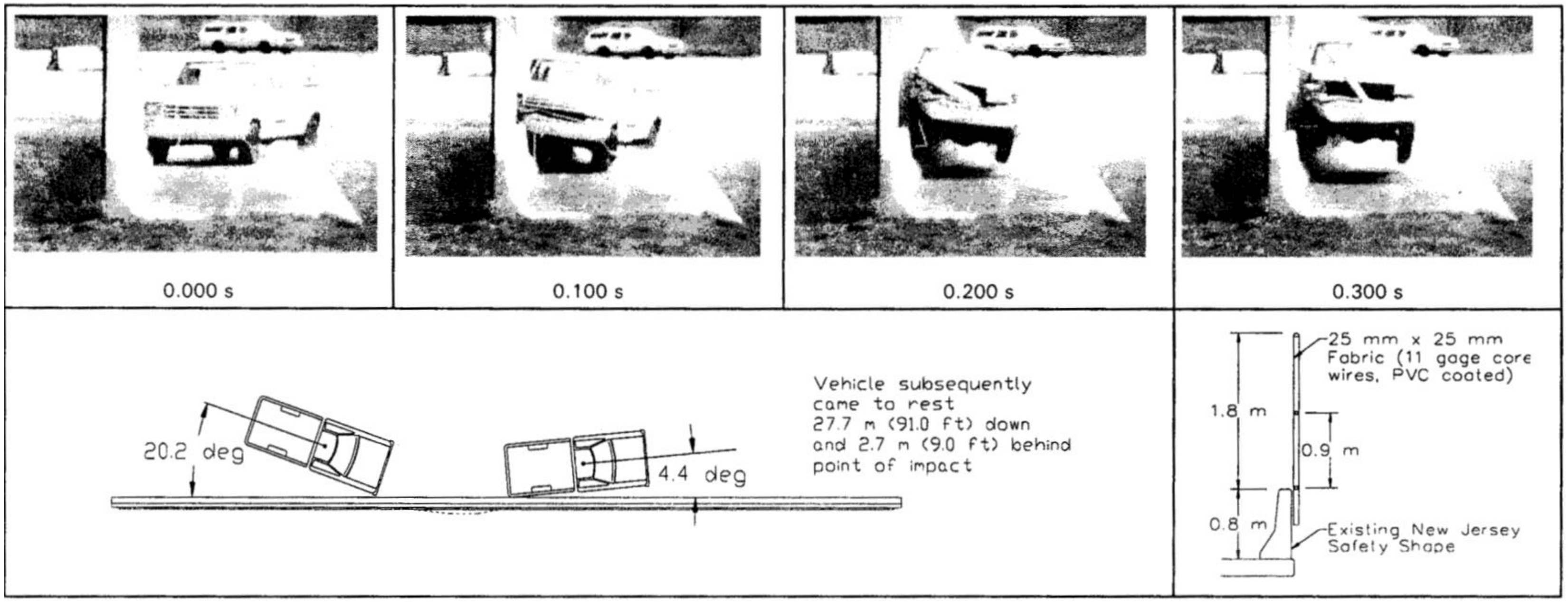

General Information	
Test Agency	Texas Transportation Institute
Test No.	472070-6
Date	03/10/95
Test Article	
Type	Retrofit Bridge Rail
Name	Vandal Protection Fence on NJSS
Installation Length (m)	30 m (100 ft)
Size and/or dimension and material of key elements	1.8 m (6.0 ft) tall 25 mm x 25 mm (1 in x 1 in) Fabric (11 gauge core wires,PVC coated)
Soil Type and Condition	on bridge deck, dry
Test Vehicle	
Type	Production
Designation	Pickup
Model	1991 Ford F250
Mass (kg) Curb	2208 (4863 lb)
Test Inertial	2450 (5397 lb)
Dummy	75 (165 lb)
Gross Static	2525 (5562 lb)

Impact Conditions	
Speed (km/h)	101.1 (62.8 mi/h)
Angle (deg)	20.2
Exit Conditions	
Speed (km/h)	79.6 (49.5 mi/h)
Angle (deg)	4.4
Occupant Risk Values	
Impact Velocity (m/s)	
x-direction	5.0 (16.5 ft/s)
y-direction	2.8 (9.1 ft/s)
THIV (optional)	
Ridedown Accelerations (g's)	
x-direction	-5.6
y-direction	-7.6
PHD (optional)	
ASI (optional)	
Max. 0.050-s Average (g's)	
x-direction	-8.4
y-direction	-5.4
z-direction	-8.0

Test Article Deflections (m)	
Dynamic	0.14 (0.47 ft)
Permanent	0.08 (0.25 ft)
Vehicle Damage	
Exterior	
VDS	0IRFQ5
CDC	01FREK2 & 01RDES3
Interior	
OCDI	RS0000000
Maximum Exterior Vehicle Crush (mm)	170 (6.7 in)
Max. Occ. Compart. Deformation (mm)	70 (2.8 in)
Post-Impact Behavior	
Max. Roll Angle (deg)	30
Max. Pitch Angle (deg)	9
Max. Yaw Angle (deg)	-19

Figure 9. Summary of Test Results [9]

2.3.3 Errant Motorcycle Rider Containment Fence: TTI Test NO. 469688-2-1

In 2019, TTI researchers published a report detailing the design and crash testing of a containment fence developed to improve errant motorcycle riders' safety. This research effort also included chain-link fence pendulum testing and finite element modeling of a chain-link fence.

A total of three design concepts were developed and evaluated using finite element analysis. These concepts consisted of a vertical weak post system, a system with vertical post bent near the top of the barrier, and a system with U-shaped posts where posts were curved away from the front face of the barrier at the top and bottom. An injury evaluation was performed on the simulations to identify the probability that an errant motorcyclist would sustain significant injury when interacting with these systems. Based on the results of this analysis and the protrusion of the simulated errant rider, researchers decided to continue the design with the U-shape post concept.

After modifying the U-shape post design, researchers proceeded to conduct full-scale crash testing evaluation of this system. The test installation of this system consisted of a 32-in. tall New Jersey style barrier spanning a 75-ft long arc on a 500-ft radius. Chain-link fabric was attached near the top-back side of the barrier which used 9-guage, 2x2-in mesh standing 48 in. tall. Horizontal rails were located near the top and bottom of the fence which the chain-link fabric attached to using 9-gauge steel secure ties. Posts consisted of HSS1.9x.1875 round tube spaced 96 in. on center and were anchored to the back side of the barrier.

Full-scale crash testing involved a 410-lb motorcycle which impacted the system at a speed of 34.6 mph and at a 15.2-degree angle. The authors of the reported noted that the chain-link fence successfully contained and redirected the errant rider which did not interact with the fence posts [11]. A maximum dynamic deflection of 9.4 in. was reported and the system damage mainly consisted of fence fabric permanent deformation of 7 in laterally.

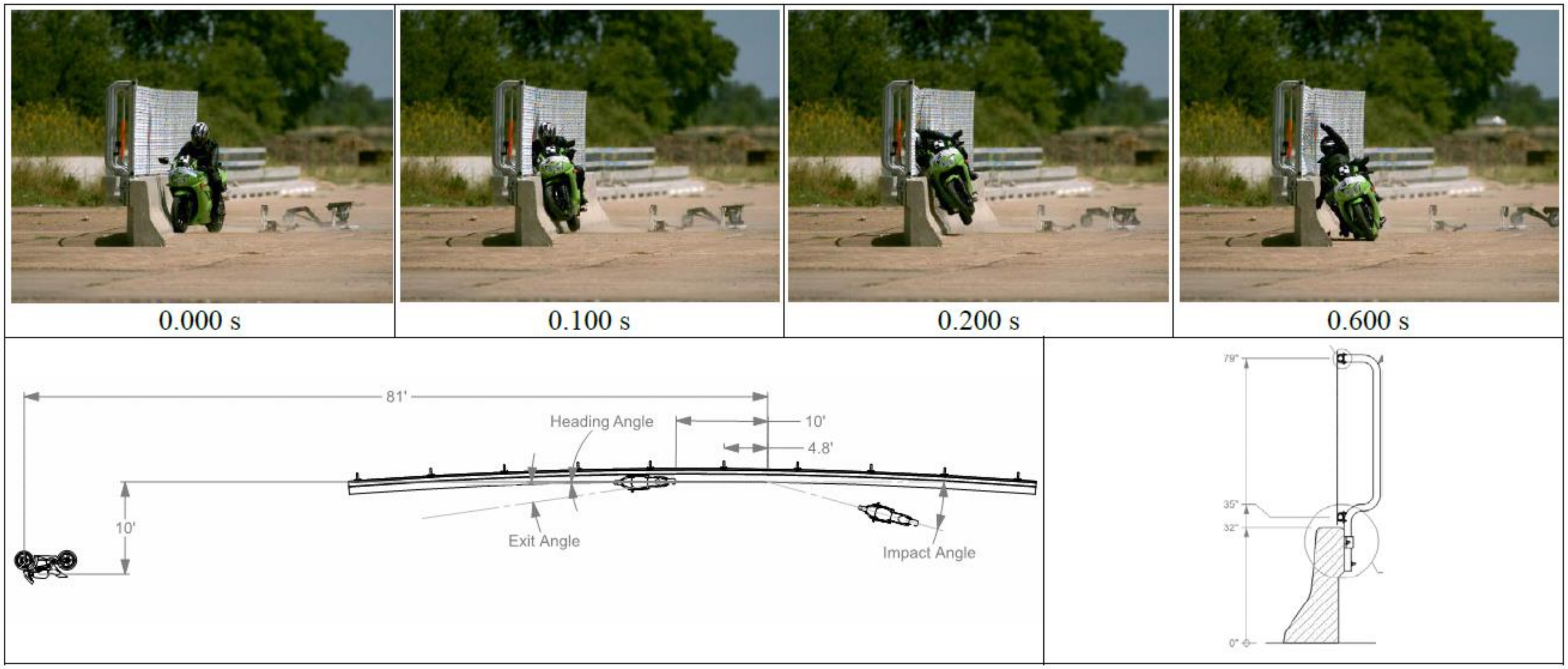

General Information
- Test Agency .... Texas A&M Transportation Institute (TTI)
- Test Standard Test No. .... Non-Standard Test
- TTI Test No. 469688-2-1
- Test Date 2018-07-05

Test Article
- Type .... Fence Barrier
- Name .... TXDOT Fence Barrier for Motorcycles
- Installation Length .... 75 ft
- Material or Key Elements ... Chain Link Fence, Tubular Posts, Concrete barrier

Soil Type and Condition ..... Concrete pavement, damp

Test Vehicle
- Type/Designation .... Motorcycle
- Make and Model .... 2012 Kawasaki 250 Ninja
- Curb .... 374 lb
- Test Inertial .... 410 lb
- Dummy .... 190 lb
- Gross Static .... 600 lb

Impact Conditions
- Speed .... 34.6 mi/h
- Angle .... 15.2°
- Location/Orientation .... 57-inches upstream of center of post 5

Exit Conditions
- Speed of motorcycle .... 28.1 mi/hr
- Angle of motorcycle .... 8.3°

Post-Impact Trajectory
- Stopping Distance .... 81 ft downstream

Test Article Deflections (Mesh)
- Dynamic .... 9.4 inches
- Permanent .... 7 inches
- Working Width .... 26.6 inches
- Working Width Height .... 79 inches

Injury Criteria
- HIC15 Value 92

Figure 10. Summary of Test Results, TTI Test No. 469688-2-1 [11]

2.3.4 Minnesota Combination Traffic-Bicycle Bridge Rail: MwRSF Test Nos. MNPD-1,MNPD-2, and MNPD-3

In 1998, Midwest Roadside Safety Facility researchers published a report pertaining to the design and crash tests of a bicycle bridge rail for the Minnesota DOT. Two full-scale crash tests were performed on this design, as shown in Figures 11 through 13, which was deemed acceptable in accordance with requirements dictated by NCHRP Report 350 [12].

The test construction included two cables placed within the tubular rails to prevent detachment of large pieces of debris from causing hazardous conditions to vehicles and pedestrians below and/or behind the bridge rail. The two cables also tapered down and attached to the backside of the rail. This configuration allows the cables to be terminated safely and moves the tensioning components to the backside of the rail and farther away from any impacting vehicles.

In 2020, Researchers at the Midwest Roadside Safety Facility conducted full-scale crash testing of this system under MASH 2016 requirements. The test article was similar to that which was tested in the effort conducted in 1998 with minor design modifications. One such modification was that the rail spindles were welded to the back of the railing instead of being welded to railing centerline [13]. The vehicle's ZOI past the front barrier face was reported in this document which achieved a 12.75-in. lateral offset. Ultimately, the safety performance of this test article was deemed acceptable according to MASH 2016 requirements.

.

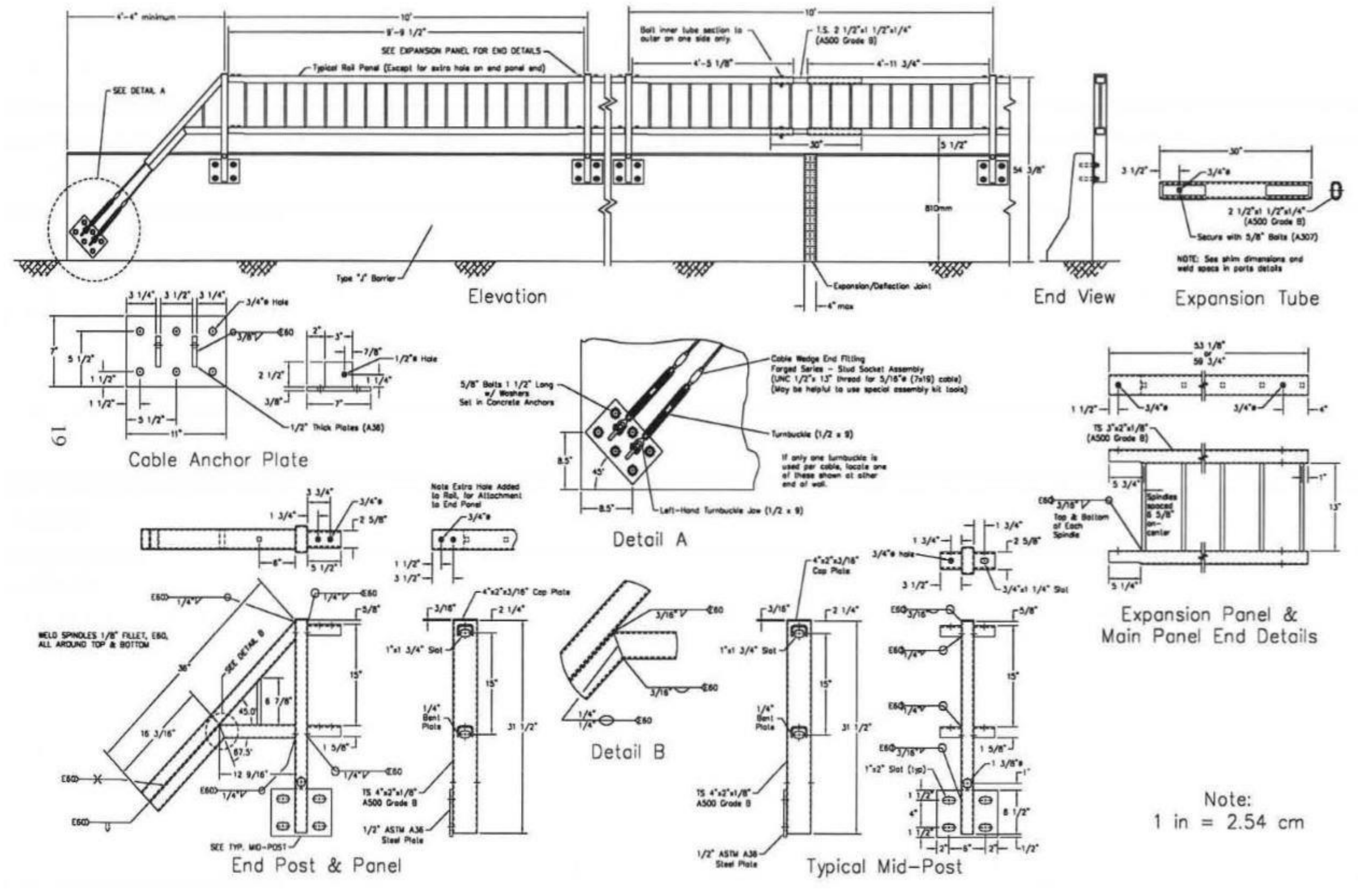

Figure 11. Minnesota Combination Traffic-Bicycle Bridge Rail Design Details [12]

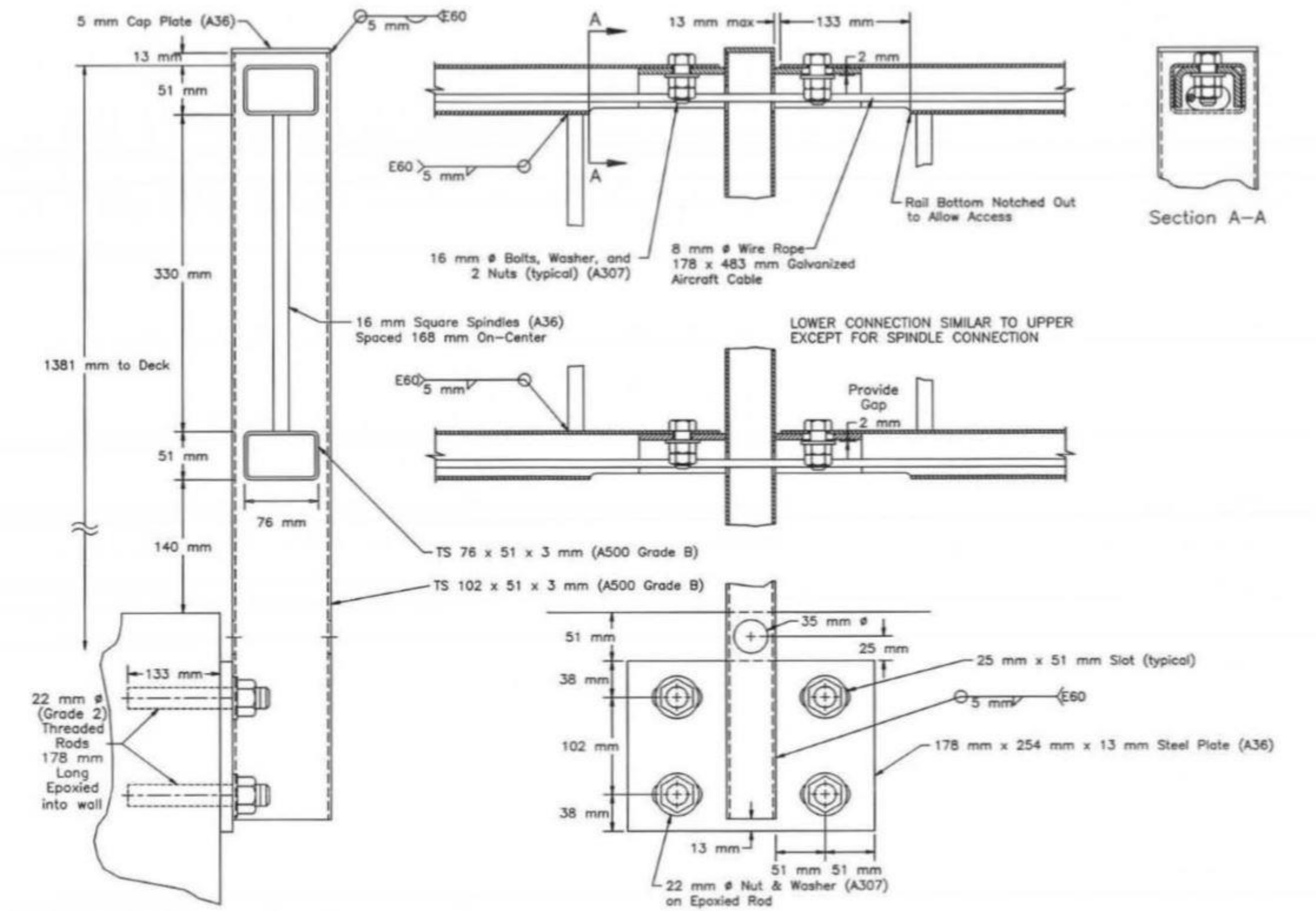

Figure 12. Minnesota Combination Traffic-Bicycle Bridge Rail Design Details [12]

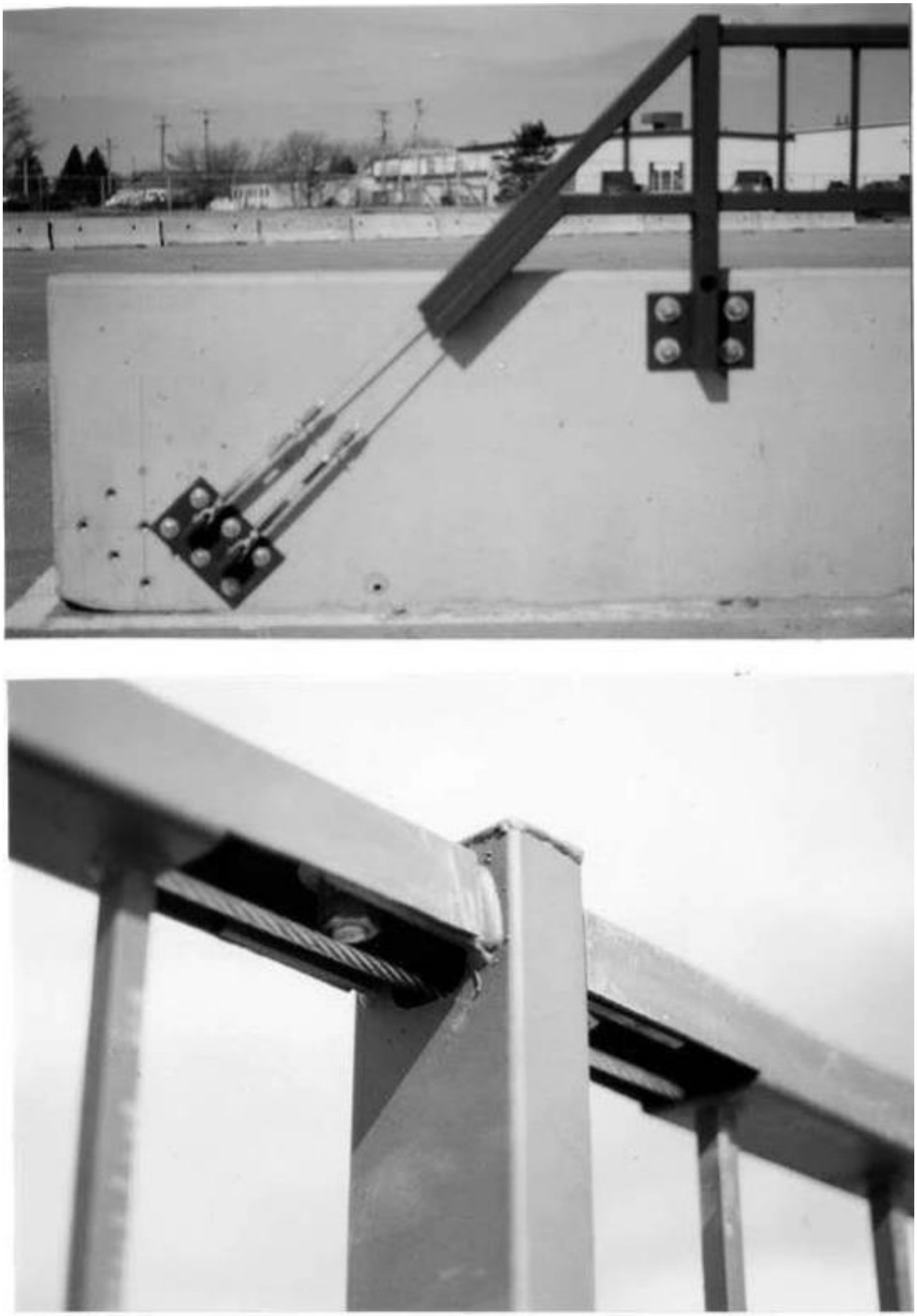

Figure 13. Tension Cable Taper and Rail Design [12]

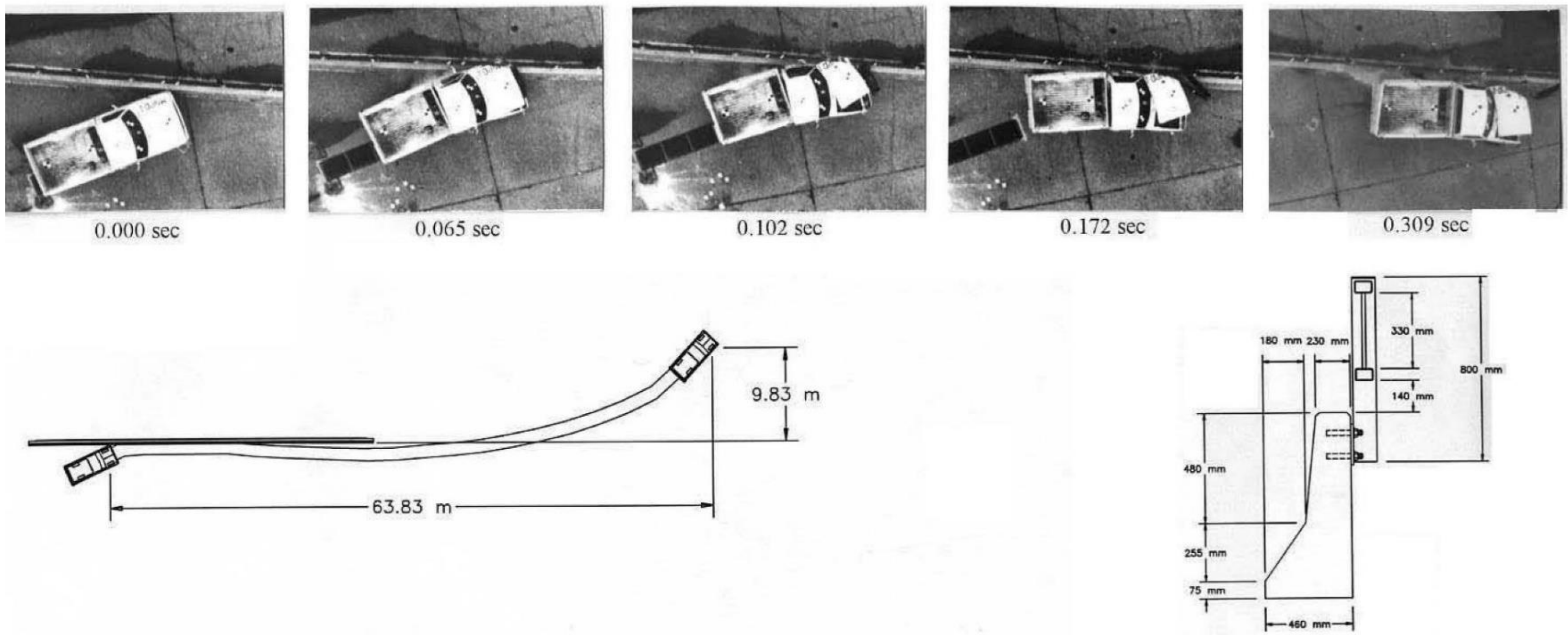

- Test Number MNPD-1
- Date 4/3/97
- Appurtenance . . . . Minnesota Combination Traffic/Bicycle Bridge Rail
- Total length . . . . 36.6 m
- Concrete Traffic Rail . . . . New Jersey Safety Shape
  - Length . . . . 6.1 m
  - Height . . . . 810 mm
  - Base Width . . . . 460 mm
  - Top Width . . . . 230 mm
- Steel Rail . . . . TS 76 x 51 x 3 mm - A500 Grade B
- Steel Spindles . . . . 16 mm Square Bars - A36
- Steel Posts . . . . TS 102 x 51 x 3 mm - A500 Grade B
- Vehicle Model . . . . 1988 Ford F-250 ¾-Ton Pickup
  - Curb . . . . 2,020 kg
  - Test Inertia . . . . 2,001 kg
  - Gross Static . . . . 2,001 kg
- Vehicle Speed
  - Impact . . . . 105.2 km/hr
  - Exit . . . . 15.3 km/hr
- Vehicle Angle
  - Impact . . . . 25.5 deg
  - Exit . . . . 1.7 deg
- Vehicle Stability . . . . Satisfactory
- Occupant Ridedown Deceleration (10 msec avg.)
  - Longitudinal . . . . 5.06 G's < 20 G's
  - Lateral (not required) . . . . . 7.57 G's
- Occupant Impact Velocity (Normalized)
  - Longitudinal . . . . 6.58 m/s < 12 m/s
  - Lateral (not required) . . . . . 7.83 m/s
- Vehicle Damage . . . . Moderate
  - TAD [21] 11-LFQ-6
  - SAE [22] 11-LDAW4
- Vehicle Stopping Distance . . . . . 63.8 m downstream
  9.8 m lateral behind
- Bridge Rail Damage . . . . Minimal
- Maximum Deflections
  - Permanent Set . . . . NA
  - Dynamic . . . . 69 mm

Figure 14. MNDP-1 Test Summary [12]

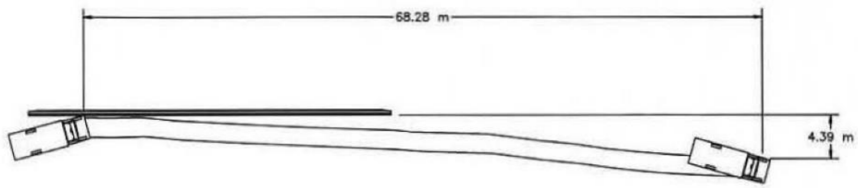

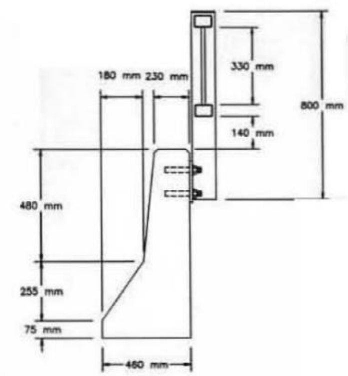

- Test Number MNPD-2
- Date 4/15/97
- Appurtenance .... Minnesota Combination Traffic/Bicycle Bridge Rail
- Total length .... 36.6 m
- Concrete Traffic Rail .... New Jersey Safety Shape
  - Length .... 6.1 m
  - Height .... 810 mm
  - Base Width .... 460 mm
  - Top Width .... 230 mm
- Steel Rail .... TS 76 x 51 x 3 mm - A500 Grade B
- Steel Spindles .... 16 mm Square Bars - A36
- Steel Posts .... TS 102 x 51 x 3 mm - A500 Grade B
- Vehicle Model .... 1986 Ford F-800 Single-Unit Truck
  - Curb .... 5,254 kg
  - Test Inertia .... 8,002 kg
  - Gross Static .... 8,002 kg
- Vehicle Speed
  - Impact .... 82.1 km/hr
  - Exit .... NA
- Vehicle Angle
  - Impact .... 14.7 deg
  - Exit .... NA
- Vehicle Stability .... Satisfactory
- Occupant Ridedown Deceleration (10 msec avg.)
  - Longitudinal .... 5.18 G's < 20 G's
  - Lateral (not required) ..... 4.30 G's
- Occupant Impact Velocity (Normalized)
  - Longitudinal .... 2.37 m/s < 12 m/s
  - Lateral (not required) ..... 2.69 m/s
- Vehicle Damage .... Moderate
  - TAD [21] 11-LFQ-3
  - SAE [22] 11-LFWL2
- Vehicle Stopping Distance ..... 68.3 m downstream
  4.39 m lateral
- Bridge Rail Damage .... Moderate
- Maximum Deflections
  - Permanent Set .... NA
  - Dynamic .... 456 mm

Figure 15. MNPD-2 Test Summary [12]

0.000 sec 0.150 sec 0.250 sec 0.350 sec 0.450 sec

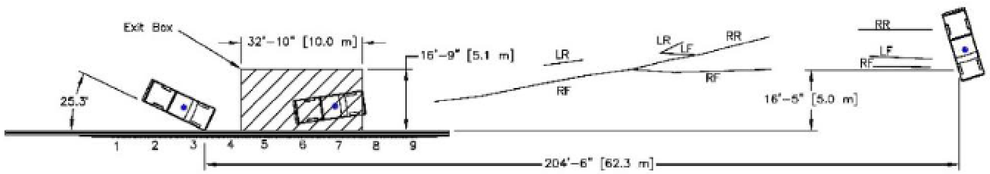

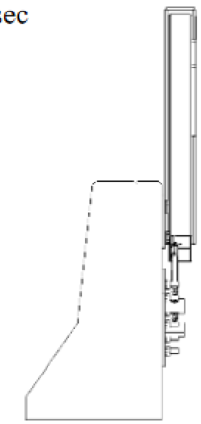

- Test Agency .... MwRSF
- Test Number MNPD-3
- Date 6/4/2020
- MASH 2016 Test Designation No. 3-11
- Test Article .... Minnesota Bicycle and Pedestrian Bridge Railing System
- Total Length .... 120 ft – 2 in.
- Key Component - Post
  - Length .... 31½ in.
  - Width .... 4 in.
  - Spacing .... 2 in.
- Key Component – Concrete Barrier
  - Length .... 120 ft – 2 in.
  - Width .... 9 in.
  - Height .... 32 in.
- Vehicle Make /Model .... 2014 Dodge Ram
  - Curb .... 4,994 lb
  - Test Inertial .... 5,001 lb
  - Gross Static .... 5,182 lb
- Impact Conditions
  - Speed .... 63.4 mph
  - Angle .... 25.3 degrees
  - Impact Location .... 71¼ in. upstream from post no. 4
- Impact Severity .... 122.7 kip-ft > 52 kip-ft limit from MASH 2016
- Exit Conditions
  - Speed .... 53.0 mph
  - Angle .... 5.1 degrees
- Exit Box Criterion .... Pass
  Vehicle Stability .... Satisfactory
- Vehicle Stopping Distance ..... 204 ft – 6 in. downstream and 16 ft – 5 in. laterally in front
- Vehicle Damage .... Moderate
  - VDS [12] 01-RFQ-5
  - CDC [13] 01-RYEW-5
  - Maximum Interior Deformation .... 2.9 in.
- Test Article Damage .... minimal
- Maximum Test Article Deflections
  - Permanent Set .... 0.4 in.
  - Dynamic .... 0.6 in.
  - Working Width .... 23.2 in.
  - ZOI .... 12.75 in.
- Transducer Data

Evaluation Criteria		Transducer		MASH 2016 Limit
		SLICE-1	SLICE-2 (primary)	
OIV ft/s	Longitudinal	-14.77	-14.37	±40 (12.2)
	Lateral	-23.36	-24.87	±40 (12.2)
ORA g's	Longitudinal	-5.90	-5.87	±20.49
	Lateral	-11.21	-10.53	±20.49
Maximum Angular Displacement degrees	Roll	22.9	22.8	±75
	Pitch	-9.2	-10.3	±75
	Yaw	-43.7	-43.9	Not required
THIV – ft/s		28.31	29.26	Not required
PHD – g's		11.51	10.87	Not required
ASI		1.41	1.51	Not required

Figure 16. MNPD-3 Test Summary [13]

2.3.5 Signs Installed on Concrete Median Barriers

Researchers from the Texas A&M Transportation Institute (TTI) completed a study in April 2013 to determine the safety of mounting signs on the top of concrete median barriers [7]. This report detailed study efforts, including a literature review, simulation effort, and four full-scale crash tests.

The four full-scale crash tests completed by TTI occurred with a 2270P pickup truck under MASH TL-3 guidelines. During the first three tests in this testing series, a 2 ½ -in. outside diameter schedule 80 pipe was used to mount to the sign and the parapet, and different connection methods were evaluated for each test. The fourth test, test no. 466462-4, included a 2½ -in. 10BWG pipe with four section-reducing slots located at the base of the post. During all of the crash tests, the vehicle extended over the front face of the barrier and contacted the sign and sign support assembly, causing the damage to the hood and the pickup truck's fender to tear off. The authors determined that that the addition of the sign assembly did not decrease the safety of the concrete parapet [7].

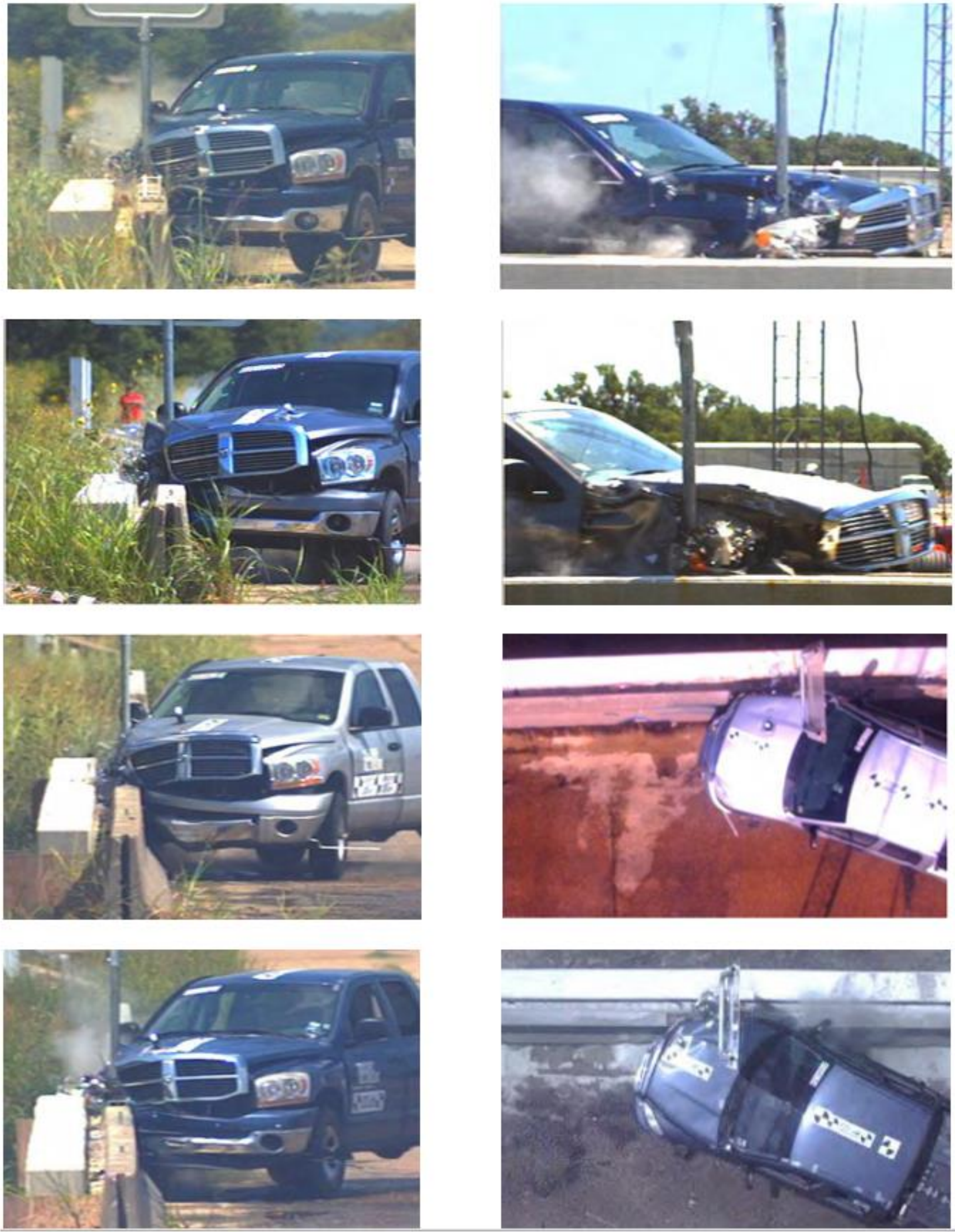

Figure 17. Vehicle-Sign Interaction, Test Nos. 466462-1, 466462-2a, 466462-3, 466462-4 [7]

2.3.6 Caltrans Barrier Mounted Sign and Signpost: Full-Scale Test No. SS641

In 2011, Caltrans researchers published a report detailing a full-scale crash test of a barrier mounted sign and signpost. One full-scale crash test was performed on this design, as shown in Figures 18 and 19. The barrier redirected the vehicle, but the impact created a high risk to occupants due to the occupant compartment deformation and was not deemed acceptable in accordance with requirements dictated by NCHRP Report 350 [14].

The sign post consisted of a 108-in. tall post with a 4-in. outside diameter. The sign configuration consisted of two rectangular 36 in. by 60 in. panels placed back-to-back. The post was mounted to the top of a 36-in. tall, 12½-in. thick, single slope barrier through the usage of a ⅜-in. thick saddle bracket, connected with two 1-in. bolts.

The structural adequacy and vehicle trajectory for the test were deemed acceptable but the occupant risk was deemed unacceptable. The hood was displaced backwards during the impact with the sign support and penetrated the windshield which is prohibited by NCHRP Report 350 criteria. Additionally, the driver side occupant compartment was excessively deformed.

Figure 18. Barrier Mounted Sign Test Article [14]

Figure 19. Barrier Mounted Sign Vehicle Impact [14]

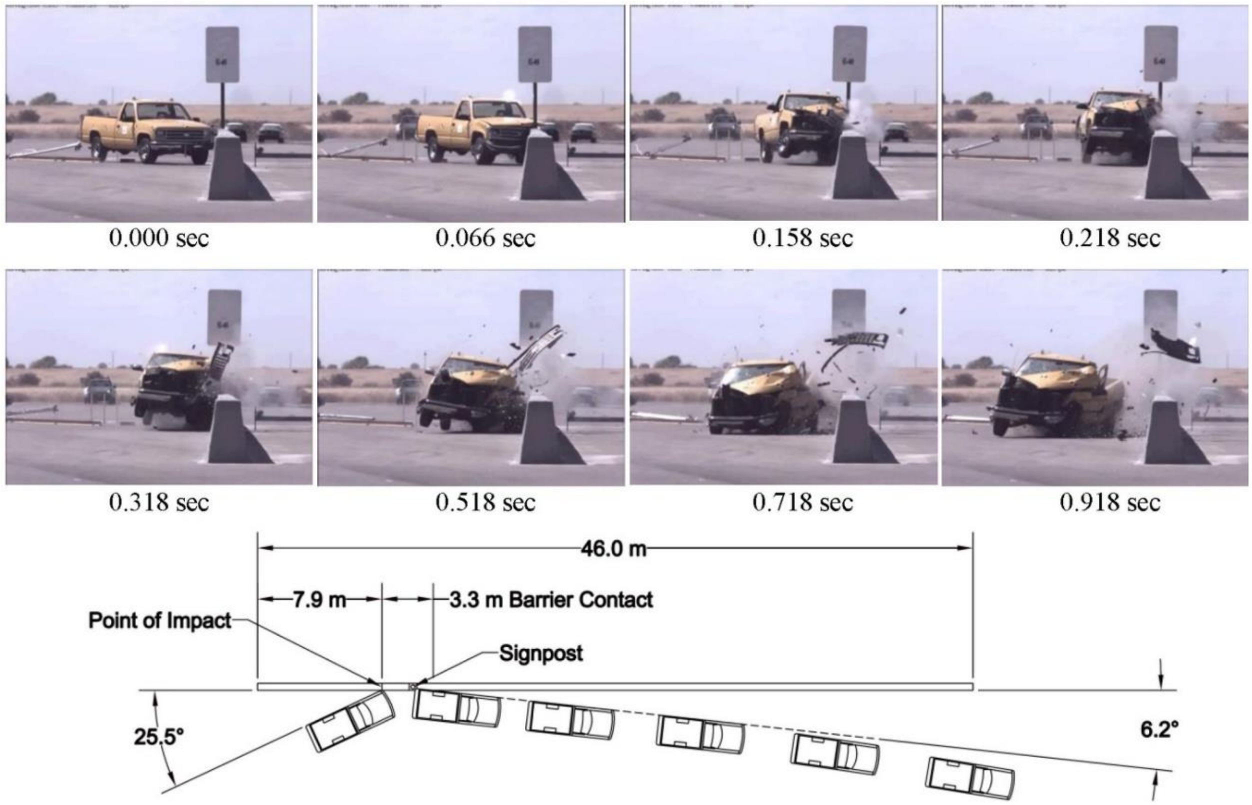

Figure 2-18 Test SS641 – Impact Sequence and Diagram

General Information	
Testing Agency	California DOT
Test Number	SS641
Test Date	August 30, 2007
Test Article	
Type	Type 60 concrete barrier w/barrier mounted metal post 101.6 mm (4.0 in) O.D.
Installation Length	46 m (150 ft)
Height	910 mm (36 in)
Test Vehicle	
Type	¾-Ton Pick-up Truck
Designation	2000P
Model	1993 Chevy Cheyenne
Mass Curb	1882.2 kg (4149.5 lb_m)
Test Inertial	1952.6 kg (4304.7 lb_m)
Impact Conditions	
Impact Velocity	99.1 km/h (61.6 mph)
Impact Angle	25.5°

Exit Conditions	
Exit Velocity	~62.3 km/h (38.7 mph)
Exit Angle	6.2°
Test Data	
Occupant Impact Velocity	
Long	n/a*
Lat	n/a*
Ridedown Acceleration	
Long	n/a*
Lat	n/a*
Vehicle Exterior:	
VDS[5,6]	FL-6, LD-4, LFQ-7
CDC[7]:	11FFAW5
Vehicle Interior:	
O.C.D.I.[1]:	LF3111121
Post-Impact Vehicular Behavior	(*Data Analysis/Video Analysis*)
Maximum Roll Angle	n/a* / -7.2°
Maximum Pitch Angle	n/a* / 5.9°
Maximum Yaw Angle	n/a* / 31.7°

Figure 20. Test No. SS641 Summary [14]

2.4 Full-Scale Crash Testing of Slope End Treatments

Terminating the debris fences at upstream and downstream ends will likely require a vertical taper of the fence element. Therefore, to determine a vertical taper rate for termination of the fence framework, researchers reviewed previously tested systems with tapered horizontal rails. In terms of the end termination geometry, steeper vertical tapers posed an advantage as they reduced the length and complexity of the overall end termination section.

Review of previously tested barriers with vertical tapers found that tapers as steep as 2H:1V have performed acceptably when used in systems with tube rail terminations. Researchers from TTI evaluated a thrie beam transition to the Wisconsin Type M tubular steel bridge rail under NCHRP Report 350 test designation no. 3-21 [15]. The top tube of the Type M tubular bridge rail had a top mounting height of 42 in. and was tapered downward at a 2H:1V slope to extend below the 31.5 in. tall thrie beam AGT, as shown in Figure 21. In test no. 401021-3, a 2000P vehicle impacted the transition upstream from the tapered tube attachment at a speed of 62.6 mph and an angle of 25.2 degrees. The pickup truck traversed across the sloped bridge rail tube with both the left-front fender and hood contacting the tube, as shown in Figure 22. However, this contact did not adversely affect vehicle redirection by the transition nor post an occupant risk hazard. The 2000P vehicle was safely redirected and test no. 401021-3 was deemed acceptable under NCHRP Report 350 TL-3.

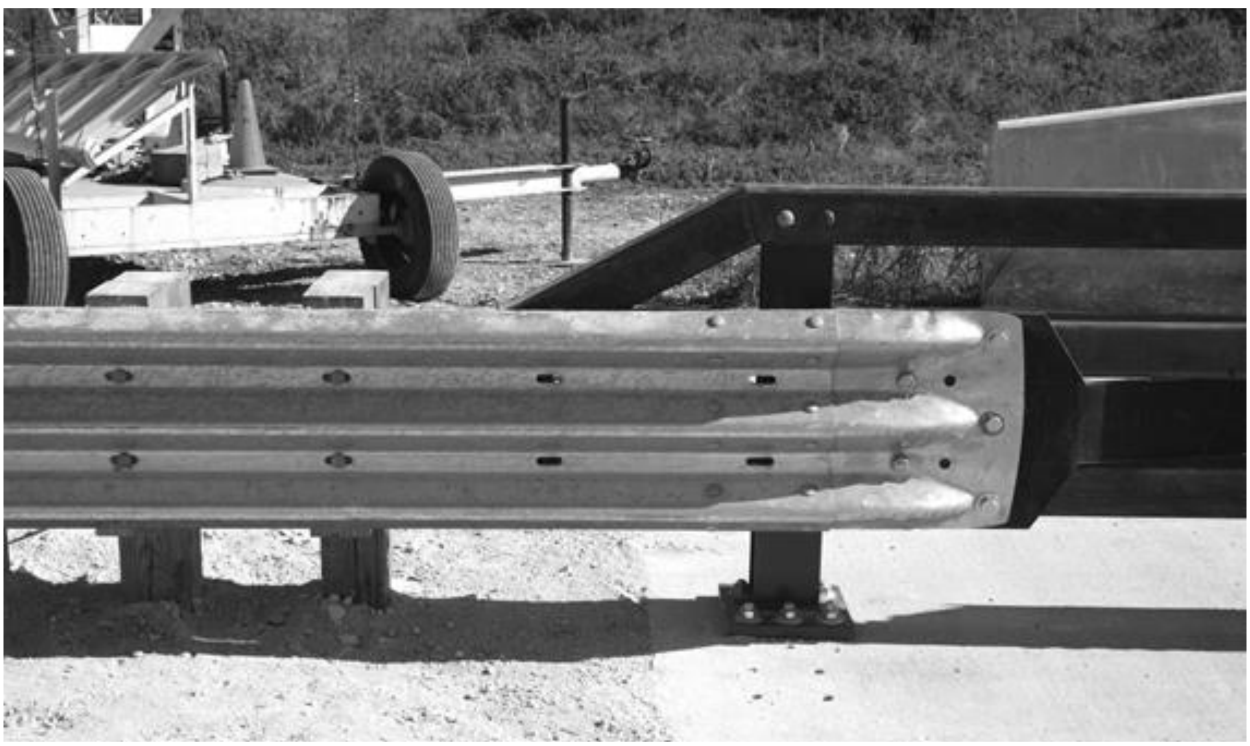

Figure 21. Thrie Beam Transition to Wisconsin Type M Tubular Steel Bridge Rail [15]

Figure 22. Tapered Tubular Rail Contact, Test No. 401021-3 [15]

TTI researchers also performed testing and evaluation of a New York State DOT box-beam transition to four-tube bridge rail under NCHRP Report 350 test designation no. 3-21 [15]. The top tube of the four-tube bridge rail had a top mounting height of 42 in. and was tapered downward at a 2H:1V slope to attach to the top of the third tube of the bridge rail near the end of the bridge rail prior to the box beam approach transition, as shown in Figure 23. The third tube of the bridge rail had a 32.7-in. top height. In test no. 401021-7, a 2000P vehicle impacted the transition upstream from the tapered tube attachment at a speed of 62.1 mph and an angle of 24.4 degrees.

Figure 23. Box Beam Transition to Four-Tube Steel Bridge Rail [15]

During the test, the pickup truck traversed the sloped bridge rail tube with both the left-front fender and hood contacting the tube, as shown in Figure 24. However, this contact did not adversely affect vehicle redirection by the transition nor pose an occupant risk hazard. The 2000P vehicle was safely redirected and test no. 401021-7 was deemed acceptable under NCHRP Report 350 TL-3.

Figure 24. Tapered Tubular Rail Contact, Test No. 401021-7 [15]

2.5 Real-World Crashes

While the safety performance of fences within the ZOI have not been clearly identified in MASH 2016 crash testing, real-world crash evidence was useful for evaluating the relative risk of these fences to occupants in impacting vehicles. Three anecdotal vehicular impact events were analyzed to understand the real-world performance of these devices.

2.5.1 Ohio Vandal Protection Fence Crash

An article published on April 5, 2018 describes an impact between a vehicle and a fence mounted on a parapet on the Valley View Bridge in Valley View, Ohio. A sedan travelling on the bridge lost control, careened across multiple lanes, and impacted another vehicle that was heading in the same direction. The second vehicle was then pushed into the bridge and fence system [16].

The vertical posts of the fence were anchored directly into the top of the parapet, and the fence structure extended 10 ft above the concrete. One horizontal stiffener was placed in the middle 5 ft above the parapet. The article stated that it is believed that if the vandal protection fence was not there, the vehicle would have most likely plummetted more than 200 ft off the bridge. The individual who impacted the barrier was taken to the hospital for minor injuries [16].

Figure 25. Valley View Vandal Protection Fence Crash [16]

2.5.2 NASS Crash Data

The National Highway Transportation Traffic Safety Administration (NHTSA) compiles information regarding vehicular crashes within the United States [17]. This resource was used to locate two real-world crashes between motor vehicles and parapet-mounted containment fences.

One such impact event occurred in April 2014 between a sedan and a parapet-mounted fence located in the median. The vehicle was travelling approximately 59.5 mph at an angle of 15 degrees when it departed the travelled way and impacted the parapet and fence combination, as shown in Figure 26. The vehicle careened across the road and impacted a traffic barrier on the other side. During this event, the vehicle did not extend over the top of the parapet and interact with the fence, which resulted in no vehicle snag. Overall, the parapet damage was minimal, but the vehicle damage was extensive, as shown in Figure 27, and concentrated on the front passenger side of the vehicle. It is believed that damage was related to the second impact event [18].

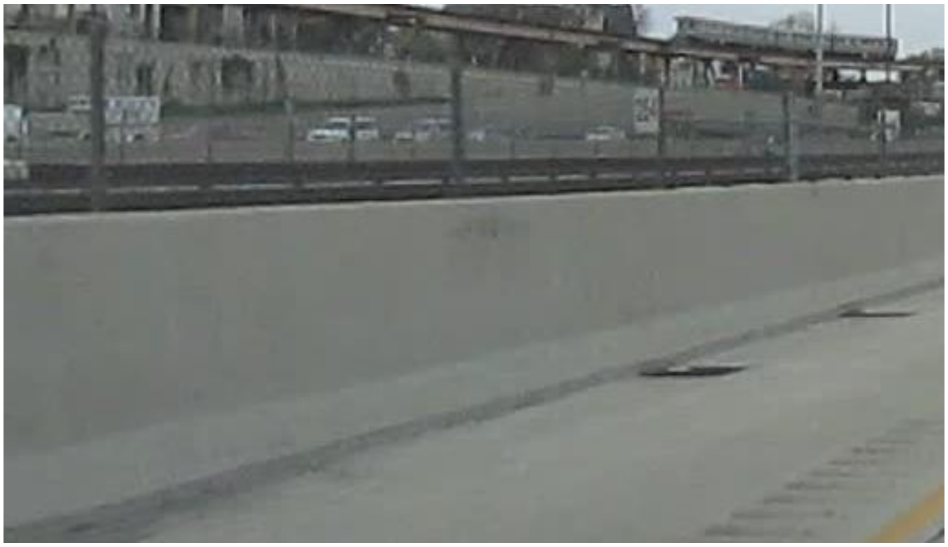

Figure 26. View of Barrier at Point of Impact [18]

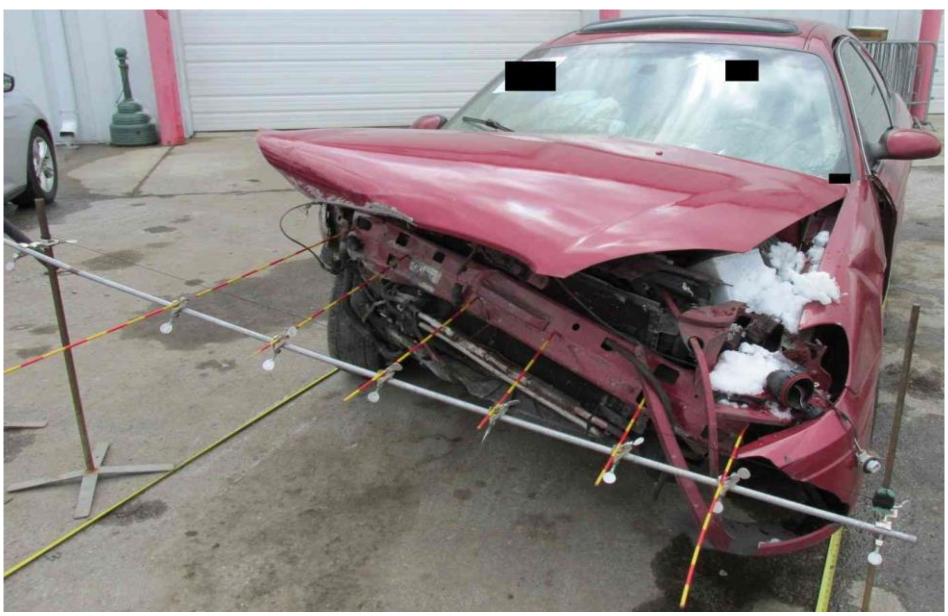

Figure 27. Vehicle Damage [18]

Another event consisted of a crash with a sequence of hazards, where the most severe impact was with a concrete barrier. Vehicle speed at the point of barrier impact was estimated to be 41 mph, and the impact angle was 6 degrees with respect to the roadway. No snagging or intrusion occurred into the fence during impact. The vehicle and system damage were minimal, but concrete spalling occurred near one vertical post anchor. The impact location and vehicle damage are shown in Figures 28 and 29 [19].

Figure 28. Point of Impact [19]

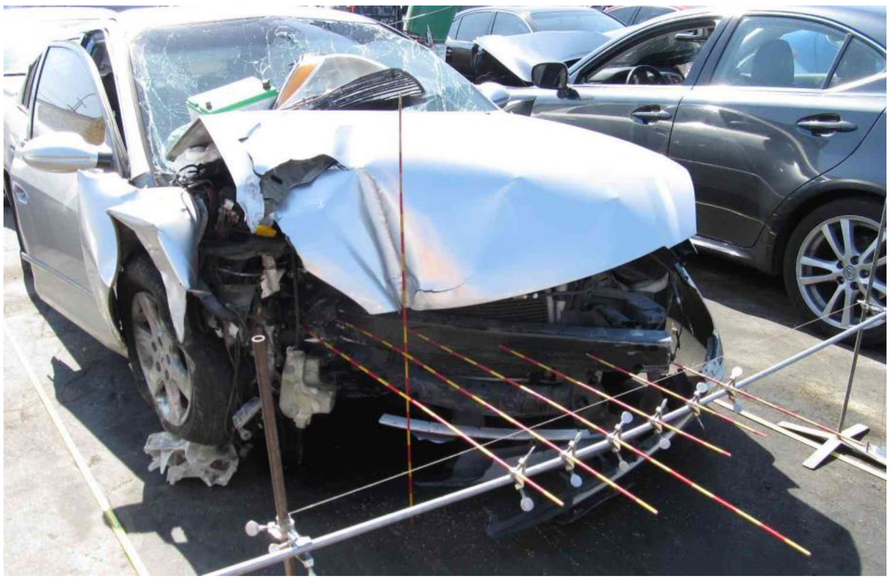

Figure 29. Vehicle Damage [19]

2.6 State Designs

State Departments of Transportation (DOTs) are responsible for maintaining design standards for roadside structures, including barriers and barrier attachments. A literature search was conducted to identify standard debris fence designs, also known as vandal protection fences, bridge safety fences, and railroad approach fences. Key design features that were reviewed consisted of the type of post used, post mounting location on the barrier, and fence attachment methods. A total of 15 State DOT design fences were reviewed, some of which had multiple fence designs. Results of this review are summarized in Table 2 and Table 3. Most of the designs included a fence with vertical posts which were either mounted to the top or back side of the barrier which combined comprised of 61% of fence systems reviewed. 28% of fence systems included fence posts which were curved and were either mounted the barrier top surface or the barrier back face. There were also some designs which included top mounted fences that used vertical post which were bent at an angle. A more detailed review of each debris fence option is shown in the following sections. State designs were then ranked based on criteria established from the fence design objectives, discussed in detailed in Chapter 4.

Table 2. State Fence Design Summary

State Fence Desgins				
Vertical Top Mounted	Vertical Back Mounted	Curved Top Mounted	Curved Back Mounted	Angled Top Mounted
33%	28%	17%	11%	11%

Table 3. State Parapet Attachment Method Summary

State Parapet Attachment Methods		
Base Plate	Clamps	Concrete Embedment
50%	39%	11%

2.6.1 Iowa

The Iowa DOT sponsored this research study to evaluate and optimize the design of a debris fence installed over railroad tracks which could potentially be full-scale crash tested according to MASH TL-3 impact conditions in a secondary phase of this project. Researchers reviewed and documented features of existing Iowa DOT standard plans and compared design features with other state DOTs.

Iowa DOT standard plans call for the use of a chain-link fence in conjunction with a pedestrian rail for debris and pedestrian containment purposes. The design consists of a 6-ft tall chain-link fence containing a 2-in. diamond mesh, made out of no. 9 wire and has knuckled selvages at the top and bottom of the fence. The vertical posts used in this design are 6 ft – ¾ in. tall, Extra Strong pipes with 2½ in. nominal diameters. Additionally, 2-in. nominal diameter pipes were utilized on the bottom of the fence, and 1¼-in. nominal diameter pipes were used along the top of the fence. The wire mesh was connected to the vertical posts by using wire ties or clips spaced every 12 in., and the mesh was connected to the horizontal members using wire ties or clips spaced at 24 in. intervals [20].

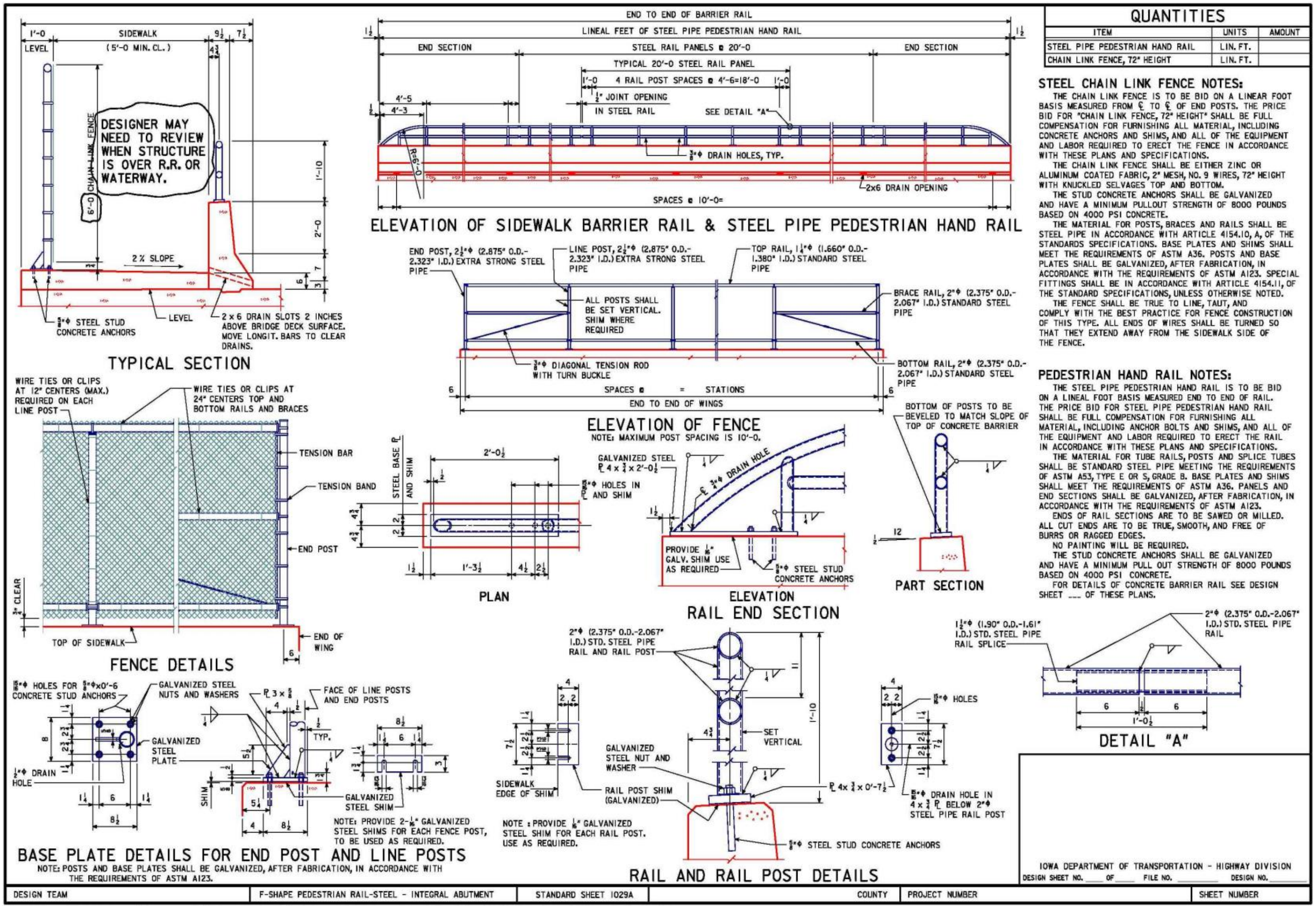

Figure 30. Iowa Protection Fence Design [20]

2.6.2 California

The California Department of Transportation (Caltrans) standard plans specify the combination of a vertical-shaped, concrete parapet and a top-mounted, vertical fence to safely keep pedestrian debris away from railroad tracks. The concrete railing presented in Caltrans plans has a height of 40 in., and the debris containment fence is mounted 6 in. behind the front face of the parapet. This design is shown in Figure 31 [21].

The debris fence is attached to the top of parapet by anchoring the vertical posts 8 in. into the concrete barrier using a mortar backfill. The rectangular vertical posts extended a total of 6 ft – 1½ in. above the concrete parapet and were placed along the barrier every 5 to 10 ft. The chain-link fabric specified by Caltrans plans is 6 ft tall and is made of up a 1-in. diamond-shaped mesh and has a knuckled selvage on the top and bottom of the wire mesh. This mesh is connected to the fence structure by clamping the fence horizontally along the top of the system and vertically at the beginning and end of the parapet. The mesh is additionally connected to the vertical members with ¼-in. self-tapping screws spaced at 1 ft – 2 in. maximum increments. This design is shown in Figure 32 [21].

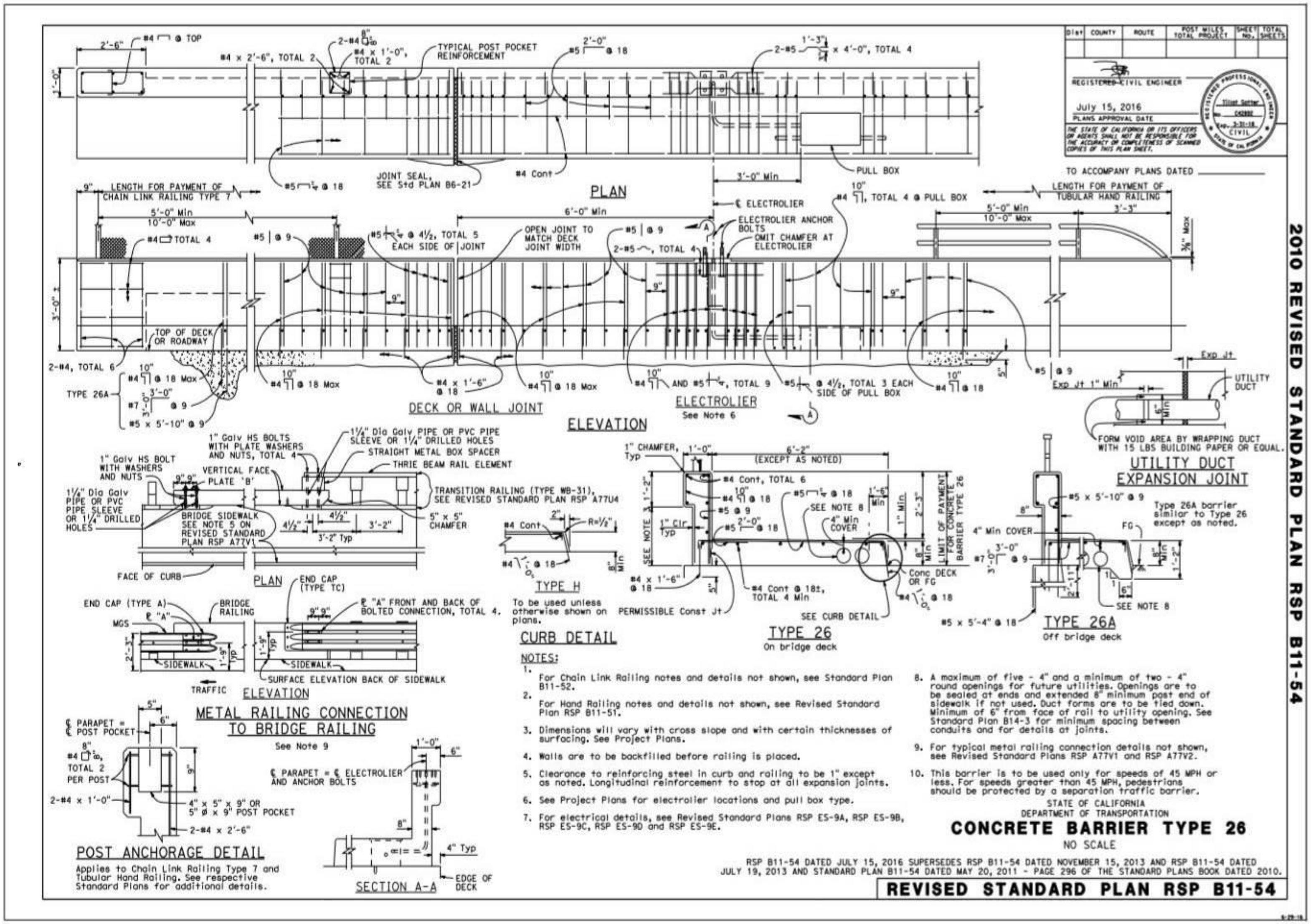

Figure 31. California Concrete Barrier [21]

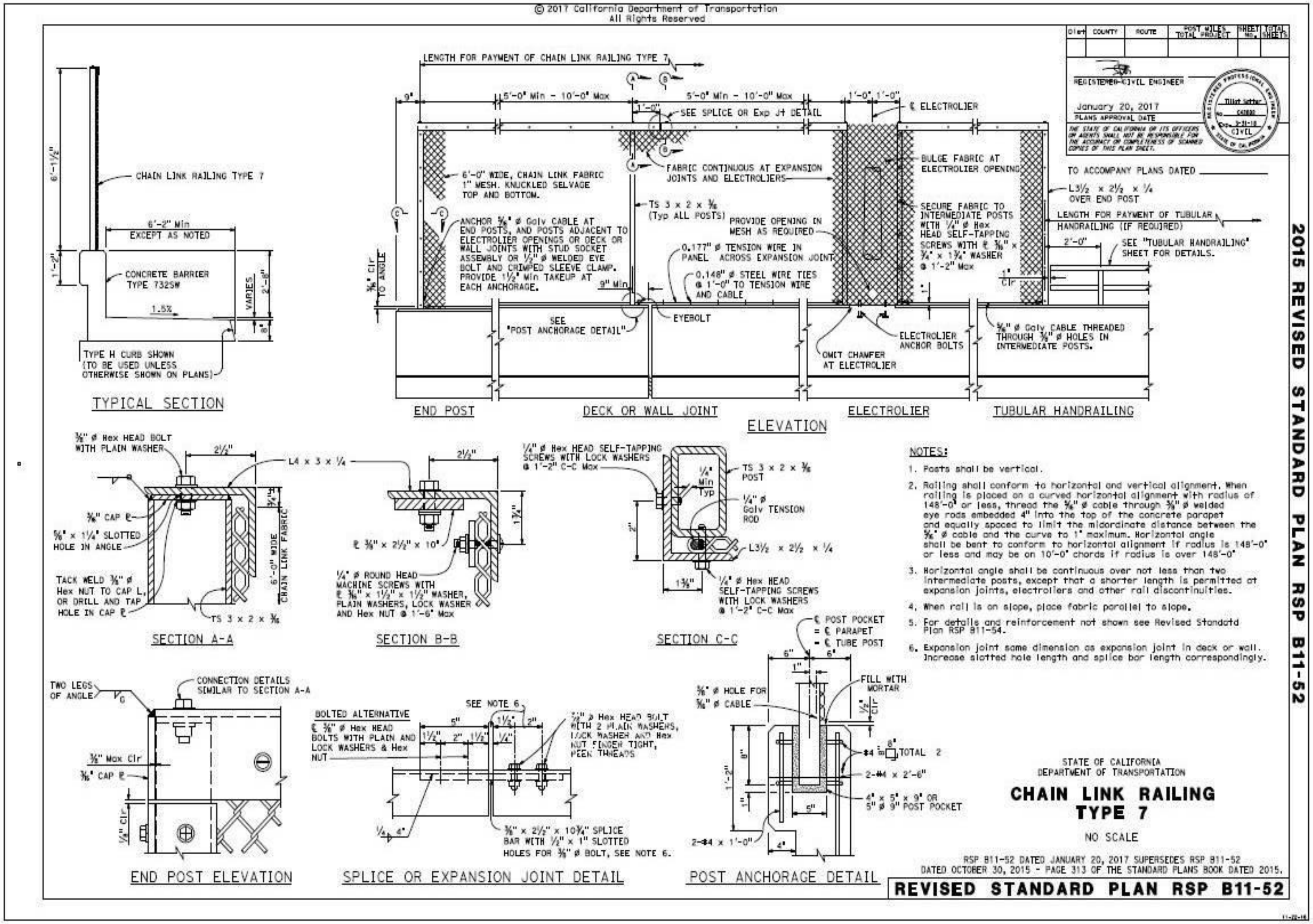

Figure 32. California Chain Link Railing [21]

2.6.3 Delaware

Delaware DOT standard plans specify two different designs for debris fences. The first design is a vertical chain-link fence mounted on top of a parapet with a baseplate and four ⅝-in. diameter threaded anchor studs. The chain-link fabric of this system measures 5 ft in height and contains a 1-in. diamond mesh made out of #9-gauge wire. The system uses 2½-in. nominal diameter pipes spaced in 10 ft increments as vertical support posts and two 1¼-in. nominal diameter pipes as longitudinal stiffeners. Single #9 gauge or double #13 gauge ties are used to connect the wire mesh to the vertical and horizontal members. The fence system is shown in Figure 33, and mounting and connection details are shown in Figure 34 [22].

Delaware utilizes a different design when when a sidewalk is located adjacent to the barrier. This design consists of a curved chain-link fence structure mounted on the top of a concrete rail, with a wire mesh height of 7 ft. The base plate configuration is the same as the first design. The sizing and spacing of the vertical members, horizontal stiffeners, and the connection of the wire mesh to the members and stiffeners are the same for both Delaware designs, but a total of four horizontal stiffeners are used in this design. The mounting and connection details are shown in Figure 34, and the fence system is shown in Figure 35 [22].

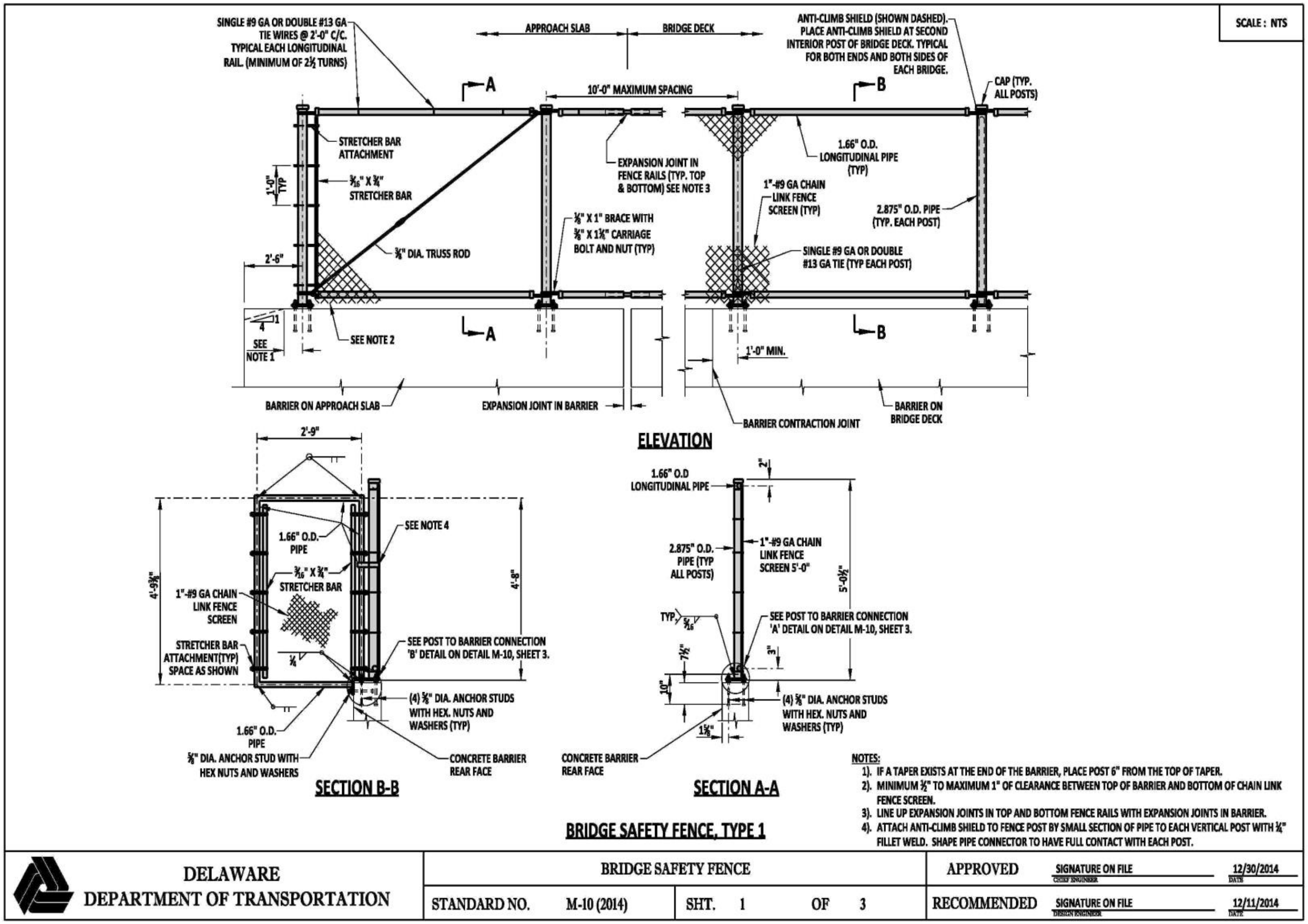

Figure 33. Delaware Bridge Safety Fence, Type 1 [22]

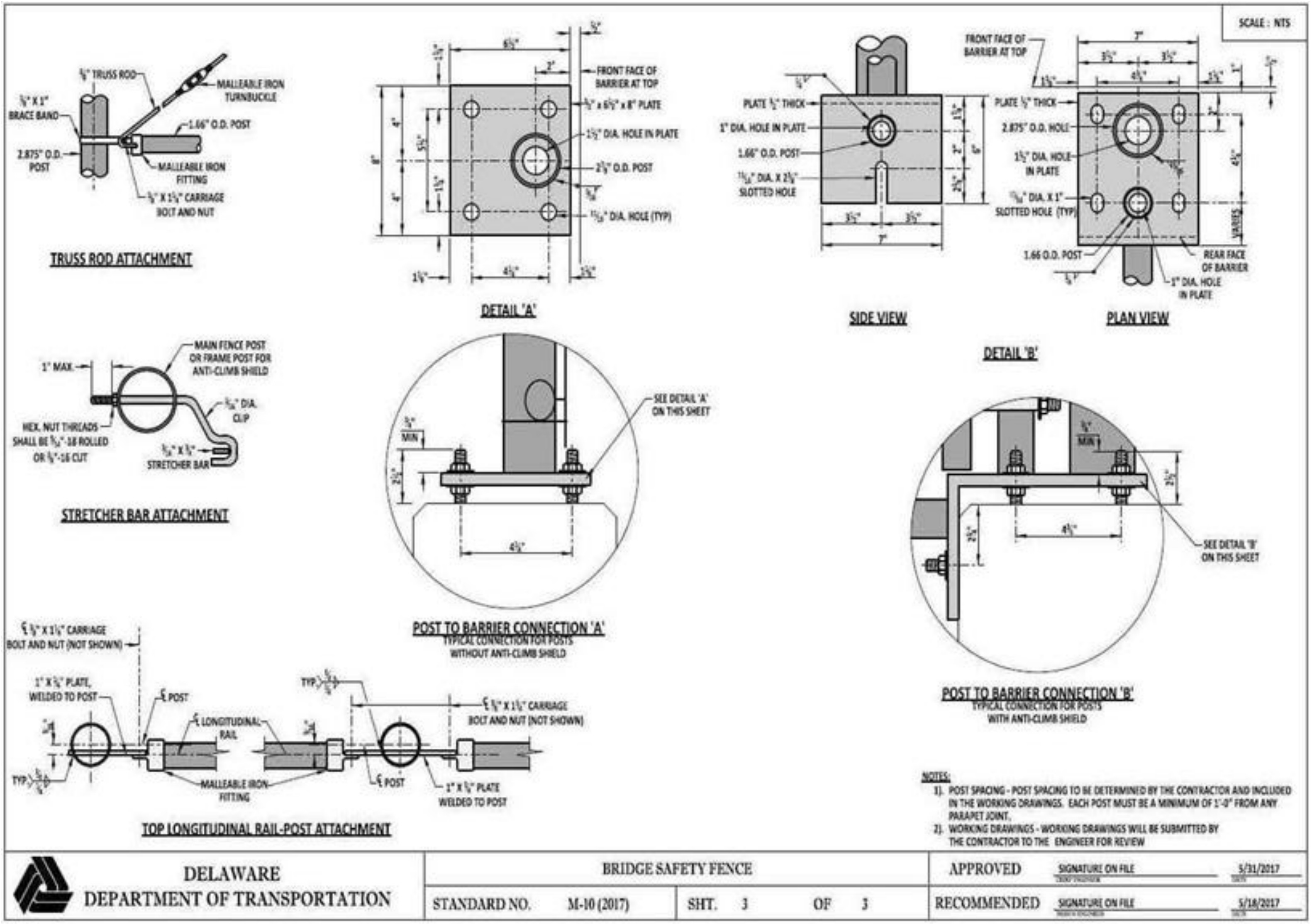

Figure 34. Delaware Bridge Safety Fence, Connection Details [22]

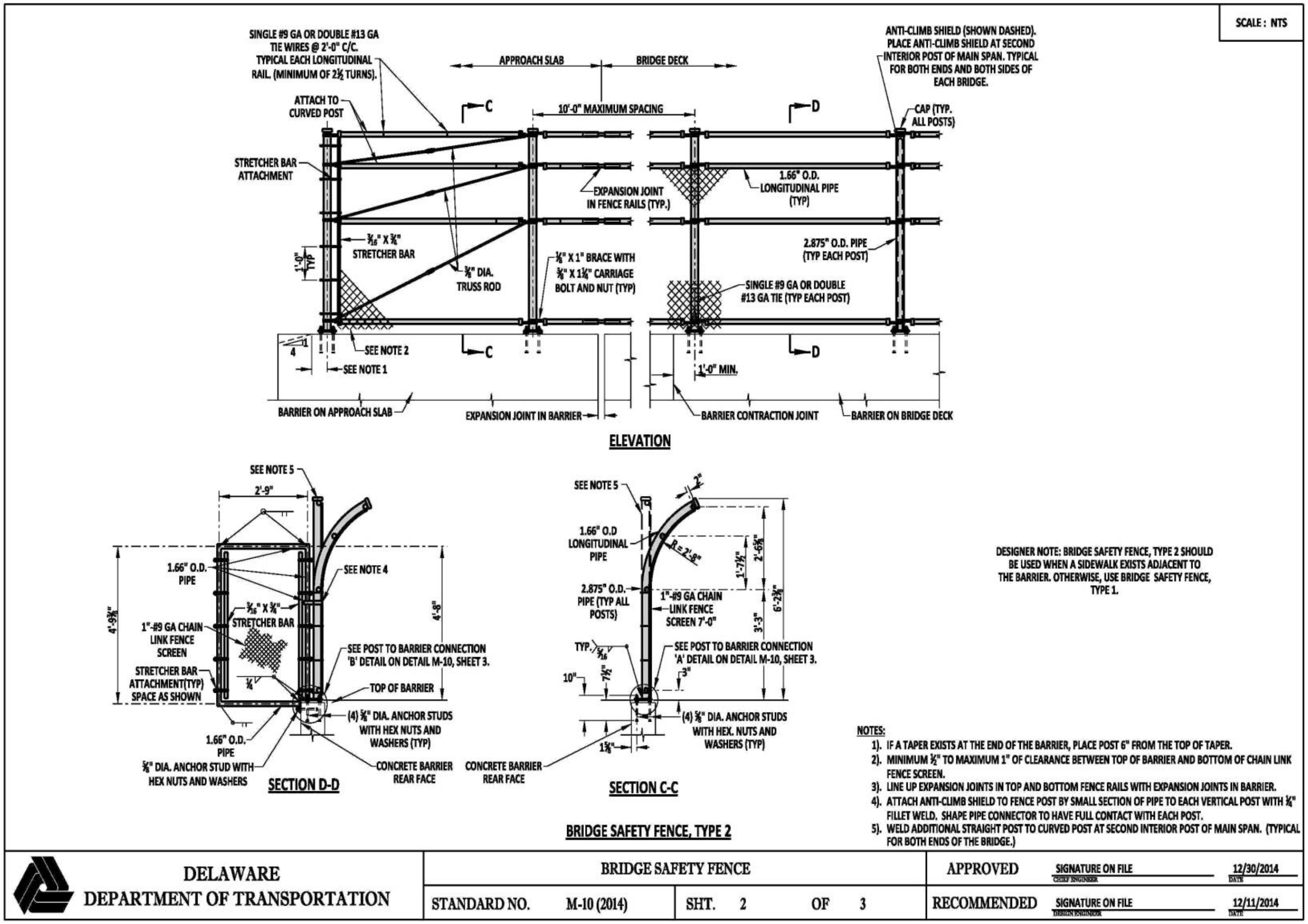

Figure 35. Delaware Bridge Safety Fence, Type 2 [22]

2.6.4 Florida

The Florida DOT uses a curved fence mounted on the back of a concrete parapet to reduce debris on and around railroad tracks. Florida DOT's design standards show that this fence can be used in conjunction with a 36-in. tall, single-slope concrete parapet, but the size and type of barrier can vary [23].

Vertical posts consist of galvanized, schedule 40 pipes, with a 3 in. nominal diameter. There are no structurally-stiff horizontal members, and lateral stiffness is obtained by using four tension wires, three near the top and one additional tension wire located near the bottom portion of the fence. Each vertical post is attached to the parapet with two pipe clamps, which are fastened to the concrete parapet with ⅝-in. adhesive anchors. The chain-link fabric is composed of a 2-in. diamond mesh that is twisted at the top and has a knuckled selvage at the bottom of the fence. The mesh is connected to the posts with wire ties and to tension wires with hog rings. System drawings and connection details are shown in Figures 36 through 38 [23].

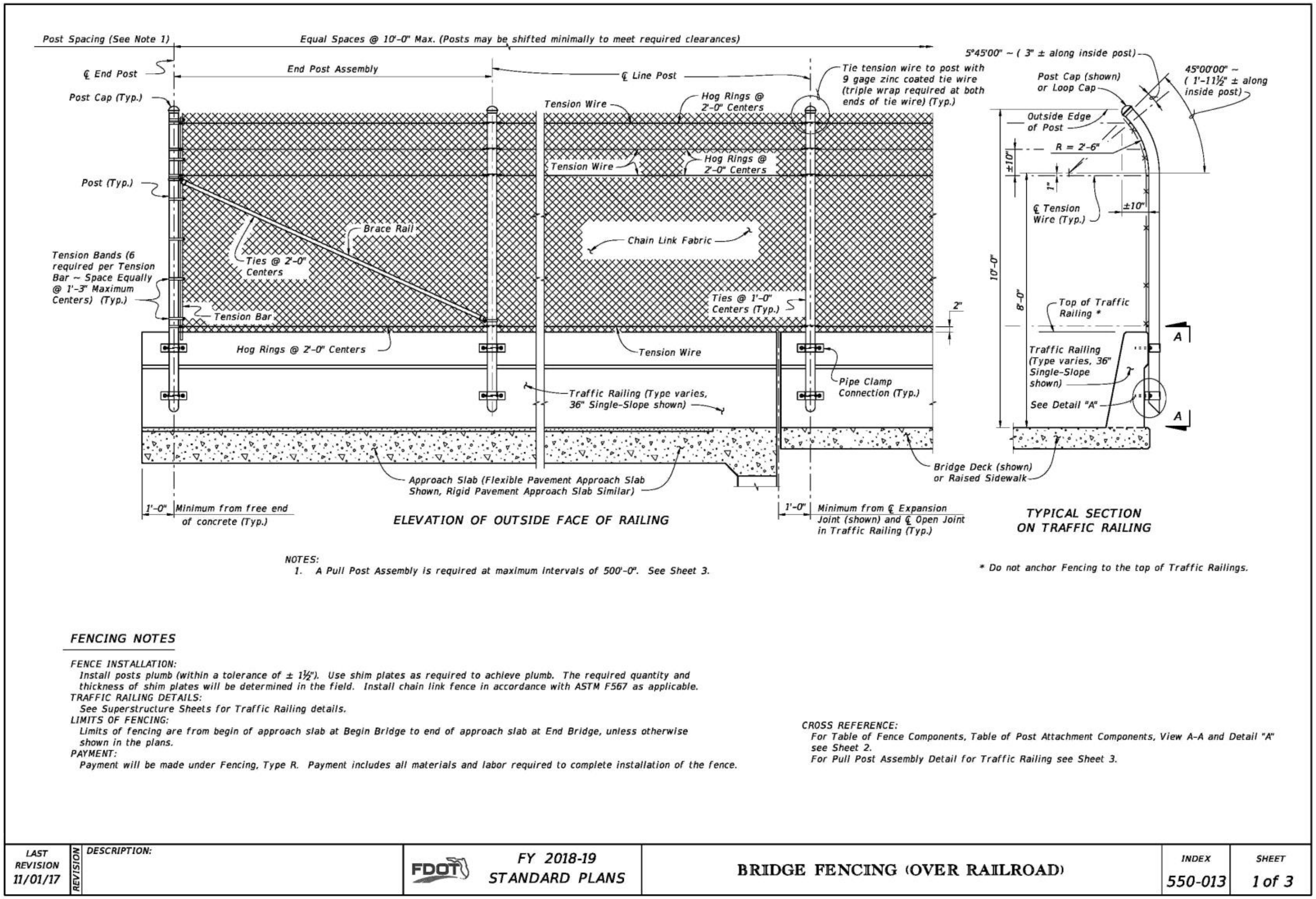

Figure 36. Florida Debris Fence Over Railroad, Sheet 1 [23]

TABLE OF CHAIN LINK FENCE COMPONENTS

COMPONENT	ASTM DESIGNATION	COMPONENT INFORMATION
Posts	F1083	Galvanized Steel Pipe - 3" NPS, Schedule 40 Regular Grade
Chain Link Fabric (2" mesh with twisted top and knuckled bottom selvage)	A392	Zinc Coated Steel - 9 gage (coated wire diameter), Class 2 Coating
	A491	Aluminum Coated Steel - 9 gage (coated wire diameter)
	F668	Polyvinyl Chloride (PVC) Coated Steel - 9 gage Class 2b
Tie Wires	F626	Zinc Coated Steel Wire - 9 gage
Brace Bands	F626	12 Gage (Min. thickness) x ¾" (Min. width) Steel Bands (Beveled or Heavy)
Tension Bars	F626	3⁄16" (Min. thickness) x ¾" (Min. width) x 6'-10" (Min. height) Steel Bars
Tension Bands	F626	14 Gage (Min. thickness) x ¾" (Min. width) Steel Bands
Miscellaneous Fence Components	F626	Zinc Coated Steel ~ (includes post or loop caps, horizontal and brace rail ends, combination rail ends, boulevard clamps and all other miscellaneous fittings & hardware)
Tension Wire	A824 & A817	Type II (Zinc Coated Steel Wire) - 7 gage, Class 4 Coating
		Type I (Aluminum Coated Steel Wire) - 7 gage
Hog Rings	F626	Zinc Coated Steel Wire - 12 gage
Brace Rails	F1083	Galvanized Steel Pipe - 1¼" NPS, Schedule 40 Regular Grade

TABLE OF POST ATTACHMENT COMPONENTS

COMPONENT		ASTM DESIGNATION	COMPONENT INFORMATION
Pipe Clamps		A36 or A709 Grade 36	¼" Steel ℞
Base Plates		A36 or A709 Grade 36	¾" Steel ℞
Shim Plates		A36 or A709 Grade 36 or B209 Alloy 6061-T6 or B221 Alloy 6063-T5	Plate thicknesses as required; Holes in shim plates will be ¾" Ø
Spacers		-	Plate thickness varies based on traffic railing type (See Detail "A")
Pipe Clamp Connection	Adhesive Anchor Rods	F1554 Grade 36	Fully threaded Headless Anchor Rods ~ ⅝" Ø x 6" (no spacer) or ⅝" Ø x (6" + spacer thickness)
	C-I-P Anchor Rods	F1554 Grade 36	Hex Head Anchor Rods ~ ⅝" Ø x 6" (no spacer) or ⅝" Ø x (6" + spacer thickness)
Bolts		A307	⅝" Ø x 4¾" Hex Head Bolts for Pipe Clamp Connections to Posts
Nuts		A563	Hex Nuts for Pipe Clamp Connections
Washers		F436	Flat Washers for Pipe Clamp Connections
Bearing Pads (Plain Neoprene)		-	In accordance with Specification Section 932 for Ancillary Structures

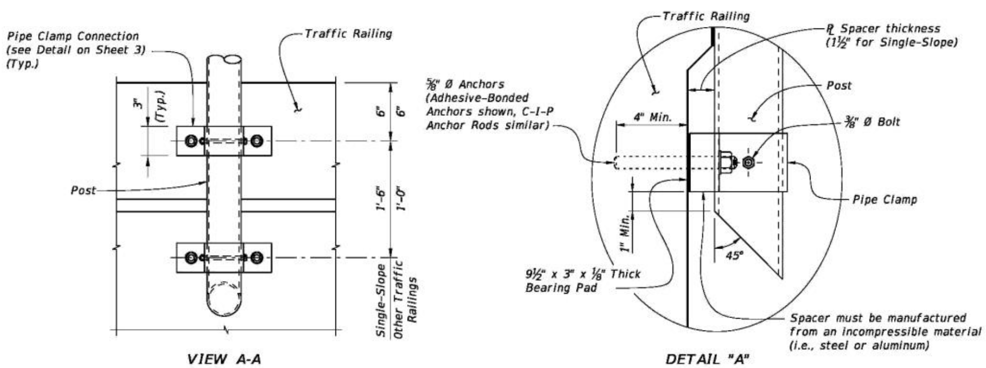

POST ATTACHMENT NOTES

ANCHOR RODS, NUTS AND WASHERS:
After the nuts have been tightened, distort the Anchor Rod threads to prevent removal of the nuts. Coat distorted threads and exposed trimmed ends of anchors with a galvanizing compound in accordance with Specification Section 562.

COATINGS:
Hot-dip galvanize all Nuts, Washers, Bolts, C-I-P Anchor Rods, Adhesive Anchors and Fence Framework (Posts, Internal Sleeves, Shim Plates, Base Plates, Pipe Clamps and Spacers) in accordance with Specification Section 962. Hot-dip galvanize Fence Framework after fabrication.

ADHESIVE-BONDED ANCHORS AND DOWELS:
Adhesive Bonding Material Systems for Anchors and Dowels will comply with Specification Section 937 and be installed in accordance with Specification Section 416. Cutting of reinforcing steel is permitted for drilled hole installation.

WELDING:
All welding will be in accordance with the American Welding Society Structural Welding Code (Steel) ANSI/AWS D1.1 (current edition). Weld metal will be E60XX or E70XX. Nondestructive testing of welds is not required.

CROSS REFERENCE:
For location of View A-A and Detail "A" see Sheet 1.

LAST REVISION	REVISION	DESCRIPTION:			INDEX	SHEET
11/01/17			FDOT FY 2018-19 STANDARD PLANS	BRIDGE FENCING (OVER RAILROAD)	550-013	2 of 3

Figure 37. Florida Debris Fence Over Railroad, Sheet 2 [23]

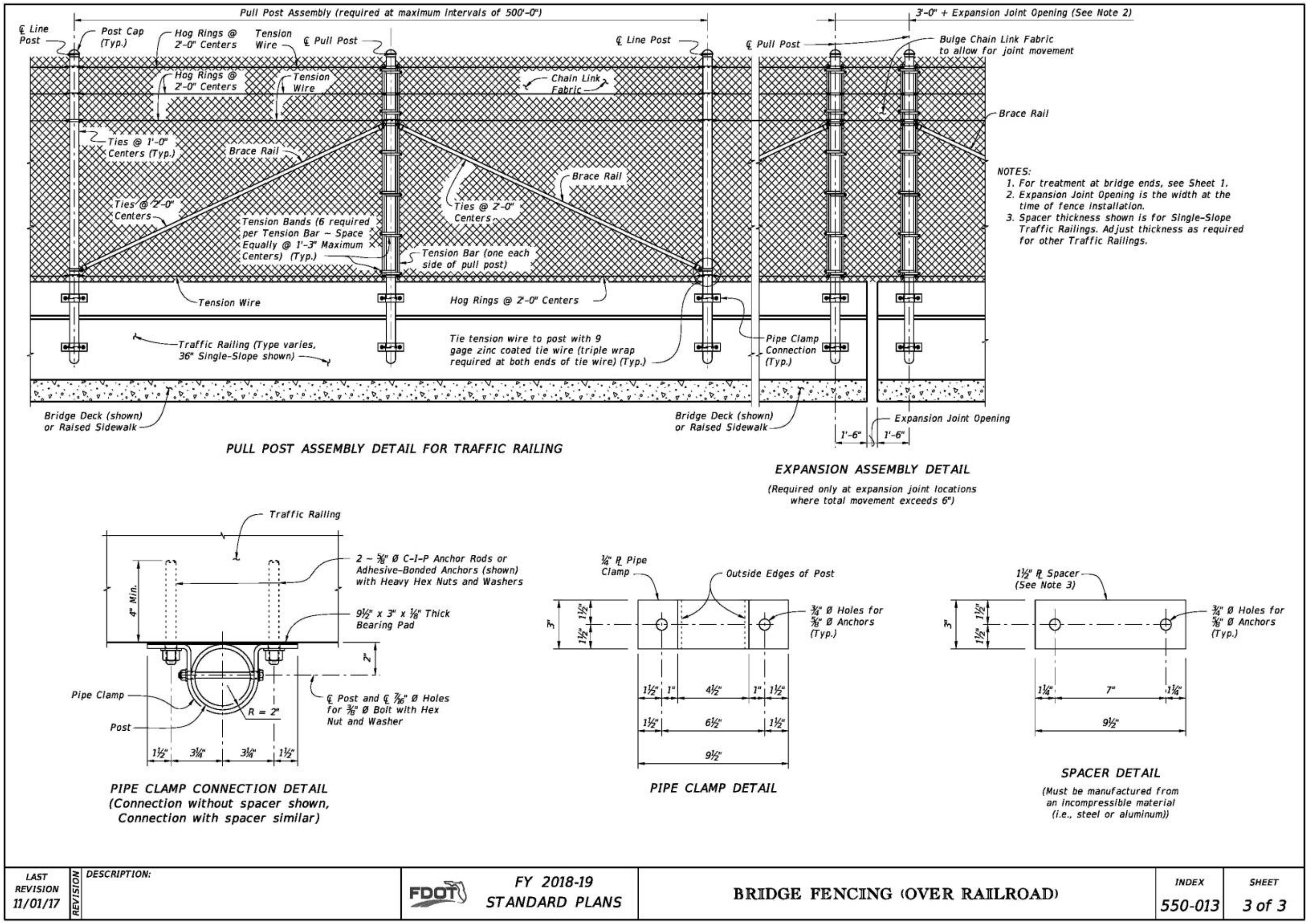

Figure 38. Florida Debris Fence Over Railroad, Sheet 3 [23]

2.6.5 Idaho

The Idaho DOT design for pedestrian protection near the travelled way consists of posts embedded into the concrete of a 27-in. tall vertical barrier rail system which support a chain link debris fence and are placed along the centerline of a 9-in. wide barrier [24].

The combination pedestrian fence system and parapet measure have a total height of 10 ft-1 in. in with respect to the road surface. The vertical posts consist of hollow steel tubes measuring 4 in. x 2 in. x $\frac{3}{16}$ in., which are spaced between 5 ft and 6 ft – 8 in. apart. Fence posts are made from welded tubes to form a 41-degree angle bend. The lower portion of the posts are 5 ft – 7 in. tall, and the upper portion of the tubes are 3 ft long. The system uses five horizontal stiffeners comprised of 2-in. x 2-in. x $\frac{3}{16}$-in. hollow structural steel tubes. There is an additional 4-in. x 2-in. x $\frac{3}{16}$-in. horizontal member located 15 in. above the parapet, which could mitigate potential snag with vertical posts when vehicle components protrude over the top surface of the barrier. A 2-in. square mesh, welded wire fabric is attached to posts and horizontal stiffeners using $\frac{3}{8}$-in. diameter stainless steel threaded studs. Details of this design are shown in Figure 39 [24].

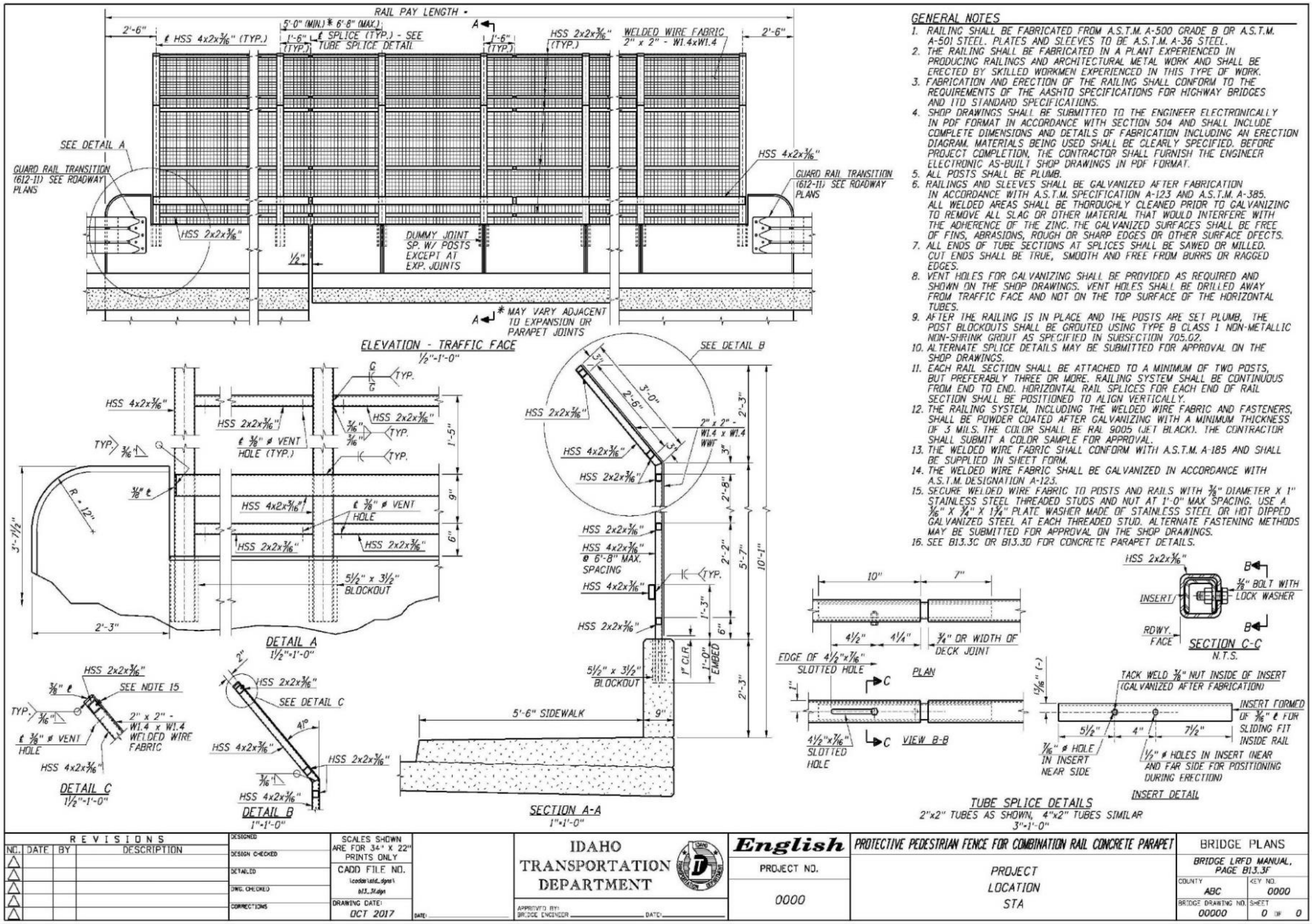

Figure 39. Idaho Protective Fence for Combination Rail and Parapet [24]

2.6.6 Indiana

Indiana DOT standard plans designate a vertical pedestrian fence mounted on top of a Type FT or FC safety shape concrete parapet. A 5-ft tall fence is installed on Type FT bridge railings whereas a 6-ft fence is installed on Type FC bridge railings [25]. This difference in fence installation height is related to the 33-in. Type FC bridge rail height compared to the 45-in. height of the Type FT bridge rail [26]. The fence structure uses 2½-in. nominal diameter steel pipes as vertical posts, which are spaced 10 ft on center. These posts are connected to 1¼-in. nominal diameter upper and lower horizontal stiffeners. Wire ties spaced at 15 in. maximum intervals are used to connect the chain-link fabric to the steel frame. The vertical posts are then secured to the concrete parapet through a base plate that is connected with four ⅝-in. diameter anchor bolts. CAD details are shown in Figure 40 [25].

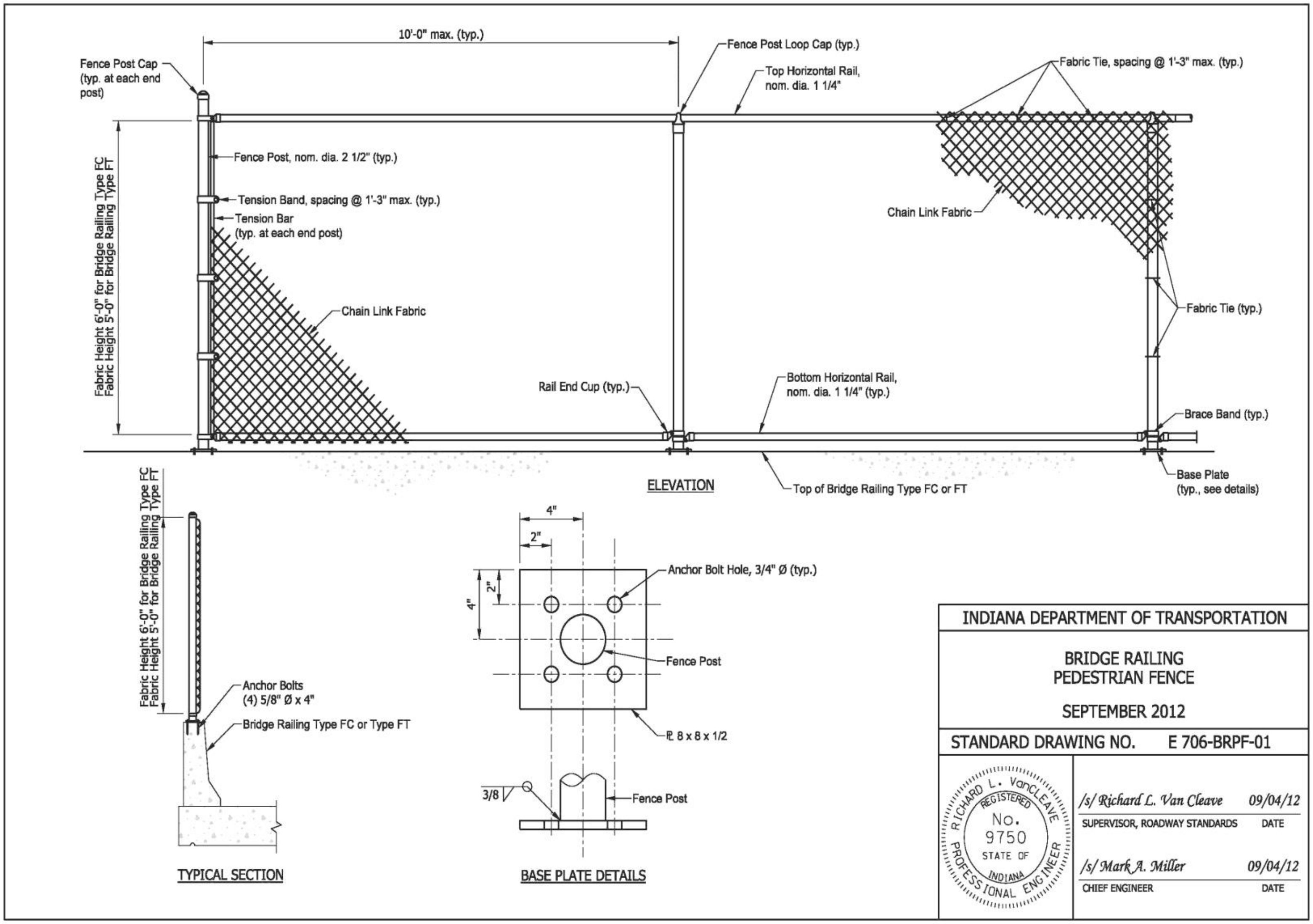

Figure 40. Indiana Bridge Railing Pedestrian Fence [25]

2.6.7 Kansas

The Kansas DOT utilizes two different fences for pedestrian and debris control over railroads, which vary based on height and concrete anchorage arrangements. Each fence configuration is mounted to the back of safety-shape concrete parapets. An 8-ft tall fence is attached to a 42-in tall barrier while a 6-ft tall fence is attached to a 36-in. tall barrier [27].

According to the Kansas DOT plans, these are railroad protective fences for Union Pacific (UP) and BNSF railroads and specifies that the 8-ft tall fence configuration is required when the shoulders of the bridge are less than 6 ft wide, and the 6-ft tall fence configuration is used when the bridge shoulders are greater than or equal to 6 ft. These configurations use 2½-in. nominal diameter Extra Strong steel pipes as vertical posts spaced 8 ft on centers. Two 1¼-in. nominal diameter Extra Strong steel pipes are used as horizontal stiffeners at the top and bottom of the fence. The vertical posts are mounted to the back of the parapet with two pipe clamps and U-bolts, and the base of each vertical member is connected to a piece of angle iron that is attached to the parapet using a ⅝-in. diameter anchor bolt. The fence is made from galvanized or PVC coated, 2-in. chain-link fabric, with knuckled selvage on both the top and bottom of the fence. This wire mesh is then connected to the fence structure with #9 gauge wire ties. The taller design is shown in Figure 41, and the shorter design is shown in Figure 42 [27].

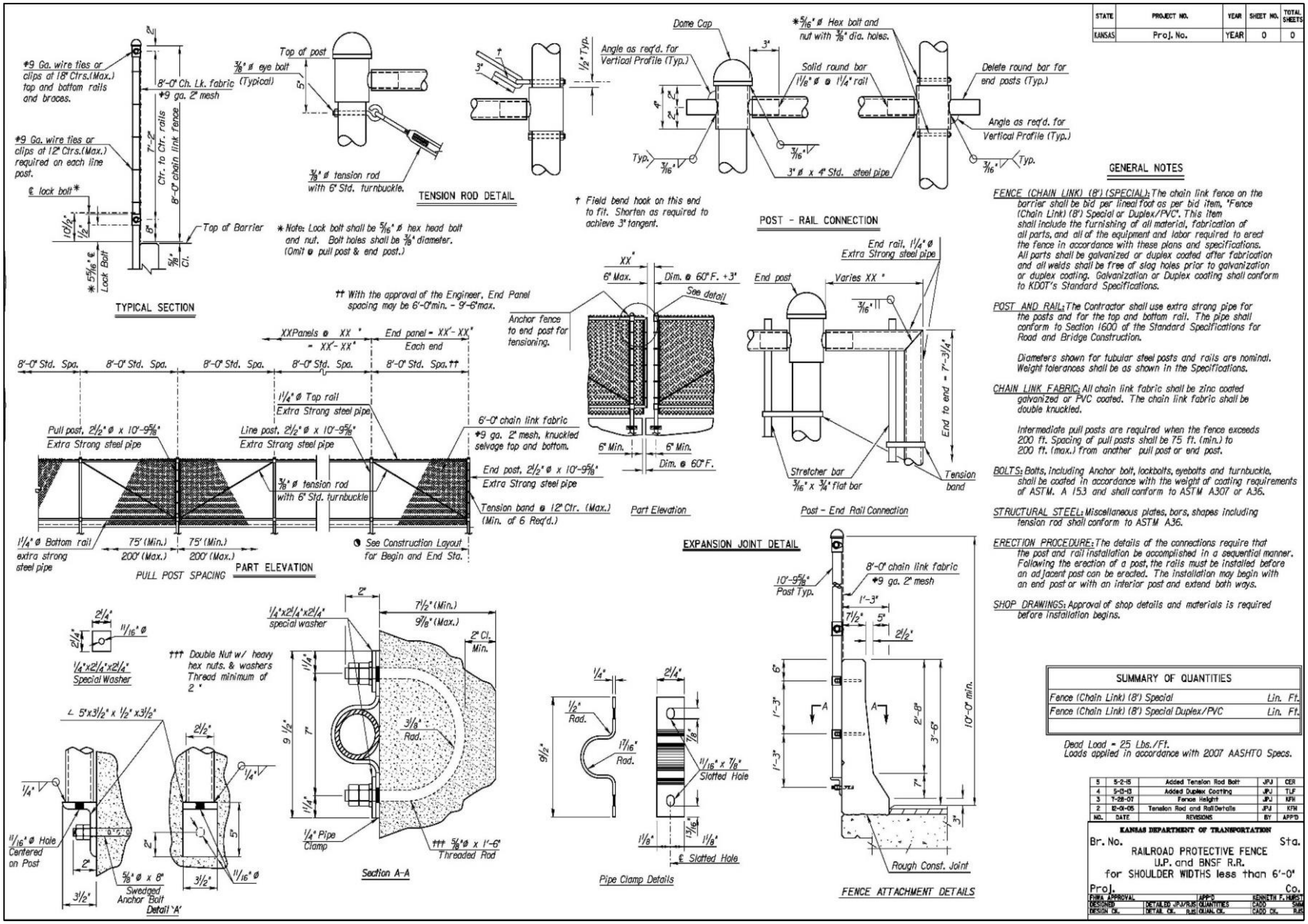

Figure 41. Kansas Railroad Protective Fence for Shoulders Less than 6 ft [27]

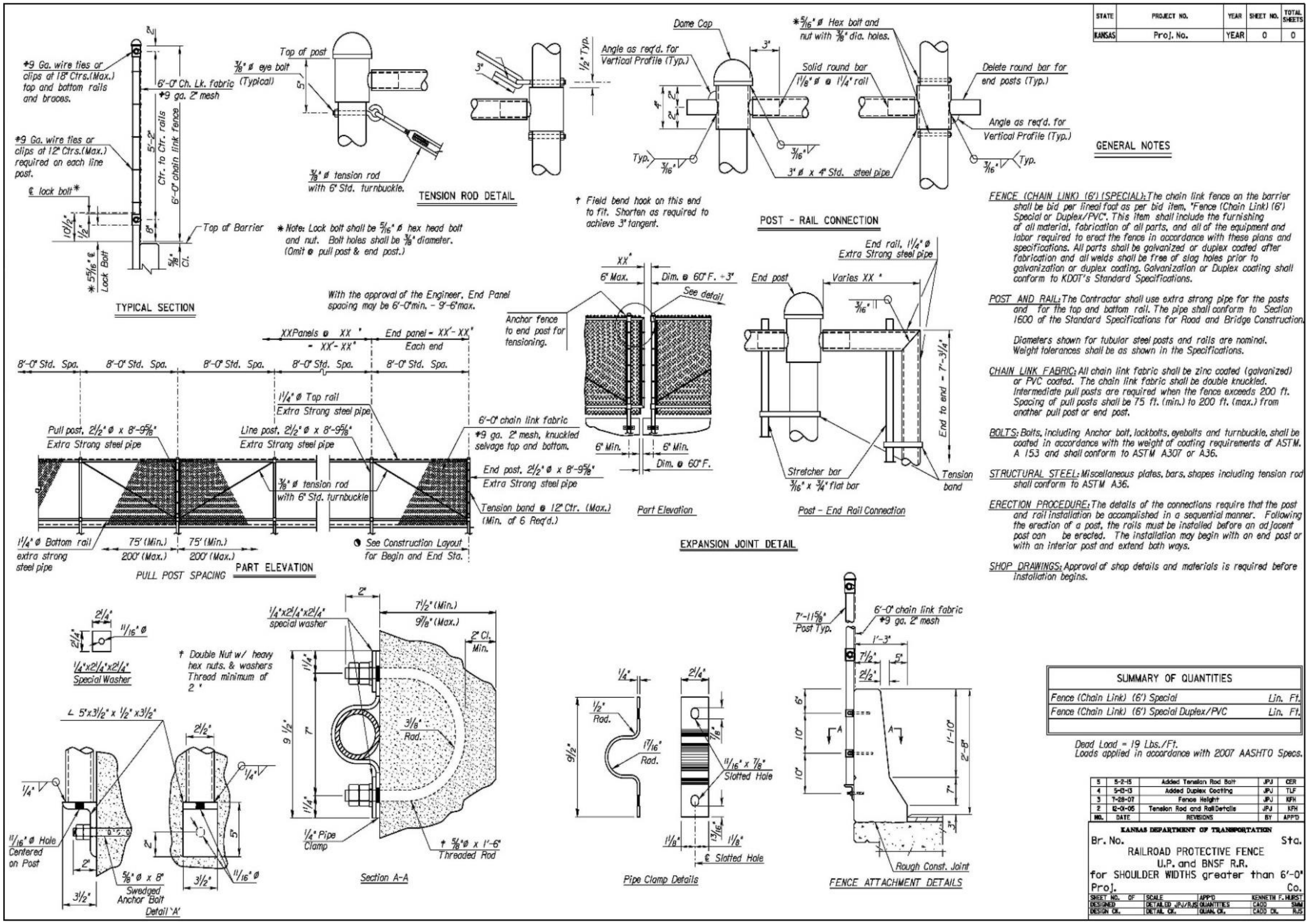

Figure 42. Kansas Railroad Protective Fence for Shoulders Greater than 6 ft [27]

2.6.8 Maryland

Maryland DOT utilizes two debris fence designs. The first system has a curve at the top of the fence and is mounted on top of a 32-in. tall vertical parapet. The other design is not curved and is vertical, flat, and mounted on top of an F shape concrete parapet [28].

The curved fence design is shown in Figures 43 and Figure 44. The round vertical posts are 2½ in. nominal diameter schedule 80 pipes, which are welded to base plates. Four ⅝-in. diameter bolts are used to attach the base plate to the top of the parapet. Four 1¼-in. nominal diameter schedule 80 pipes are used as horizontal stiffeners for the fence frame. The fence fabric is comprised of a #6 gauge mesh with a 2-in. gap opening connected to the frame with #9 gauge wire or double #13 gauge wire [28].

The vertical fence design is shown in Figures 45 and 46. Vertical posts were 2½-in. nominal diameter schedule 80 pipes welded to base plates and bolted to the top of the parapet with four ⅝-in. bolts. Two 1¼-in. nominal diameter schedule 80 pipes are used as horizontal stiffeners attached to the post with brace bands. The fence is constructed with a #6 gauge mesh and a 2-in. gap opening. The chain-link fabric is then connected to the vertical and horizontal members of the system with #9 gauge wire or double #13 gauge wire [28].

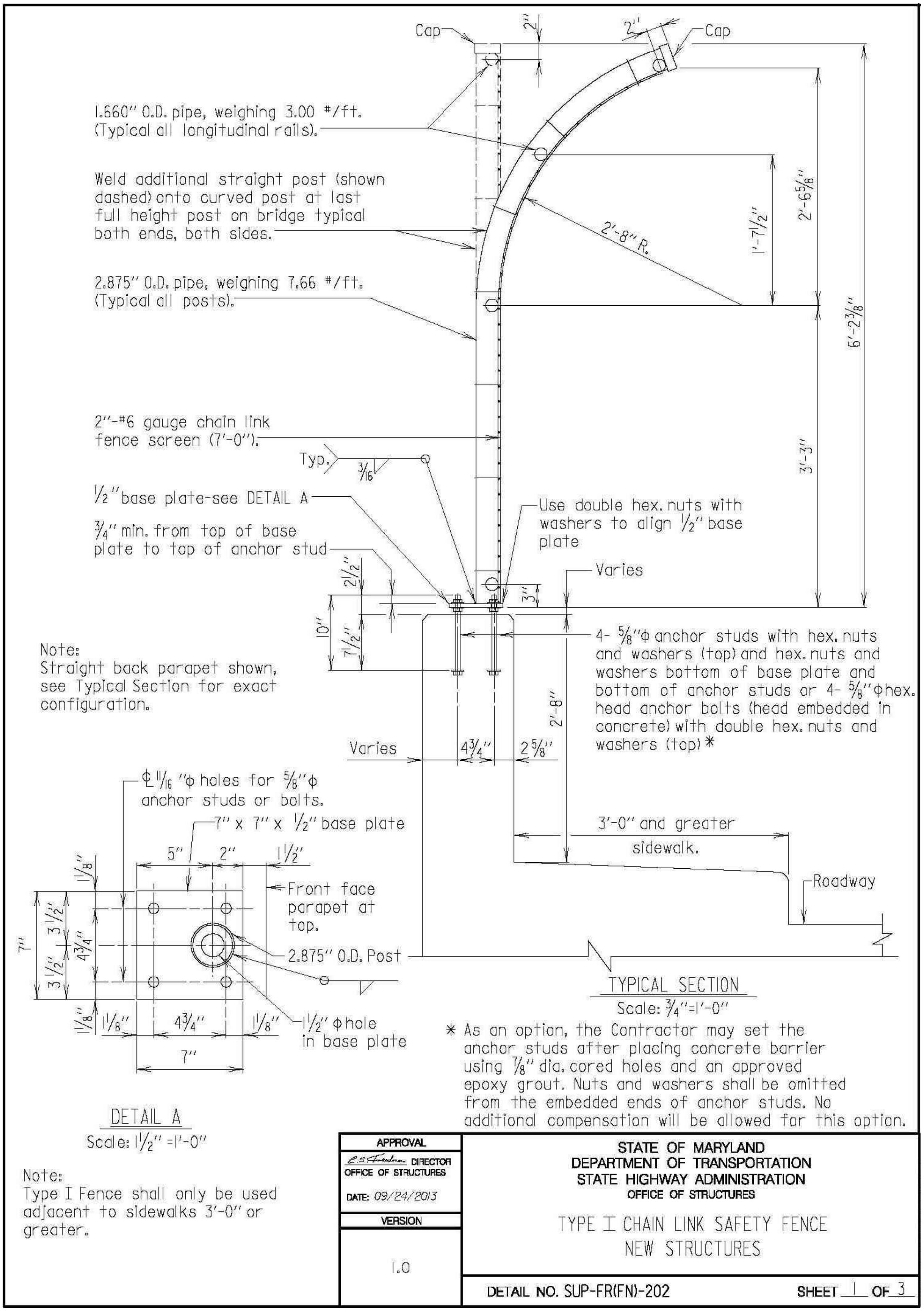

Figure 43. Maryland Type I Chain Link Safety Fence [28]

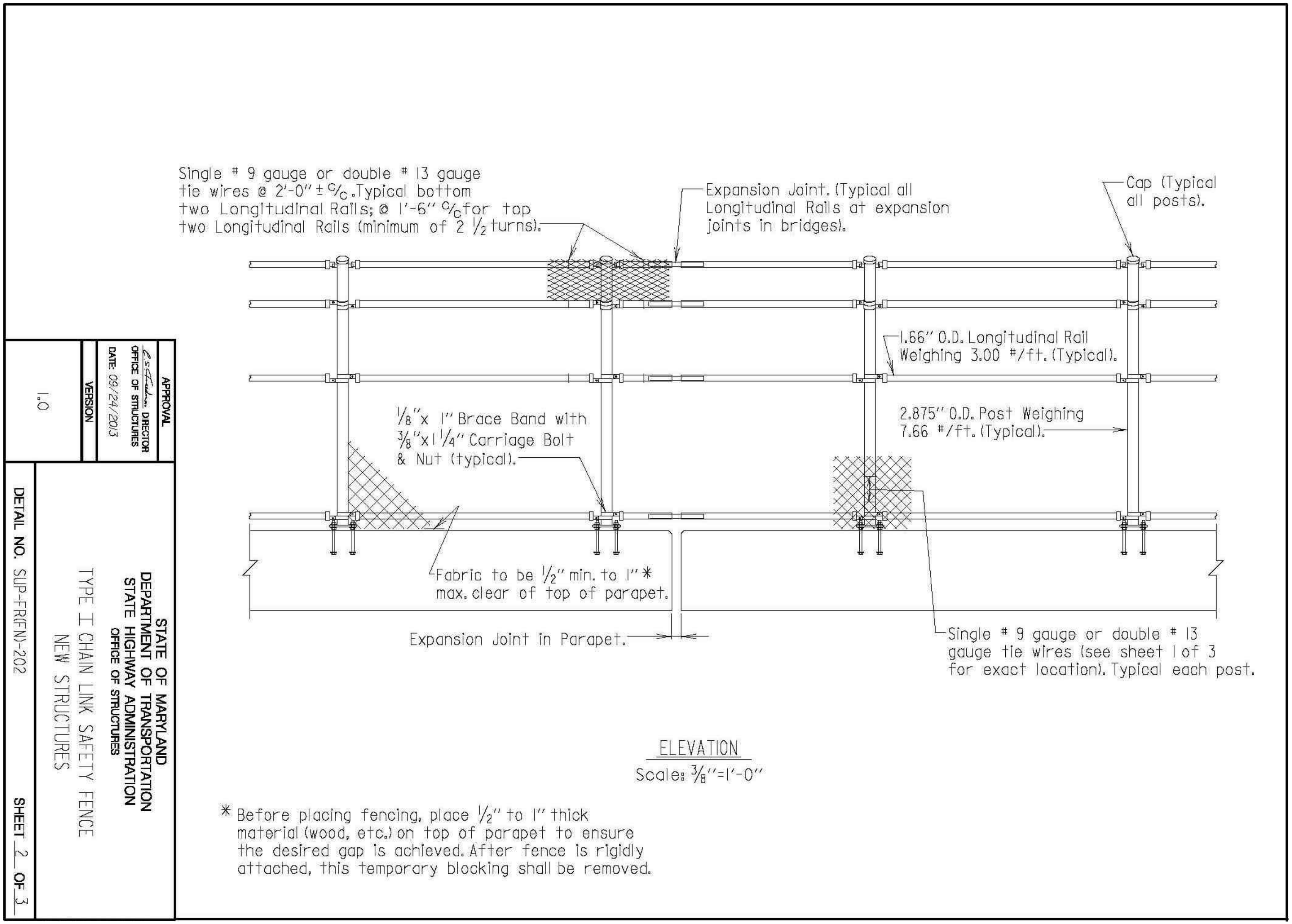

Figure 44. Maryland Type I Chain Link Safety Fence [28]

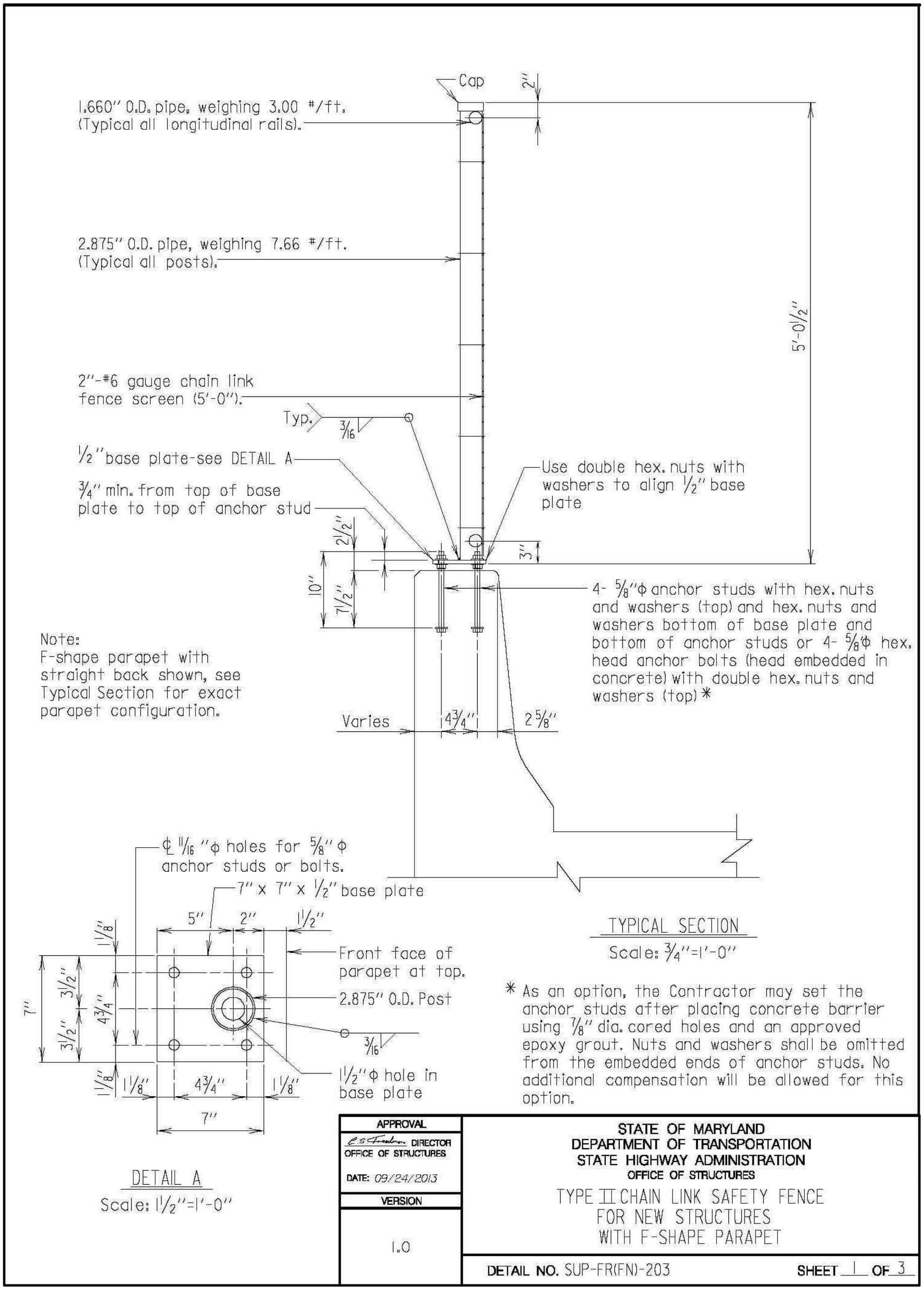

Figure 45. Maryland Type II Chain Link Safety Fence [28]

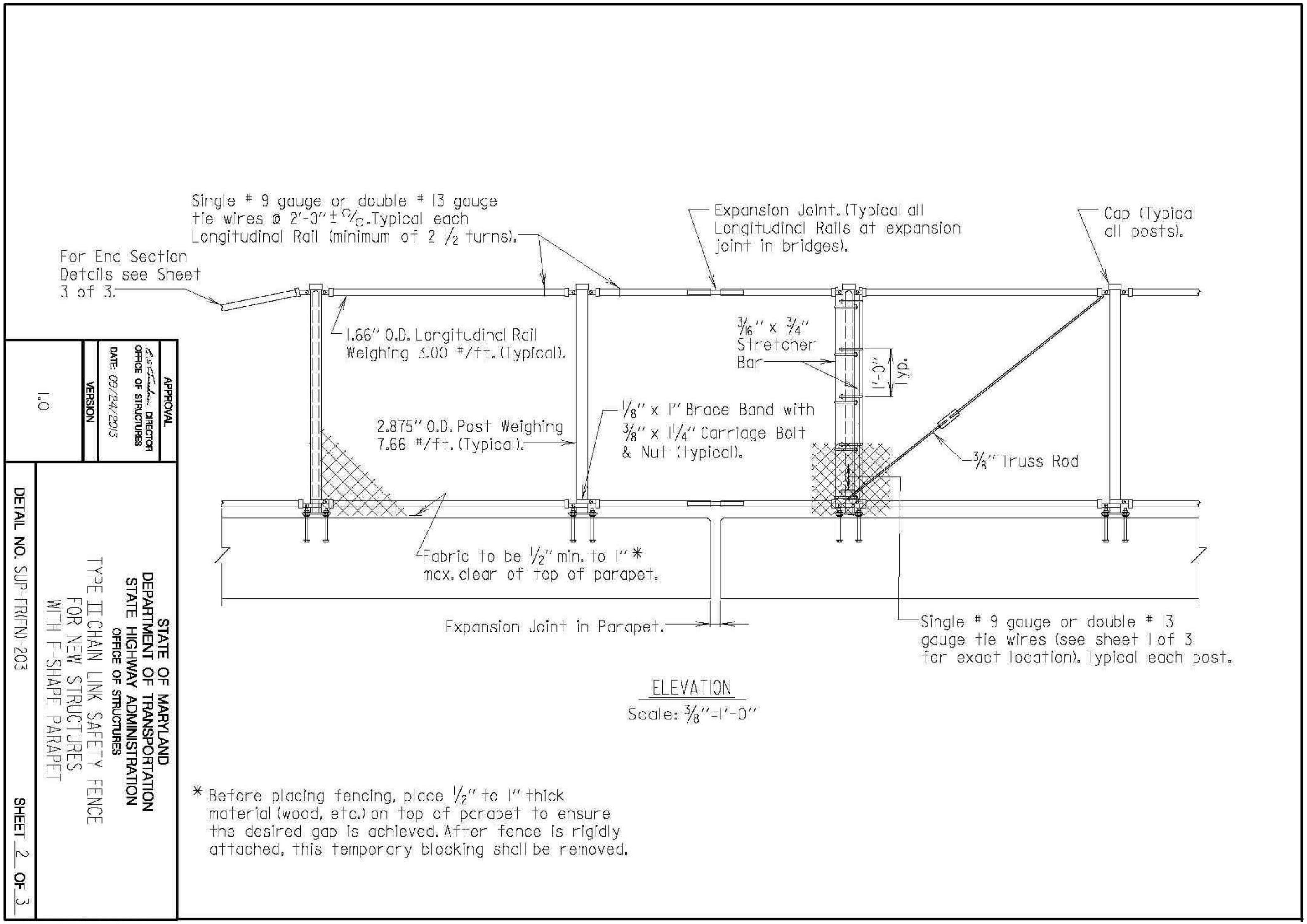

Figure 46. Maryland Type II Chain Link Safety Fence [28]

2.6.9 Minnesota

Minnesota DOT utilizes a debris fence mounted on top of a vertical concrete parapet. The concrete railing that is implemented in Minnesota can vary between 32 and 44 in. in height, depending on the application. The top of the parapet measures 15 in. wide, and the front face of the fence is placed at a minimum of 4½ in. away from the front of the concrete parapet, as is shown in Figure 47 [29].

The 6-ft tall, top-mounted chain-link wire mesh utilizes vertical posts consisting of 2½-in. nominal diameter standard pipes spaced at 10-ft centers. Cylindrical, 1¼-in. nominal diameter standard pipes were used as longitudinal stiffeners along the bottom of the mesh and along the top at expansion joints, connected to vertical members using pipe clamps. An additional 7-gauge, galvanized steel tension wire was located at the top of the fence which could potentially prevent fence elements from falling off the parapet during high wind loading events. A baseplate is used to connect the vertical posts to the concrete parapet. The wire mesh is connected to steel pipe members with vinyl coated fabric ties and to tension wire with hog rings. Additional details are shown in Figure 48 [29].

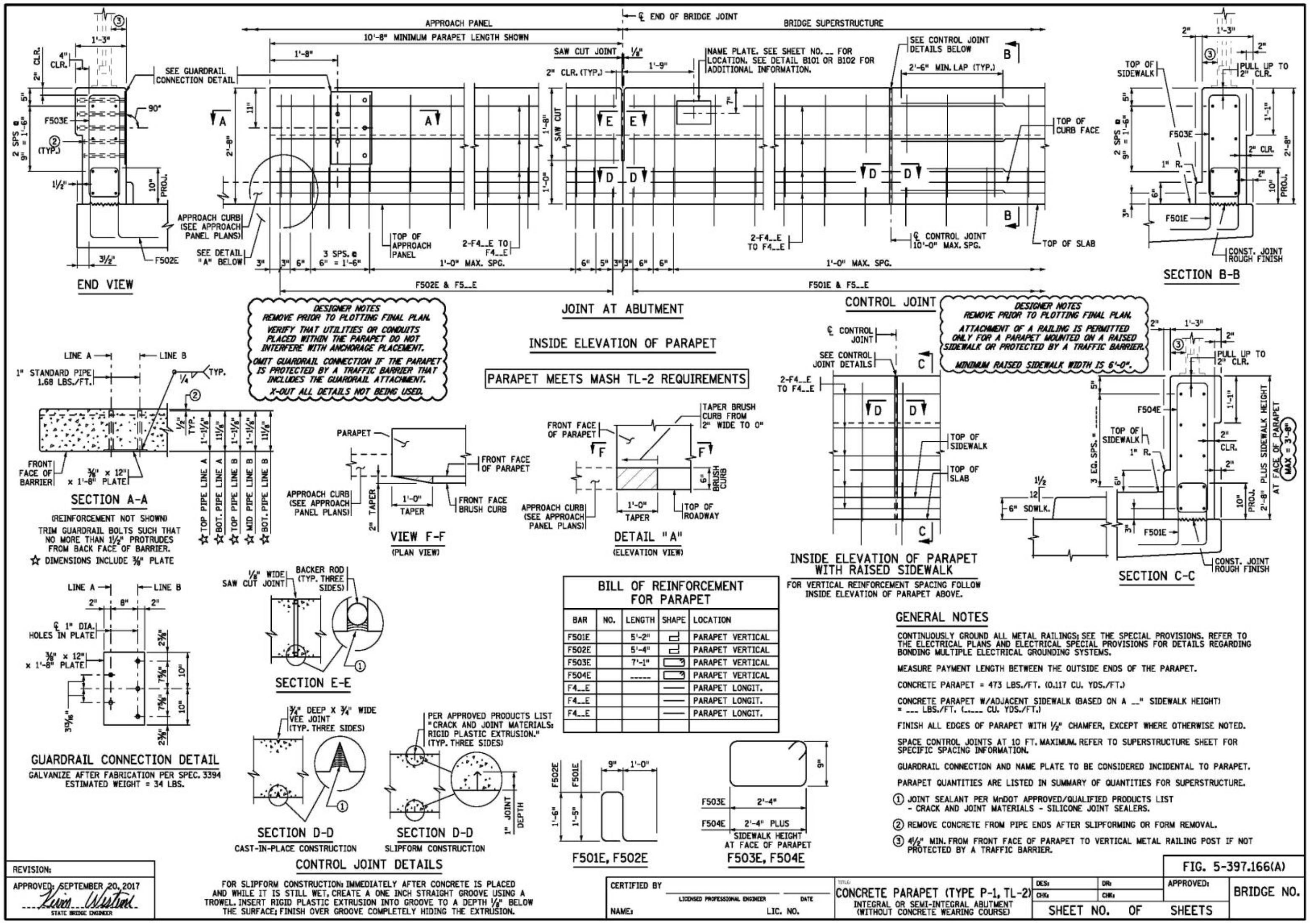

Figure 47. Minnesota Concrete Parapet Type P-1 [29]

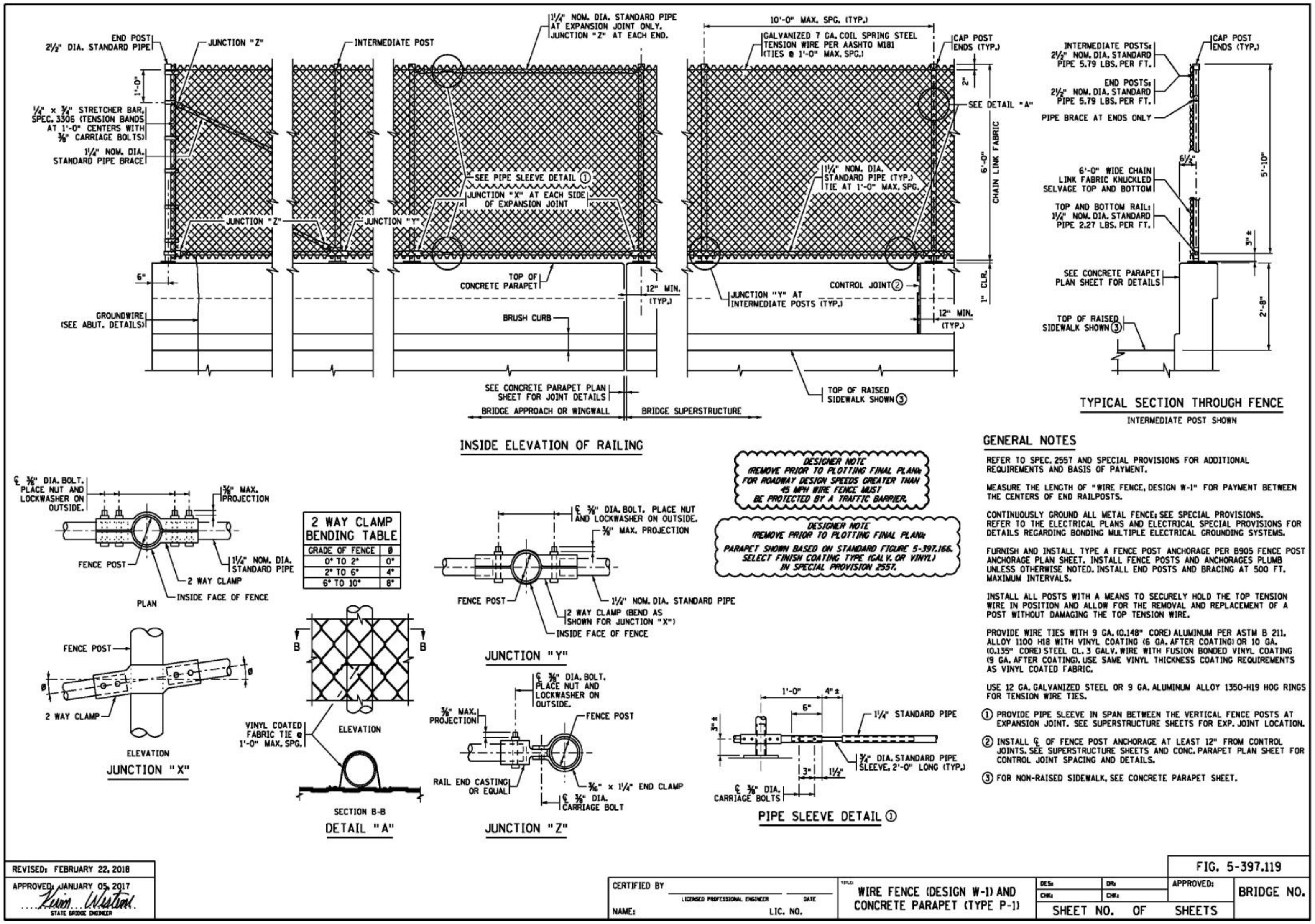

Figure 48. Minnesota Wire Fence Design W-1 [29]

2.6.10 Nebraska

The Nebraska DOT utilizes two different fence designs for debris mitigation over railway overpasses. Both of these fence designs are used in conjunction with a concrete parapet bridge rail. This concrete bridge rail parapet is shown below in Figure 49 [30].

One of the fence designs used by Nebraska contains a vertical 6-ft tall, galvanized chain-link fence, with knuckled selvage at the top and bottom, mounted to the top of a concrete parapet with a base plate. The fence is placed at the centerline of the parapet, 7 in. back from the front face. Vertical posts are 3-in. nominal diameter standard pipes spaced 8 ft on center on top of the parapet. The bottoms of the vertical posts are connected to a base plate that is bolted to the top of the concrete parapet using ¾-in. diameter U-bolts. This design also contains three, 1¼-in. nominal diameter standard pipes functioning as longitudinal stiffeners. This fence design is shown in Figure 50 [30].

Nebraska also utilizes a back-mounted, 7-ft tall, galvanized chain-link fence debris fence system. The vertical posts of the system, are 3-in. nominal diameter standard pipes, spaced 8 ft on center. The bottom of the post are inserted onto a receiver, made with a 2½-in. nominal diameter pipe, attached to a bracket on the back side of the barrier. An addition bent bracket fastens the vertical posts to the parapet with two ½-in. diameter bolts. Three, 1¼-in. nominal diameter standard pipes are used to provide horizontal support to the fence frame. This fence design is shown in Figure 51 [30].

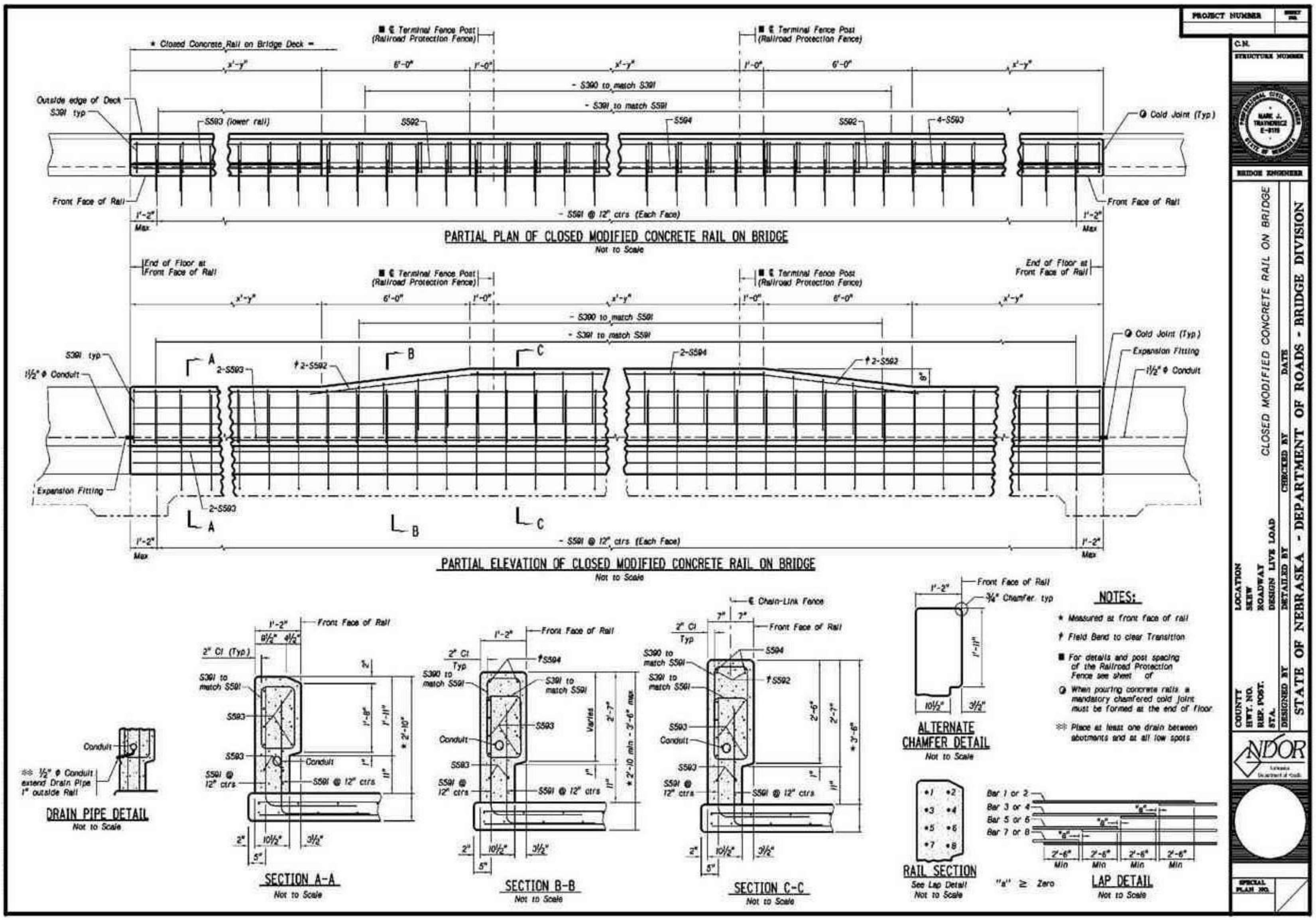

Figure 49. Nebraska Closed Concrete Rail Parapet Reinforcement Details [30]

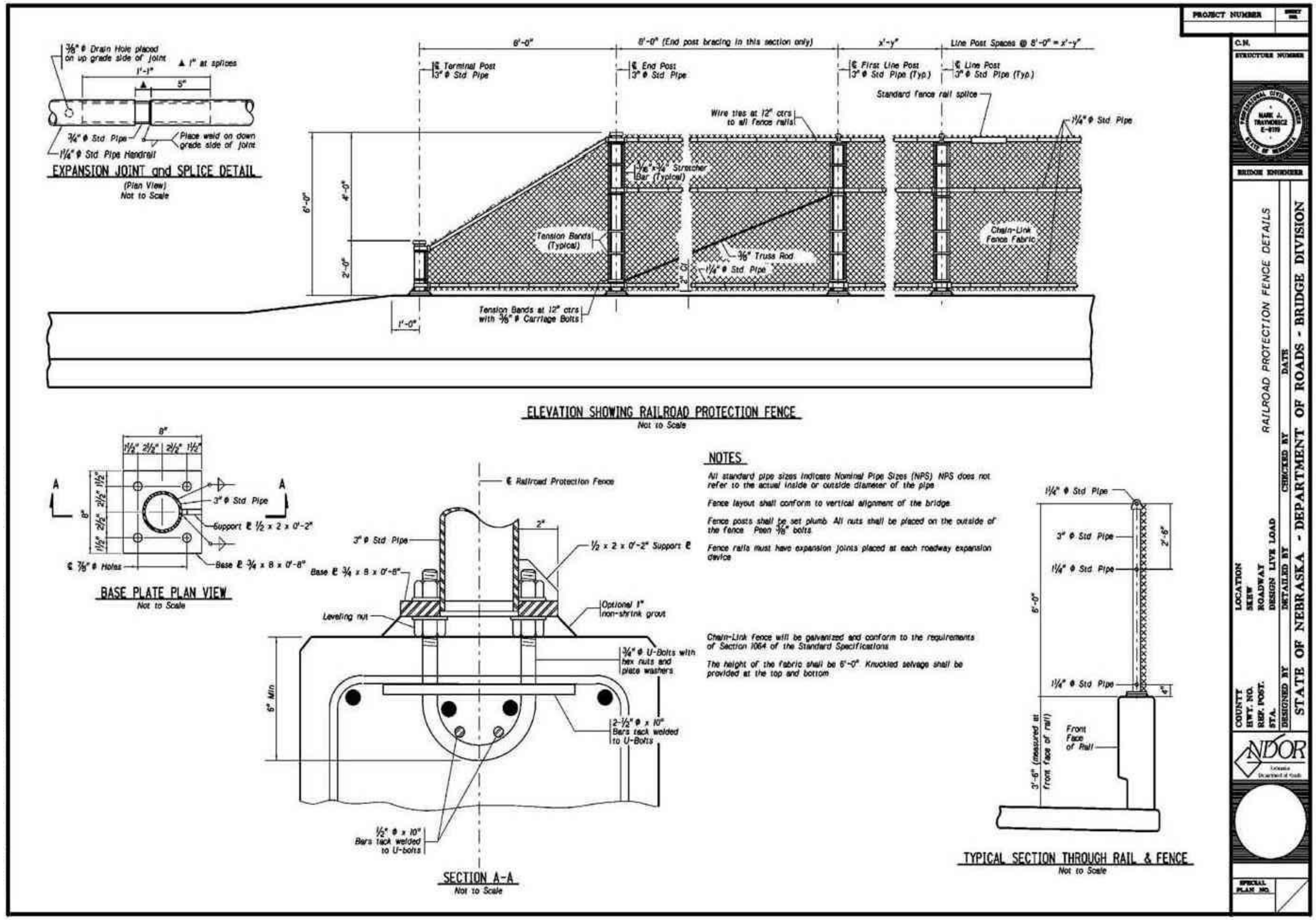

Figure 50. Nebraska Railroad Protection Fence Details [30]

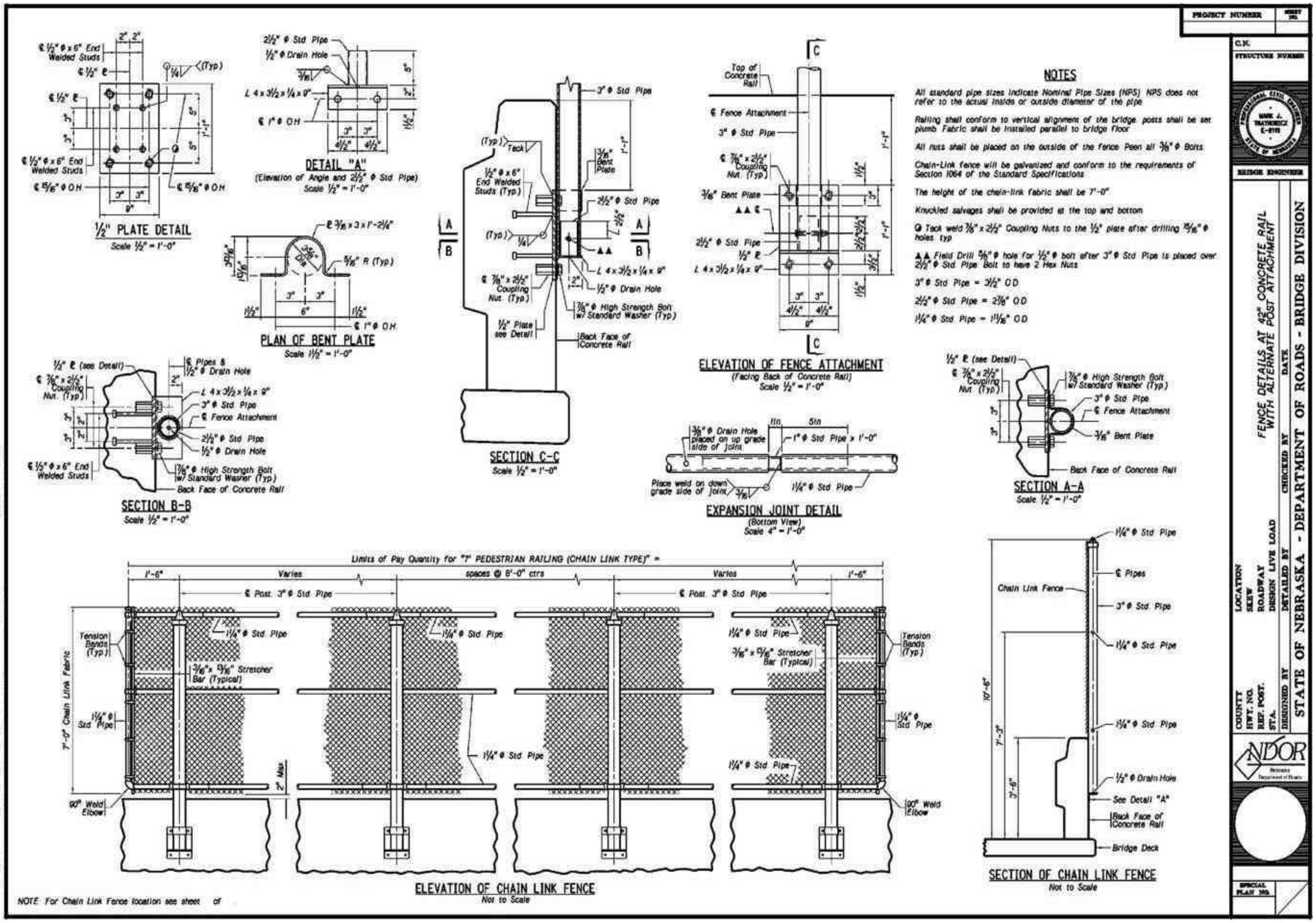

Figure 51. Nebraska Fence Details with an Alternate Post Attachment [30]

2.6.11 New Jersey

The New Jersey DOT curved fence mounted on top of a 32-in. tall vertical parapet. The curved fence is constructed using 2-in. square, ¼-in. wall thickness, ASTM B221 aluminum-alloy tubes functioning as vertical posts. Four 1½-in. square, ⅛-in wall thickness aluminum-alloy tubes are used to longitudinally stiffen the fence frame. Each vertical member is connected to a baseplate that is anchored to the parapet using two ¾-in. diameter corrosion resistant steel bolts. A 1-in. mesh is connected to the fence framework with fabric ties spaced every 6 in. for the top horizontal stiffeners and every 12 in. for the vertical posts. The geometric details of this design are shown in Figure 52 [31].

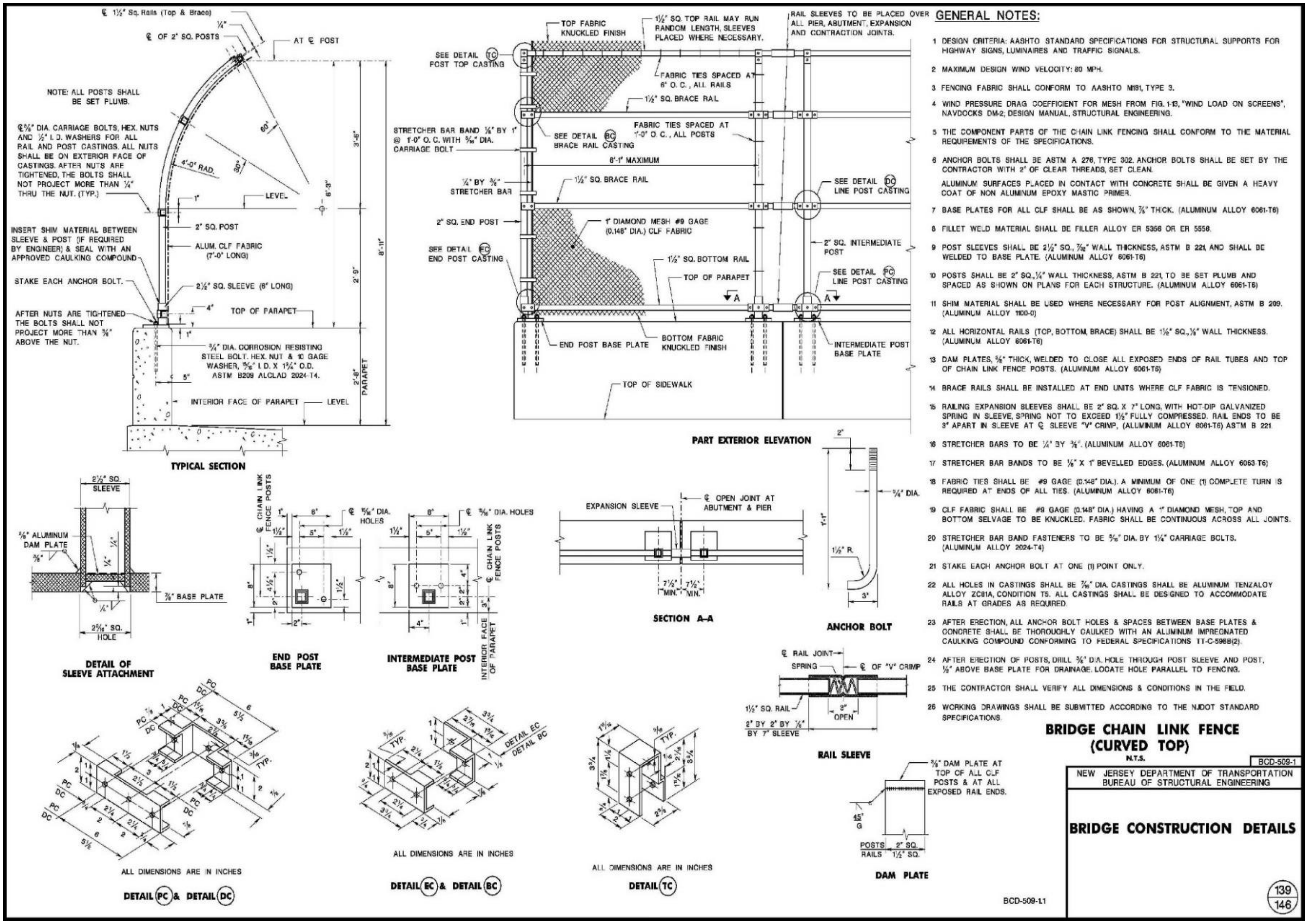

Figure 52. New Jersey Curved Chain Link Fence [31].

2.6.12 New York

The New York State DOT utilizes a vertical fence mounted directly on the back of either a 34-in. tall, safety-shape barrier or a 42-in. tall, vertical barrier as a debris fence. The design uses 2½-in. nominal diameter standard pipes spaced in 10 ft increments. The posts are attached to the back of the parapet with two clamps and four ⅝-in. diameter bolts. Three 1¼-in. nominal diameter standard pipes are used as horizontal stiffeners located at the top, middle, and bottom portion of the fence. The fence uses a 1-in. gap opening, diamond chain-link wire mesh made with 11-gauge wire. The system design is shown in Figure 53 [32].

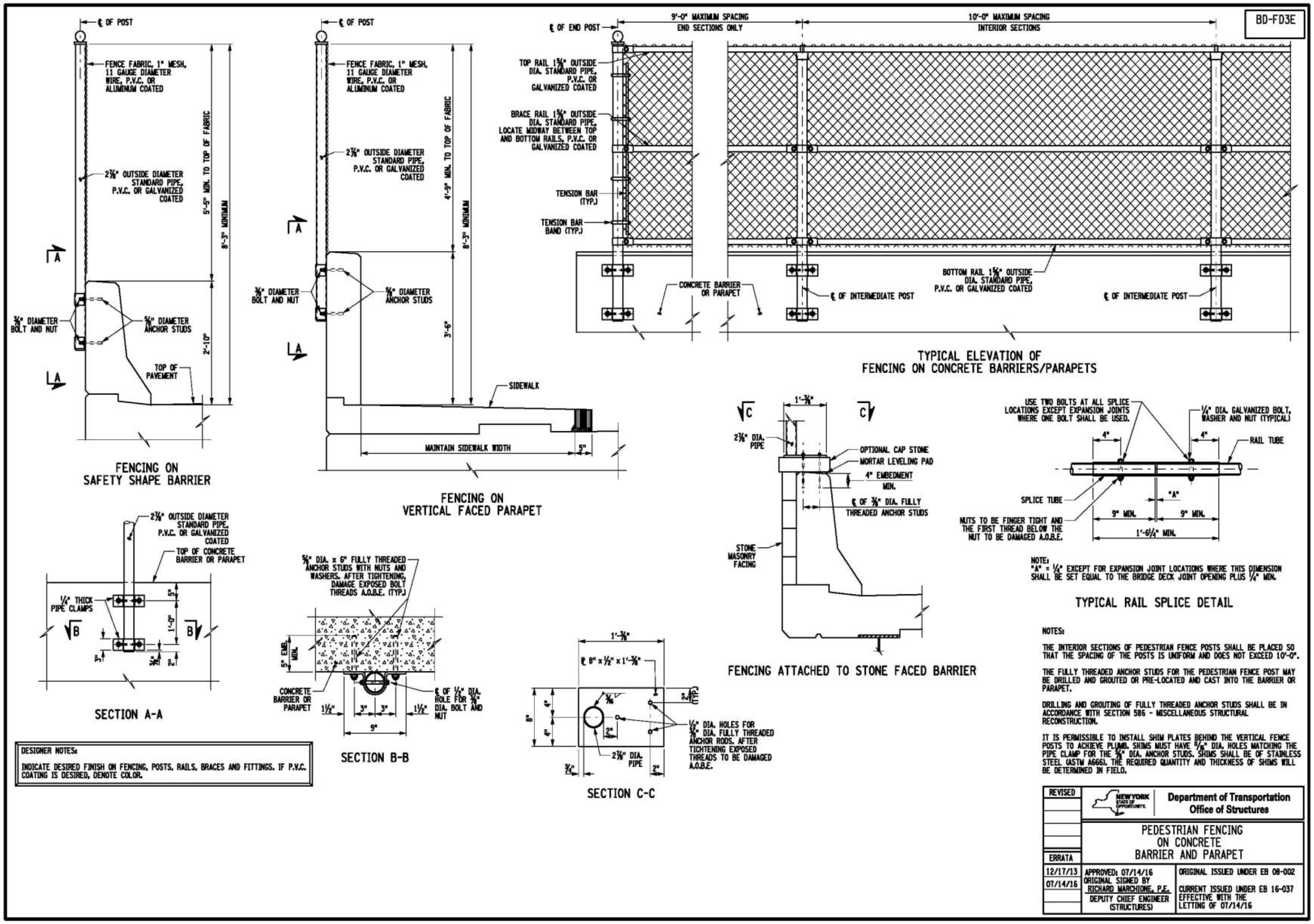

Figure 53. New York Pedestrian Fencing on Concrete Barrier and Parapet [32]

2.6.13 Oregon

The Oregon DOT utilizes a vertical pedestrian fence mounted on the back of an F-shape concrete bridge rail and a curved pedestrian fence mounted on the back of a vertical bridge rail [33].

Posts in the vertical fence design are 3-in. nominal diameter and 3½-in. nominal diameter Extra Strong pipes for 6-ft and 8-ft tall chain-link fence configurations, respectively. These posts are spaced 10 ft on center and connect to the backside of the bridge rail with two clamps, which are fastened to the rail with ¾-in. diameter resin-bonded anchors. Two horizontal stiffeners consisting of 1¼-in. nominal diameter standard pipes are located at the top and bottom of the fence frame. A 2-in. diamond chain-link fabric is attached to the traffic side of the fence frame. This fence design is shown in Figure 54, which is labeled as a Type C Fence Section. Connection details are shown in Figure 55 [33].

The curved fence design contains vertical posts made of 3½-in. nominal diameter and 4-in. nominal diameter Extra Strong pipes for parapet-mounted fence configurations with a total height of 9 ft – 1⅜ in. and 11 ft –1 in., respectively. These posts are spaced 10 ft apart and connect to the backside of the bridge rail with a clamp anchored to the concrete with two ¾-in. diameter resin bonded anchors. Additionally, a plate connected to the post is also attached to the top of the barrier using ⅝-in. diameter anchor bolts. Four horizontal stiffeners composed of 1¼-in. nominal diameter standard pipes are used along the length of the system. The chain-link fabric, consisting of a 2-in. gap diamond mesh, is attached to the traffic side of the curved fence frame. This fence design is shown in Figure 54, and is labeled as a Type A Fence Section. Connection details are shown in Figure 55 [33].

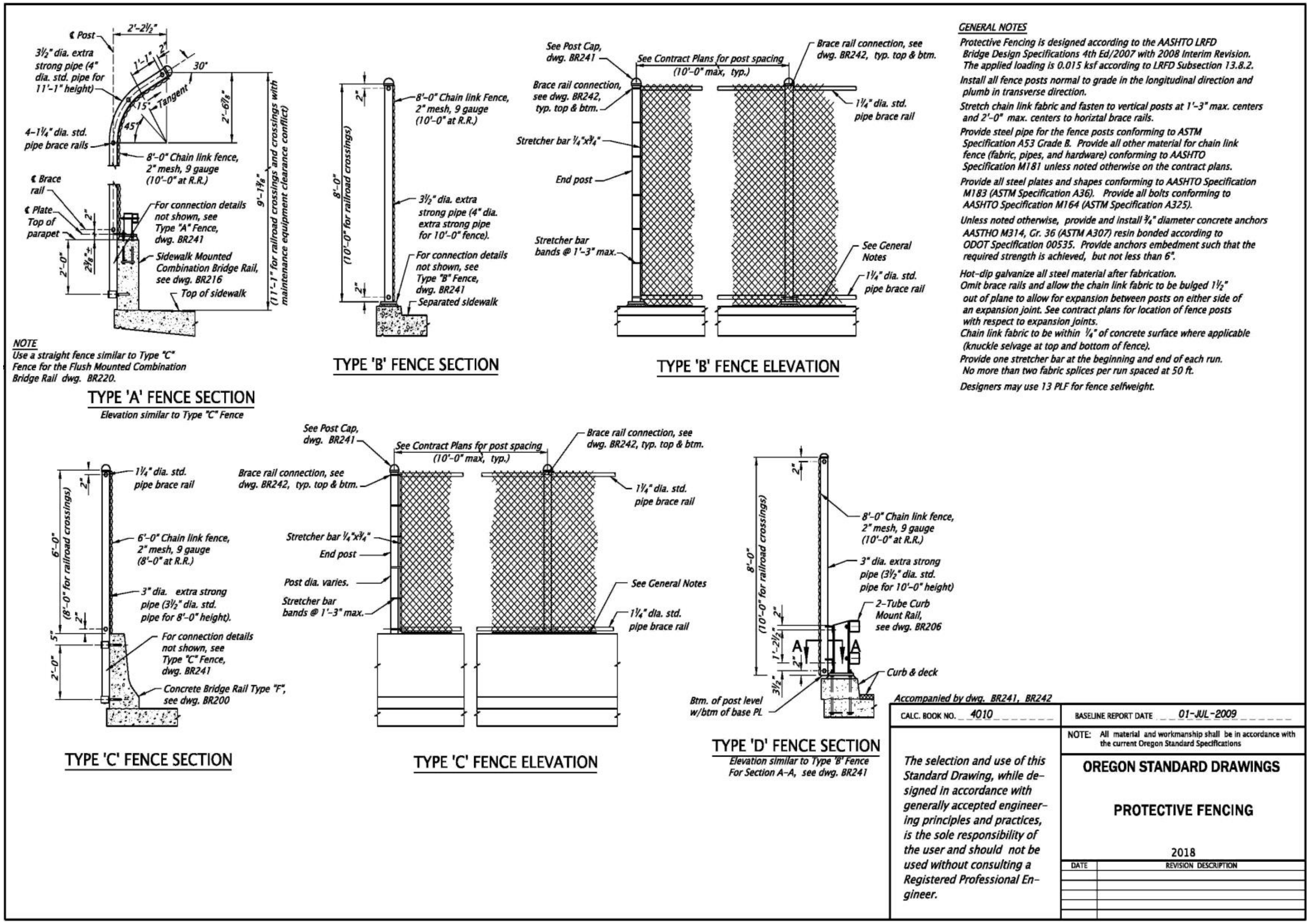

Figure 54. Oregon Pedestrian Fence [33]

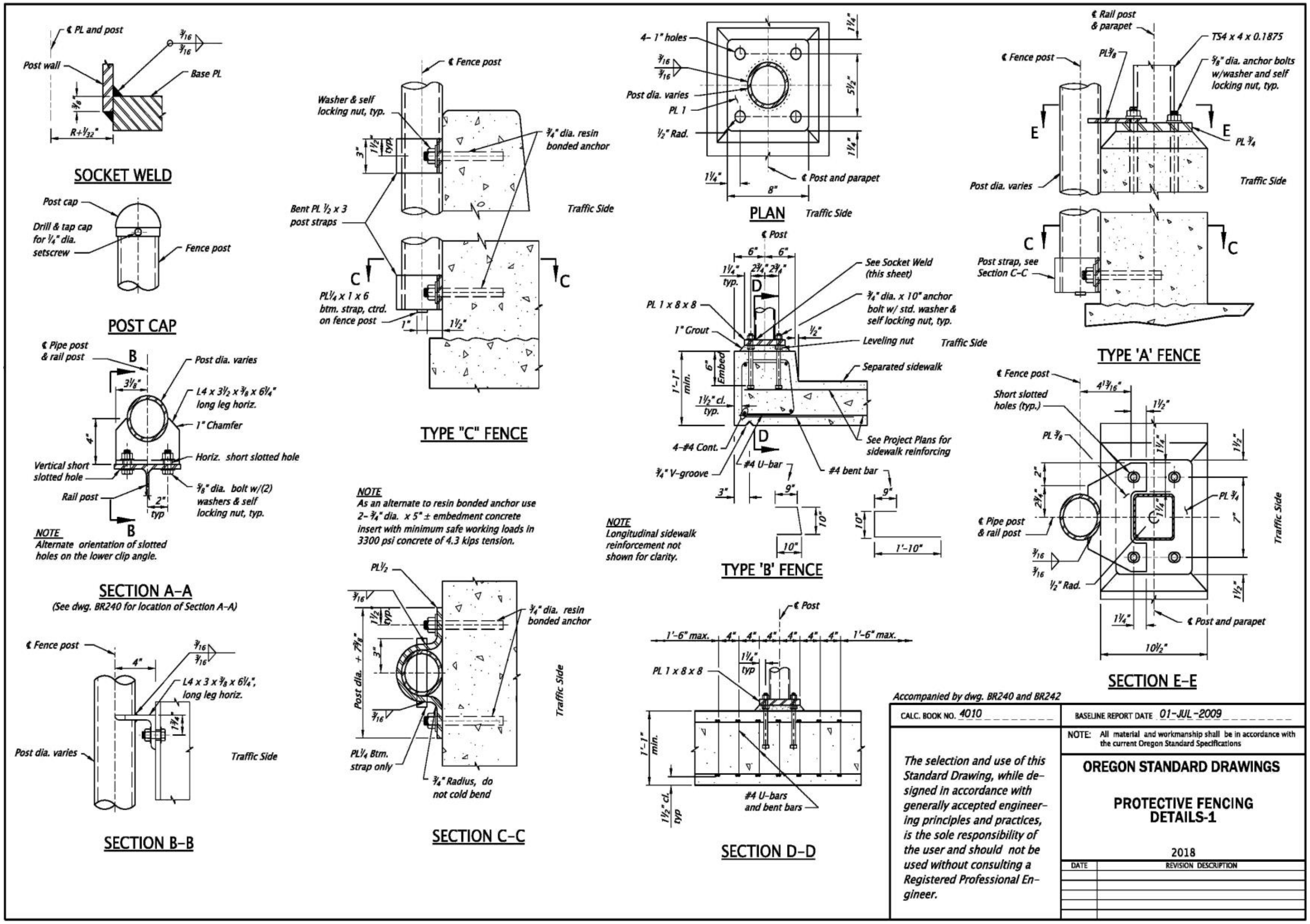

Figure 55. Oregon Protective Fencing Details [33]

2.6.14 Texas

The Texas DOT standard utilizes a debris fence mounted to the back of a concrete bridge rail. The Texas T211 vertical concrete parapet or the Texas T551 safety shape concrete parapet are recommended for use in combination with the debris fence.

Vertical posts, consisting of HSS3.5x0.216 round structural steel tubes conforming to either ASTM A1085 or ASTM A500 Gr B, are spaced 8 ft on center. The vertical posts are connected to the backside of the concrete parapet with a bracket and two ⅝-in. diameter anchor bolts. A third ⅝-in. diameter anchor bolt attached the post to the barrier directly. One horizontal stiffener, which consists of HSS1.660x0.140 in. conforming to either ASTM A 1085 or ASTM A500 Gr B, is threaded through sleeves mounted on the top of the posts. The mesh is constructed from 9-gauge steel fabric with a 2-in. diamond gap opening, and it is attached to the posts and stiffeners using 9-gauge steel wire ties. A tension wire is also attached to the bottom portion of the fence using 9-guage steel hog rings. The debris fence and concrete parapet are shown in Figures 56 and 57 [34].

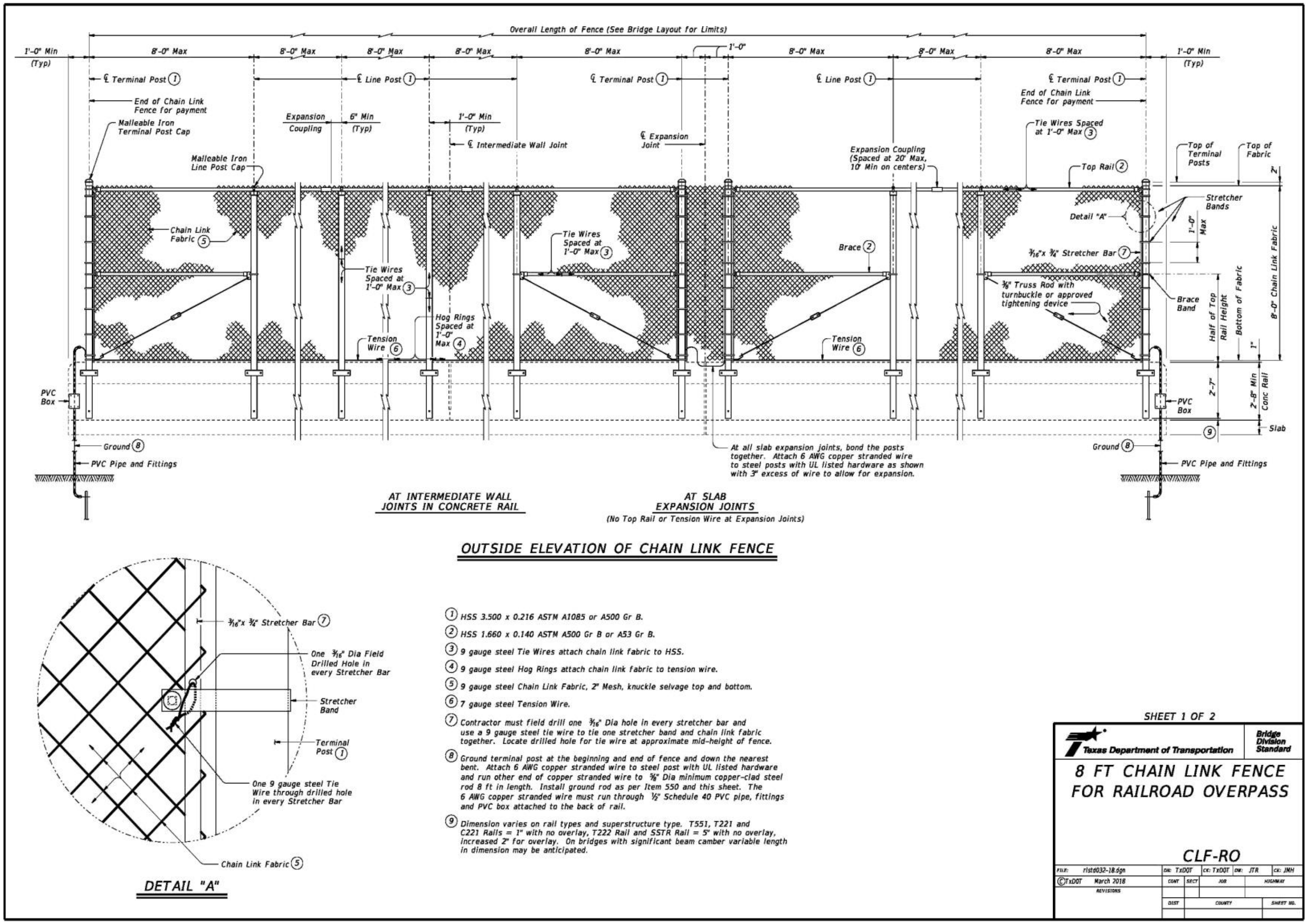

Figure 56. Texas 8 ft Chain Link Fence for Railroad Overpass [34]

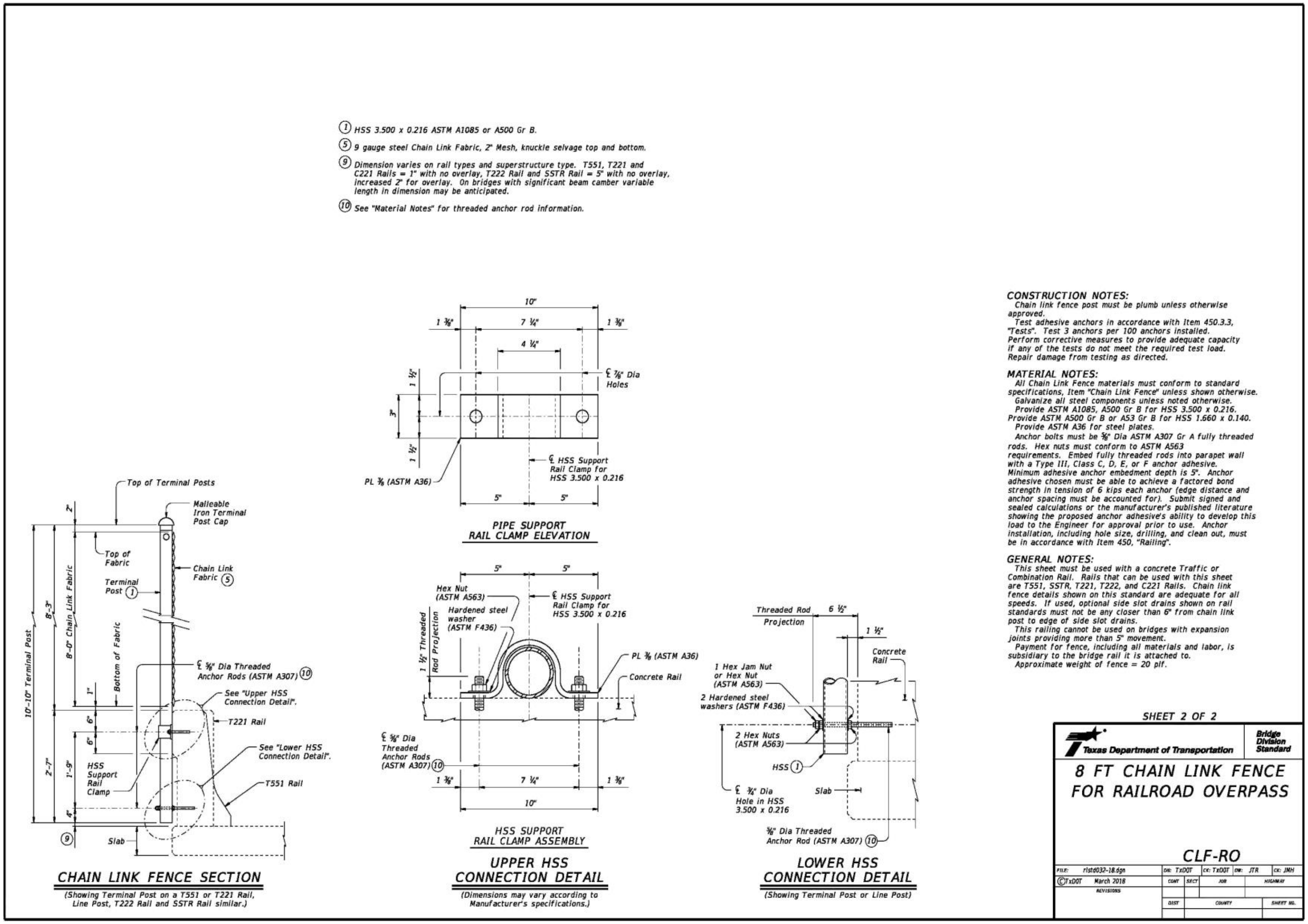

Figure 57. Texas 8 ft Chain Link Fence for Railroad Overpass Details [34]

2.6.15 Wisconsin

The Wisconsin DOT utilizes two types of debris fences: a flat, vertical fence; and a curved option. Both fences are installed in conjunction with a 32-in. tall concrete barrier on raised sidewalks, or behind traffic barriers and in conjunction with sidewalks. For traffic barrier applications, a straight fence is mounted on a 31⅞-in. tall single slope parapet [35].

End posts and overhang posts are composed of 2½-in. nominal diameter standard pipes, while line posts use 2-in. nominal diameter standard pipes. The posts are spaced 8 ft on center and are welded to base plates which are used to attach posts to the top of the parapet with two ½-in. diameter anchor bolts. Three 1¼-in. nominal diameter standard pipes function as horizontal stiffeners, attached to the vertical posts using rail ends and brace bands. The fence is constructed from 9-gauge, 2-in. diamond mesh, and chain-link fence attached to the posts and stiffeners with 9-guage wire ties. The system and connection details are shown in Figure 58 [35].

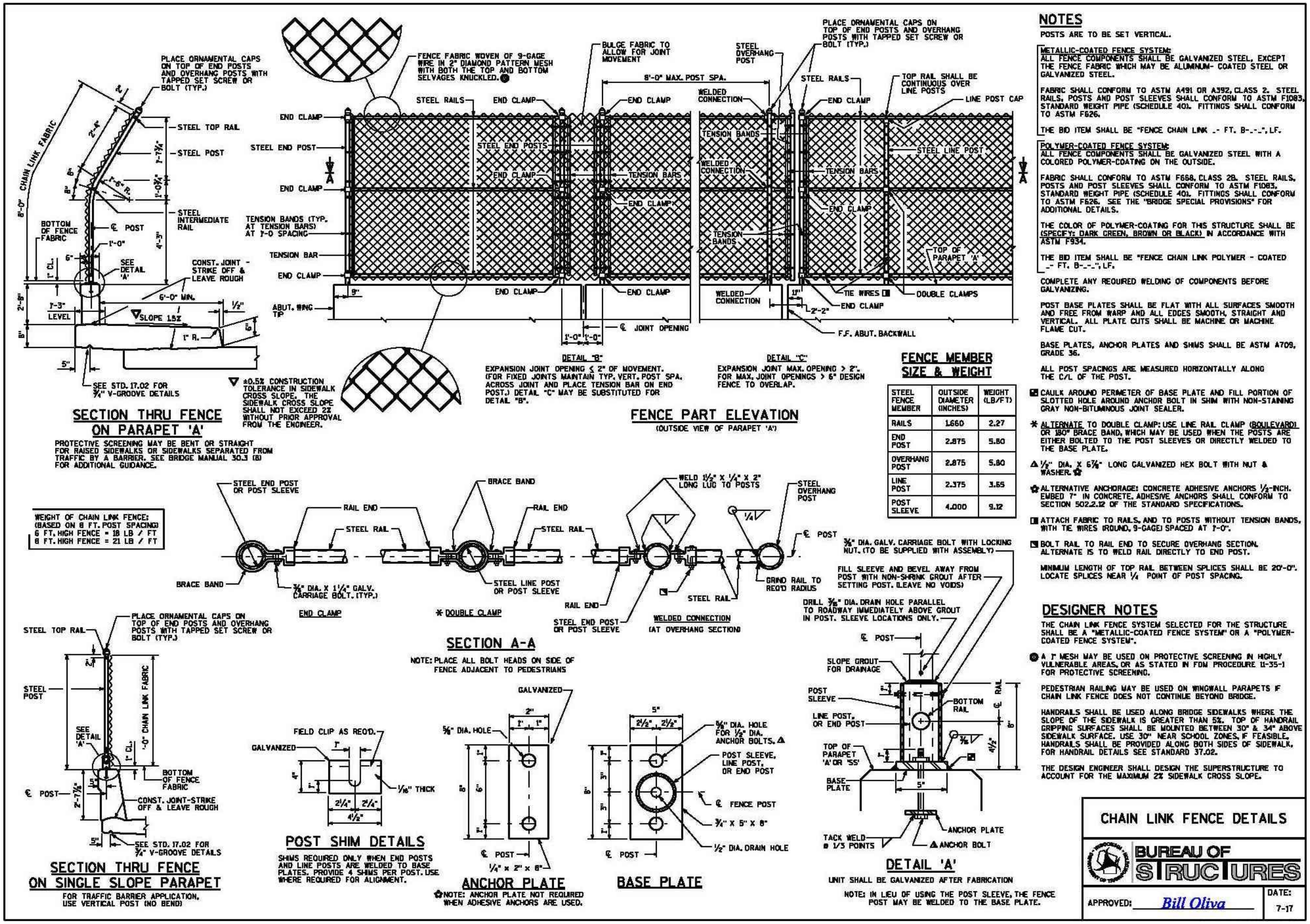

Figure 58. Wisconsin Chain Link Fence Details [35]

2.7 Lincoln, Nebraska Fence Examples

A survey of two different fences used in close proximity to the travelled way was completed in Lincoln, Nebraska. The first design consisted of an aesthetic vertical debris fence mounted on top of a concrete parapet. The second system was similar to the protective fence used by Iowa, which is shown in Figure 30. No evidence was observed that either of the local fences had been impacted during a vehicle impact with the adjacent barrier.

2.7.1 Aesthetic Debris Fence

The first fence example that was analyzed in Lincoln, Nebraska is located near the corner of North Antelope Parkway and Salt Creek close to the design headquarters of MwRSF. This example is different from Nebraska DOT standard fence plans, as can occur on local roads and municipalities. For this design, a fence is mounted on the top of a vertical concrete bridge rail using a base plate. This rail measures 42 in. tall, and the debris fence is mounted in the middle of the rail, 8 in. behind its front face.

The aesthetic fence design is composed of wire mesh panels containing cyclic wave designs on both the top of the mesh structure and on panels that are bolted to the mesh. Rectangular vertical posts measuring 8 ft – 7½ in. were placed 8 ft on center. These posts were connected to panels containing two horizontal stiffeners, one at the bottom and one 4 ft above the parapet. An additional aesthetic stiffener is located at the top of the fence mesh. These panels also contained vertical posts at the beginning and end of each panel section. All vertical posts and longitudinal stiffeners located in the mesh structure were fabricated with 2-in. x 2-in. x ¼-in. rectangular steel tube. The wire mesh panels were connected to the vertical posts with a total of six ¼-in. self-tapping screws. A baseplate measuring 8 in. x 8 in. x ½ in. was used to secure the vertical posts to the concrete bridge rail and was held in place with four 6-in. long by ⅜-in. diameter anchor bolts. CAD details of both the fence and parapet design are shown in Figures 59 through 61.

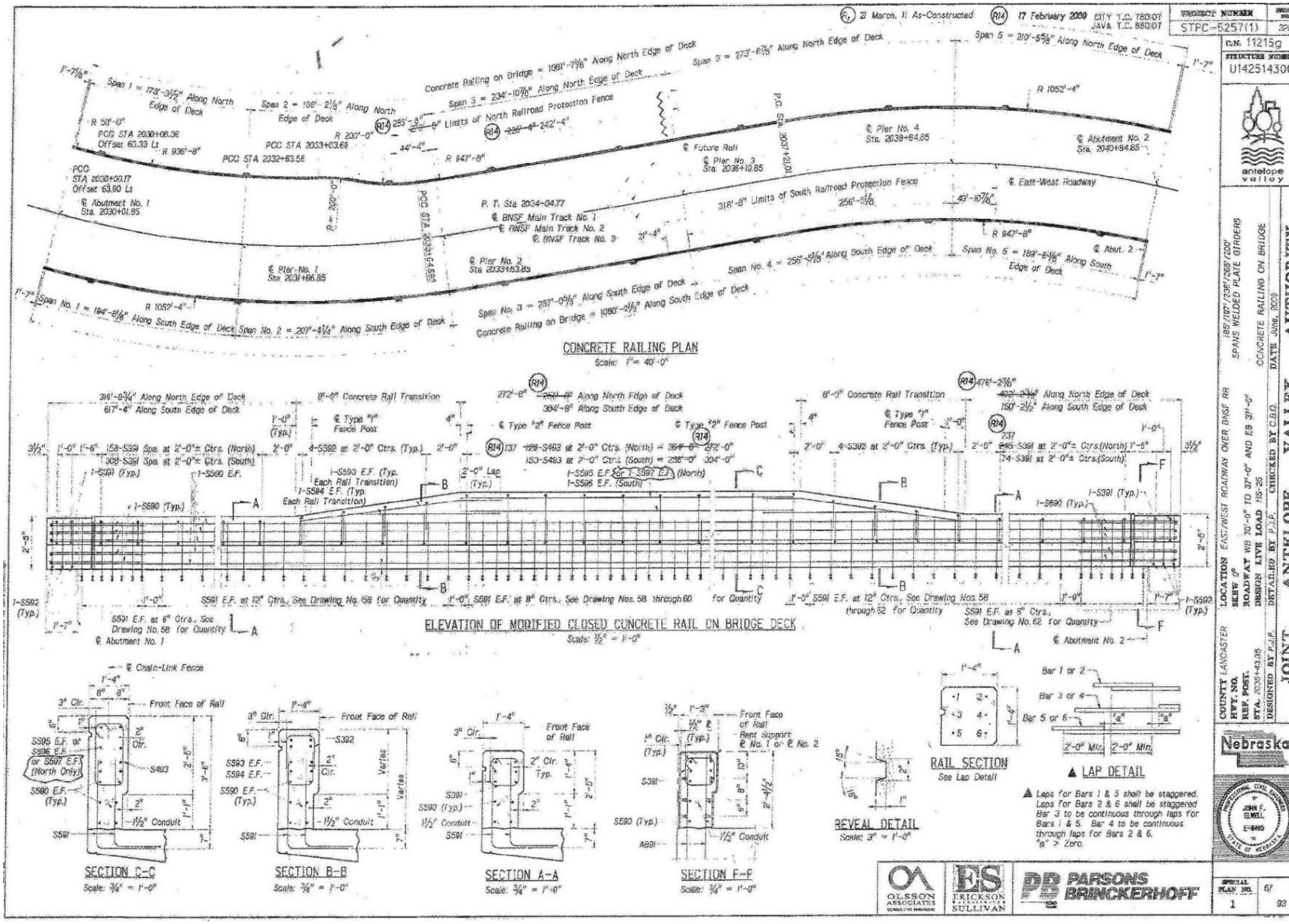

Figure 59. Aesthetic Debris Fence Bridge Rail Details

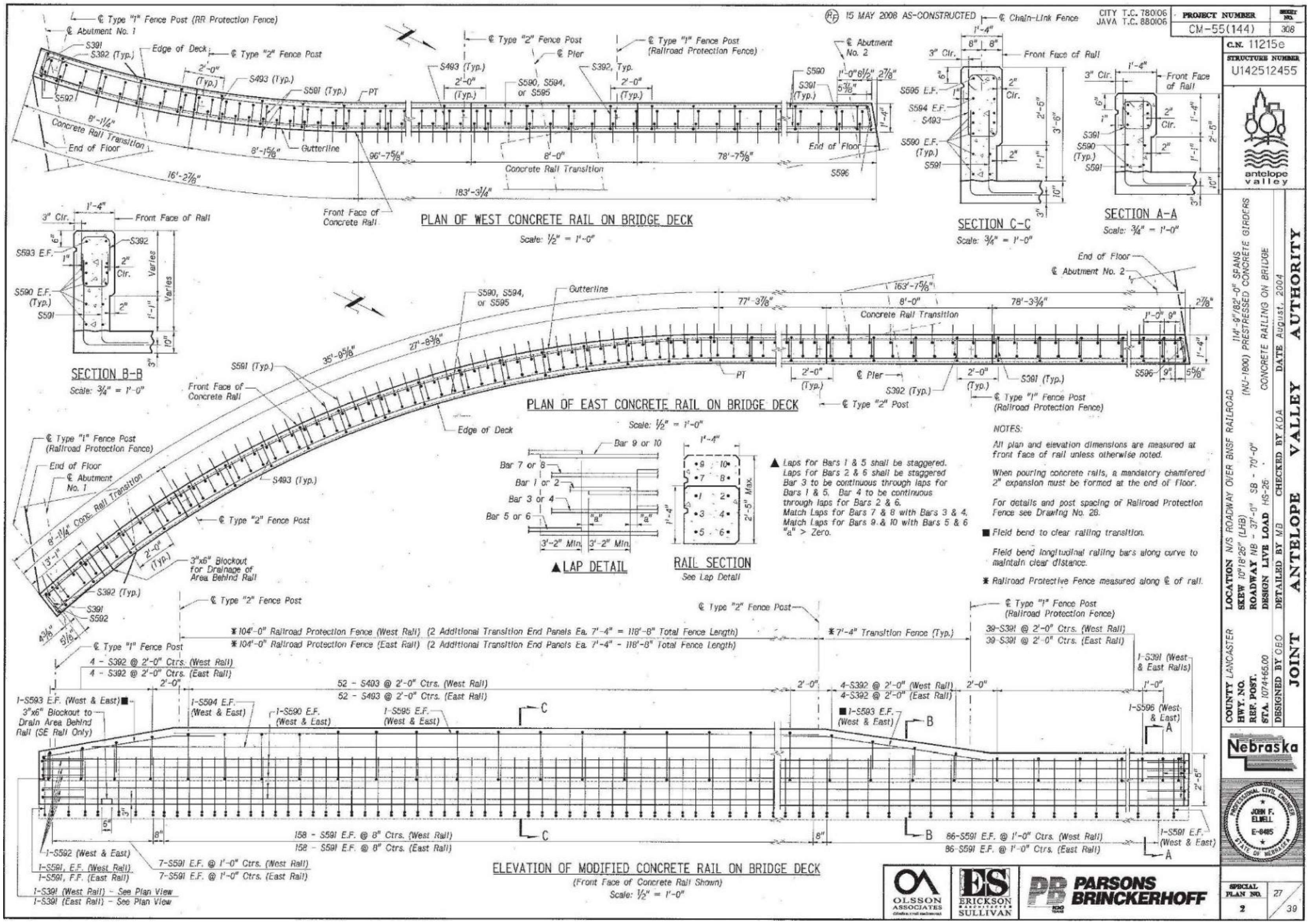

Figure 60. Aesthetic Debris Fence Bridge Parapet and Placement Details

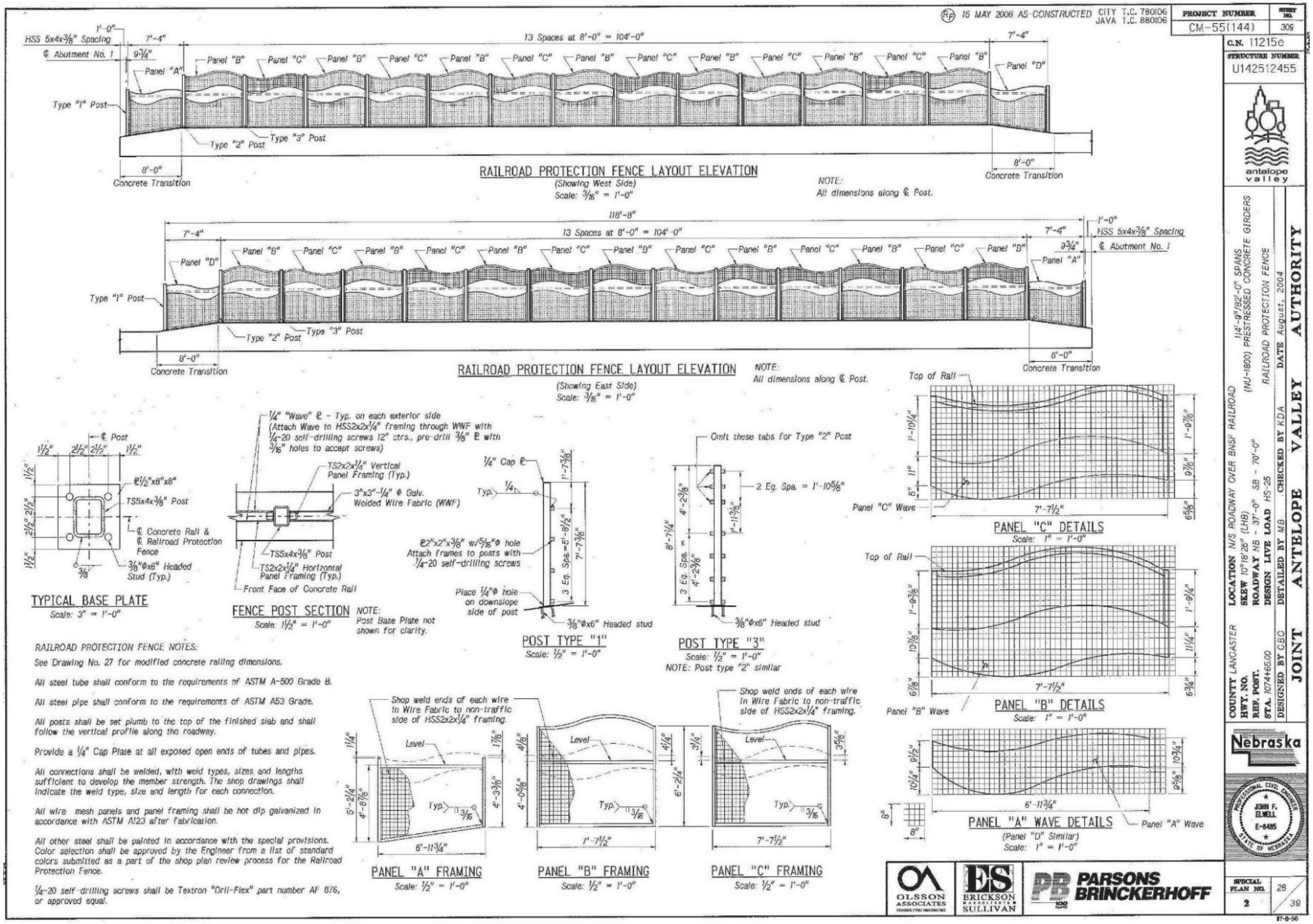

Figure 61. Aesthetic Debris Fence Details

Upon examination, some panels within the fence structure were missing, as shown in Figures 62 through 64. Closer inspection revealed that some of the self-drilling screws used to secure the fence panels to the vertical posts had fractured and ratchet straps were being used to secure the panels to the posts, as shown in Figures 64 and 65.

Figure 62. Aesthetic Debris Fence Overview

Figure 63. Aesthetic Design Missing Panels

Figure 64. Aesthetic Design Missing Panel

Figure 65. Aesthetic Design Broken Screws

2.7.2 Combination Rail and Pedestrian Fence

Another design used in Lincoln, Nebraska, and located on the 27th Street and Salt Creek Roadway overpass, is very similar to the Iowa combination pedestrian rail and debris fence shown in Figure 30. This design, as shown in Figure 66, is representative of the common, curved, fence designs used by states for pedestrian and debris containment. There are three longitudinal stiffeners used within the fence framework, one is placed at the bottom of the fence and the other two are within the curved upper section of the structure. There is also a handrail that runs longitudinally along the length of the system.

Figure 66. Lincoln Pedestrian Fence

2.8 Design Standards

2.8.1 Iowa Chain-Link Fence Standards

Iowa DOT currently specifies criteria for the installation and maintenance of chain-link fence near the roadway. These guidelines were analyzed to determine design requirements for a debris fence installed in conjunction with a concrete parapet [36].

The structural elements used for both the vertical posts and horizontal stiffeners must meet one of the following requirements:

1. AASHTO M 181 Grade 1 guidelines or ASTM F1083 Schedule 40
2. AASHTO M 181 Grade 2 or ASTM F1043 Group IC

The chain-link fabric used in the debris fence design, unless otherwise noted in contract documents, must include:

1. 9-gauge coated wire with a breaking strength of 1,290 pounds;
2. Height of fabric of 72 inches;
3. Selvage knuckled at both the top and bottom; and
4. Mesh size 2 ± ⅛ inches.

Additionally, the chain-link fabric must conform to one of the following options:

1. Zinc coated fabric meeting requirements of ASTM A 392, Class 2 or AASHTO M 181 Type 1, Class D;
2. Aluminum coated fabric meeting requirements of AASHTO M181, Type II; and
3. PVC coated fabric requirements of ASTM F668, Class 2b or AASHTO M181, Type IV, Class B Fused.

Any tension wires used within a parapet-mounted debris fence design in Iowa shall either meet requirements of one of the following:

1. AASHTO M 181
2. ASTM A 824 or A 817, Type II, Class 3;
3. ASTM A 824 or A 817, Type 1; and
4. ASTM F 1664, PVC (Vinyl) Coated, Class 2b.

Brace and tie wires must meet requirements of ASTM F 626 and be either zinc or aluminum coated. They must also meet these additional requirements:

1. Where specified, round metallic-coated tie wires, clips and hog rings shall be polymer coated to match the color of the chain-link fabric as selected from ASTM 934 and

2. The coating process and metallic-coated core wire materials shall be in accordance with ASTM F 668.

Recommendations for the fittings used to secure the chain link to the structural members include the following:

1. Attach braces to posts using fittings which will hold both the post and the post and brace rigidly;

2. Use diagonal truss rods of ⅜-in. diameter, round steel rods with appropriate commercial means for tightening;

3. Furnish a locknut or other device to hold the tightening device in place;

4. Furnish a suitable sleeve or coupling device, recommended by the manufacturer, to connect sections of top rail and to provide for expansion and contraction;

5. Use stretcher bars no less than ⅜ in. diameter, or equivalent cross sectional area, with suitable clamps for attaching fabric to corner, end, or gate posts; and

6. All fittings should conform to AASHTO M 181 or ASTM F 626.

Anchor bolts used to secure the debris fence to the parapet should comply with the following requirements:

1. Use full-length galvanized bolts;

2. Comply with ASTM F 1554, Grade 105, S4 (-20°F);

3. Threads are to comply with ANSH/ASME B1.1 for UNC thread series, Class 2A tolerance;

4. The end of each anchor bolt intended to project from the concrete is to be color coded to identify the grade; and

5. Do not bend or weld anchor bolts.

Nuts that are used within the debris fence design should conform to the following specifications:

1. Comply with ASTM A 563, Grade DH or ASTM A 194, Grade 2H;

2. Use heavy hex;

3. Use ANSI/ASME B1.1 for UNC thread series, Class 2B tolerance; and

4. Nuts may be over-tapped according to the allowance requirements of ASTM A563.

Washers used in the system should comply with ASTM F 436 Type 1 requirements. The debris fence design may include the need to weld some of the structural members, and Iowa Department of Transportation states that these welds must comply with ANSI/AWS D1.1 Structural Welding Code procedures and requirements. The Iowa standards require that items along the roadway be able to withstand three-second wind gusts up to 90 mph (144.8 kmh).

2.8.2 Union Pacific and BNSF Standards

Rail companies, such as Union Pacific and BNSF, recommend guidelines for debris fences adjacent to railway properties. Their guidelines state that the fence should be designed to prevent climbing and provide means of protecting the railroad facility and employees from debris being thrown off the overhead structure and components from falling off the structure. These guidelines also require a minimum 8 ft combined height for barriers with curved fences and a minimum 10 ft combined height for barriers with straight fences [37]. The geometric details of the barrier and fences on overhead structures requirements is shown in Figure 67. The Iowa DOT has policies on barriers and fencing over railways which mentions that when BSNF and Union Pacific ask for parapet-mounted fences, the Iowa DOT generally proposes that the fence be omitted in lieu of a 44-in. tall concrete barrier [38].

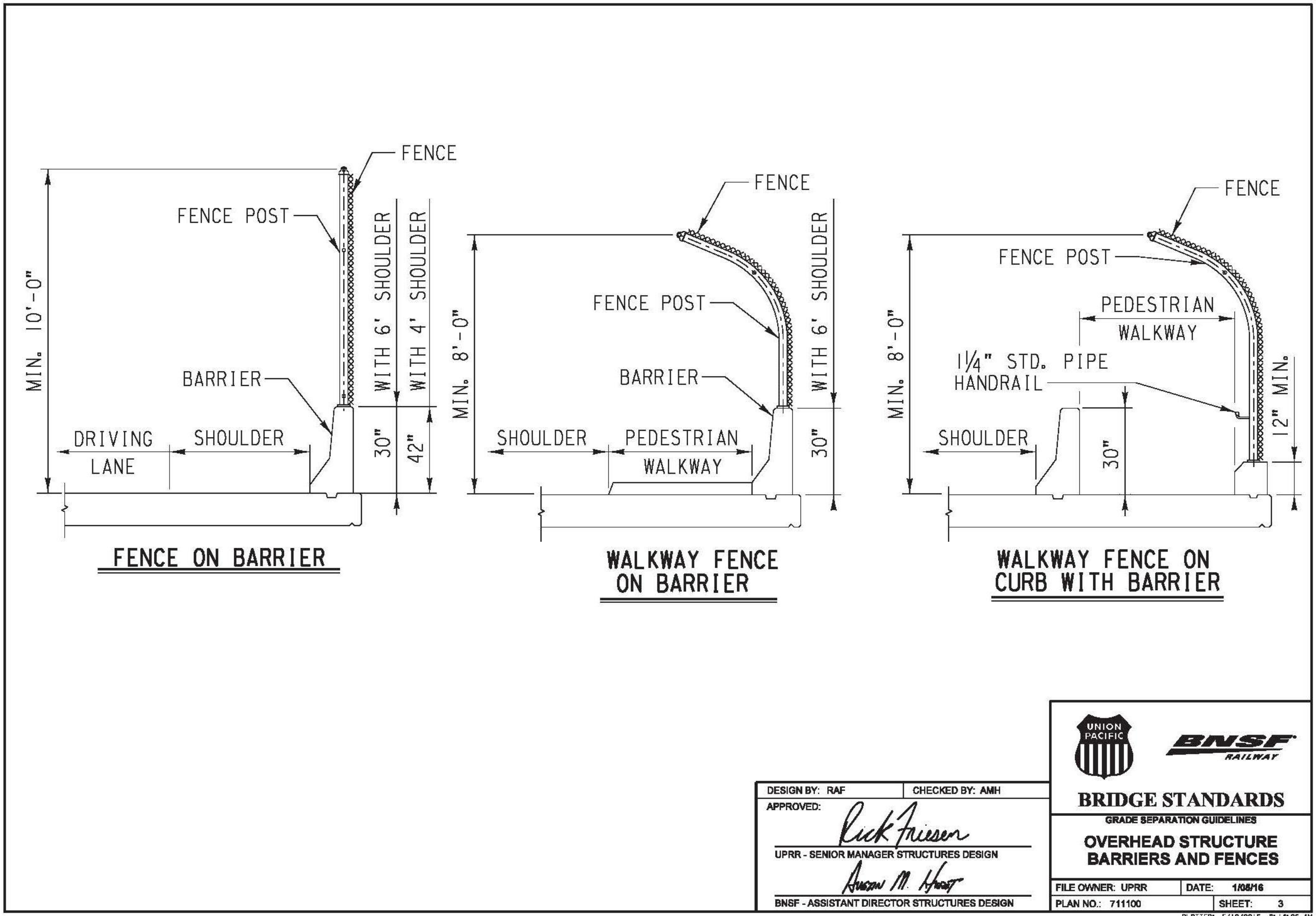

Figure 67. UP-BNSF Overhead Structure Barrier and Fence Details [37]

3 MASH TL-3 TEST REQUIREMENTS AND EVALUATION CRITERIA

3.1 Test Requirements

Longitudinal barriers, such as the parapet-mounted debris fence system design in this effort, must satisfy impact safety standards in order to be declared eligible for federal reimbursement by the Federal Highway Administration (FHWA) for use on the National Highway System (NHS). For new hardware, these safety standards consist of the guidelines and procedures published in MASH 2016 [1]. According to TL-3 of MASH 2016, longitudinal barrier systems must be subjected to two full-scale vehicle crash tests, as summarized in Table 4. Note that there is no difference between MASH 2009 and MASH 2016 for longitudinal barriers such as the system tested in this project, except that additional occupant compartment deformation measurements are required by MASH 2016. Full-scale crash testing was not in the scope of this project, however the parapet-debris fence combination was design to meet MASH 2016 TL-3 requirement.

Table 4. MASH 2016 TL-3 Crash Test Conditions for Longitudinal Barriers

Test Article	Test Designation No.	Test Vehicle	Vehicle Weight, lb	Impact Conditions		Evaluation Criteria [1]
				Speed, mph	Angle, deg.	
Longitudinal Barrier	3-10	1100C	2,420	62	25	A,D,F,H,I
	3-11	2270P	5,000	62	25	A,D,F,H,I

[1] Evaluation criteria explained in Table 5.

3.2 Evaluation Criteria

Evaluation criteria for full-scale vehicle crash testing are based on three appraisal areas: (1) structural adequacy, (2) occupant risk, and (3) vehicle trajectory after collision. Criteria for structural adequacy are intended to evaluate the ability of the concrete parapet to contain and redirect impacting vehicles. In addition, controlled lateral deflection of the test article is acceptable. Occupant risk evaluates the degree of hazard to occupants in the impacting vehicle. Post-impact vehicle trajectory is a measure of the potential of the vehicle to result in a secondary collision with other vehicles and/or fixed objects, thereby increasing the risk of injury to the occupants of the impacting vehicle and/or other vehicles. These evaluation criteria are summarized in Table 5 and defined in greater detail in MASH 2016.

Table 5. MASH 2016 Evaluation Criteria for Longitudinal Barrier

<table>
<tr><td>Structural Adequacy</td><td>A.</td><td colspan="3">Test article should contain and redirect the vehicle or bring the vehicle to a controlled stop; the vehicle should not penetrate, underride, or override the installation although controlled lateral deflection of the test article is acceptable.</td></tr>
<tr><td rowspan="12">Occupant Risk</td><td>D.</td><td colspan="3">Detached elements, fragments or other debris from the test article should not penetrate or show potential for penetrating the occupant compartment, or present an undue hazard to other traffic, pedestrians, or personnel in a work zone. Deformations of, or intrusions into, the occupant compartment should not exceed limits set forth in Section 5.2.2 and Appendix E of MASH 2016.</td></tr>
<tr><td>F.</td><td colspan="3">The vehicle should remain upright during and after collision. The maximum roll and pitch angles are not to exceed 75 degrees.</td></tr>
<tr><td rowspan="4">H.</td><td colspan="3">Occupant Impact Velocity (OIV) (see Appendix A, Section A5.2.2 of MASH 2016 for calculation procedure) should satisfy the following limits:</td></tr>
<tr><td colspan="3">Occupant Impact Velocity Limits</td></tr>
<tr><td>Component</td><td>Preferred</td><td>Maximum</td></tr>
<tr><td>Longitudinal and Lateral</td><td>30 ft/s</td><td>40 ft/s</td></tr>
<tr><td rowspan="4">I.</td><td colspan="3">The Occupant Ridedown Acceleration (ORA) (see Appendix A, Section A5.2.2 of MASH 2016 for calculation procedure) should satisfy the following limits:</td></tr>
<tr><td colspan="3">Occupant Ridedown Acceleration Limits</td></tr>
<tr><td>Component</td><td>Preferred</td><td>Maximum</td></tr>
<tr><td>Longitudinal and Lateral</td><td>15.0 g’s</td><td>20.49 g’s</td></tr>
</table>

4 DESIGN OBJECTIVES

4.1 Overview

The MwRSF research team developed a debris fence system for the Iowa DOT which included the selection or design of the following components:

- Bridge rail / parapet
- Vertical posts
- Post-to-rail attachments
- Concrete anchorage
- Wire rope
- Upper horizontal fence stiffeners (frame)
- Lower horizontal fence stiffener
- Chain link mesh

Design objectives for the system and each component were discussed with and approved by Iowa DOT. Each fence component was designed to satisfy component design criteria defined in this chapter, the Iowa DOT fence standards, and UP-BNSF requirements.

Per Iowa DOT, the fence design was to be full-scale tested during a subsequent phase according to MASH TL-3 impact conditions, but researchers also considered the effects that a TL-4 impact could have on debris fence components. This test condition specifies the use of a 10000S single-unit truck impacting at 56 mph and a 15-degree angle. MASH TL-4 test conditions could result in significant vehicle-to-fence system intrusion of the box behind the barrier system [3]. Therefore, researchers considered options for retaining damaged fence components in the event of significant fence damage due to an impact consistent with TL-4 conditions.

4.2 Debris Fence General Objectives

The debris fence was intended to be used in combination with a bridge parapet railing which satisfied MASH TL-4 crashworthiness criteria. Design concepts were only considered which satisfied Iowa's fundamental strength criterion: the debris fence could not deform from 3-second duration 90-mph wind gusts. In addition to this requirement, additional design objectives were identified:

- Prevent damage from loading events
- Crashworthiness
- Low cost and constructible

- Fence component retention
- Aesthetically pleasing
- Optimized weight

It was believed that the optimization of fence component sizes would include the minimization of weight when possible, and the control of maximum component strengths for any component which was in the barrier's ZOI. Controlling both the minimum and maximum strengths of fence components was intended to balance design performance and operation in non-impact conditions and weather events and to improve occupant safety in the event of vehicle snag from passenger vehicles or larger trucks. However, component failure could contribute to fence debris falling onto railroad tracks. Therefore, additional fence retention components were also considered to mitigate concerns of debris ejection during various impact events. Design aesthetics were also considered for components and connection configurations.

4.3 State DOT Fence Design Ranking

Before fence concepts were developed, researchers reviewed State DOT standards and summarized attributes of those systems. Each design attribute was ranked based on compliance with the overall design objectives which were abbreviated into four main criteria consisting of crashworthiness, constructability, cost, and aesthetics. Design attributes of interest consisted of vertical post shapes and sizes, post-to-barrier attachments, horizontal stiffeners, and chain-link fabric to fence framework attachments.

4.3.1 Crashworthiness

Crashworthiness was deemed the most important criterion and therefore weighed the heaviest when ranking design attributes. Placing vertical post farther behind the front barrier face reduces the likelihood of vehicle engagement during impact scenarios; therefore, back-mounted post configurations were preferred over fence designs with top-mounted vertical posts. Designs which use smaller section posts were also preferred because if posts are impacted by a vehicle, smaller posts will have a lower plastic hinge force which reduces potential vehicle snag. Moreover, using verticals posts with round sections instead of square or rectangular sections eliminates edges where exterior vehicle components could snag if contact with fence posts occurs. Thus, preference was given to designs with smaller, round posts over large open-section or rectangular posts.

The Ohio vandal protection fence anecdotal crash results indicated that horizontal fence members can detach during impact events and potentially act as spearing hazards. Thus, designs with limited number horizontal stiffeners within the barrier ZOI were preferred. Attachment between these members and vertical post are typically achieved through slip joints and bolted connections, respective examples of these attachments are incorporated in Delaware's fence design shown in Figure 34 and the splice tube connections detailed in New York's standard plans, shown in Figure 53. Bolted and welded connections were considered more crashworthy since slip connections could allow these members to detach during impact or fence flexure. Posts mounted to the back side of the bridge rail were deemed preferable to top-mounted posts, due to a desire to minimize the interaction of the vehicle and posts which may be in the ZOI. As well, mounting the chain link mesh to the traffic side of the posts was preferred, as some propensity for snagging on posts and horizontal stiffeners may be mitigated. Therefore, designs were classified as having a higher potential for crashworthiness with posts mounted on the back side of the parapet and with the mesh located on the traffic side of the posts.

Chain-link fabric-to-fence framework connections were also ranked based on their potential for crashworthiness. This attribute was considered since using hardware that produces reliable connections is more likely to retain fence elements during incidents that severely damage the fence structure, such as large vehicle impacts. Additionally, during these impact conditions, reliable connections could also reduce the amount railroad-cluttering debris. The Lincoln aesthetic fence example shows the importance of correctly securing the fence and highlights the need for strong connections to decrease the potential for the fence components to fall onto the roadway or railway tracks.

4.3.2 Constructability

Next, researchers considered the ease of fabricating and assembling the fence components on bridge parapets. Attributes that influenced the constructability of fence included post-to-bridge rail attachments, horizontal stiffer configurations and fence fabric connections.

Top mounted post-to-parapet configurations were considered more easily constructible when compared to back-mounted designs. This is true since, for designs where the fence is mounted to the back side of the barrier, installers must lean over the barrier to align and install vertical posts, and the installers may be required to support and maintain the weight of the post and brackets during the alignment to map the locations for drilling holes for the fasteners.

Technicians have noted that minimizing bolted or threaded fasteners as well as specialized equipment is preferred to expedite construction. As well, construction or repairs during winter months which do not require construction crews to remove gloves during cold weather was preferred. In general, designs which minimized the total number of fasteners, as well as number of unique sizes of those fasteners, were preferred.

Typical chain-link fence installation practices suggest fastening the chain-link fabric to vertical posts and horizontal stiffeners at a maximum spacing of 15 and 24 in., respectively [39]. Meeting these specifications requires an extensive number of connections and therefore the simplicity each connection will greatly influence the overall fence construction effort.

4.3.3 Cost

Material costs are a significant expense for all DOT construction projects, so researchers prioritized designs which minimized the amount of material, and which prioritized standard, readily-available materials, grades, and treatments to minimize cost. Factors which affected materials and fabrication costs included post shapes, fence-to-post attachments, post-to-bridge rail attachments, and horizontal stiffeners and attachments.

4.3.4 Aesthetics

Roadside designs which are considered “aesthetic” often have elements of consistency, smooth transitions, good coloration, and a seamless appearance. If the fence is impacted or laterally displaced, the imposed lateral variations of the chain-link fence will be magnified near the top of the fence due to its height. For example, for a 7-ft tall fence with posts mounted to 10 in. from the barrier top, a 1-in. lateral deflection near the top of the barrier will produce a 9.4-in. lateral deflection at the top of the fence. Some control mechanisms were desired to maintain good fence aesthetics by limiting lateral displacement that could occur due to construction tolerances or imposed by impacts with the fence. Horizontal frame members laterally stiffen the fence framework, improving its ability to prevent swaying during high wind events and correct irregularities caused by installation tolerances. Designs which were conducive for good aesthetic properties and simple, smooth construction and transitions were preferred.

4.3.5 Summary

The results of state fence design review were evaluated using the criteria above, based on a five-point scale. An importance factor was also considered to amplify the desirability of crashworthy designs over the other criteria. Based on this review, the preferred configurations were the Florida DOT design, which utilized vertical round posts and two saddle brackets to the back side of the parapet, and the Texas DOT design, which utilized a single saddle bracket and a lower bolt which passed through the post into the back side of the parapet. These designs also possess fence frameworks with a limited number of stiff horizontal members within ZOI envelope of passenger vehicles. The Florida DOT design is shown in Figures 36 through 38 [23] while details of the Texas DOT design are shown in Figures 56 and 57 [34].

Researchers then reviewed components of those systems and established component design objectives. These component design objectives were also shaped by additional guidelines brought forth from information gathered in the literature review.

- A strong moment connection should be established with the post to bridge rail attachment. It was anticipated this would be accomplished using a minimum of two distinct bracket connections.

- Post-to-parapet attachments (specifically, bolted attachments) should not experience damage or produce concrete damage during design impacts. Post-to-parapet attachments should not require replacement when an impact occurs.

- If possible, no structurally-stiff horizontal members should be placed within passenger vehicle ZOI.

- Parapet connection was standardized. Adaptation may be required for alternative bridge rail configurations.

4.4 Debris Fence Specific Component Objectives

4.4.1 Vertical Posts

Vertical posts are used as the primary structural component in erecting a chain-link fence. All components such as fence stiffeners and chain-link mesh are fixed to the vertical post and any loads applied to these components are transferred to the vertical post. It is required that the post not be damaged by wind loads and vertical loads consisting of dead, dead ice, live, and snow loads as well as the combination of these loads applied to the fence system. As well, it was desired that vertical posts minimize the risk of vehicle component snag during impact, based on the shape, location, and strength of the post.

Researchers decided to investigate the potential for designs that included back-mounted vertical posts to increase the posts offset from the barrier front face and therefore minimize the potential for vehicle snag. Top mounted designs were avoided based on the observation of the top mounted sign test article crash tested by Caltrans researchers shown in Figure 18. The sign and post configuration was well within the ZOI and ultimately resulted in vehicle snag that caused occupant safety concerns [14]. This failed test demonstrates the importance of moving any barrier attachments as far out of the ZOI as possible.

4.4.2 Post-to-Parapet Attachment

Many state DOTs use bent clamps to attach vertical post to the back side of concrete barriers anchored to the top or back side of the bridge rail with drilled or adhesive anchors. While drilling to install post-installed anchors, reinforcement may be encountered and the construction team may choose to drill a new hole adjacent to the first one. Researchers preferred designs which permitted construction tolerances to allow construction teams to have flexibility, allowing the option to avoid barrier reinforcement if necessary.

4.4.3 Concrete Anchorage

Researchers only considered designs in which satisfactory concrete anchor strength could be achieved, such that the anchors would not be damaged during design wind, dead, or impact loads. As well, because post installation on the back side of the parapet was preferred, anchor configurations which simplified construction procedures including installation requirements for post-installed anchors were preferred.

To achieve this, the concrete anchorage must be designed to develop the full capacity of the vertical post, preventing damage to the anchorage from vertical loads, wind loads or loading that occur from vehicle impact scenarios. Anchor fasteners should not be damaged in any way that will diminish their functionality and the concrete should not need repairs after design impact events.

4.4.4 Wire Rope, Attachments and Termination

Wire rope was considered an efficient and optimized method of maintaining fence aesthetics and controlling component debris. In the Minnesota bicycle bridge rail system, the wire rope prevented the detachment of large rail structure, particularly in the full-scale crash test involving the single-unit truck. Wire rope is a primarily tensile element with little shear or bending resistance, making it a conducive element for use within the ZOI on the top of the barrier as a horizontal fence stiffener and fence alignment tool. Examples of tensile elements used in fence design were reviewed from state DOT designs such as the Florida DOT fence design shown Figure 36, which used tension wire along the top and bottom of the fence framework. Tension wire was also considered in the design due to similarity with wire rope. Note that tension wire consists of a single wire of increased thickness (e.g, 6- or 9-gauge) of the same nominal diameter as wire rope, but as a single wire and not a braided bundle of strands of wire.

A wire rope element was selected to span the entire length of the chain-link fence and terminate at the ends of the fence span. If the termination of the wire rope were to fail, the wire rope would lose tension and its ability to contain dislodged components of the debris fence. As such, all connections to the wire rope must be designed to develop the capacity of the wire rope.

Connections between the wire rope and fence components should not longitudinally fix the wire rope. Connections should be designed in this manner so that elongation from fence deformations is distributed over a nonlocal area. If the wire rope were fixed at each vertical post, the displacement of the fence framework during impact scenarios would be distributed over small wire rope sections, potentially producing large strains. Therefore, allowing longitudinal displacement reduces the wire rope's strain, consequently minimizing the potential for wire rope breakage.

4.4.5 Upper Horizontal Stiffener

A fence design which uses wire rope without longitudinal frame elements could reduce the aesthetics of the system. High wind loading environments may cause the fence to sway, and tolerances in the fence construction may cause the top of the fence to wander or appear irregular, which decreases the overall aesthetic quality. A laterally-stiff frame on the top of the fence may fix or hide fence irregularities and provide a "clean" appearance for the system, without compromising safety. A laterally-stiff structural member was incorporated on the top portion the parapet-mounted fence framework to provide continuity between each vertical post. This horizontal member should support the top of the chain-link mesh and function as a reliable connection point between the mesh, post and wire rope.

Any deformation of a horizontal stiffener would reduce the aesthetics of the fence and should not occur from vertical loads which include dead and ice or snow loads, plus the concern that a person could attempt to climb the fence. The horizontal stiffener should also incorporate a retention cable, wire rope, or tension wire which will prevent debris from falling onto railroad tracks in the event of the fracture of fence post components during a vehicle impact. The upper stiffener should also allow access to the wire rope for repairs, if needed.

4.4.6 Lower Horizontal Stiffener

States commonly use small diameter pipes or tension wires as horizontal stiffening members in debris fence designs. A lower longitudinal member will also be incorporated in the debris fence to help maintain the chain-link fabric during high wind situations. The appearance of the bottom portion of the fence is especially important since it is located in the horizontal line of sight of drivers. Additionally, this member will serve as a means of vandal protection by increasing the difficulty of lifting the bottom portion of the fence fabric, preventing debris from being shoved under the fence. The addition of a lower horizontal member however must not reduce the crashworthiness of the fence by introducing any potential spear or snag hazards during impact events.

5 DEBRIS FENCE DESIGN CONCEPTS

5.1 Overview

Design of the debris fence included the development of various debris fence component concepts. The components and features considered were the post shape, post failure mode, and post-to-parapet attachments. Design objectives such as crashworthiness, cost, constructability, and aesthetics were considered when selecting these concepts.

5.2 Post Shape

Five post shape concept were identified which consisted of vertical, offset, bent, and curved post shapes as shown in Figure 68. The first and second concepts use vertical posts. In the second concept, additional components would be placed in between the barrier and posts to achieve a larger post offset from the front barrier face. Concepts three and four consist of the fence posts bent backwards near the barrier top face. The last concept consists of curving the top of post, similar to the Florida DOT fence design.

Curving the fence at the barrier was not pursued due to the complexity of curving the fence fabric to close the gap between the barrier back face and the post offset. The offset vertical post option was not selected for this same reason. Curved or bent post options were also not desired due to the increased post fabrication cost. Fences with posts curved at the top are typically used adjacent to walkways since they increase the difficulty of climbing over the top of the fence. Curving the top of the posts has limited benefits since the Iowa parapet-mounted fence is designed to be installed adjacent to the roadway which typically will not have pedestrian traffic.

The bent post concept was not pursued since the maximum barrier-post offset is achieved well above the barrier top face. Post offset near the barrier top is limited in this concept and is of most importance since the vehicle intrusion over the barrier is the largest in this region for TL-3 impacts. For the reasons mentioned here, the debris fence design continued with the vertical, straight post attached directly on the barrier back face.

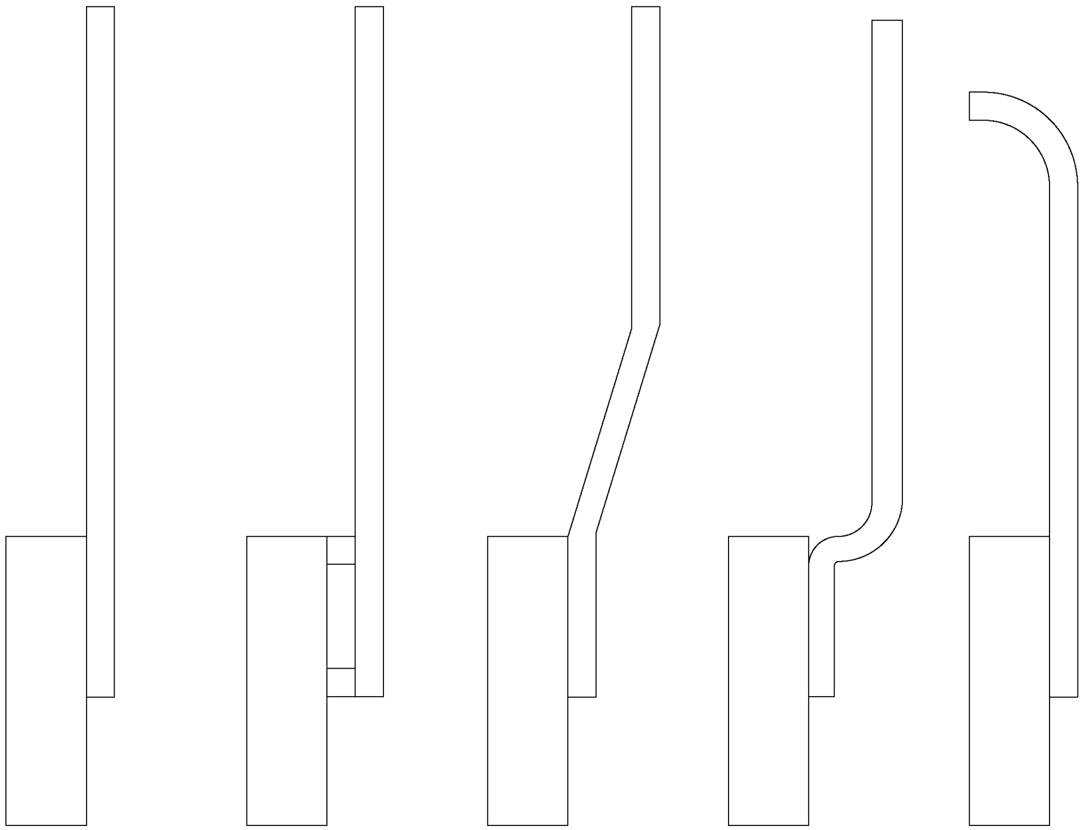

Figure 68. Post Shape Concepts

5.3 Post Failure Mode

Next, fasteners and post-to-concrete parapet attachments were designed to withstand design loading without damaging the concrete bridge rail. Fasteners were designed to withstand the total failure of post members, which is dependent on the selected post and the post mounting location. For example, increasing the vertical distance between the barrier top and the post-to-parapet attachment bracket magnifies the bending moment on the vertical post.

The two vertical post failure modes that are applicable for impact loading scenarios is bending and shear failure. Shear failure was not preferred since this would most likely result in the vertical posts detaching near the post-to-parapet bracket, which could result in fence debris becoming a hazard for railroad operations. This was the same reason why section reduction methods, such as cutting material from the vertical posts, were not considered in the design. Removing material from vertical posts increases the likelihood of post detachment. The vertical post size and post connection was selected to promote bending rather than section reduction via material removal.

5.4 Post-to-Parapet Attachment Design

Saddle brackets, shown on the top left corner of Figure 69, where initially selected as the post- to-concrete parapet attachment hardware. This was primarily due to the simplicity of this part and since they are typically used by other state DOTs with back-mounted fences. The impact loading analysis, outlined in Section 6.3.9, indicated that a large anchor spacing would be required to develop the vertical post capacity. This in turn required the saddle bracket to be much longer and would therefore fail in flexure. To mitigate flexural failure, gussets were added to the saddle brackets and to simplify fabrication, square HSS was used to house the vertical posts. The design of the gusseted post bracket is shown on the bottom left corner of Figure 69.

In state DOT designs with saddle-mounted vertical posts, installation of the saddle brackets requires that the vertical post be held in place while the saddle brackets are bolted to the barrier. Researchers considered an additional bracket concept that would simplify the fence installation by eliminating the need to hold the vertical post in place during installation. This design, shown in Figure 69, merges both saddle brackets by using one long square HSS tube socket. Installation of this part would consist of bolting the bracket to the barrier followed by inserting the vertical post into the tube socket that would rest on a tab welded to the underside of the tube socket. The drawback of this concept is that the added tube material increases the weight of this part. Researchers decided that the benefit of simplifying installation outweighed the increased weight and continued the design of the post-to-parapet attachment bracket with the tube socket design concept.

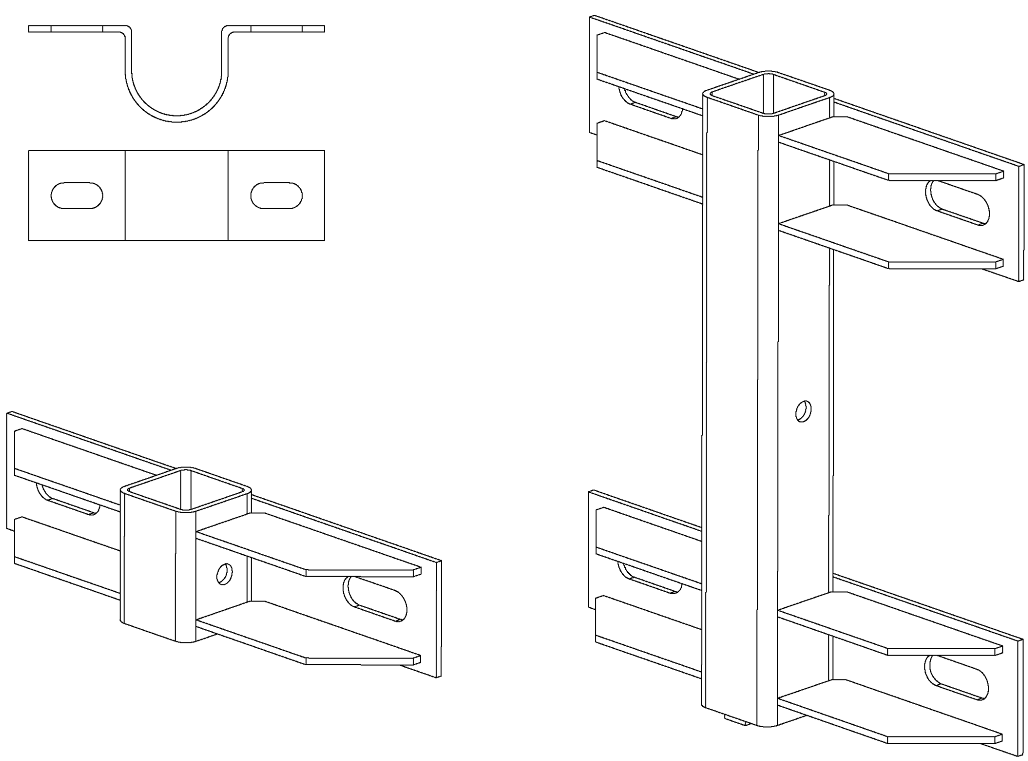

Figure 69. Post-to-Parapet Attachment Concepts

6 PARAPET-MOUNTED DEBRIS FENCE DESIGN

6.1 Overview

During the service life of the debris fence, severe loading could occur from high wind events, atmospheric icing, and from individuals climbing the fence. Fence components and associated connections were configured to withstand the combined loading at design load conditions. The analysis process used to evaluate hardware is illustrated in Figure 70. First, design loads were established in accordance with ASCE 7-16 *Minimum Design Loads and Associated Criteria for Buildings and Other Structures* [40]. Next, the fence vertical post was selected to meet the capacity needs for bending, ice, wind, and live load combinations, but minimized to mitigate snag risk for vehicles impacting the bridge rail and extending into the ZOI. The impact load was identified based on the assumption that a vehicle would plastically deform the post in bending at the connection to the post-to-parapet attachment bracket. These impact loads were used to design the post-to-parapet attachment bracket and concrete anchorage to meet the minimum capacity. Lastly, the upper horizontal stiffener, also referred to as cap rail, and debris retention connection with wire rope were designed.

Vertical posts, post-to-parapet brackets, cable brackets, and cap rails were designed utilizing the *AISC Steel Construction Manual* [41]. The concrete anchorage was designed using the *Building Code Requirements for Structural Concrete (ACI 318-14)* [42]. Additional procedures outlined in the *AISC Steel Design Guide 9* [43] were followed to develop the cap rail. Detailed design procedures that include equation references are shown in Figures 71 through 73. The design procedure and associated assumptions are discussed in this chapter, while complete design calculations are presented in Appendix A through Appendix F.

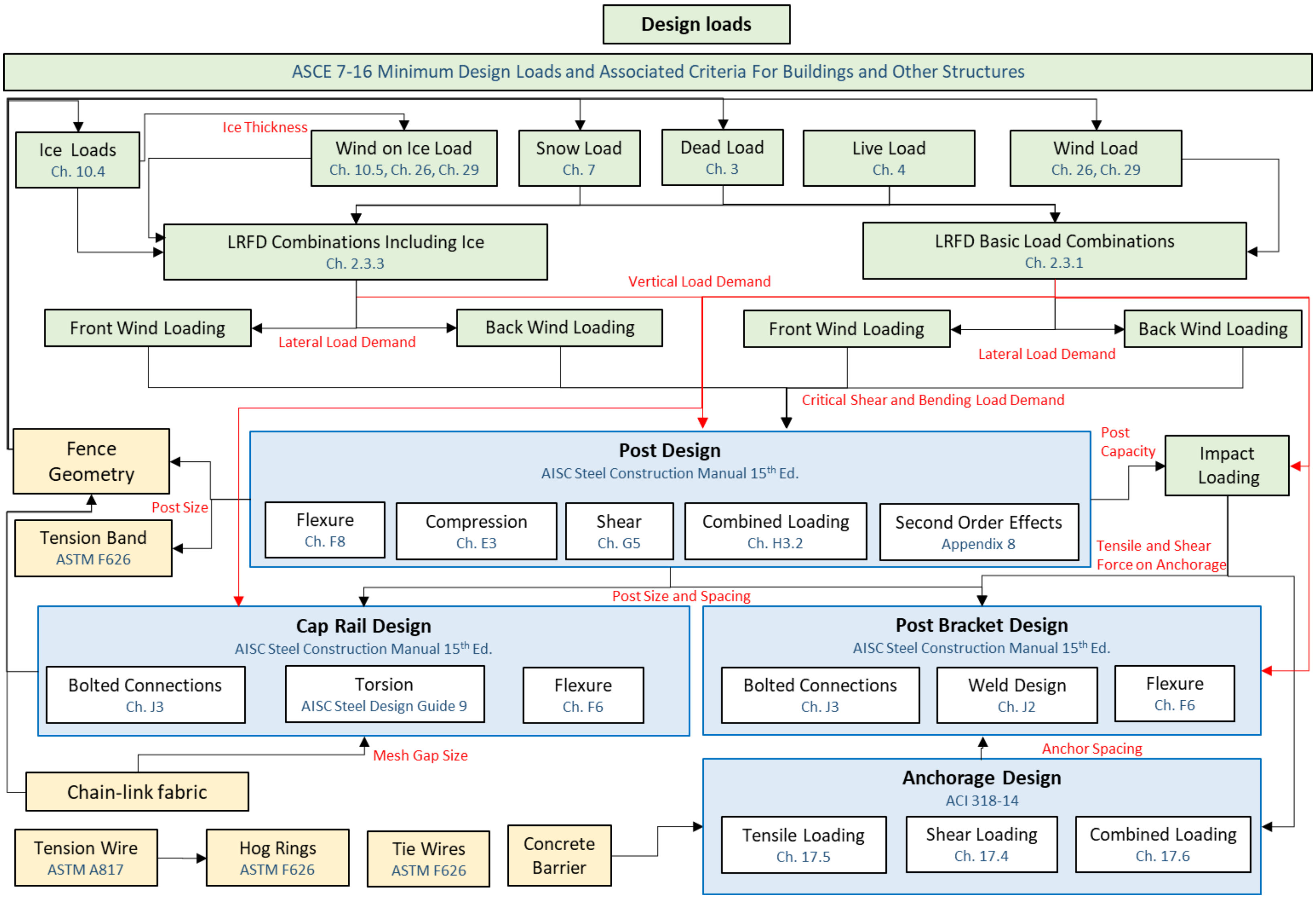

Figure 70. Iowa Parapet-Mounted Fence Design Procedure

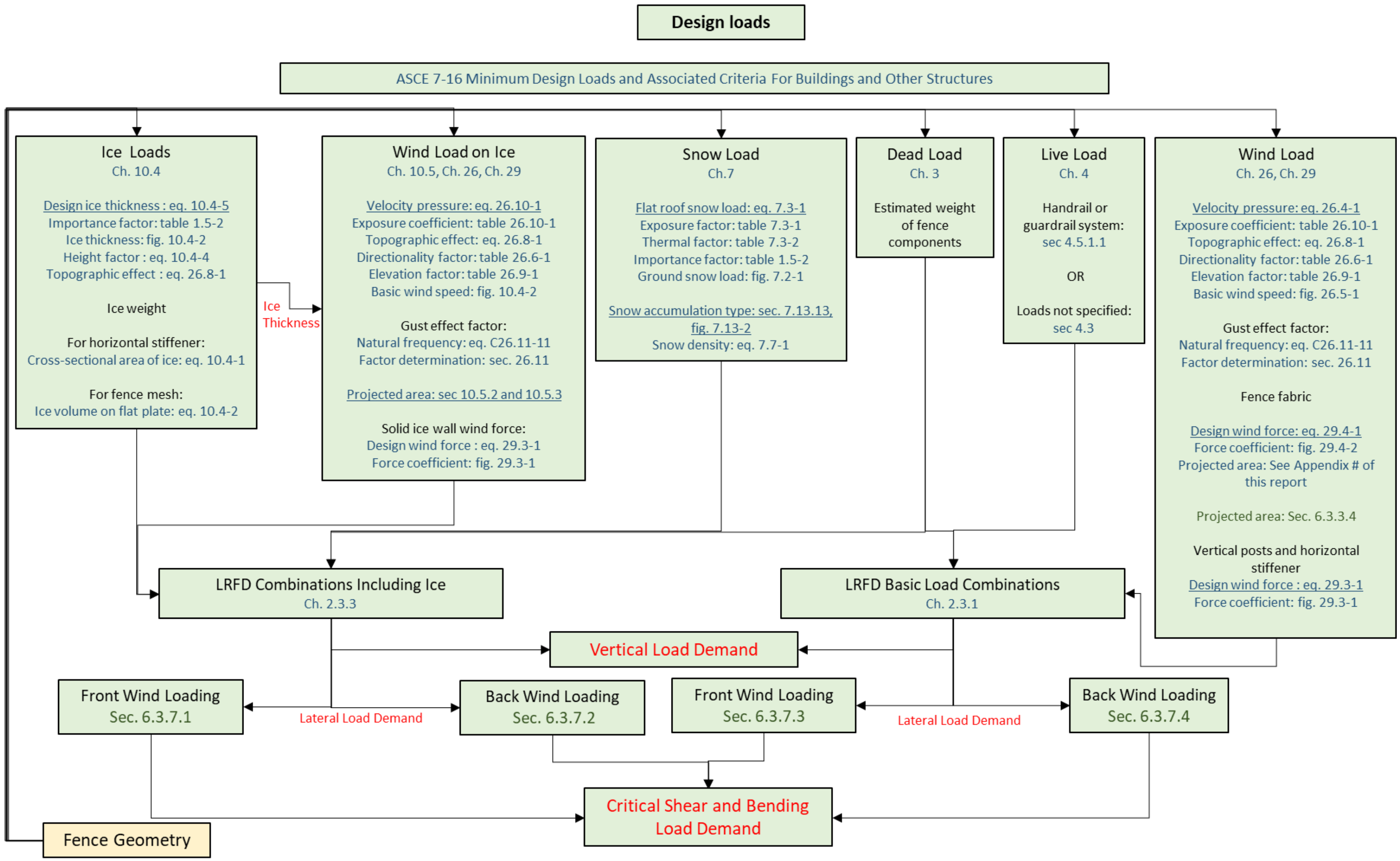

Figure 71. Iowa Parapet-Mounted Fence Design Procedure (continued)

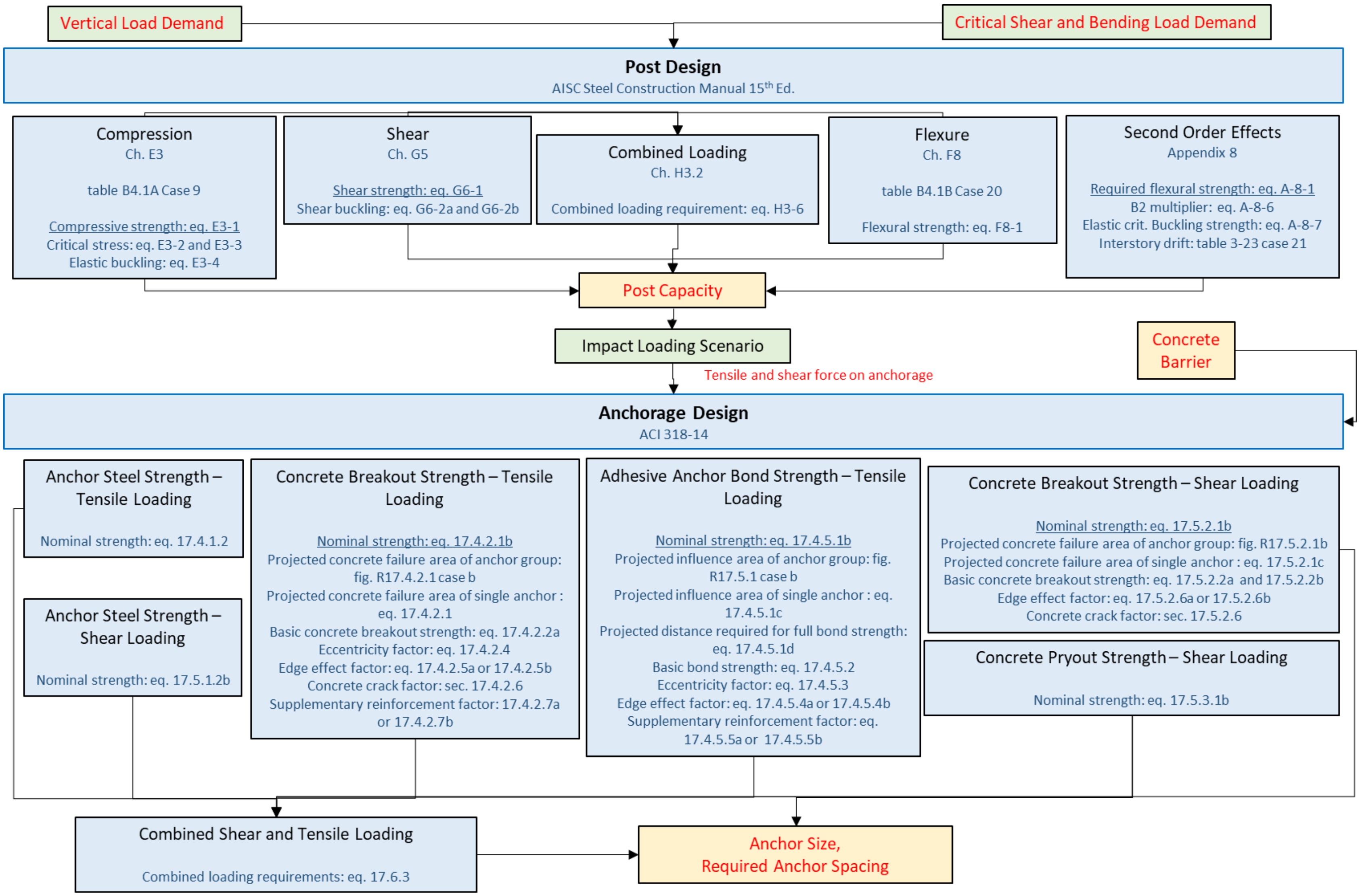

Figure 72. Iowa Parapet-Mounted Fence Post and Anchorage Design Procedure

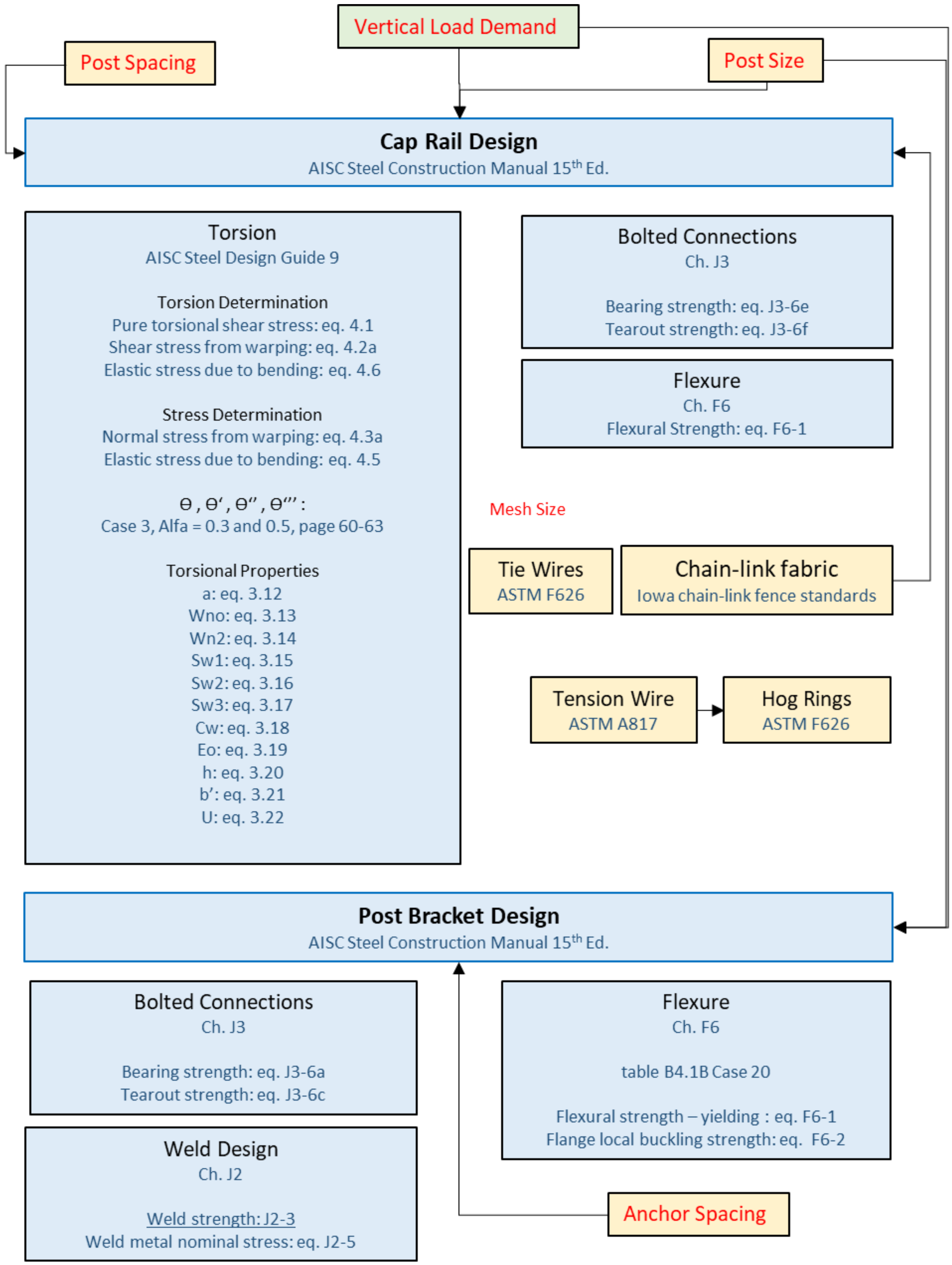

Figure 73. Iowa Parapet-Mounted Fence Horizontal Stiffener and Post Bracket Design Procedure

6.2 Preliminary Vertical Post Selection and Post Spacing

Prior to the establishment of design loads and subsequent fence hardware design, the *Chain Link Fence Wind Load Guide for the Selection of Line Post and Line Post Spacing (WLG 2445)* [44] was consulted to determine a baseline post size and post spacing used at the initial revisions of the fence design. To determine the recommended post size and post spacing, general design parameter were identified.

Current Iowa DOT requirements dictate the following:

1. Any item placed along the roadway must withstand wind gusts up to 90 mph.
2. Standards state that the wire height of the structure must be at least 6 ft tall.
3. The mesh gap size must be at least 2 in. and should be composed of #9 gauge wire.

In discussion with Iowa DOT, a 36-in. tall standardized parapet was identified for the candidate exemplar parapet to attach the debris fence. Parapet selection is discussed in Chapter 8. As a result, it was determined that a 7-ft fence would be required to meet UP-BNSF height requirement for parapet-mounted fencing on railway overpasses. Next, researchers selected a maximum wind speed of 105 mph based on Risk Category I from ASCE 7-16, which was higher than Iowa's guidelines. Using this information, the requirements set by Iowa DOT, geographical and weather conditions in Iowa along with Equation (1), post spacing and their respective post options were determined.

$$S' = S(C_1)(C_2)(C_3) \tag{1}$$

Where: S'= Recommended post spacing (ft)

S= S value based on post properties

C_1= 7.26, Coefficient for mesh and fabric size

C_2= 0.55, Wind exposure category coefficient

C_3= 0.45, Ice exposure coefficient

A table of relationships between post spacing and size based on different standard material grades was developed, as shown in Table 6. State DOT chain-link fence designs incorporate post spacing configurations that range from 5 ft to 10 ft. As such, candidate post options which could be spaced between 5 and 10 ft were identified, with preference for the optimization of least number of posts and smallest post section. Of the post spacing options, an 8-ft post spacing was preferred which would satisfy Iowa DOT requirements and which could be suitable for other state DOTs as well. Based on the WLG 2445 recommendations, the optimized post option with a post spacing near 8 ft was the 2⅞ -in. diameter ASTM F1043 Group 1C post and was adopted as the baseline post size.

Table 6. Calculated Vertical Post Spacing for Pipe Options Based on Post Strength

Post Diameter (in.)	WLG 2445 Recommended Post Spacing (ft)		
	ASTM F1043 Sch. 40 Group IA (30 ksi)	ASTM F1043 Sch. 40 Group IA (50 ksi)	ASTM F1043 Group 1C (50 ksi)
1.875	N/A	N/A	2.2
2.375	2.9	4.9	4.1
2.875	5.7	9.5	7.9
3.5	9.5	15.8	12.4
4	13.5	N/A	16.5
6.625	48.2	80.3	N/A
8.625	95.2	N/A	N/A

N/A – Not Applicable

In the following sections additional design analysis will be discussed which were completed to determine design loads on the fence structure and individual fence components. Further analyses of vertical posts were conducted to verify that the WLG 2445 post recommendation was capable of withstanding the combined LRFD load effects for an 8-ft post spacing configuration and to identify additional post options.

6.3 Design Loads

Debris fence evaluations were performed on a fence section spanning between the midpoints between consecutive posts, with loads acting on a single post. This was done such that the fence design was less dependent on the installation length as it may vary depending on the construction site needs. For the design to be completed on a fence section basis, the vertical post spacing had to be established since this will affect how much loaded area of fence each vertical post must sustain. An 8-ft post spacing was considered when developing design loads and other fence design aspects based on the WLG 2445 recommendations. The determination of design loads per ASCE 7-16 guidelines will be described in the following section while a summary of the design load determination is provided in Section 6.3.6.

6.3.1 Dead and Live Loads

Dead loads of the fence system were determined by estimating the weight of each fence component acting per post, which was defined as one fence section. Live loads are specified in ASCE 7-16 for handrail or guardrail systems; however, live loads of fences or other lattice structure are not specified. There exists a potential that individuals could climb on the fence fabric, and though this is undesirable, the fence was designed not to experience permanent deflection resulting from a 750-lb live load of three 250-lb persons hanging on an 8-ft fence section.

Live loads are specified for pedestrian and bicycle railings in the AASHTO LRFD Bridge Design Specifications guidelines [45]. However, these guidelines apply to pedestrian and bicycle railings which are to be installed on sidewalks with curbs for low-speed applications or on sidewalks shielded by concrete barriers for high speed applications. The parapet-mounted fence designed in this effort was developed to meet MASH 2016 TL-3 requirements which is not considered a low-speed application. Therefore, if this parapet-mounted debris fence were to be used to protect pedestrians and bicyclists, it must be shielded by an additional barrier. However, designing a fence that was shielded by an additional barrier was not the aim of this effort. This parapet mounted-debris fence is to be installed adjacent to the roadway and is not expected to typically experience pedestrian live loads. For these reasons, the loads specified in the AASHTO LRFD Bridge Design Specifications were not considered.

These provisions do specify a design load for chain link fences which is 0.015 k/sf acting normal to the fence when used as a pedestrian railing. Also, for bicycle railings, these provisions specify that when the rail height exceeds 54 in. above the riding surface, that design loads shall be determined by the Designer [45]. It also mentions that for railings taller than 54 in. the design live load for posts should be applied 54 in. above the riding surface with the post live load determined using Equation (2). As previously mentioned, the debris fence was not specifically designed to meet these design loads.

$$P_{LL} = 0.20 + 0.050L \; (AASHTO\ 13.8.2 - 1\,) \tag{2}$$

Where: P_{LL}= Concentrated design live load, (kips)

L=Post spacing, (ft)

6.3.2 Snow Load

The ASCE published information regarding snow loading experienced by buildings and other structures based on geographical placement of the structure. ASCE 7-16 guidelines mention that snow loading should be considered on any structure that will accumulate snow and were followed to determine its effects on the fence structure. The snow loading that would be experienced by a flat roof (with narrow width) was found using Equation (3).

$$p_f = 0.7C_eC_tI_sp_g(ASCE\ 7 - 16\ 7.3 - 1\,) \tag{3}$$

Where: p_f= Flat roof snow load, (lb/ft^2)

C_e=0.9, Exposure factor for fully-exposed, roughness C

C_t=1.2, Thermal factor for unheated, open air structure

I_s=0.8, Snow importance factor

p_g=40 lb/ft^2, Ground snow load

The exposure factor for the fence structure was selected as full-exposed installed near terrain with a Surface Roughness category C. Roughness Category C was selected since it is the worst-case scenario for the exposure factor determination. Additionally, the fence could be installed near flat, open country or grasslands, which are defined as Surface Roughness C by ASCE 7-16 guidelines. The thermal factor was then selected for an unheated open-air structure since these conditions are expected for most fence installations. Ground snow loading was determined from Figure 7.2-1 of ASCE 7-16 for conditions in Iowa.

Snow, ice, and wind load determinations per ASCE 7-16 are modified by an importance factor for each respective load type. The magnitude of these importance factors, defined in ASCE 7-16, are dictated by the selected Risk Category of the structure. ASCE 7-16 gives guidance for selection of Risk Category for certain structures such as unoccupied buildings (Risk Category I), commercial buildings (Risk Category II), and hospitals (Risk Category IV), however, no guidance is given on structures designed for roadside safety purposes. Chapter C1.5 of ASCE 7-16 gives additional guidance in the selection of Risk Category, relating it to number of lives placed at risk. Risk Category I is applicable when approximately two people may be affected by the structure's failure while Risk Category II is associated with about two to two hundred people affected by the structure failure [40].

For the debris fence designed for the Iowa DOT, researchers decided to assign a Risk Category I to the debris fence for two reasons. First, failure of the fence due to severe weather effects would most likely cause the fence to plastically bend which would not pose a significant risk to occupants in vehicles on the roadways. Adding to this, an extreme weather event may occur that imposes more severe wind loading, for example an EF4 or EF5 tornado, which could cause the fence to fully detach and pose a much higher risk. However, elevating the Risk Category to Category II will most likely not prevent the detachment of the fence during these extreme weather events. The second reason being that increasing the Risk Category would require a stiffer vertical post which increases loads transmitted to the concrete anchorage and, more importantly, reduces the crashworthiness of the fence-barrier structure. This is because elevating the Risk Category will increase the load demand, requiring a stiffer vertical post which could subsequently increase the snag potential between the post and an errant vehicle during impact scenarios.

Once the flat roof snow was determined, it was adapted for use with the fence structure by guidelines in section 7.13.3 of ASCE 7-16 [40]. These provisions apply snow loading effects to components with limited widths such as pipes and cable trays and were followed to identify the weight of snow that could accumulate on the fence's horizontal stiffeners. Snow accumulation on the fence fabric was not considered in establishing snow loads as is it expected that snow accumulation on the fabric will be minimal compared to that on the cap rail. On the cap rail, snow accumulation can occur with triangular or trapezoidal cross-sections, depending on the cap rail width.

When $w \leq \frac{0.73p_f}{\gamma}$ snow loading is calculated in accordance with Figure 74

When $w > \frac{0.73p_f}{\gamma}$ snow loading is calculated in accordance with Figure 75

Where: w = Width of cable tray or diameter of pipe, (in.)

p_f = Flat roof snow load, (lb/ft^2)

γ = Snow density, (lb/ft^3)

Snow density is calculated using Equation (4) and shall not exceed 30 lb/ft^3.

$$\gamma = 0.13p_g + 14\ (ASCE\ 7-16\ 7.7-1) \tag{4}$$

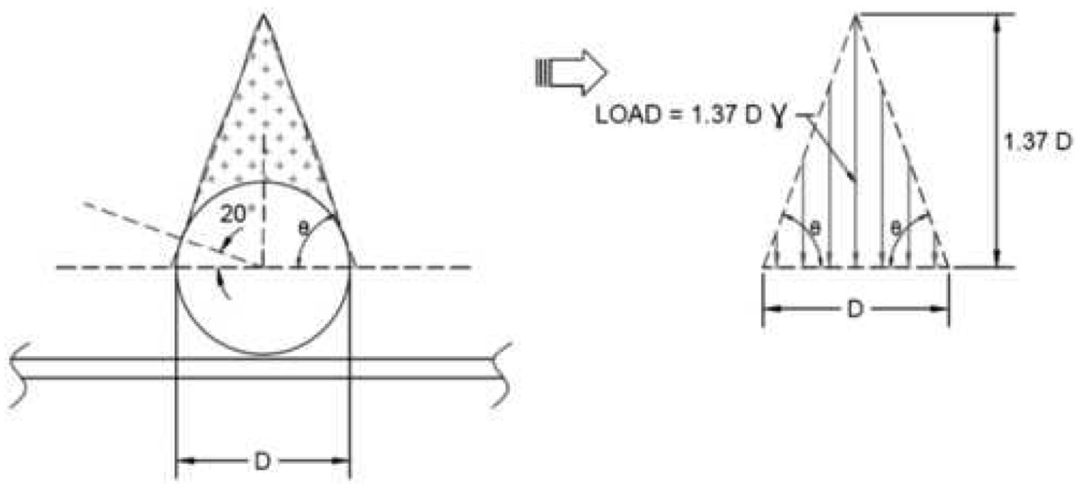

Note: D, pipe diameter $+2x$ insulation thickness (as applicable); P_f, flat roof snow load; θ, assumed angle of repose = 70°

Figure 74. Triangular Snow Loading on Pipes and Cable Trays [40]

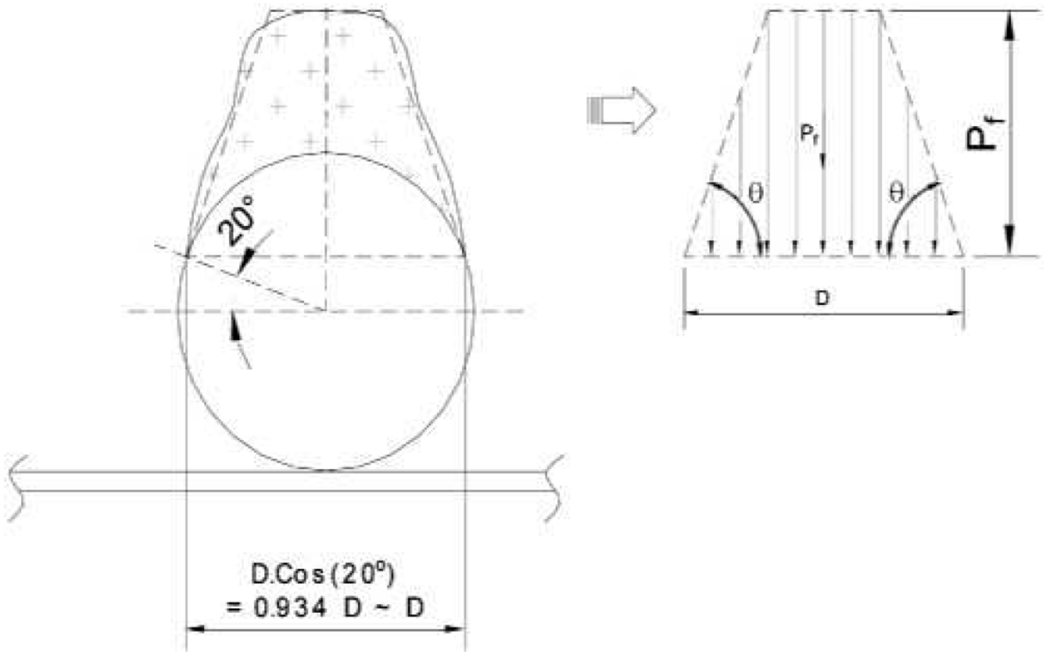

Note: D, pipe diameter $+2x$ insulation thickness (as applicable); P_f, flat roof snow load; θ, assumed angle of repose = 70°

Figure 75. Trapezoidal Snow Loading on Pipes and Cable Trays [40]

6.3.3 Minimum Design for Wind Loading

The ASCE published information regarding the typical wind loads that buildings and other structures experience based on expected wind velocities and geographical placement of the structure. These guidelines were followed to determine maximum wind loading on the debris fence structure. The equation for calculating the maximum expected wind loads on the fence fabric, vertical post, and upper horizontal stiffener is shown below.

$$F = q_z G C_f A_f \ (ASCE\ 7 - 16\ 29.4 - 1) \tag{5}$$

Where: F = Maximum wind load, (lb)

q_Z = Velocity pressure at height z, (lb/ft^2)

G = 0.85, Gust-effect factor

A_f = Projected area normal to the wind, (in^2)

C_f = Force coefficient

For the determination of wind force on the fence post and upper horizontal stiffener, the projected area (A_f) was replaced with the gross area of each respective member.

6.3.3.1 Velocity Pressure

The first step in determining wind loads was to calculate the maximum overall velocity pressure imparted on the fence structure. The equation for this pressure calculation is shown below and is given in Section 26.10.2 of the ASCE guidelines. Using this equation, the velocity pressure imposed on the debris fence structure was determined for the fence, vertical post, and upper horizontal stiffener.

$$q_z = 0.00256 K_z K_{ZT} K_d K_e V^2 \ (ASCE\ 7-16\ 26.10-1) \tag{6}$$

Where: q_z = Velocity pressure, (lb/ft^2)

K_Z= Velocity pressure exposure coefficient

K_{ZT} =1, Topographic factor

K_d = Wind directionality factor

K_e= 1, Ground elevation factor

V =105 mph, Basic wind speed in Iowa

The velocity pressure exposure coefficient is dependent on the height above ground level of the installed structure and the ground surface roughness surrounding the structure. Since fences will be installed on railway overpasses, a 100-ft roadway height was assumed for the determination of the velocity pressure exposure coefficient. Considering this, along with the 10-ft fence height as specified by UP-BNSF requirements, the fence fabric and vertical post velocity pressure was determined at a 105-ft height while that of the upper horizontal stiffener was defined for a 110-ft height. Surface roughness D, defined as flat unobstructed areas, was considered for the selection of the velocity pressure exposure coefficient since it is possible that fence installations in Iowa may be located near flat grass planes.

Wind speed rise effects, shown Figure 76, can occur when structures are installed on unobstructed hills, ridges, or escarpments [40]. These wind speed rise effects occur as wind gusts interact with hills causing the velocity to increase as the wind gust passes over the hill. This effect may occur in Iowa since there may be some topographic regions where fences are installed near reasonably flat, undulating grass planes. Considering that fences will be installed on elevated structures over railways, wind speed-up effects will be mitigated since wind can flow through the railway passage. An illustration of this effect is shown in Figure 77.

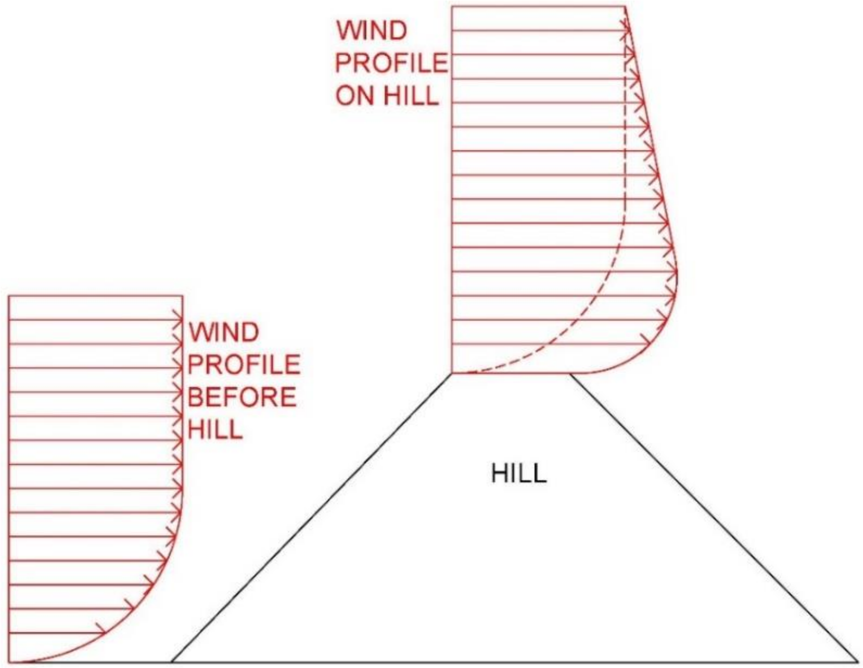

Figure 76. Topographic Wind Speed Up Effects

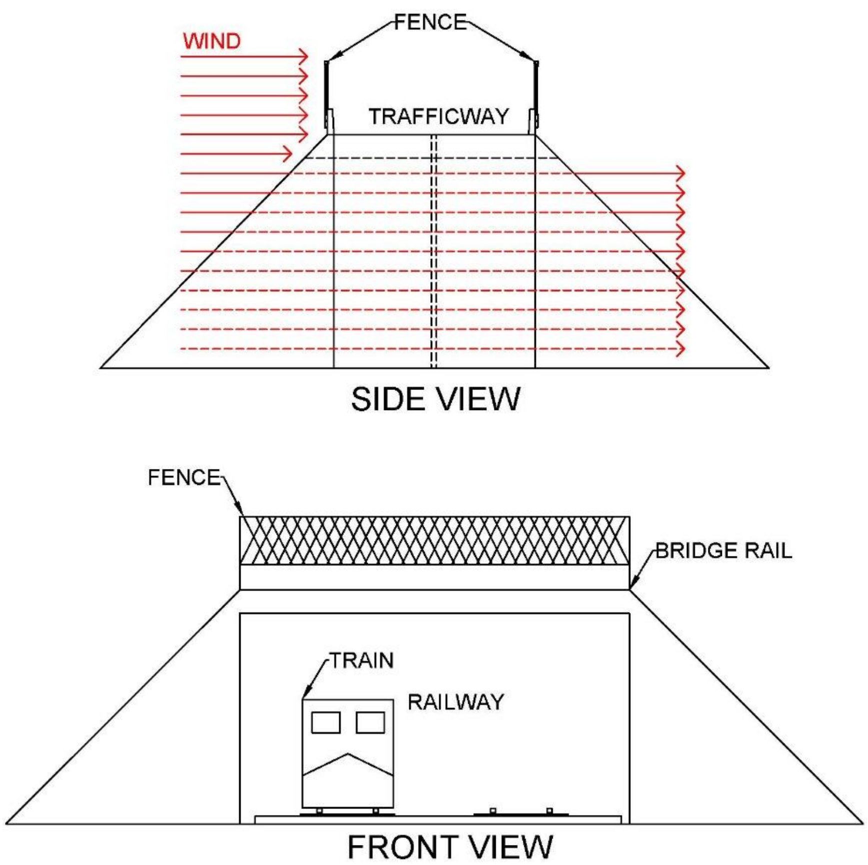

Figure 77. Reduced Topographic Effect Due to Railway

For the fence fabric, the wind directionality factor was selected for single plane open frame structures while the upper horizontal stiffener was considered a solid-free standing sign with the directionality factor selected as such. As for the vertical post, Table 26.6-1 of ASCE 7-16 specifies a directionality factor of 0.95 for round structures used with non-axisymmetric structural systems.

A ground elevation factor equal to 1 was used as a conservative approximation based on ASCE guidelines [40]. The basic wind speed used to calculate the velocity pressure on the fence fabric, vertical post, and upper horizontal stiffener was determined from Figure 26.5-1A of ASCE 7-16 for conditions in the state of Iowa. Note that the design wind speed of 105 mph exceeded Iowa's fence criteria to withstand wind loads of 90 mph for 3-second increments.

6.3.3.2 Gust Effect Factor

For rigid structures, which are structures with fundamental natural frequencies greater than or equal to 1 Hz, the gust effect factor is permitted to be taken as 0.85 [40]. In the debris fence structure, the natural frequency of the vertical post was selected and determined using equation (7). It was determined that the potential post options in deliberation had a natural frequency greater than one, and therefore the fence system was considered a rigid structure. For example, using this equation, an HSS round tube with a diameter of 2⅞ in. and a 0.188-in. wall thickness had a natural frequency of 11.6 Hz.

$$n_1 = \frac{0.56}{h^2}\sqrt{\frac{EI}{\mathrm{m}}}\ \ (ASCE\ 7-16\ C26.11-11) \tag{7}$$

Where: n_1 = Fundamental natural frequency, (Hz)

E = Modulus of elasticity, (MPa)

I = Second moment of area, (m^2)

h = Height, (m)

m = Mass per unit height, (kg/m)

6.3.3.3 Force Coefficient

The force coefficient for wind loading on the fence fabric was found using Figure 29.4-2 of the ASCE 7-16 guidelines. The fabric's wire diameter and solidity ratio along with the velocity pressure posed on the fabric were used in the determination of the force coefficient. Derivation of the solidity ratio, which is the ratio between net area and gross area in one diamond mesh spacing, was determined for the selected 9-gauge fence fabric size. An illustration of how the net and gross area of one chain-link fence diamond was considered is shown in Figure 78 and full details of this procedure are presented in Appendix A. The projected area in one fence section was then determined by the product of the solidity ratio and area of fence in one fence section.

Force coefficients for wind loading on the post and horizontal stiffener were found using figure 29.3-1 of the ASCE 7-16 guidelines. To use these guidelines, the horizontal stiffeners and vertical posts were considered solid free-standing signs with the wind acting normal to these components. The gross area of each of these components was determined and used to identify the wind force on each component.

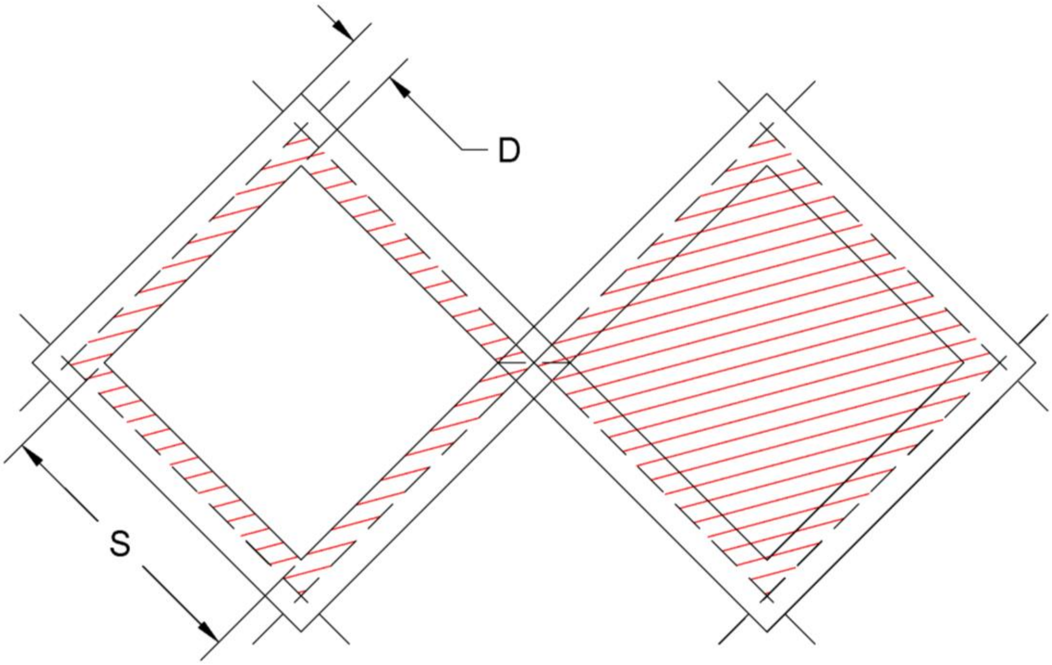

Figure 78. Net (Left) and Gross (Right) Projected Area of a Chain-Link Diamond

6.3.4 Ice Load

The ASCE published information regarding the typical icing effects that buildings and other structures experience based on geographical placement. These guidelines were followed to determine ice loading that occurs from the accumulation of ice. This was done by calculating the design ice thickness which can accumulate on each component the fence system. Prior to this calculation, the nominal ice thickness accumulation in Iowa was determined from Figure 10.4-2 of ASCE 7-16.

$$t_d = tI_i f_z (K_{zt})^{0.35} \ (ASCE\ 7-16\ 10.4-5\ ) \tag{8}$$

Where: t_d=Design ice thickness, (in.)

t= 1.5 in., Nominal ice thickness in Iowa

I_i= 0.8, Importance factor for ice thickness

f_z= 1.12, Height factor

K_{zt}= 1, Topographic factor

A structure at an increased vertical distance above the ground will result in elevated winds speeds that intensify icing effects. In the height factor formulation, z represents the height above ground level, defined as 105 ft., as used in Equation (9)

$$F = (\frac{z}{33})^{0.10} (ASCE\ 7-16\ 10.4-4\ ) \quad (9)$$

The weight of ice accumulated on all exposed surfaces of the fence structure was found by first calculating the cross-sectional area of ice on these surfaces. The cross-sectional area of ice on structural shapes was found using Equation (10).

$$A_i = \pi t_d (D_c + t_d)\ (ASCE\ 7-16\ 10.4-1\ ) \quad (10)$$

Where: A_i= Cross-sectional area of ice, (in.^{2})

t_d= Design ice thickness, (in.)

D_c= Diameter of a cylinder circumscribing an object, (in.)

Applying Equation (10) to the fence fabric would over-compensate the cross-sectional area and consequently overcompensate the weight of ice imposed on the fence framework. This occurs since the cross-sectional area of ice on one chain-link wire segment overlaps with the cross-sectional area of ice on other chain-link wire segments in the same chain-link diamond. For this reason, the fence fabric was treated as a flat plate and Equation (11) was used to find the volume of ice accumulated on the fence fabric.

$$V_i = \pi t_d A_s\ (ASCE\ 7-16\ 10.4-2\ ) \quad (11)$$

Where: V_i= Volume of ice, (in.^{3})

t_d= Design ice thickness, (in.)

A_s= Area on one side of plate, (in.)

6.3.5 Minimum Design for Wind Loading on Ice Covered Structures

Wind loading on the ice-covered fence structure was investigated to ensure that the fence could withstand increased wind speeds during icing effects. This condition must be studied since the surface area of the fence fabric normal to the direction of wind increases as ice accumulates on the fence structure. In a worse case scenario, the accumulation of ice could cover the openings in the fence fabric, producing a solid wall. For this reason, the ice-covered fence structure was treated as a solid free-standings sign and section 29.3 of the ASCE 7-16 guidelines were followed to find the force coefficient used for wind on ice-covered structures load calculations. These assumptions were considered highly conservative as icing which causes full impedance of the fence with 2-in. typical gap openings would likely be a rare event.

6.3.6 ASCE 7-16 Design Loads Summary

The established ASCE 7-16 design loads pertaining to the debris fence are summarized in Table 7. Loads are organized by what component they apply to consisting of the chain-link fabric, vertical post, and upper horizontal stiffener. Although these loads are presented with the component they are initially applied to, loads will transfer to other components via their connections. Note that the vertical post dead load includes the weight of the splice connection used to attach horizontal stiffeners to posts. Additionally, the wind loading with ice effects produces a single wind load applied to the ice-covered fence structure. These loads were used to determine load combinations that could be imposed on the fence structure in the following section.

Table 7. ASCE 7-16 Design Loads Summary, 8-ft Fence Section

Load Direction	Load Type	Chain-link Fabric	Vertical Post	Horizontal Stiffener
Applied to fence vertically	Dead (lb)	39.8	112.9	87.7
	Live (lb)	750	0	0
	Snow (lb)	0	0	55.9
	Dead Ice (lb)	855.1	0	127.1
Lateral loads on fence	Wind (lb)	284.4	107.3	212.9
	Wind on Ice (lb)	744.6		

6.3.7 LRFD Load Combinations

The combination of lateral wind loads and vertical loads consisting of dead, dead-ice, live, and snow loads must be accounted for to ensure that fence components and their connections do not fail. The LRFD Load combination provisions of the ASCE 7-16 guidelines were followed to identify the worst-case combined loading scenarios. Loading effects are separated into two combinations, a basic set and a set including atmospheric icing loads, shown Tables 8 and 9, respectively. Note that roof and rain loads were not included since their effects do not critically load the fence structure.

Table 8. LRFD Basic Load Combinations

Comb. No.	Combination	Vertical Load (lb)	Lateral Load (lb)		
			Mesh	Post	Cap Rail
1	1.4Dead	336.5	0	0	0
2	1.2Dead+1.6Live+0.5Snow	1516.5	0	0	0
3a	1.2Dead+1.6Snow+Live	1127.9	0	0	0
3b	1.2Dead+1.6Snow+0.5Wind	377.9	142.2	53.7	106.5
4	1.2Dead+Wind+Live+0.5Snow	1066.5	284.4	107.3	212.9
5	0.9Dead+Wind	216.3	284.4	107.3	212.9

Table 9. LRFD Combinations Including Atmospheric Ice Loading

Comb. No.	Combination	Vertical Load (lb)	Lateral Load (lb)
1	1.2Dead+1.6Live+0.2Dead-Ice+0.5Snow	1712.9	0
2	1.2Dead+Live+Dead-Ice+Wind-Ice+0.5Snow	2048.5	744.6
3	1.2Dead+Dead-Ice	1198.5	0
4	0.9Dead+Dead-Ice+Wind-Ice	1270.7	744.6

The worst-case load combination of each fence component was used for its respective design. For the vertical post design, basic combination number 4 and ice combination 2 were identified as the worst-case load combination since they produced the largest combination of vertical and lateral loads, and subsequent moment-bending. When determining critical loads for impact loading situations, the largest vertical load from these combinations was applied as a shear load onto the anchorage. This was done since the vertical force will combine with the shear load imposed on the anchorage from longitudinal impact forces. Correspondingly, lateral impact forces (perpendicular) will impose a tensile force on the anchorages. Vertical forces did not have the same effect during impact loading when considering the vertical post since the section is circular and loading is therefore omnidirectional.

6.3.8 LRFD Static Load Analysis

Once design worst-case critical load combinations were determined, a static analysis was conducted to determine critical forces and moments experienced by the fence framework caused by LRFD loads. The components of this debris fence can potentially be subjected to a total of four different LRFD loading conditions:

1. A wind load on the front, traffic side, of the fence;

2. A wind load on the back of the fence;

3. An ice-covered fence, front wind load scenario; and

4. An ice-covered fence, back wind load scenario.

For loads to be calculated for these conditions, it was assumed that the top and bottom anchorage would be located 10 in. and 27½ in. from the barrier top surface, respectively. This anchor spacing configuration was determined from the concrete anchorage design which was selected to maximize the anchorage capacity.

6.3.8.1 Front Wind Loading

Lateral wind blowing onto the front side of the fence structure, consisting of the vertical posts, chain-link mesh, and cap rail, will place a shear and subsequent moment load onto the vertical post. Note that for a cantilever beam, the distributed wind loads can be simplified to effective point loads and produce an equivalent maximum shear and maximum bending moment. Shear forces will then be transferred to the post-to-parapet bracket and anchors as a tensile load. In this loading scenario, the largest tensile load will be transferred into the top anchor connections. Thus, the lower anchorage did not represent a worst-case design scenario. A diagram showing the effective point load front wind loading scenario and its corresponding shear and moment diagrams are shown in Figure 79, a definition of the variables is shown in Table 10, a summary of critical loads is shown in Table 11,and the full mathematical derivation is given in Appendix A.7.

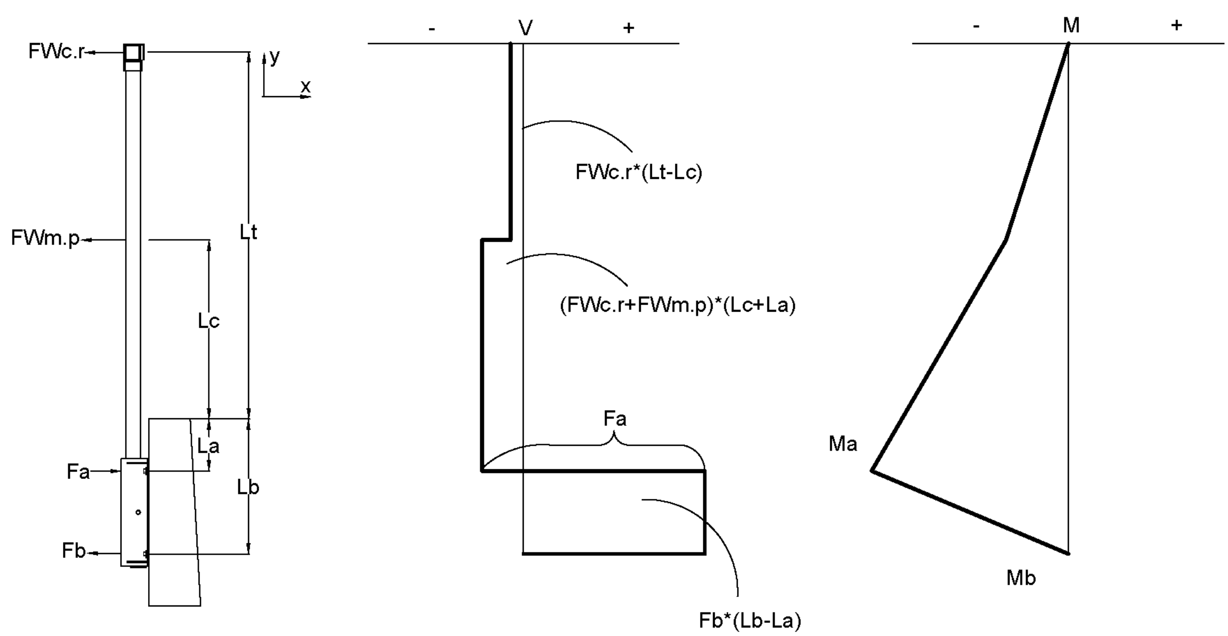

Figure 79. Front Wind Loading Configuration

Table 10. Front Wind Loading Variable Definition

Variable	Definition
FWc.r.	Wind force on cap rail
FWm.p.	Wind force on mesh and post
Fa	Tensile force at top anchorage
Fb	Reaction force at bottom anchorage
Lt	Distance from cap rail wind force location to barrier top
Lc	Distance from mesh and post wind force location to barrier top
La	Distance from top anchorage to barrier top
Lb	Distance from bottom anchorage to barrier top

Table 11. Critical Loads for Front Wind Loading

FWc.r (kips)	FWm.p. (kips)	Fa (kips)	Fb (kips)	Ma (kip-in.)
-0.21	-0.39	2.9	-2.3	-39.8

6.3.8.2 Back Wind Loading

Lateral wind blowing onto the back side of the fence structure, consisting of the vertical posts, chain-link mesh, and cap rail, will place a shear and subsequent moment load onto the vertical post. Note that for a cantilever beam, the distributed wind loads can be simplified to effective point loads and produce an equivalent maximum shear and maximum bending moment. Shear forces will then be transferred to the post-to-parapet bracket and anchors as a tensile load. In this loading scenario, the largest tensile load will be transferred into the bottom anchor connections. Thus, the reaction force at the top anchor connections was neglected. A diagram showing the effective point load back wind loading is shown in Figure 80, a definition of the variables is shown in Table 12, and critical loads are summarized in Table 13. Note that the back wind loading scenario produces the same load magnitudes as that of the front wind loading, with only a difference in compression of the top anchors and tensile loading at the bottom anchors.

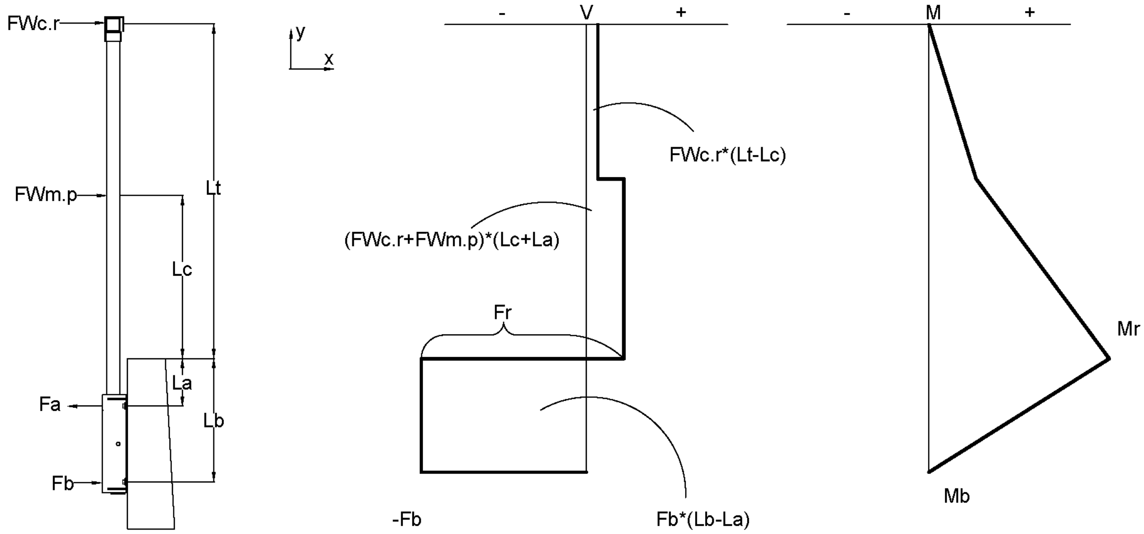

Figure 80. Back Wind Loading Configuration

Table 12. Back Wind Loading Variable Definition

Variable	Definition
FWc.r.	Wind force on cap rail
FWm.p.	Wind force on mesh and post
Fa	Reaction force at top anchorage
Fb	Tensile force at bottom anchorage
Lt	Distance from cap rail wind force location to barrier top
Lc	Distance from mesh and post wind force location to barrier top
La	Distance from top anchorage to barrier top
Lb	Distance from bottom anchorage to barrier top

Table 13. Critical Loads for Back Wind Loading

FWc.r (kips)	FWm.p. (kips)	Fa (kips)	Fb (kips)	Ma (kip-in.)
0.21	0.39	-2.9	2.3	39.8

6.3.8.3 Front Wind on Ice Loading

Lateral wind blowing onto the front side of the ice-covered fence structure will place a load onto the ice-covered fence system which will result in a shear and subsequent moment load onto the vertical post. Note that for a cantilever beam, the distributed wind load can be simplified to effective point load and produce an equivalent maximum shear and maximum bending moment.

Shear forces will then be transferred to the post-to-parapet bracket and anchors as a tensile load. In this loading scenario, the largest tensile load will be transferred into the top anchor connections. Thus, the lower anchorage did not represent a worst-case design scenario. A diagram showing the effective point load front wind on ice loading scenario and its corresponding shear and moment diagrams are shown in Figure 81, a definition of the variables is shown in Table 14, critical loads are summarized in Table 15, and the full mathematical derivation is given in Appendix A.7.

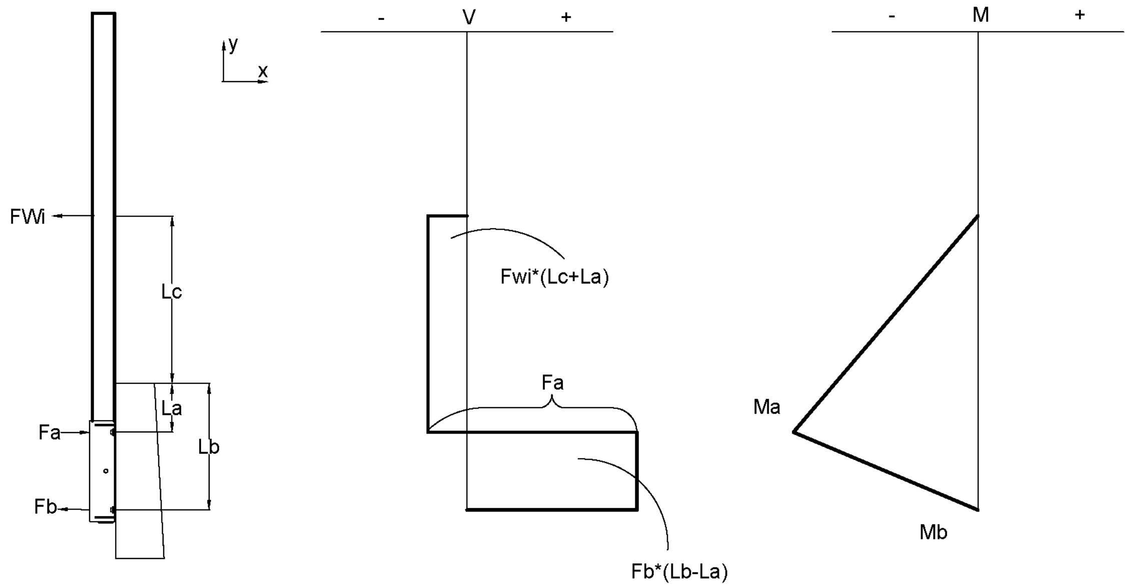

Figure 81. Front Wind on Ice Loading Configuration

Table 14. Front Wind on Ice Loading Variable Definition

Variable	Definition
FWi	Concentrated wind force on ice-covered fence
Fa	Tensile force at top anchorage
Fb	Reaction force at bottom anchorage
Lc	Distance wind on ice point force location to barrier top
La	Distance from top anchorage to barrier top
Lb	Distance from bottom anchorage to barrier top

Table 15. Critical Loads for Front Wind on Ice Loading

FWi (kips)	Fa (kips)	Fb (kips)	Ma (kip-in.)
-0.74	3.0	-2.3	-40.2

6.3.8.4 Back Wind on Ice Loading

Lateral wind blowing onto the back side of the ice-covered fence structure will place a shear and subsequent moment load onto the vertical post. Note that for a cantilever beam, the distributed wind load can be simplified to effective point load and produce an equivalent maximum shear and maximum bending moment. Shear forces will then be transferred to the post-to-parapet bracket and anchors as a tensile load. In this loading scenario, the largest tensile load will be transferred into the bottom anchor connections. As such, the reaction force at the top anchor connections were neglected. A diagram showing the effective point load back wind on ice loading is shown in Figure 80, a definition of the variables is shown in Table 16, and critical loads are summarized in Table 17.

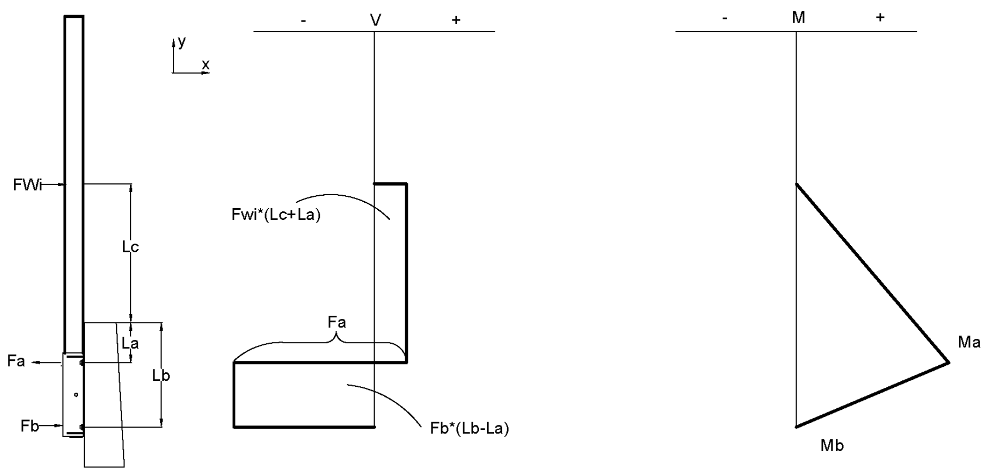

Figure 82. Back Wind on Ice Loading Configuration

Table 16. Back Wind on Ice Loading Variable Definition

Variable	Definition
FWi	Concentrated wind force on ice-covered fence
Fa	Reaction force at top anchorage
Fb	Tensile force at bottom anchorage
Lc	Distance wind on ice point force location to barrier top
La	Distance from top anchorage to barrier top
Lb	Distance from bottom anchorage to barrier top

Table 17. Critical Loads for Back Wind on Ice Loading

FWi (kips)	Fa (kips)	Fb (kips)	Ma (kip-in.)
0.74	-3.0	2.3	40.2

6.3.9 Design Impact Loading

6.3.9.1 Design Methodology

The design methodology used to determine the estimated impact load was to identify the load on the anchorage, F_a and F_b at a theoretical impact force F_i, which causes the post to plastically hinge. The actual impact forces that may be imposed directly on the vertical posts is unknown, but this approach will increase the likelihood that the maximum force in the posts during yielding and buckling does not exceed the anchorage capacity. A schematic showing the impact loading scenario is shown in Figure 83.

Using this design approach, anchor forces become dependent on post capacity. It is noted that the yield stress of any structural part can vary due to the manufacturing process, and materials greatly in excess of the design strength may have a deleterious effect on the anchorage assemblies. To account for potential yield stress variations, the yield stress listed in the ASTM material specification for the selected posts was increased by 20 ksi for the estimation of practical worst-case design impact loading. For the results discussed in the following section, impact forces were determined from a 2½ in. schedule 80 pipe conforming to ASTM A53 Gr. B with a specified minimum yield strength of 35 ksi. This post is one of the recommended options that meets vertical post design loading requirements and yield the highest load demand for the impact loading analysis.

Lateral and longitudinal impact scenarios were considered when determining forces on the anchorage to determine the maximum shear and tensile forces that could may occur from impacts with errant vehicles. The impact forces were estimated using the following assumptions:

- The maximum moment will be located near the top surface of the post bracket, equal to the post flexural capacity;
- Top and bottom anchorage connections are located 10 in. and 27½ in. below the top of the barrier;
- The impact force would be applied 3 in. above the top of the barrier;

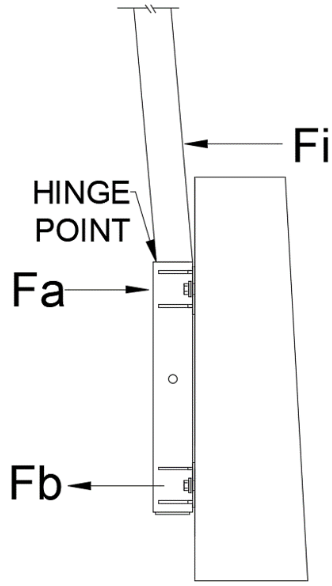

Figure 83 Impact Load Design Methodology

6.3.9.2 Lateral Impact Loading

A lateral impact force would place a load directly on the vertical post which will then be transferred into the post bracket and anchor connections. In this loading scenario, the largest load will be transferred into the top anchor connection as a tensile load. Thus, the lower anchorage did not represent a worst-case design scenario. A diagram showing the lateral impact loading scenario and its corresponding shear and moment diagrams are shown in Figure 84, a definition of the variables is shown in Table 18, a summary of critical loads is shown in Table 19, and the full mathematical derivation is given in Appendix C.

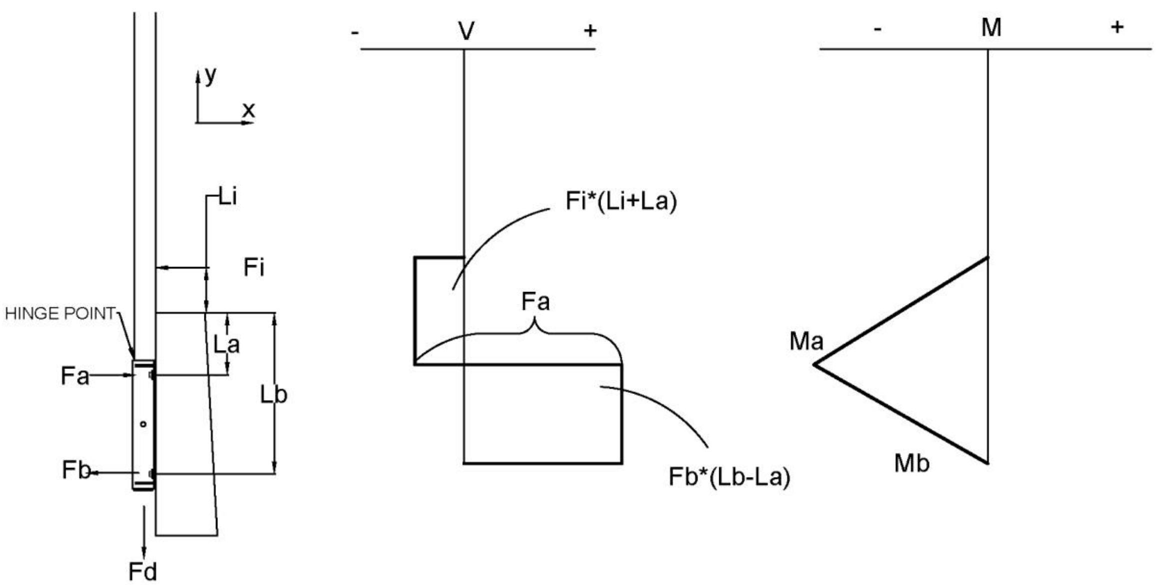

Figure 84. Lateral Impact Loading Configuration

Table 18. Lateral Impact Loading Variable Definition

Variable	Definition
Fi	Concentrated impact force on ice-covered fence
Fa	Tensile force at top anchorage
Fb	Reaction force at bottom anchorage
Fd	Vertical Load determined from LRFD load combinations
Li	Distance from impact force location to barrier top
La	Distance from top anchorage to barrier top
Lb	Distance from bottom anchorage to barrier top

Table 19. Critical Loads for Lateral Impact Loading

Fi (kips)	Fa (kips)	Fb (kips)
-9.3	-16.2	6.9

6.3.9.3 Longitudinal Impact Loading

A longitudinal impact force would place a load directly on the vertical post which will then be transferred into the post bracket and anchor connections as a shear load. In this loading scenario, the largest shear load will be transferred into the top anchor connections. Thus, the lower anchorage did not represent a worst-case design scenario. A diagram showing the longitudinal impact loading scenario and its corresponding shear and moment diagrams are shown in Figure 85, a definition of the variables is shown in Table 20, and critical loads are summarized in Table 21.

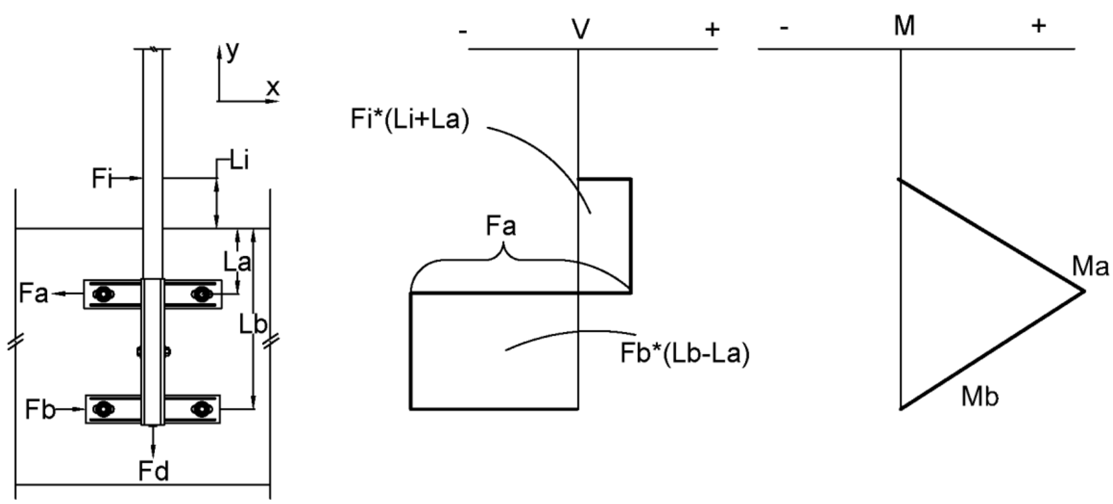

Figure 85. Longitudinal Impact Loading Configuration

Table 20. Longitudinal Impact Loading Variable Definition

Variable	Definition
Fi	Concentrated impact force on ice-covered fence
Fa	Shear force at top anchorage
Fb	Shear force at bottom anchorage
Fd	Vertical Load determined from LRFD load combinations
Li	Distance from impact force location to barrier top
La	Distance from top anchorage to barrier top
Lb	Distance from bottom anchorage to barrier top

Table 21. Critical Loads for Longitudinal Impact Loading

Fi (kips)	Fi (kips)	Fb (kips)
9.3	16.2	6.9

6.4 Vertical Post Design

6.4.1 Design of Members for Flexure

Chapter F of the *AISC Steel Construction Manual* [41] was consulted to determine the maximum allowable flexural capacity to design vertical posts that must resist lateral wind loads. Sections F1, General Provisions, and F8, Round HSS, are of particular interest in the design of the parapet-mounted debris containment fence since post options were limited to round sections. To determine the plastic flexural design strength, Equation (12) was utilized.

$$\phi_b M_n = \phi_b F_y Z \; (AISC\ F8-1) \tag{12}$$

Where: $\phi_b M_n$ = Design flexural strength (kip-in.)

F_y = Specified minimum yield stress (ksi)

Z = Plastic section modulus (in.^{3})

ϕ_b = 0.9, Resistance factor for flexure

6.4.2 Design of Members for Shear

Wind loading on the fence will apply a bending moment on vertical post which produces a shear force at the top anchorage connection. Chapter G of the *AISC Steel Construction Manual* [41] was consulted to determine the maximum shear capacity of the vertical posts. The shear capacities of round posts were determined using Equation (13).

$$\phi_v V_n = \frac{\phi_b F_{cr} A_g}{2} \quad (AISC\ G5-1) \tag{13}$$

Where: $\phi_v V_n$ = Design shear strength (kips)

F_{cr} =0.6 F_y, Critical stress, (ksi)

F_y = Specified minimum yield stress, (ksi)

A_g = Gross cross-sectional area (in.^{2})

ϕ_v = 0.9, Resistance factor for shear

6.4.3 Design of Members for Compression

Chapter E of the *AISC Steel Construction Manual* [41] was consulted to determine the design compressive strength of vertical posts. Compression loading was considered since its effects due to vertical loads combined with wind loading could cause vertical posts to fail. Design compressive strength of non-slender round posts were determined using Equation (14). This equation was used since the readily-available post options were all categorized as non-slender elements per chapter B of the AISC manual.

$$\phi_c P_n = \phi_c F_{cr} A_g \quad (AISC\ E3-1\ ) \tag{14}$$

Where: $\phi_c P_n$ = Design compressive strength (kips)

F_{cr} = Critical stress (ksi)

A_g = Gross cross-sectional area (in.^{2})

ϕ_c = 0.9, Resistance factor for compression

The available column strength of compression members is dependent on the effective slenderness ratio $\frac{L_c}{r}$. Two conditions for calculating the critical stress are provided by AISC manual depending on the effective slenderness ratio. To determine the effective slenderness ratio, the effective length factor (K) must be defined which is dependent on the connection of the post to the post-top-parapet bracket. As a worse-case scenario, this connection could resist moment and act fixed, which requires an effective length factor equal to 2.1 be used in the determination of effective slenderness ratio. This effective length factor was selected from Table C-A-7.1 of the AISC steel design guide for condition “e”. In condition “e”, the bottom of the post is considered fixed while the top is allowed to rotate and translate freely. This condition was considered the most appropriate since the top of multiple fence sections could sway laterally during high wind loading events, providing no rotation or translation restraint near at the top of the fence system.

When $\frac{L_c}{r} \leq 4.71\sqrt{\frac{E}{Fy}}$:

$$F_{cr} = \left[0.658^{\frac{F_y}{F_e}}\right] F_y \quad (AISC\ E3-2) \tag{15}$$

When $\frac{L_c}{r} \geq 4.71\sqrt{\frac{E}{Fy}}$:

$$F_{cr} = 0.877F_e \quad (AISC\ E3-3) \tag{16}$$

$$F_e = \frac{\pi^2 E}{\frac{L_c}{r}^2} \quad (AISC\ E3-4\ ) \tag{17}$$

Where: L_c= KL= Effective length of member, (in.)

K=2.1, Effective length factor

L= Laterally-unbraced length, (in.)

r = Radius of gyration, (in.)

E= Modulus of elasticity, (ksi)

F_y= Yield stress, (ksi)

F_e= Elastic buckling stress, (ksi)

ϕ_c = 0.9, Resistance factor for compression

6.4.4 Design of Members for Combined Forces

Chapter H of the *AISC Steel Construction Manual* [41] was consulted to determine if the vertical post satisfied combined loading criteria. These criteria verify that the combination of bending and shear from wind loading and compression from dead, live, and ice loading does not exceed the vertical post's capacity. Sections H3, Members Subject to Torsion and Combined Torsion, Flexure, and/or Axial Force provisions were followed for HSS members. It was assumed that wind would act normal to the fence structure and would therefore not produce torsional loading on the vertical posts. Thus, the ratio of required and design torsion strengths was neglected in this calculation.

$$\left(\frac{P_r}{P_c}+\frac{M_r}{M_c}\right)+\left(\frac{V_r}{V_c}+\frac{T_r}{T_c}\right)^2 \leq 1.0 \quad (AISC\ H3-6) \tag{18}$$

Where: P_r= Required axial strength using LRFD Load Combinations, (kips)

P_c= Design axial strength, (kips)

M_r= Required flexural strength using LRFD load combinations, (kip-in.)

M_c= Design flexural strength, (kip-in.)

V_r= Required shear strength using LRFD load combinations (kips)

V_c= Design shear strength, (kips)

T_r= Required torsional strength using LRFD load combinations (kip-in.)

T_c= Design torsional strength, (kip-in.)

6.4.5 Approximate Second Order Analysis

Appendix 8 of the *AISC Steel Construction Manual* [41] was consulted to determine the required bending strength of vertical posts under the action of second-order load effects. These second order effects may occur when wind loads cause the vertical post to deflect laterally and created a lateral moment arm for vertical loads to act on, creating a secondary bending moment action. Axial loads are also amplified due to second order effects, however axial load condition was not as critical as the bending condition and was therefore not analyzed. The required second-order flexural strength is calculated using Equation (19) which consists of the moment contributions from P-Δ and P-δ effects. In the case of the parapet-mounted fence, P-δ effects will most likely not occur since the top of multiple fence sections will laterally deflect during wind loading and provide limited lateral constraint near the top of the fence. Without this lateral constraint, the vertical post cannot deflect in a manner that produces P-δ effects. For this reason, P-δ effects were neglected. Examples of P-Δ and P-δ deflections are shown in Figure 86.

$$Mr = B_1 M_{nt} + B_2 M_{lt} \quad (AISC\ A-8-1) \tag{19}$$

Where: M_r= Required second order flexural strength, (kip-in.)

B_1= P-δ effect multiplier

B_2= P-Δ effect multiplier

M_{nt} = First-order moment using LRFD load combinations, with structure resisting latera translation, (kip-in.)

M_{lt} = First-order moment using LRFD load combinations, due to lateral translation only, (kip-in.)

The B2 multiplier was identified using Equation (20). This multiplier is a function of the ratio between the total vertical load and the elastic critical buckling strength, calculated using equation (21). For the design of this fence system, the interstory drift (Δ_H) was calculated by finding the lateral deflection at the top of the fence that occurs from 1 kip of force and therefore, the total story shear (H) was set equal to 1 kip since it was used to calculate interstory drift.

$$B_2 = \frac{1}{1 - \frac{\alpha P_{story}}{P_{e\ story}}} \geq 1 \quad (AISC\ A-8-6) \tag{20}$$

$$P_{e\ story} = R_M \frac{HL}{\Delta_H} \quad (AISC\ A-8-7) \tag{21}$$

Where: α=1 for LRFD design

$P_{e\ story}$= Elastic critical buckling strength, (kips)

P_{story}= Total vertical load being supported by story using LRFD load combinations, (kips)

R_M = 0.85, Selected for moment frames

H = 1 kip, Total story shear produced by the lateral force used to compute Δ_H,

L = Height of vertical post, (in.)

Δ_H = First-order interstory drift due to lateral forces, (in.)

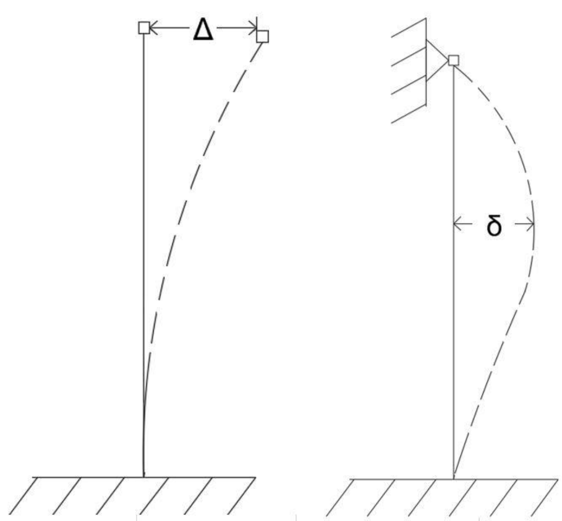

Figure 86. P-Δ (Left) and P-δ (Right) Effects

6.4.6 Second Order Effects Using Deflection Method

To verify that vertical posts had the capacity to withstand second-order bending effects, the secondary moment effects were calculated using the deflection method. In this method, the vertical post deflection caused by lateral loads is calculated and multiplied by vertical loads to determine the secondary moment. During basic wind loading, lateral forces are applied at two vertical locations along the post. Similarly, vertical loads are applied at different heights on the fence structure. The deflection caused by wind loading on the cap rail and the deflection form the fence fabric mesh and post was added by superposition to determine the total lateral deflection. To simplify these calculations, the vertical center of gravity (c.g.) location of the fence weight was determined. Once the deflection was determined by superposition, the product of the lateral translation of the c.g. and the vertical weight of the c.g. were taken to determine the secondary moment. A similar procedure was followed to determine the secondary moment on the fence structure during wind on ice loading however, in that situation, one lateral wind load occur at the center of the fence. Details of this analysis are presented in Appendix B.3.

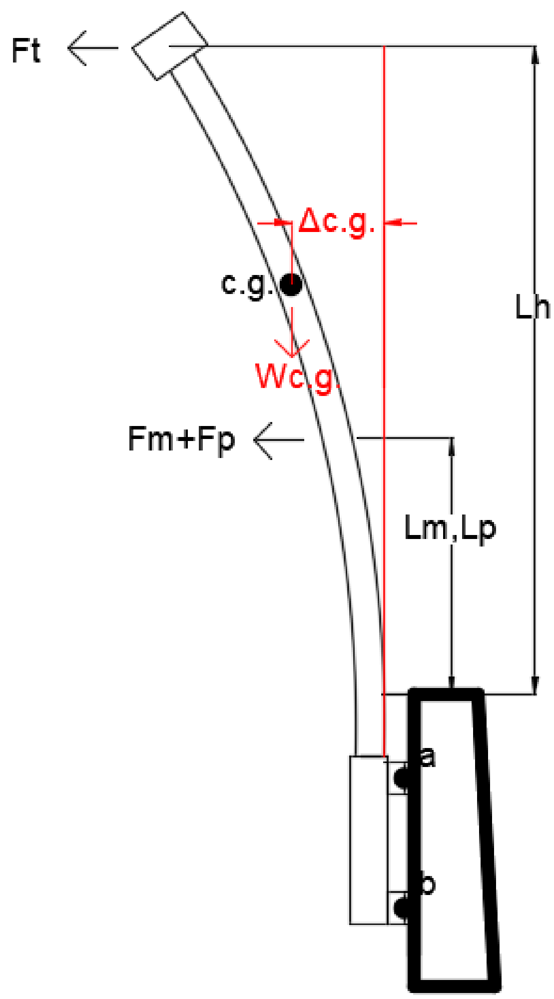

Figure 87. Deflection during Wind Loading and Evaluation of Secondary Moments

Table 22. Front Wind Loading Variable Definition

Variable	Definition
Ft.	Wind force on cap rail
Fm+Fp	Wind force on mesh and post
Lm,Lp	Distance from mesh and post wind force location to barrier top
Lh	Distance from cap rail wind force location to barrier top
Wc.g.	Cumulative weight on the fence structure
c.g.	c.g. location of the cumulative fence weight
Δ c.g.	Lateral deflection of fence weight c.g.

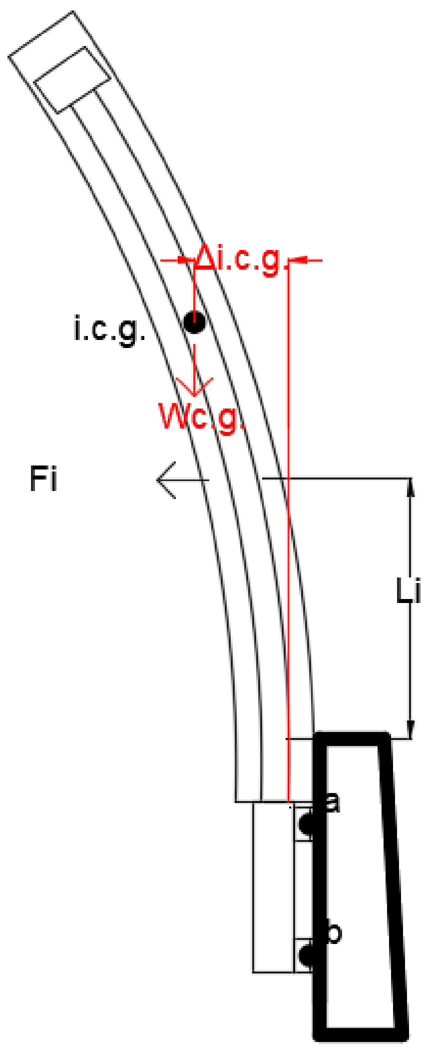

Figure 88. Deflection during Wind on Ice Loading and Evaluation of Secondary Moments

Table 23. Second Order Effects Variable Definition, LRFD Combinations with Ice Loads

Variable	Definition
Fi	Concentrated wind force on ice-covered fence
Li	Distance from wind on ice point force location to barrier top
Wc.g.	Cumulative weight on the ice-covered fence structure
Ic.g.	c.g. Location of ice-covered fence weight
Δ c.g.	Lateral deflection of fence weight c.g.

6.4.7 Vertical Post Design Summary

A summary of the vertical post design is shown in Table 24. The design summary of LRFD ice loading combinations is presented here since they posed a higher load demand than that of the LRFD basic load combinations. These calculations are for a HSS2.875x0.188 round tube conforming to ASTM A1085 material specifications which specify a 50 ksi minimum yield stress. Below is a list of additional post options that met load requirements:

- HSS2.875x0.203 ASTM A500 Gr C
- Pipe 2-1/2 SCH40 ASTM F1083 High Strength
- Pipe 2-1/2 SCH80 ASTM A53 Gr. B

Table 24. Vertical Post Design Summary, LRFD Ice Loading Combination No. 2

Load Condition	Demand	Capacity
Compression (kips)	2.1	7.86
Shear (kips)	3.0	20.0
Bending (kip-in.)	40.2	57.2
Approximate Second Order Analysis (kip-in.)	52.0	
Deflection Method Second Order Analysis (kip-in.)	43.1	
Combined Forces Requirement	1.0 ≥	0.99

6.5 Post-to-Parapet Attachment Design

The research team decided to design the post-to-parapet attachments subject to the condition that it should not be damaged by LRFD loads or the determined design impact load, to minimize the number of components that need replacement in the event of system damage. Possible post bracket failure modes are shown in Figure 89. During tensile loading caused by a longitudinal impact load, the welds between the tube and flat bar can fail and the flat bars could flex. During shear loading caused by a lateral impact load condition, hole bearing, hole tearout, or tensile tearing of the bracket could occur. The design of this bracket considered the load capacity of each failure mode and met or exceeded the load demand for each condition. The following sections discuss this design process.

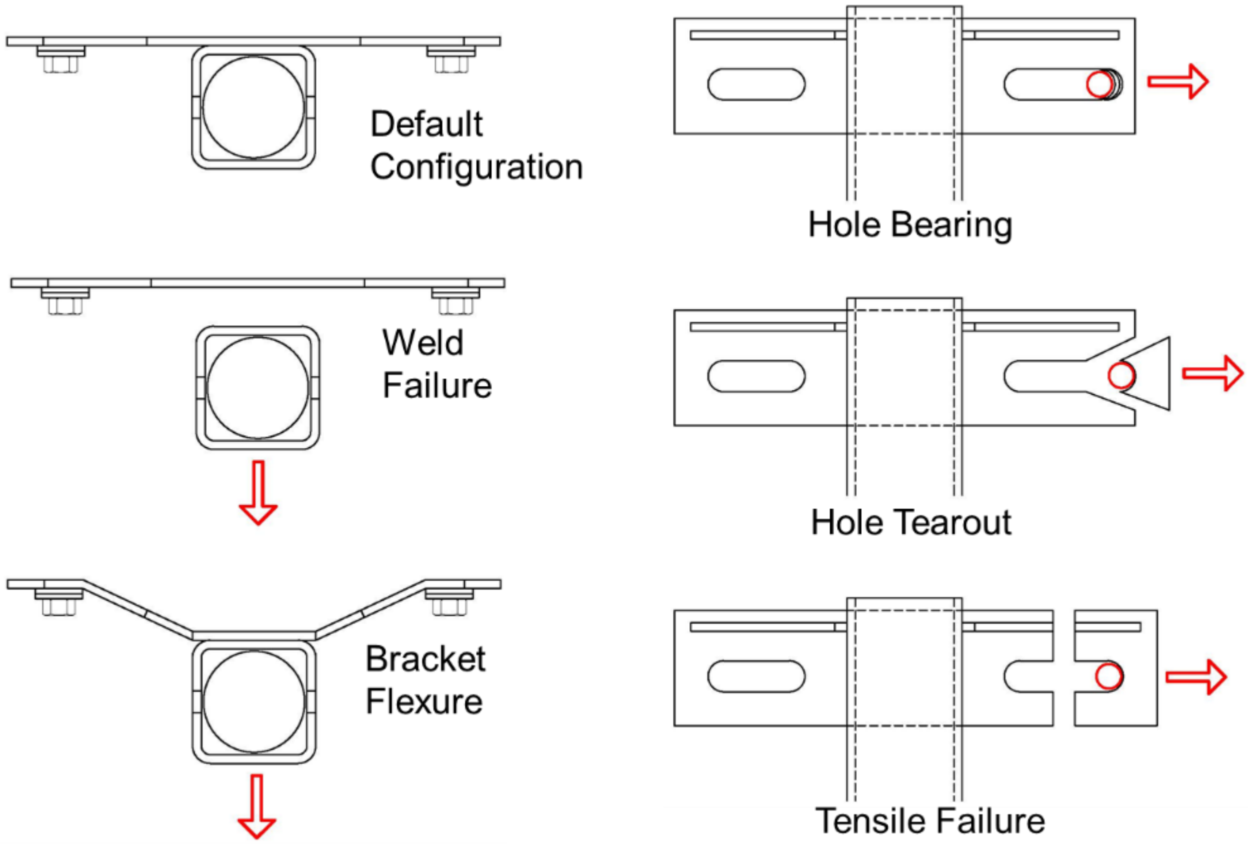

Figure 89. Bracket Failure Modes

6.5.1 Design of Bolted Connections

Chapter J of the *AISC Steel Construction Manual* [41] was consulted to determine the required post-to-parapet attachment geometry for impact loading conditions. These provisions were followed to design the attachment and its connections to develop the capacity of the vertical post. This manual was used to determine bearing, tearout, and tensile strength at bolt holes.

Bearing and tear-out strength were determined from the provisions of the *AISC Steel Construction Manual* section J3.10. Specifically, provisions where deformation at the bolt hole were a design consideration were followed. This was done to satisfy the objective of minimizing damage to reduce the number of components that require replacement after impact loading events. Bearing and tear-out strength were found using Equation (22) and Equation (23), respectively.

$$\phi R_n = \phi 2.4 d t F_u \ \ (AISC\ J3-6a) \tag{22}$$

$$\phi R_n = \phi 1.2 l_c t F_u \ \ (AISC\ J3-6c) \tag{23}$$

Where: ϕR_n = Design strength at bolt holes (kips)

l_c= Clear distance, in the direction of force, between the edge of the hole and edge of adjacent hole or edge of material, (in.)

t = Thickness of connected material, (in.)

d = Nominal bolt diameter, (in.)

F_u = Specified minimum tensile strength, (ksi)

ϕ = 0.75, Resistance factor

Design tensile strength of the bracket at the bolt hole location was determined using provisions of the *AISC Steel Construction Manual* section J4.1. The tensile strength is taken as the lower value obtained from tensile yielding and tensile rupture Equation (24) and Equation (25) , respectively.

$$\phi R_n = \phi F_y A_g \ \ (AISC\ J4-1) \qquad \phi = 0.90 \tag{24}$$

$$\phi R_n = \phi F_u A_e \ (AISC\ J4-2) \qquad \phi = 0.75 \tag{25}$$

Where: ϕR_n= Design tensile strength of connecting elements, (in.)

F_y = Specified minimum yield stress, (ksi)

F_u = Specified minimum tensile strength, (ksi)

A_g = Gross area, (in.^{2})

A_e = Effective net Area, (in.^{2})

ϕ = Resistance factor

6.5.2 Design of Welded Connections

Chapter J of the *AISC Steel Construction Manual* [41] was consulted to determine the required weld strength for impact loading conditions. Provision for fillet welds accounting for directional strength increases were followed since loading of fillet welds could occur in any direction.

$$\phi R_n = \phi F_{nw} A_{we} \ (AISC\ J2-4\ ) \tag{26}$$

Where: ϕR_n = Design weld strength (kips)

$F_{nw} = 0.6F_{EXX}(1.0 + 0.50sin^{1.5}\theta)$, (ksi)

F_{EXX}= Filler material classification strength, (ksi)

$A_{we} = t_e l$, Effective weld area, (in.^{2})

$t_e = 0.707t$, Effective throat thickness, (in.)

$t =$ Weld thickness, (in.)

$l =$ Weld length, (in.)

ϕ = 0.75, Resistance factor for weld strength

6.5.3 Design of Members for Flexure

A flexure analysis was conducted on the post-to-parapet attachment to ensure that the tensile impact force would not produce a moment that caused bracket bending. Flexure calculations were performed with Equation (12) using the elastic section modulus instead of the plastic section modulus. This allowed for a more conservative analysis, described in Appendix E.

To identify the bending demand, the bracket was considered a beam with a center load transferred to it via the vertical post. Since it is desired that the concrete anchorage remain robust, the bolted connections were assumed to be rigid and inflexible.

During this loading condition, the peak bending moments occur at the center of the bracket and at each anchor location, shown in Figure 90. Since the bracket section is the largest at the center due to the square tube, bending about the anchor connections was considered the critical load location. The section modulus was determined for cross section A-A of the bracket. Section A-A and the section at the anchor location only differ due to the slot where the anchor passes through.

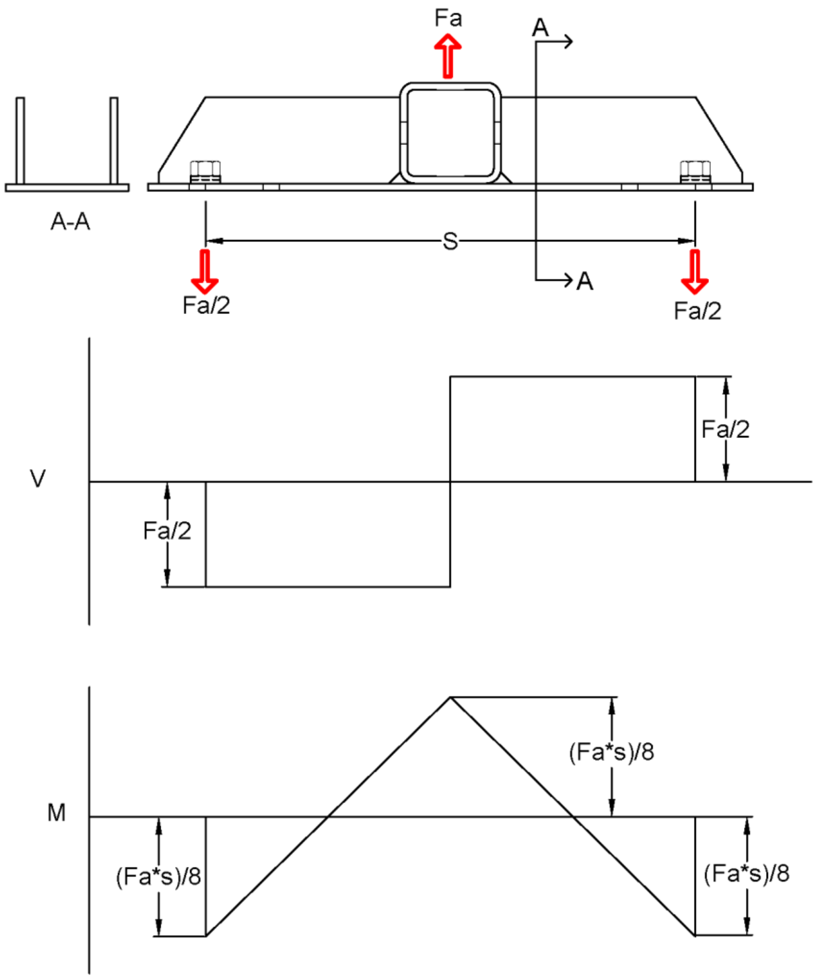

Figure 90. Bracket Flexure Configuration

6.5.4 Post Bracket Design Summary

A summary of the post-to-parapet attachment design is shown in Table 25. These calculations are for a post bracket built up with ¼-in. ASTM A572 Grade 50 plate. This post bracket also has 2-in. slotted holes with ¼-in. gussets on either side of the 3½-in. x 3½-in. x ¼-in. HSS A500 Gr B tube socket. ¼-in. thick fillet welds formed with 60-ksi filler material will be used in the fabrication of the post bracket.

Table 25. Post-to-Parapet Bracket Design Summary

Failure Mode	Demand	Capacity
Weld Failure (kips)	16.2	33.4
Hole Bearing (kips)	8.1	25.6
Hole Tearout (kips)	8.1	21.0
Flexure (kip-in.)	34.3	57.4

6.6 Concrete Anchorage Design

The American Concrete Institution published information on design requirements for anchors used to transfer structural loads to structural concrete. These design requirements are detailed in *Building Code Requirements for Structural Concrete (ACI 318-14)* [42] and were followed to determine the required anchor size and spacing for impact loading conditions. In these provisions, the design of steel anchors, concrete and their connections under shear and tensile loading is presented.

6.6.1 Tensile Loading

A lateral impact load will apply a tensile load to the top anchorage. During tensile loading, the anchors could fail in tension, the bond connection between the anchor and concrete could release, and a section of concrete surrounding the anchors could detach. These possible failure modes are shown in Figure 91. The design strength of these failure modes was calculated to meet or exceed tensile forces from the impact loading scenario.

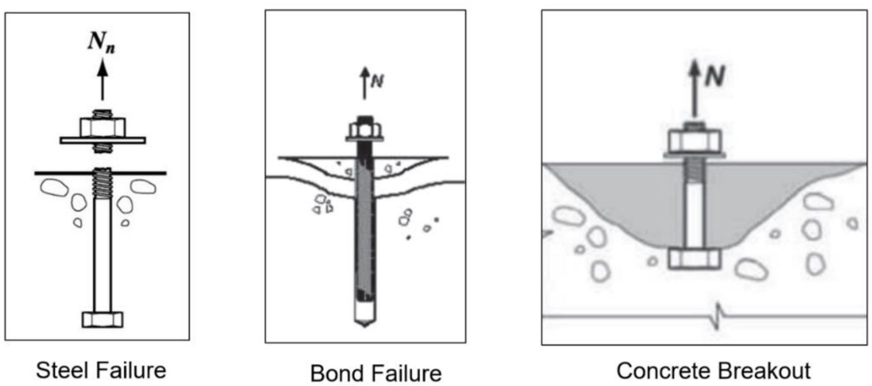

Figure 91. Concrete Anchorage Tensile Failure Modes [42]

6.6.1.1 Steel Strength of Anchor in Tension

For forces to transfer to the concrete, steel anchors must develop the capacity of the vertical post. The design strength of a steel anchor in tension is found using Equation (27).

$$\phi N_{sa} = \phi f_{uta} A_{se,N} \ (ACI \ \ 17.4.1.2) \tag{27}$$

Where: ϕN_{sa} = Design tension strength, (kips)

f_{uta}= Ultimate stress of anchor material, (ksi)

$A_{se,N}$ = Effective cross-sectional area of anchor in tension, (in.^{2})

ϕ = Strength reduction factor

6.6.1.2 Bond Strength of Adhesive Anchor in Tension

Section 17.4.5 of ACI-318 was consulted to find the bond strength of adhesive anchors in tension. Provisions for a single anchor were followed with modifications to account for anchor group action since it was expected that anchors would be installed in proximity with each other.

$$\phi N_a = \emptyset \frac{A_{Na}}{A_{Nao}} \psi_{ed,Na} \psi_{cp,Na} N_{ba} \quad (ACI\ 17.4.5.1a) \tag{28}$$

Where: ϕN_a= Design bond strength (lb)

A_{Na}= Projected influence area of single adhesive anchor or group of anchor, (in.^{2})

$A_{Nao} = (2c_{Na})^2$= Projected influence area of single adhesive anchor, (in.^{2})

$C_{Na} = 10d_a\sqrt{\frac{\tau_{uncr}}{1100}}$ = Projected distance from center of an anchor shaft on one side of the anchor required to develop the full bond strength of a single adhesive anchor, (in.)

τ_{uncr}= Characteristic bond stress of epoxy in un-cracked concrete, (psi)

$\psi_{ed,Na}$= Edge effect modification factor for adhesive anchors

$\psi_{cp,Na}$= Modification factor for adhesive anchors in un-cracked concrete without supplementary reinforcement

ϕ = Strength reduction factor

N = Subscript relating to tensile loading

$$N_{ba} = \lambda_a \tau_{uncr} \pi d_a h_{ef} \quad (ACI\ 17.4.5.2) \tag{29}$$

Where: N_{ba}= Basic bond strength of a single adhesive anchor, (lb)

$\lambda_a = 1.0$, Lightweight concrete modification factor

τ_{uncr}= Characteristic bond stress of epoxy in un-cracked concrete, (psi)

d_a= Anchor diameter, (in.)

h_{ef}= Effective anchor embedment depth, (in.)

6.6.1.3 Concrete Breakout Strength of Anchor in Tension

When the steel anchor and bond connections develop the capacity of the vertical post, loading will be transferred to the concrete barrier. Section 17.4.2 of ACI-318 was consulted to find the breakout strength of an anchor. Provisions for a single anchor were followed with modifications to account for anchor group action since it was expected that anchors would be installed in proximity with each other.

$$\phi N_{Cb} = \emptyset \frac{A_{Nc}}{A_{Nco}} \psi_{ed,N} \psi_{c,N} \psi_{cp,N} N_b \quad (ACI\ 17.4.2.1a) \tag{30}$$

Where: ϕN_{Cb}= Design concrete breakout strength (lb)

A_{Nc}= Projected concrete failure area of single anchor or group of anchor, (in.^{2})

$A_{Nco} = 9h_{ef}^2$, Projected concrete failure area of single anchor, (in.^{2})

$\psi_{ed,N}$= Edge effect modification factor

$\psi_{c,N}$= Concrete modification factor for cracked or un-cracked concrete

$\psi_{cp,N}$= Modification factor for post-installed anchors in un-cracked concrete without supplementary reinforcement

ϕ = Strength reduction factor

N = Subscript relating to tensile loading

$$N_b = 17\lambda_a \sqrt{f_C'} h_{ef}^{1.5} \quad (ACI\ 17.4.2.2a) \tag{31}$$

Where: N_b= Basic concrete breakout strength of a single anchor in cracked concrete, (lb)

$\lambda_a = 1.0$, Lightweight concrete modification factor

f_c'= Concrete strength, (psi)

h_{ef}= Effective anchor embedment depth, (in.)

6.6.2 Shear Loading

A longitudinal impact load will apply shear loads to the top and bottom anchorage. During shear loading, the anchors could fail in shear, a section of the concrete surrounding the anchor could break out in shear, and pryout of the anchor could occur. These possible failure modes are shown in Figure 92. The design strength of these failure modes was calculated to meet or exceed shear forces from the longitudinal impact loading scenario.

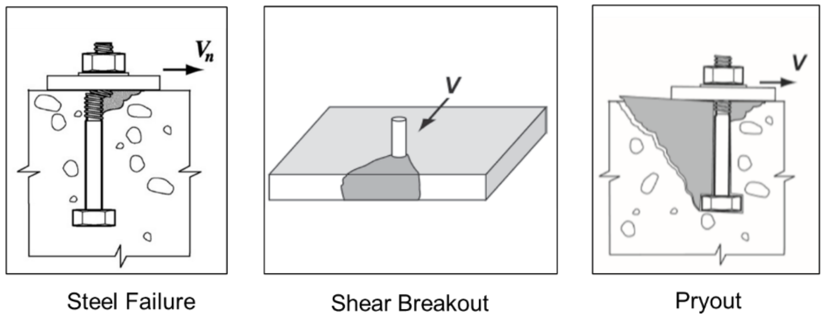

Figure 92. Concrete Anchorage Shear Failure Modes [42]

6.6.2.1 Steel Strength of Anchor in Shear

For shear forces to transfer to the concrete, steel anchors must develop the capacity of the vertical post during longitudinal impact loading. ACI 318-14 provisions were followed to find the design strength of anchors in shear using Equation (32). Specifically, provisions for post-installed anchors in shear were followed.

$$\phi V_{sa} = \phi 0.6 f_{uta} A_{se,V}\ (ACI\ \ 17.5.1.2b) \tag{32}$$

Where: ϕV_{sa} = Design shear strength, (kips)

f_{uta}= Ultimate stress of anchor material, (ksi)

$A_{se,v}$ = Effective cross-sectional area of anchor in shear, (in.^{2})

ϕ = Strength reduction factor

6.6.2.2 Design Concrete Breakout Strength of Anchor in Shear

Section 17.5.2 of ACI-318 was consulted to find the concrete breakout strength of an anchor in shear. Concrete breakout strength in shear is reduced when anchors exist near a free edge. For example, the top of the parapet is considered a free edge. Provisions for anchor groups were followed since it was expected that anchors would be installed in proximity with each other.

$$\phi V_{Cbg} = \emptyset \frac{A_{vc}}{A_{vco}} \psi_{ec,V} \psi_{ed,V} \psi_{c,V} \psi_{h,V} V_b\ (ACI\ 17.5.2.1b) \tag{33}$$

Where: ϕV_{Cbg}= Design concrete breakout strength in shear (lb)

A_{vc}= Projected concrete failure area of single anchor or group of anchor, (in.^{2})

$A_{vco} = 4.5(c_{a1})^2$, Projected concrete failure area of single anchor, (in.^{2})

$\psi_{ec,V}$= Modification factor for eccentrically loaded anchors

$\psi_{ed,V}$= Edge effect modification factor

$\psi_{c,V}$= Concrete modification factor for cracked or un-cracked concrete and for supplementary reinforcement

$\psi_{h,V}$= Modification factor for anchors located in concrete where $h_a < 1.5C_{a1}$

h_a= Concrete thickness, (in.)

c_{a1}= distance from center of anchor to edge of concrete, (in.)

V_b= Basic concrete breakout strength of single anchor in cracked concrete, (lb)

ϕ = Strength reduction factor

V = Subscript relating to shear loading

During impact loading, shear will be applied parallel to the top edge of the parapet. These provisions note that the concrete breakout strength is doubled when shear loading is applied parallel to the free edge. The basic concrete breakout strength of a single anchor in shear is taken as the smaller value calculated using Equation (34) and Equation (35).

$$V_b = \left(7\left(\frac{l_e}{d_a}\right)\sqrt{d_a}\right)\lambda_a\sqrt{f_c'}\left(C_{a_1}\right)^{1.5}\ (ACI\ 17.5.2.2a) \tag{34}$$

$$V_b = 9\lambda_a\sqrt{f_c'}\left(C_{a_1}\right)^{1.5}\ (ACI\ 17.5.2.2b) \tag{35}$$

Where: V_b= Basic concrete breakout strength in shear (lb)

l_e= Load bearing length of anchor, (in.)

d_a= Anchor diameter, (in.)

λ_a = Lightweight concrete modification factor

f_c'= Concrete strength, (psi)

c_{a1}= distance from center of anchor to edge of concrete, (in.)

6.6.2.3 Design Concrete Pryout Strength of Anchor in Shear

Shear loading can cause anchors to pry out of the concrete caused by epoxy bond failure, concrete breakout, and the combination of these two failures. In section 17.5.3 of ACI-318, the concrete pryout strength is taken as the lower of the bond strength and concrete breakout strength in tension modified by a pryout strength coefficient.

$$\phi V_{cp} = \emptyset K_{cp} N_{cp} \quad (ACI\ 17.5.3.1b) \tag{36}$$

Where: ϕV_{cp}= Design concrete pryout strength in shear (lb)

K_{cp}= Coefficient of pryout strength

N_{cp}= Basic concrete pryout strength, (lb)

ϕ = Strength reduction factor

6.6.3 Combined Loading Criteria

Vehicular impacts with the debris fence could occur at any given angle relative to the barrier, which could produce shear and tensile forces simultaneously. The concrete anchorage design was validated by satisfying combined loading provisions from section 17.6 of ACI-318. Combined loading criteria are shown in Equation (37).

$$\left(\frac{N_{ua}}{\phi N_n} + \frac{V_{ua}}{\phi V_n}\right) \leq 1.2 \quad (ACI\ 17.6.3) \tag{37}$$

Where: N_{ua}= Factored tensile force applied to anchor or anchor group (lb)

ϕN_n= Design tensile strength

V_{ua}= Factored shear force applied to anchor or anchor group, (lb)

ϕV_n= Design shear strength

6.6.4 Concrete Anchorage Design Summary

Anchor loading requirements were satisfied using a ⅞-in. ASTM A193 B7 threaded rod with an epoxy having an 1800-psi minimum characteristic bond stress. These anchors would be located 10 in. and 27½ in. below the barrier top surface and have a 15 in. longitudinal spacing. The combined loading requirement calculation yielded a ratio of 1.2 which satisfies strength criteria. Anchor design for tensile and shear loading is summarized in Table 26 and Table 27, respectively. Note that the slots on the post-to-parapet attachment bracket allow for eccentric installation which could increase the force to one anchor under some loading scenarios.

Table 26. Anchorage Design for Tensile Loading

Failure Mode	Demand	Capacity
Steel Tensile Failure (kips)	9.2	43.3
Bond Failure (kips)	9.2	12.49
Tensile Breakout (kips)	9.2	12.47

Table 27. Anchorage Design for Shear Loading

Failure Mode	Demand	Capacity
Steel Shear Failure (kips)	8.1	22.5
Shear Breakout (kips)	16.2	35.0
Anchor Pryout (kips)	8.1	24.9

6.7 Horizontal Fence Stiffener Design

A top horizontal stiffener was designed for aesthetics and controlling fence movement. Flexure analysis was conducted on the horizontal fence stiffener to ensure that vertical loads calculated according to LRFD would not produce permanent deformation. These loads consist of forces applied directly on the cap rail combined with forces transferred from the fence mesh to the cap rail through bolted connections. Vertical loads on the cap rail produce bending between vertical post spans, shown in Figure 93. In addition, loads transferred to the cap rail from the fence fabric is concentrated on the front cap rail flange, which creates a twisting moment. A schematic of this loading condition is illustrated in Figure 94, and was considered in the design to prevent permanent twisting deformations. The fence fabric bolted connection was designed to transfer vertical loads to the cap rail without the bolts experiencing damage.

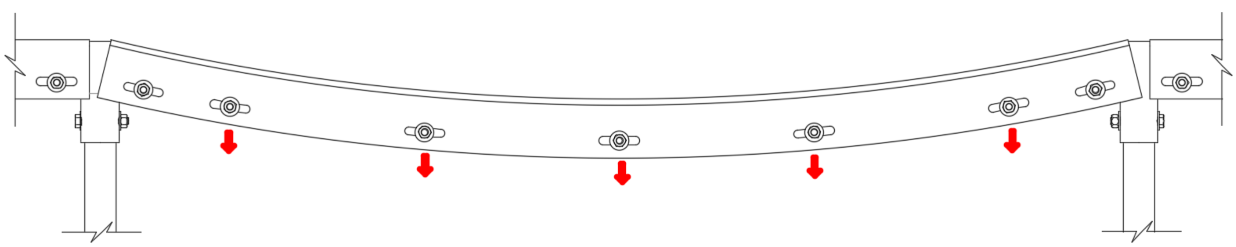

Figure 93. Horizontal Fence Stiffener Bending

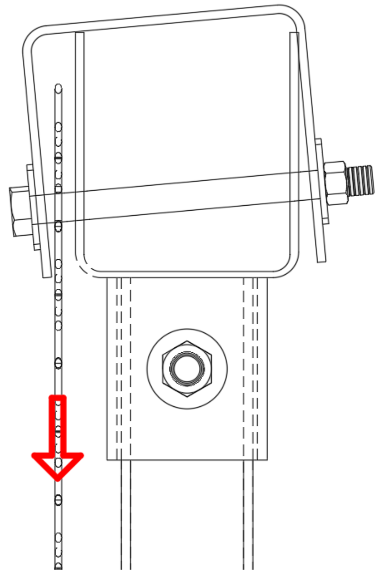

Figure 94. Horizontal Fence Stiffener Torsion Loading

6.7.1 Design of Members for Flexure

The cap rail was considered a beam with pinned constraints at each end meaning the peak moment would occur at the center of the cap rail. Pinned connections were approximated since the end attachment of the cap rail uses slots with construction tolerances that will allow the ends of the cap rail to rotate and provide minimal moment restraint. Once the peak moment was calculated from the loading analysis, it was compared to the flexure capacity obtained using Equation (12) with the use of the section modulus instead of the plastic section modulus. This allowed for a more conservative analysis, detailed in Appendix F.

6.7.2 Design of Members for Torsion

The *AISC Torsional Analysis of Structural Steel Members (Steel Design Guide 9)* [43] was consulted to determine the torsional demand and capacity of the cap rail. The cap rail was considered to be torsionally-pinned at each end since the extremities of the cap rail would be allowed to warp during torsional loading. Shear forces in the cap rail are a combination of the pure torsional shear stresses, shear stress due to warping, and the shear stress due to bending.

Pure torsional shear stress was calculated using Equation (38) and is present on the cross-section of the cap rail due to the torsional moment [43]. Note that the maximum pure torsional shear stress at every point on the cross section is equal for this component since the thickness does not vary. Shear stress due to warping distributes through four points of interest on the channel: at the ends of the flanges (0), in the flange mid span (1), in the corner where the flanges and web meet (2), and in the web mid span (3) as shown in Figure 95 [43]. The shear stress due to warping was calculated at each of these locations using Equation (39) and the warping moment was calculated at each respective point of interest. Shear stress due to bending is calculated using Equation (40) for the flange and webs. Note that shear stress flow due to bending differs slightly from shear stress due to warping, as shown in Figure 96 [46], for this loading scenario. Derivatives of rotation angles Θ were calculated using Case 3 charts for pinned connections from Appendix B of the Steel Design Guide 9 [43].

Once shear stresses were calculated they were combined at each point of interest to determine the maximum combined shear stress in the cross-section. LRFD Limit states of yielding under shear stress were determined using Equation (41) which compares this combined shear stress to the yield stress of the material. Details of this analysis are presented in Appendix F.

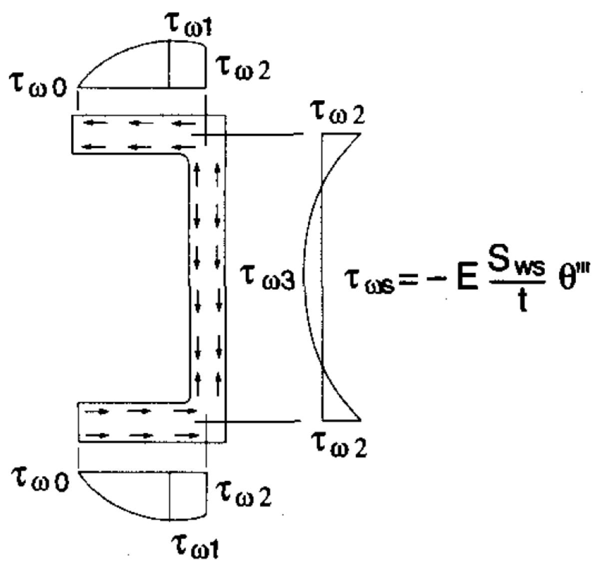

Figure 95. Shear Stress Due to Warping [43]

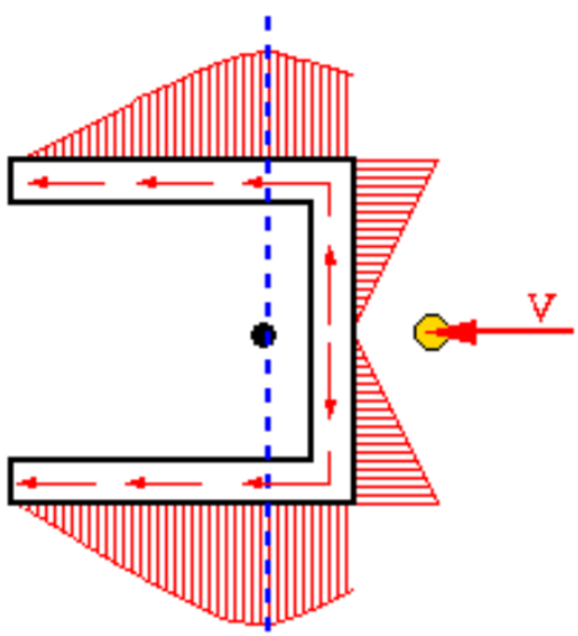

Figure 96. Shear Stress Flow Due to Bending [46]

$$\tau_t = Gt\Theta' \quad (AISC\ Design\ Guide\ 9\ \ 4.1) \tag{38}$$

Where: τ_t= Pure torsional shear stress at element edge, (ksi)

G= 11,200 ksi, Shear modulus of elasticity

t= thickness of element, (in.)

Θ'= Rate of change of twist angle

$$\tau_{ws} = \frac{-ES_{ws}\Theta'''}{t} \quad (AISC\ Design\ Guide\ 9\ \ 4.2a) \tag{39}$$

Where: τ_{ws} = Shear stress at point s due to warping, (ksi)

E = 29,000 ksi, Steel modulus of elasticity

S_{ws}=Warping statical moment at point “s”, (in.^{4})

t = thickness of element, (in.)

Θ'''= Third derivative of twist angle

$$\tau_b = \frac{VQ}{It} \quad (AISC\ Design\ Guide\ 9\ \ 4.6) \tag{40}$$

Where: τ_b= Shear stress due to applied shear, (ksi)

V= Shear, (kips)

I= Moment of inertia, (in.^{4})

Θ'= Rate of change of twist angle

t = thickness of element, (in.)

$$f_{uv} \leq \phi 0.6F_y \ (AISC\ Design\ Guide\ 9\ \ 4.13) \tag{41}$$

$$f_{uv} = \tau_t + \tau_{ws} + \tau_b \tag{42}$$

Where: f_{uv}= Factored shear stress, (ksi)

F_y= Yield strength of steel, (ksi)

ϕ= 0.9, Load resistance factor

6.7.3 Design of Bolted Connections

Bolted connections that attach the fence to the cap rail were also designed to transfer vertical loads to the cap rail without experiencing damage. As a conservative approach, these connections were designed to develop the capacity of the chain-link wire. This wire has a 1290-lb capacity, which the wire on each side of the bolt will develop bringing the vertical demand on the bolded connection to 2.58 kips. Bold bearing and tearout were calculated using Equation (22) and Equation (23), respectively. Additionally, it was desired that damage to the slotted connections be minimized. Due to the length of these slots, the material below the slots could possibly experience bending. The flexural capacity of this connection was calculated using Equation (12) and compared to the bending demand on the bolt slots.

6.7.4 Horizontal Fence Stiffener Summary

The horizontal fence stiffener design is summarized in Table 28. This component shall be formed from $\frac{3}{16}$-in. thick ASTM A572 Grade 50 plate, folded to create a channel geometry. The channels web will have a 6¼ in. width while the flanges are 5½ in. tall. The selected material, thickness and geometry culminated a cap rail design that exceeds all load demands.

Table 28. Horizontal Fence Stiffener Design Summary

Load Condition	Demand	Capacity
Bending (kips)	19.9	125.5
Torsion (ksi)	4.23	27
Maximum Twist Angle	1.58 degrees	

7 FENCE TERMINATION DESIGN

Design of fence interior sections differs from the design requirements at endpoints. For example, the retention wire or wire rope at the top of the installation is terminated at the ends, and requires separate consideration for loading and support hardware. Real-world installations of this parapet-fence system will require end terminations that safely attaches the fence ends to the barrier and provides a smooth transition for impacting vehicles which could contact the fence structure. To date, a small number of full-scale crash tests have been conducted on parapet-mounted fences, none of which included crash testing of fence terminations. For this reason, DOT fence design terminations and full-scale crash testing of test articles that included sloped features were investigated to develop a termination design for the Iowa parapet fence system.

7.1 Review of State DOT Fence Terminations Designs

Most state DOT fence designs have fences terminating at a vertical post, and in some cases, additional bracing is used to support the fence fabric loads on end posts. Some designs use a larger diameter posts as terminal posts. The additional lateral stiffening is added at terminals to prevent lateral swaying during the chain-link mesh installation, to stretch the chain link fabric under a static tension, and to prevent damage to end posts from loads occurring on the posts or fabric in the fence interior.

Of the reviewed state fence designs, only the Nebraska DOT design includes a downward-sloped fence termination, shown in Figure 50. This design also has a truss rod near the terminals used to brace the fence ends. To achieve the 2H:1V taper, pipe connections that rotate about the lateral axis were used to attach the top fence rail from the 6-ft tall end post to the 2-ft tall terminal post. Though not visible in Figure 50, these pipe connections are most likely slip-on rail end that attach to brace bands, an example of which is shown in Figure 97.

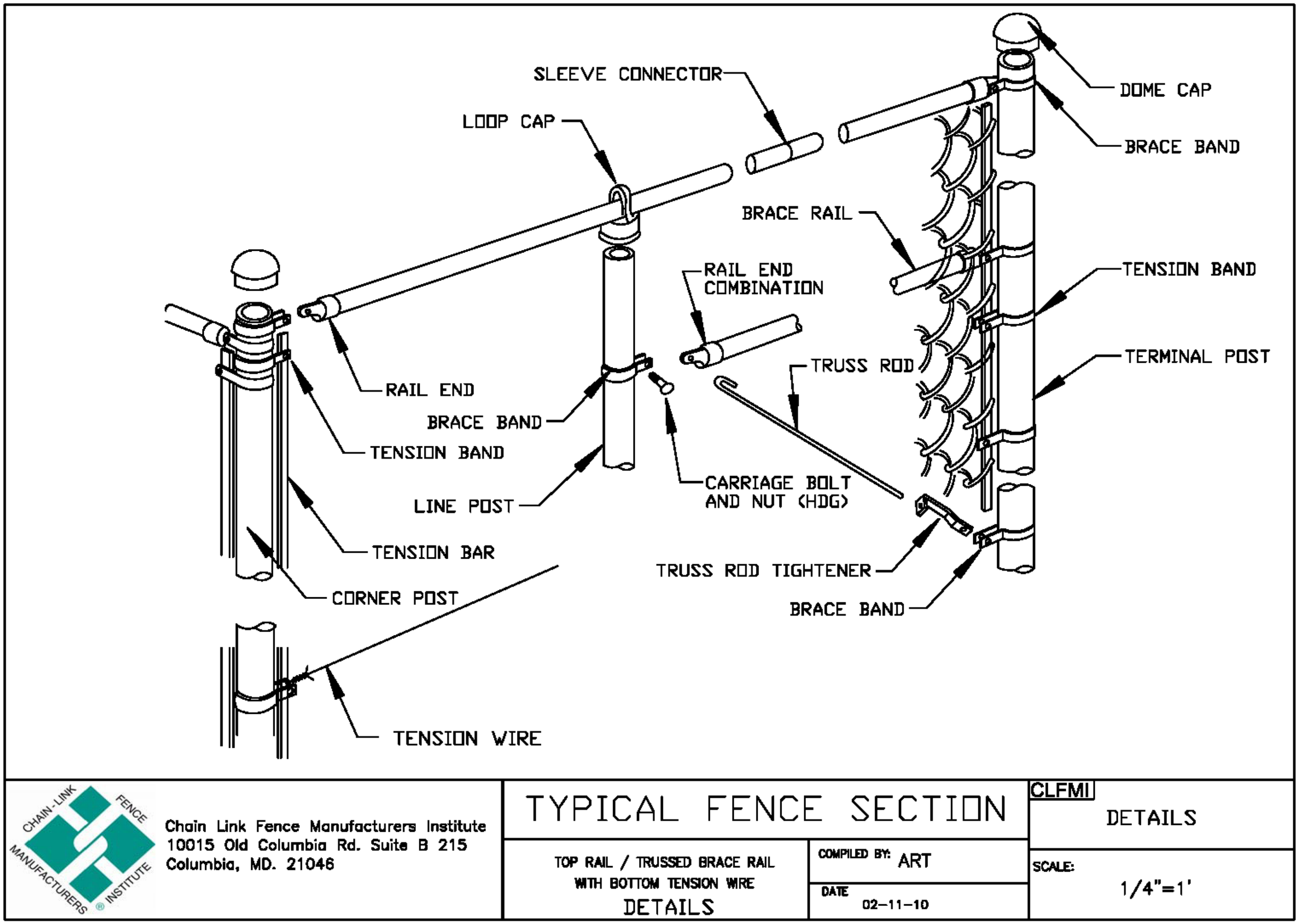

Figure 97. Typical Fence Termination Details [47]

7.2 Review of Previously Crash Tested Systems with Vertical Taper Features

The two full-scale crash tests presented in Section 2.4 suggest that a 2H:1V slope for a vertical tube transition is capable of meeting crashworthy requirements specified under NCHRP Report 350 TL-3. Thus, it was necessary to compare these installations to the selected 36-in. tall, near vertical-face, traffic barrier with a back-mounted, 7-ft chain-link fence and determine if a similar sloped end termination transition could be developed.

The two crash tested transitions had several differences when comparing them to the debris fence which was designed herein. As discussed in Section 8.3.1, the fence was designed to be mounted to the back side of a 36-in. tall, 8-in. thick at the top concrete barrier, which is 3.3-in. taller than the bridge rail crash tested in test no. 401021-7. The previously-crash tested transitions had smaller lateral offsets between the tapered rail and the face of the adjacent thrie beam or tube rails compared to the 8-in. lateral offset achieved by mounting the fence on the back side of the proposed parapet. These two factors will reduce the vehicle interaction and snag that could occur on the tapered termination during the full-scale crash testing of the parapet-mounted debris fence termination when compared to the two transition crash tests. Alternatively, the two transition crash tests were tested at NCHRP Report 350 TL-3 test conditions while this fence system is designed to meet MASH 2016 TL-3 criteria. The updated roadside testing criteria had a 590-lb increase on the target vehicle weight requirement which increases the impact severity and therefore could potentially result in larger vehicle intrusion over the barrier.

7.3 Fence Termination Design

It was decided that the fence termination would be designed with a 1H:1V slope end achieved by tapering the cap rails down towards the concrete barrier. This taper was selected primarily to reduce the termination length since the 7-ft tall fence with a 2H:1V slope would require a 14-ft long taper. Referring to the literature review, the TTI signs on concrete median barriers study indicated that placing some stiff vertical elements on top of barriers in controlled locations did not produce significant snagging that violated MASH 2016 occupant safety criteria. In this case, the sloped cap rail will be placed further behind the barrier face than vertical members in the TTI study and should therefore pose less of a snag concern. Furthermore, the connection between the cap rail and concrete barrier was designed to have a stiffness lower than that of the vertical posts used within the Iowa parapet-fence system, which would increase the propensity of cap rail deflection if impacted by a pickup. As such, this configuration was considered to pose less of a snag concern when compared to the fence vertical posts.

A connection between the wire rope and concrete barrier was achieved by means of a steel bracket that attached to the wire rope turnbuckle. For convenience, the end cap rail was also designed to attached to this cable bracket using an angled flat bar bracket to bridge the gap between the cap rail and cable bracket. The fence termination design is shown in Figure 98, details of the end cap rail to cable bracket connection are shown in Figure 99. Note that fence fabric was not included in tapered fence region to simplify construction. In the following sections, the design of the cable bracket, the concrete anchorage, and the angled bar bracket will be discussed.

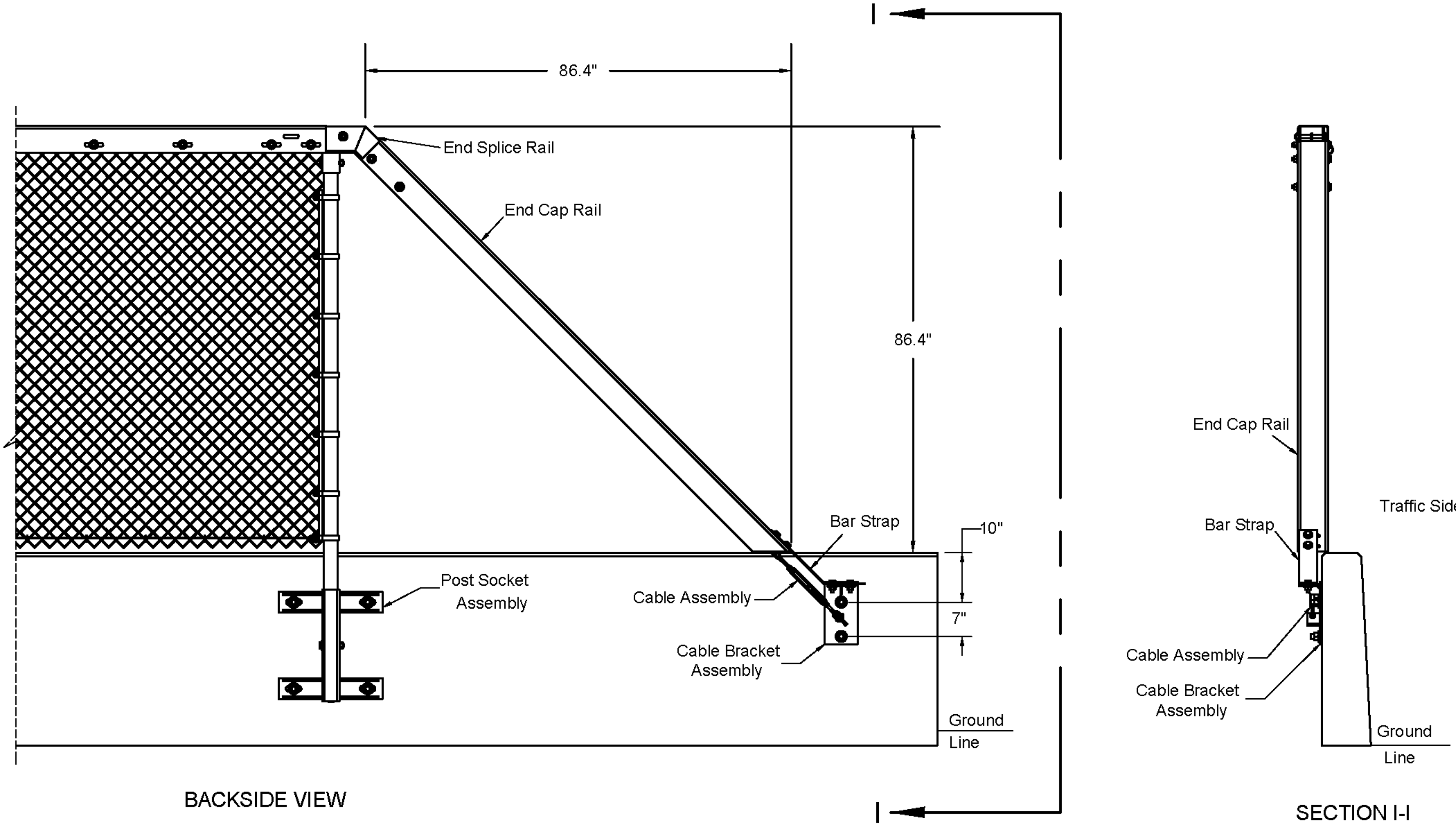

Figure 98.Sloped End Termination Design

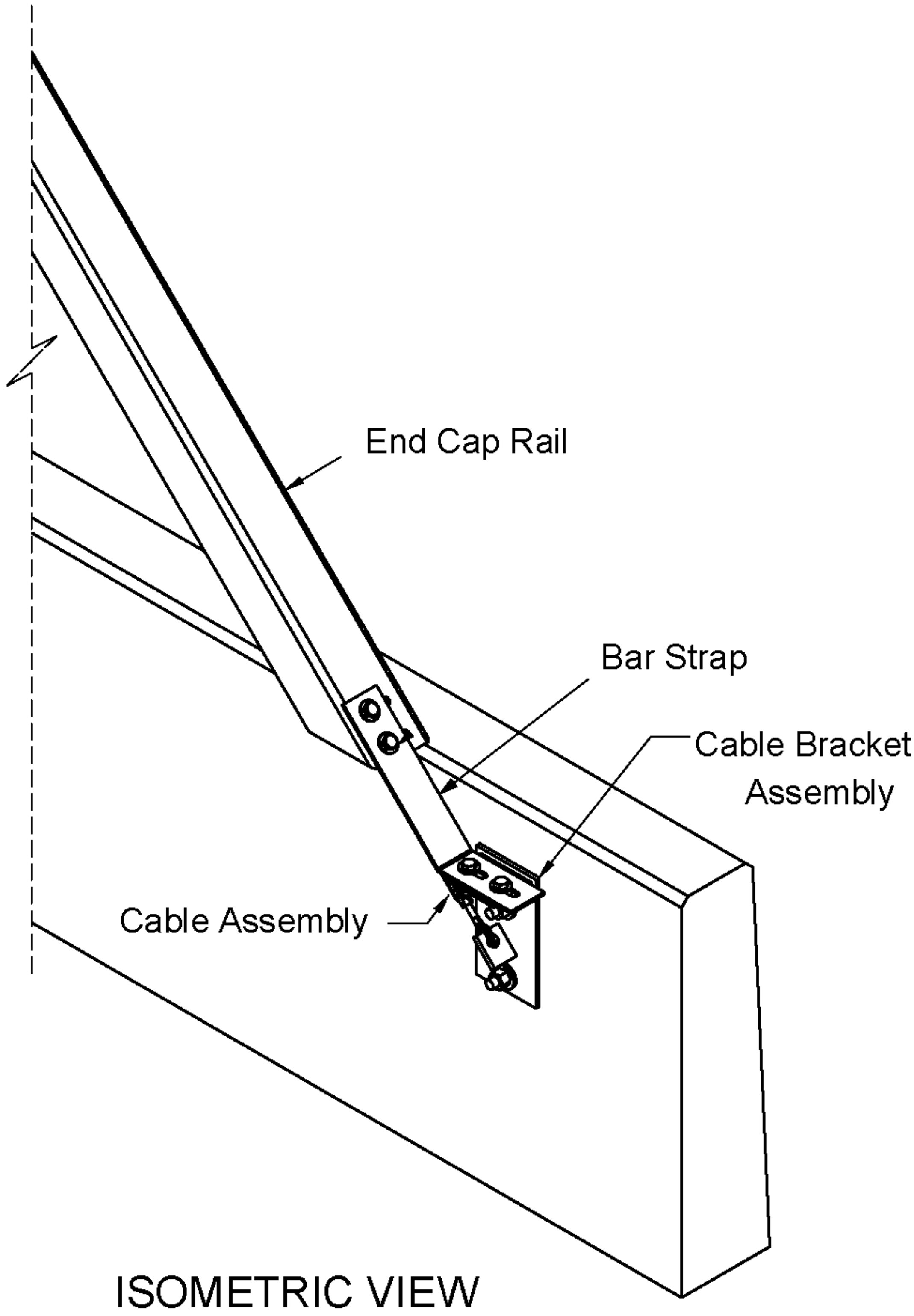

Figure 99. Isometric View of Sloped End Termination Attachment

7.4 Tapered Cap Rail Bar Strap Attachment Design

To further reduce snag concerns during errant vehicle impacts near the fence termination, the strap attaching the tapered cap rail to the wire rope bracket was designed with a lower bending capacity than that of vertical posts. This component will most likely deflect due to lateral-torsional buckling and therefore, the limit states of this failure mode were considered by following the flexural design procedure outlined in the *AISC Steel Construction Manual* [41]. These provisions specify that the lateral torsional buckling limit for flat, rectangular section must not exceed the yielding state limit, determined using Equation (12). The plastic section modulus of a rectangular bar was determined using Equation (43).

$$Z = \frac{bh^2}{4} \tag{43}$$

Where: Z = Plastic section modulus, (in.^{3})

b = Bar thickness, (in.)

h= Bar width, (in.)

7.5 Wire Rope Attachment Design

Design objectives require that the wire rope attachments and termination develop the full capacity of the wire rope. The wire rope attachment bracket consisted of a steel tab welded to a base plate which is anchored to the concrete barrier. The wire rope turnbuckle attaches directly to the mentioned steel tab. Failure of the bracket could occur via the turnbuckle pinned connection, failure of the welds between the tab and base plate, base plate flexure, and concrete anchorage failure. The potential cable bracket failure modes are illustrated in Figure 100 while the design procedure is summarized in Figure 101. Before this part could be design, a design load was established.

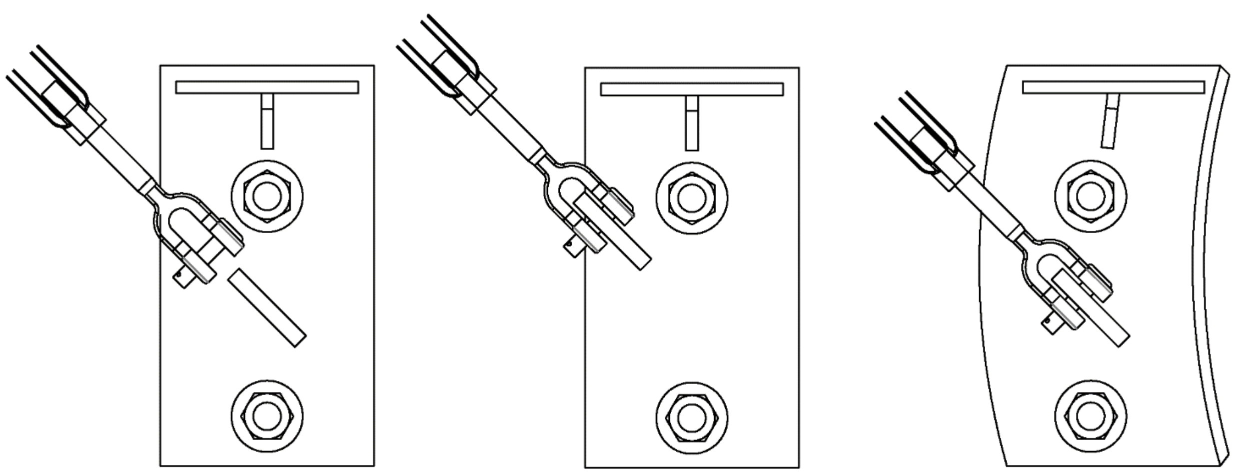

Figure 100. Wire Rope Attachment Bracket Failure Modes

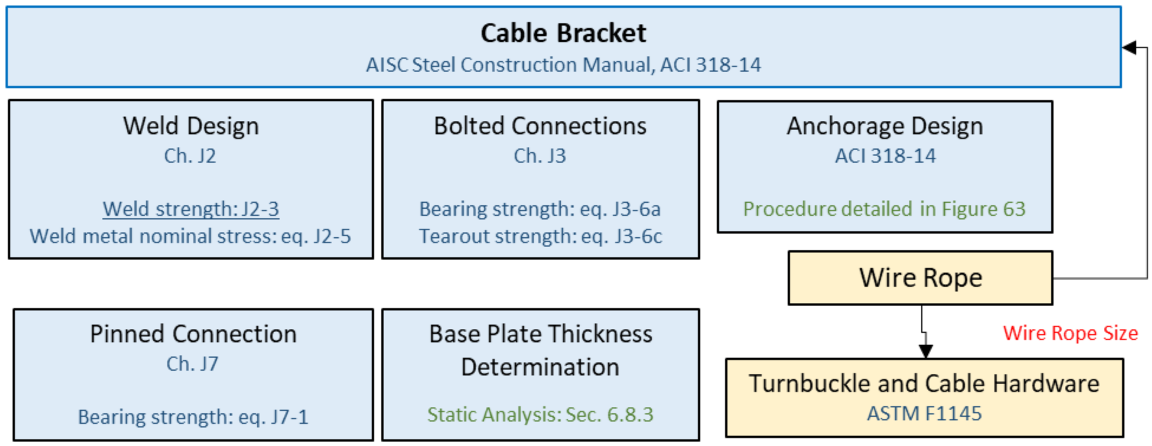

Figure 101. Wire Rope Attachment Design Procedure

7.5.1 Loading

Tensile force in the wire rope will transfer to the bracket as a direct shear force. The wire rope tensile force also acts on the distance between the turnbuckle pinned attachment and the base of the bracket creating a moment. Tensile and compressive forces at the anchors then resist the applied moment on the bracket. When designing these connections and components to develop the wire rope capacity, the design load on the bracket was established as minimum specified wire rope breaking force from ASTM A1023 designation. The reason being is, when the wire rope achieves the breaking force, any additional strain will typically not cause forces in the wire to increase due to plastic deformation. However, it is possible that the manufactured wire rope has a breaking strength higher than the ASTM specified minimum breaking strength. To account for possible variations in wire rope breaking strength, the design tensile force on the bracket was taken as the ASTM specified minimum breaking force multiplied by a factor of 1.6. This factor is consistent with the findings described by Stolle et al. where it was determined that the ASTM specified minimum breaking strength of the wire rope was 25,000 lb however, tensile testing indicated that the breaking strength was closer to 40,000 lb [48]. Note that the wire rope tested in that study consisted of a 3x7 construction while the wire rope selected for the Iowa parapet fence used a 7x19 construction.

7.5.2 Pinned Connection Design

The first region of the bracket that will experience loading will be the turnbuckle-to-bracket pinned connection. Chapter J7 of the *AISC Steel Construction Manual* [41] was consulted to determine the design bearing strength of the pinned connection between the turnbuckle and cable bracket. These provisions are specifically for pinned connections with finished surfaces; however, this connection is more closely comparable to a bolted connection where the shoulder of the bolt transfers force to the bolt hole. Regardless of this, these provisions were followed since they provide a more conservative design. The required thickness of the pin tab on the cable bracket was determined using Equation (44).

$$\phi_b R_n = \phi_b F_y A_{pb} \ (AISC\ J7-1) \tag{44}$$

Where: $\phi_b R_n$ = Design bearing strength (kips)

F_y = Specified minimum yield stress (ksi)

A_{pb} = Projected area in bearing (in.^{2})

ϕ_b = 0.75, Resistance factor for bearing strength

7.5.3 Design of Welded Connections

Chapter J of the *AISC Steel Construction Manual* [41] was consulted to determine the required weld strength for impact loading conditions. Provision for fillet welds accounting for directional strength increases were followed since loading of fillet welds could occur in any direction during severe impact loading events. Equation (26) was used to determine the capacity of the welds merging the tab to the base plate.

7.5.4 Base Plate Design

The baseplate's main function is to attach the turnbuckle to the concrete barrier and transfer shear and subsequent compressive and tensile forces to the concrete barrier via the anchors. A flexure analysis was conducted on the baseplate to minimize the potential for damage during impact events. To identify the bending demand, the baseplate was considered a beam with a center moment transferred to it via the pin tab. Since it is desired that the concrete anchorage not fail, the bolted connections were assumed rigid as they will not allow any rotation at the anchors.

Two load conditions were considered, where the design load may be applied longitudinally and vertically on the bracket, as shown in the loading diagrams in Figure 102. In the longitudinal load condition, the moment is directly applied to the rigid anchorage connection, resulting in no moment transfer to the base plate. The moment can be decomposed into a couple, and the bracket separated into two rigidly-constrained cantilever beams. For this case, the right side of the bracket poses a worse-case scenario since the concrete will resist flexure on the left side. The moment experienced by the right side of the bracket is localized on the portion of the bracket with the increased section due to the presence of the pin tab, and therefore did not reflect a critical load scenario.

In the vertical loading condition, the moment is applied at the center location between the rigid anchor connections. During this loading condition, the peak bending moments occur at the center of the bracket and at each anchor location. Since the bracket section is the largest at the center due to the pin tab, bending about a cross-section of base plate immediately in front of the pin tab a was considered the critical load location. The required thickness was determined using Equation (12) and the rectangular plastic section modulus of the base plate. This analysis is described in detail in Appendix G.

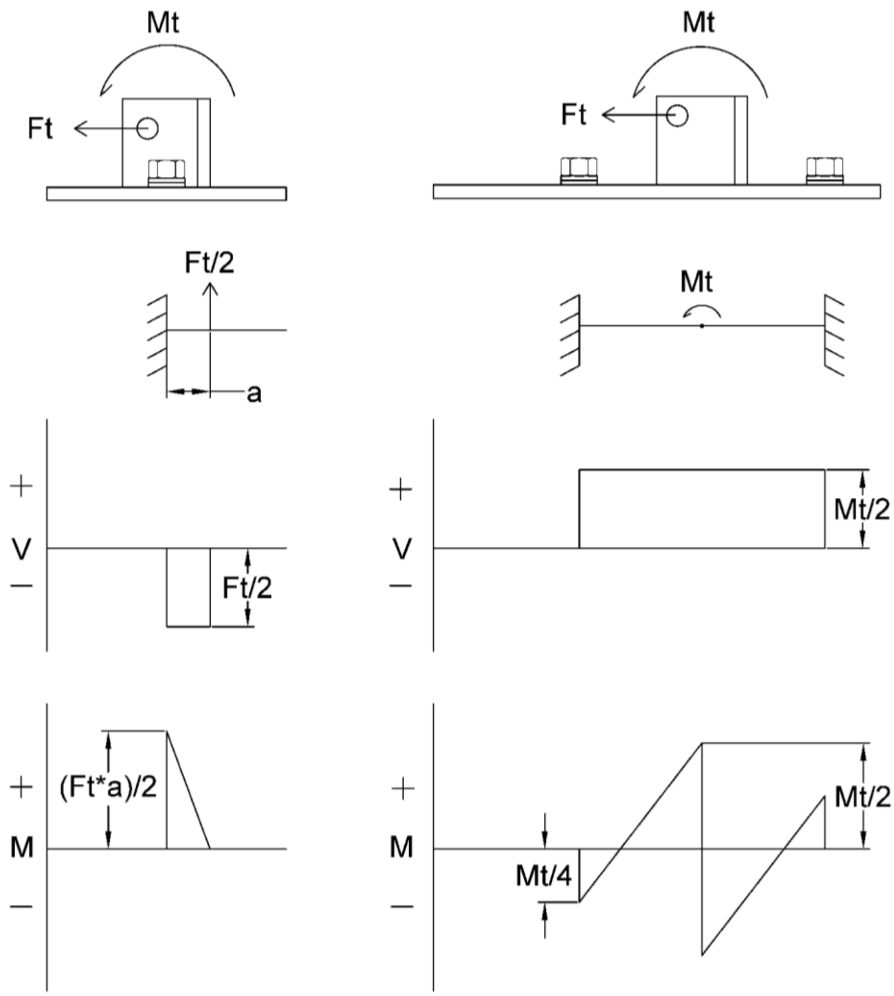

Figure 102. Cable Bracket Loaded Longitudinally (Left) and Vertically (Right)

7.5.5 Concrete Anchorage Design

The procedure outlined in Section 6.6 was followed to determine if the anchorage capacity met or exceeded the design load on the anchorage. Although the same anchors and epoxy will be used to attach this bracket to the barrier, the anchorage design was reviewed since only two vertically-spaced anchors would attach the bracket to the barrier. Additionally, to reduce the size of this bracket, a shorter anchor spacing of 9.5 in. was used which also affects the anchorage strength. The capacities of the selected anchors exceeded the expected design loading.

7.5.6 Wire Rope Attachment Design Summary

A $\frac{5}{16}$-in. diameter ASTM A1023 utility wire rope with a minimum breaking strength of 9.8 kips was selected to be used in this parapet fence system. Subsequently, the resultant design load on the cable bracket was 15.7 kips. As a conservative approach, this load was applied to the bracket as a longitudinal shear force and lateral tensile force since this loading condition applied the maximum tensile force on the anchorage which was controlled by the tensile breakout strength.

The cable bracket and anchorage connection design is summarized in Table 29. ASTM A572 Grade 50 steel plate will be used in the fabrication of all components of this bracket. To meet the pin bearing load demand, a 9⁄16-in. thick steel plate was required, attached to the base plate with 3⁄8-in. thick fillet welds. A 3⁄8-in. thick plate was selected as the base plate material to meet flexure demand. Direct shear forces, direct tensile forces, and resultant tensile forces from the moment did not exceed anchorage capacity limits. Additionally, anchorage combined loading requirements were satisfied, which were considered since severe impact loading scenarios occurring near the fence terminations could rotate the wire rope such that the bracket is under the action of combined shear and tensile forces.

Table 29. Wire Rope Attachment Bracket Design

Failure Mode	Demand	Capacity
Pin Bearing (Kips)	15.7	16.6
Weld Shear (Kips)	15.7	43.0
Base Plate Flexure (kip-in.)	7.4	10.7
Anchorage Tensile Concrete Breakout (Kips)	15.7	20.8
Anchor Shear Concrete Breakout (Kips)	7.8	17.5
Anchor Combined Loading Requirement	1.2 ≥	1.2

8 PROPOSED DESIGN DETAILS AND DISCUSSION

8.1 Overview

In this chapter, details of the parapet-mounted fence are presented followed by a discussion of each major fence component. In this discussion, each components design, including how objectives were satisfied is described. Additionally, deviations from Iowa fence standards are presented along with reasoning's for such decisions.

8.2 Design Details

The proposed system is configured with a total length of 124 ft – 6 in. and consists of approximately 104 ft of debris fence and two end sections. The chain-link debris fence is mounted to the back side of a near-vertical concrete parapet, as shown in Figures 103 through 131.

Posts used to support the debris fence are $111\frac{1}{8}$-in. long round structural steel tubes with a $2\frac{7}{8}$-in. outside diameter and a 0.188-in. wall thickness conforming to ASTM A1085 specifications. The fence fabric consists of a 7-ft tall, galvanized fence mesh with 2-in. mesh spacing, constructed with 9-gauge steel wires with knuckle selvage at the top and bottom of the fence. The chain link should satisfy ASTM A817 specifications.

The vertical post-to-barrier bracket is to be fabricated using two, 21-in. long, $4\frac{1}{4}$-in. wide steel flat bars and a $22\frac{1}{4}$-in. long, $3\frac{1}{2}$-in. square HSS tube with a $\frac{1}{4}$-in. thickness conforming to ASTM A500 grade B. Gussets between the square tube and steel flats are 8 in. long and 3 in. tall. A strap is to be welded to the bottom of the square socket which is 1 in wide and $3\frac{1}{16}$ in. long. All mentioned parts excluding the square tube are fabricated using $\frac{1}{4}$-in. thick ASTM A572 grade 50 steel plate and are connected using $\frac{1}{4}$-in. welds. After fabrication, brackets should be galvanized to meet ASTM A123 specifications.

The anchors used to attach the debris fence to the parapet are $\frac{7}{8}$-in. ASTM A193 B7 anchors, galvanized in accordance with ASTM A153, with a 6-in. concrete embedment depth. Additionally, the epoxy used to bond anchors to the concrete shall have a minimum characteristic bond stress of 1,800 psi. The top anchors are located 10 in. below the top edge of the barrier and are spaced approximately 15 in. apart longitudinally. The second set of anchors is located $27\frac{1}{2}$ in. below the top of the barrier and are also spaced approximately 15 in. apart.

The top fence retention system consists of galvanized 7x19, $\frac{5}{16}$-in. diameter utility wire rope meeting ASTM A1023 specifications. Wire rope connection hardware is comprised of an Electroline turnbuckle assembly that attaches to a $\frac{5}{16}$-in. diameter wire rope by means of a plug and sleeve mechanical connection. The cable bracket base plates are to be fabricated using $6\frac{3}{4}$-in. x $\frac{3}{8}$-in. x 13 $\frac{5}{8}$-in. steel plate. Pin tabs shall be fabricated from 3-in. x $\frac{9}{16}$-in. x $2\frac{1}{2}$-in. steel plate and include a $\frac{1}{2}$-in. pin hole. These tabs will be connected to the center of the turnbuckle bracket at a 45-degree angle using $\frac{3}{8}$-in. welds. The tab on the top of the cable bracket, shown in Figure 115, shall be fabricated from a $5\frac{3}{4}$-in. x $\frac{3}{8}$-in. x $4\frac{1}{4}$-in. steel plate. Angled brackets that attach upper horizontal stiffeners to turnbuckle brackets should be fabricated with $23\frac{9}{16}$-in x $\frac{1}{4}$-in. x $3\frac{3}{4}$-in. steel flat bar bent to a 45-degree angle. ASTM A572 grade 50 steel plate shall be used in the fabrication of all components of the cable bracket and angled bracket. After fabrication, parts must be hot dip galvanized to meet ASTM A123 specifications.

Upper horizontal stiffeners, also referred to as cap rails, are to be formed from a 3⁄16-in. thick ASTM A572 grade 50 steel plate to achieve the geometry shown in Figure 117. This plate is to be folded to a 6 3⁄16-in. x 5½-in. folded channel geometry with a 94-in. length. Splice rails shall be fabricated by folding 3⁄16-in. thick ASTM A572 Grade 50 steel plate to achieve 5⅜-in. x 4⅞-in. channel dimensions. Round HSS tube having a 3½-in. diameter and a ¼-in. wall thickness conforming to ASTM A500 grade B shall be attached to the bottom of splice rails using 3⁄16 -in. welds. End splice rails should be constructed by welding a 21½ -in. x 5⅜-in x 4⅞-in. folded segment to a 15-in. x 5⅜-in x 4⅞-in. segment to achieve a 45-degree angle. After fabrication, parts must be hot dip galvanized to meet ASTM A123 specifications.

The concrete railing, as shown in Figures 123 and 124 consists of a single-slope, half-section, reinforced concrete parapet and shall stand 36-in. tall after placement of a 3-in. overlay. The base of the barrier measures 10 in. in width and tapers up to a minimum of 8 in. at the top of the structure.

Galvanized 7-gauge steel tension wire conforming to ASTM A817 requirements shall be attached to the bottom of the fence fabric using 9-gauge steel hog rigs spaced at 24-in. increments. The 9-gauge steel wire ties shall be attached between fence fabric and posts at 12-in. spacing intervals and to cap rails at 18-in. spacing intervals. Tension bars with a ¾-in. x 3⁄16-in. cross section shall be used with 1-in. wide brace bands sized to match the 2⅞-in. diameter vertical posts. All mentioned hardware must conform to ASTM F626 requirements. Nuts conforming to ASTM A563DH, and bolts conforming to ASTM F3125 Grade A325 with ⅝-11 UNC thread shall be used within the debris fence structure. During fence installation, 21-in. x 1⁄16-in. x 4-in. shims shall be installed between the post bracket and concrete barrier to achieved plum post installation. This shim should be fabricated with steel having a yield strength of at least 25 ksi.

Fence pull-post assemblies are necessary within the fence system if the fence installation exceeds 200 ft in length. Details of the fence mid span pull post assemblies are shown in Figure 130. In this connection, two sets of tension bars are to be attached to both sides of the pull post spaced at 12-in. increment per side.

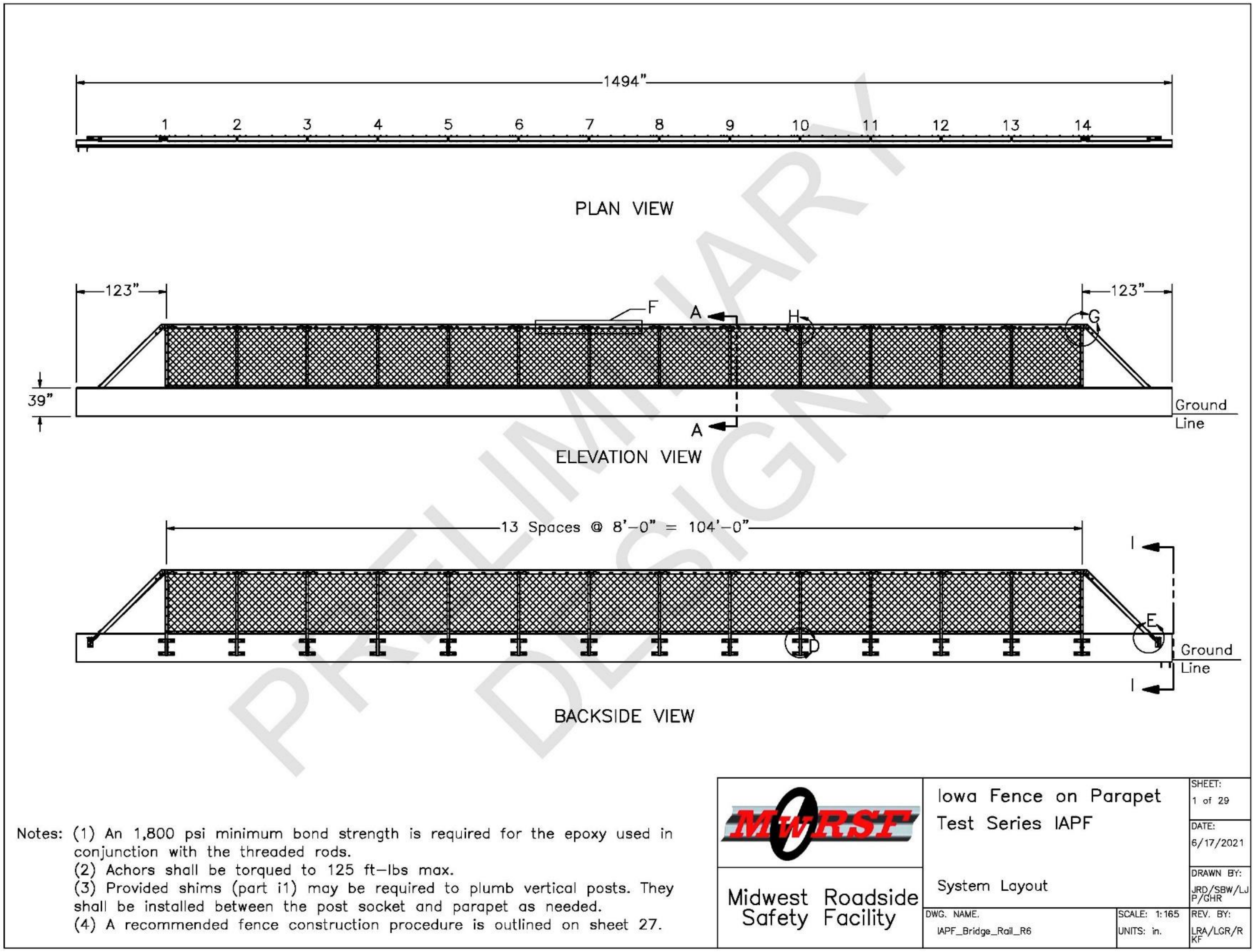

Figure 103. Preliminary Iowa Parapet Fence Design – System Layout

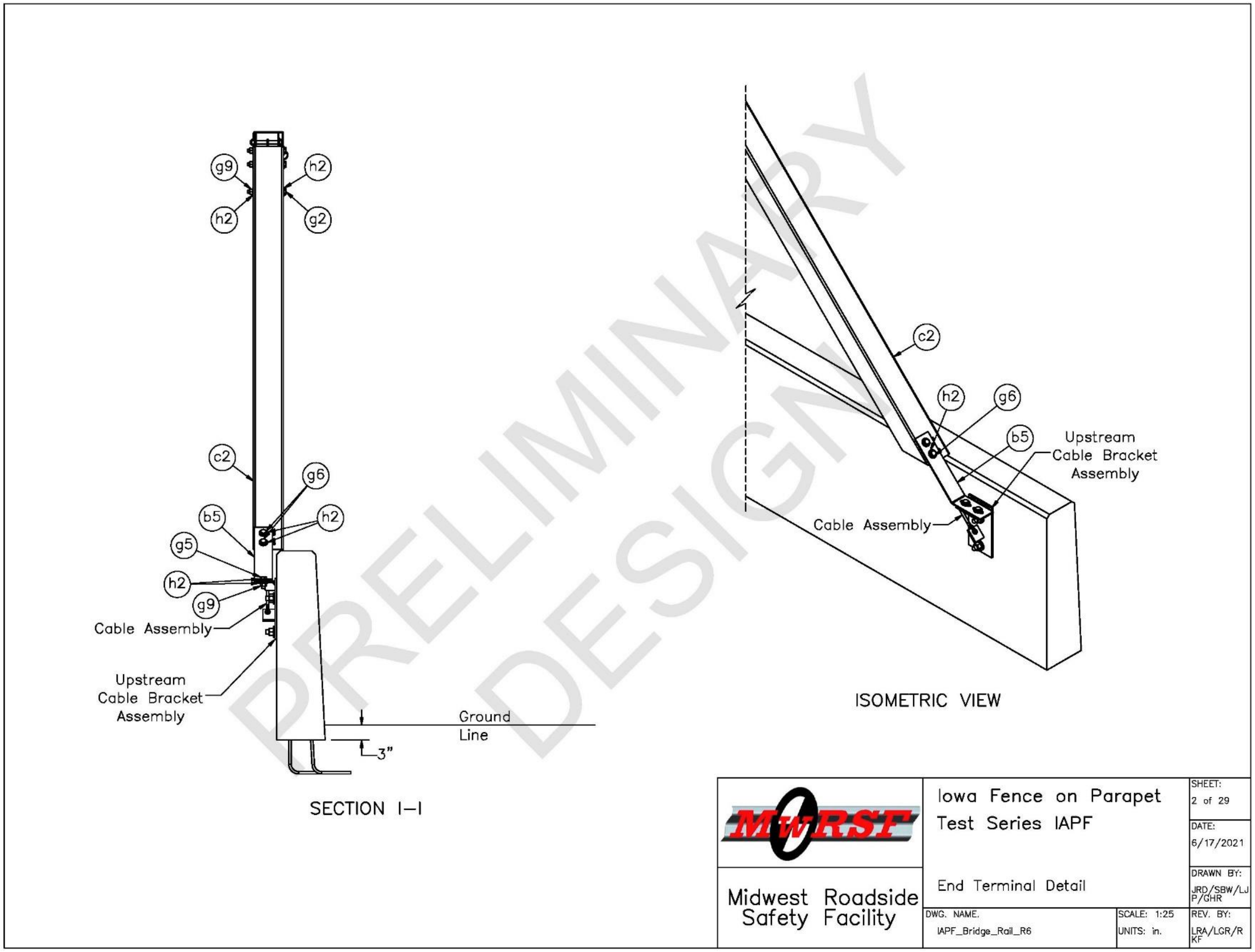

Figure 104. Preliminary Iowa Parapet Fence Design – Termination Details

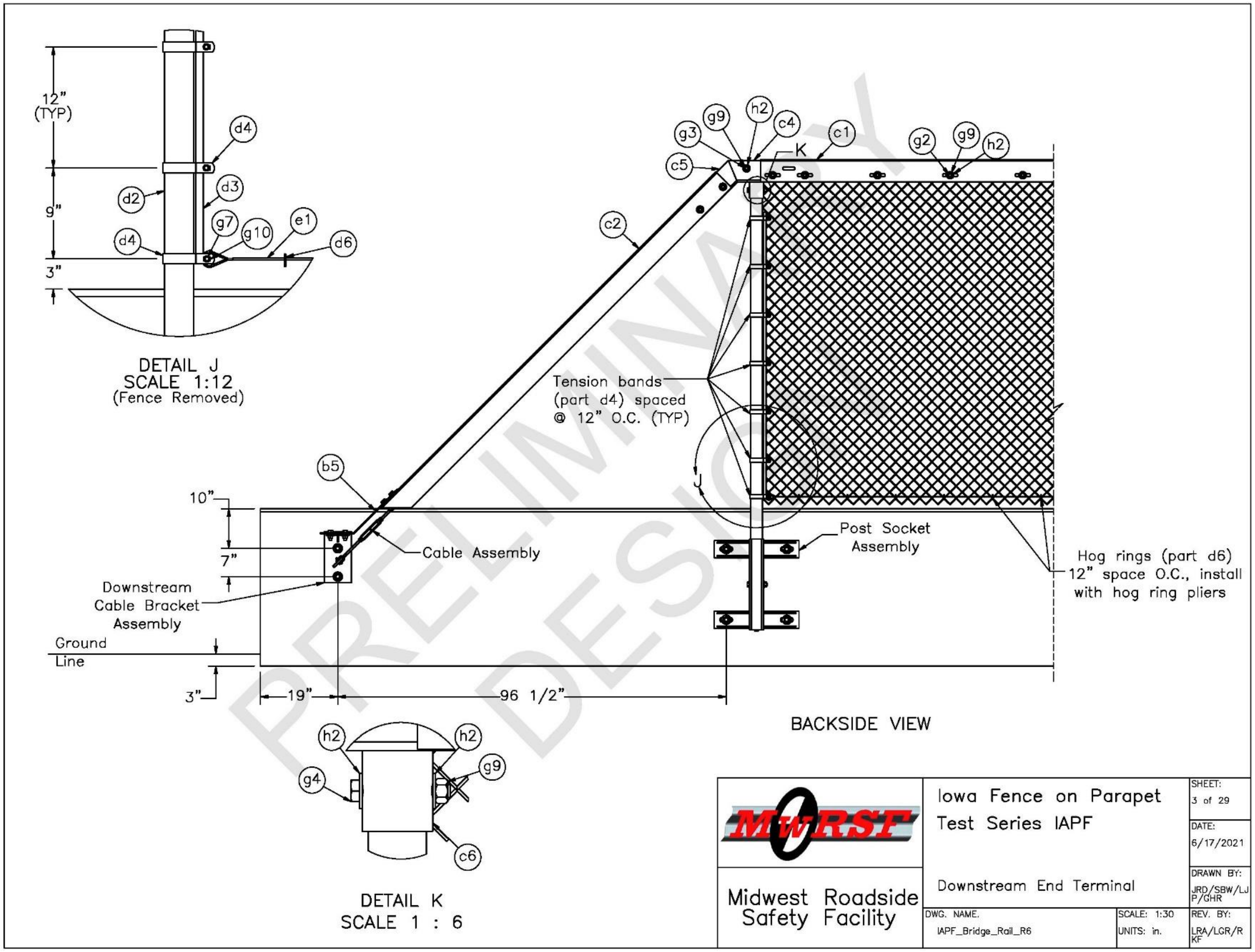

Figure 105. Preliminary Iowa Parapet Fence Design – Downstream Termination Details, Backside View

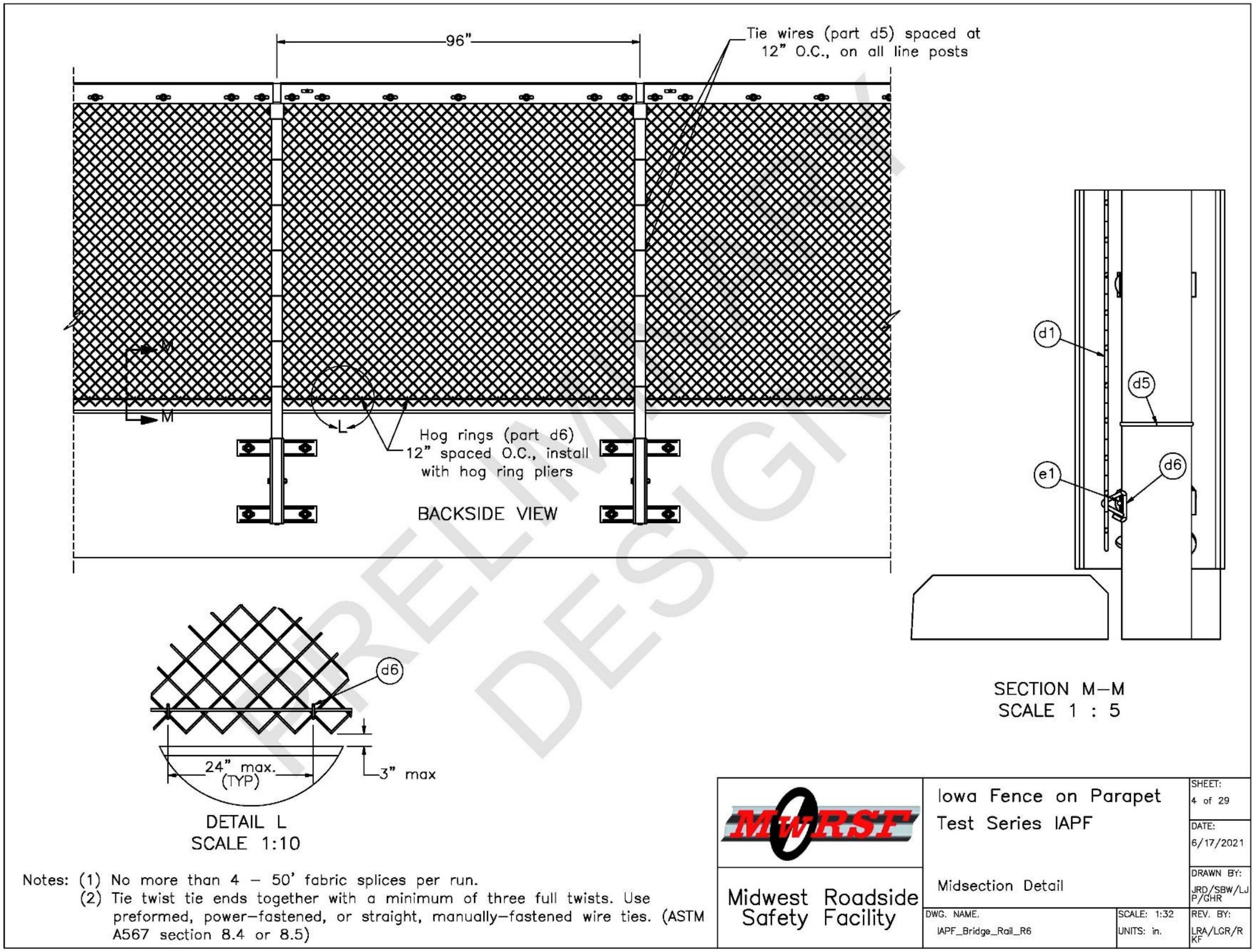

Figure 106. Preliminary Iowa Parapet Fence Design – Mid Span Details

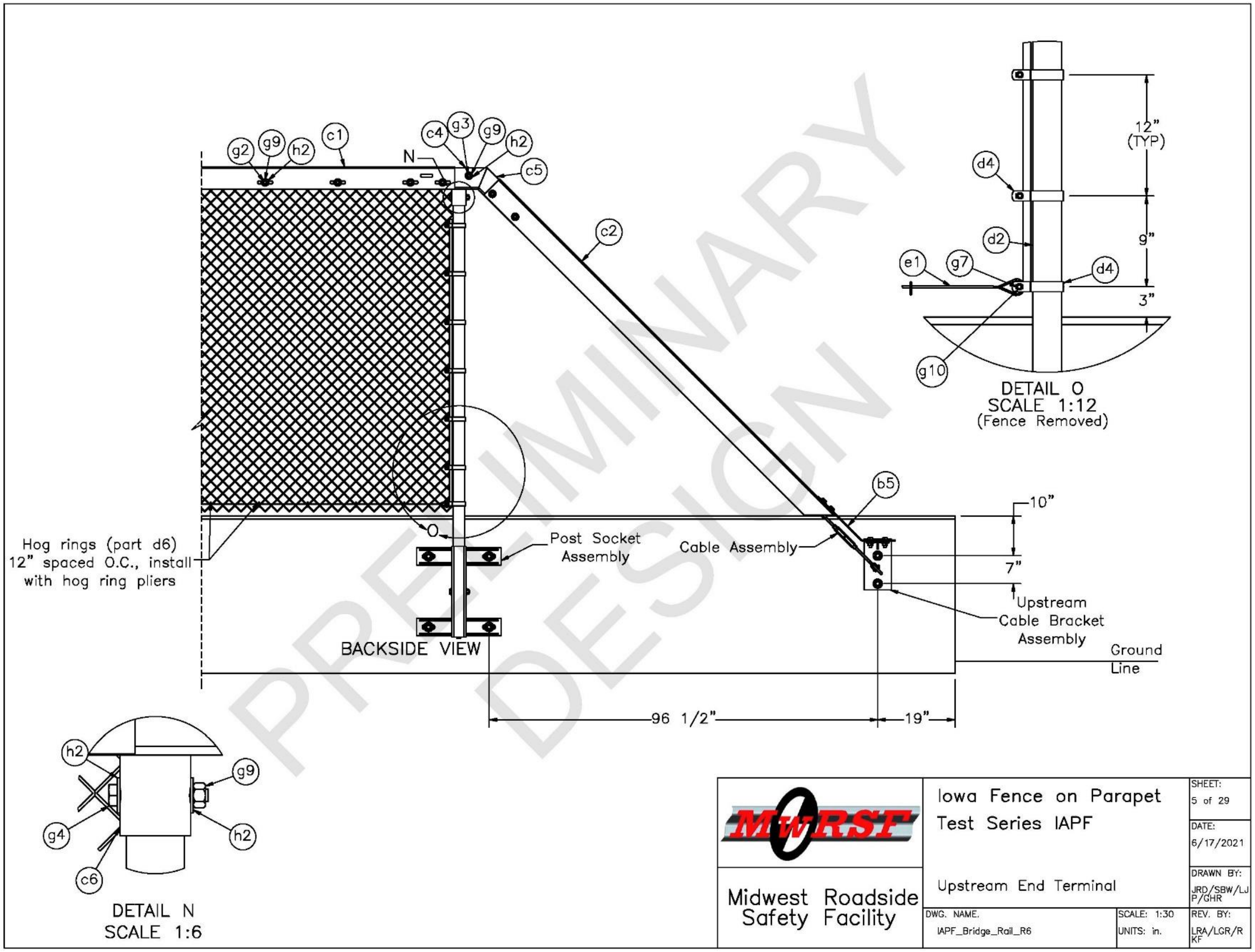

Figure 107. Preliminary Iowa Parapet Fence Design – Upstream Termination Details, Backside View

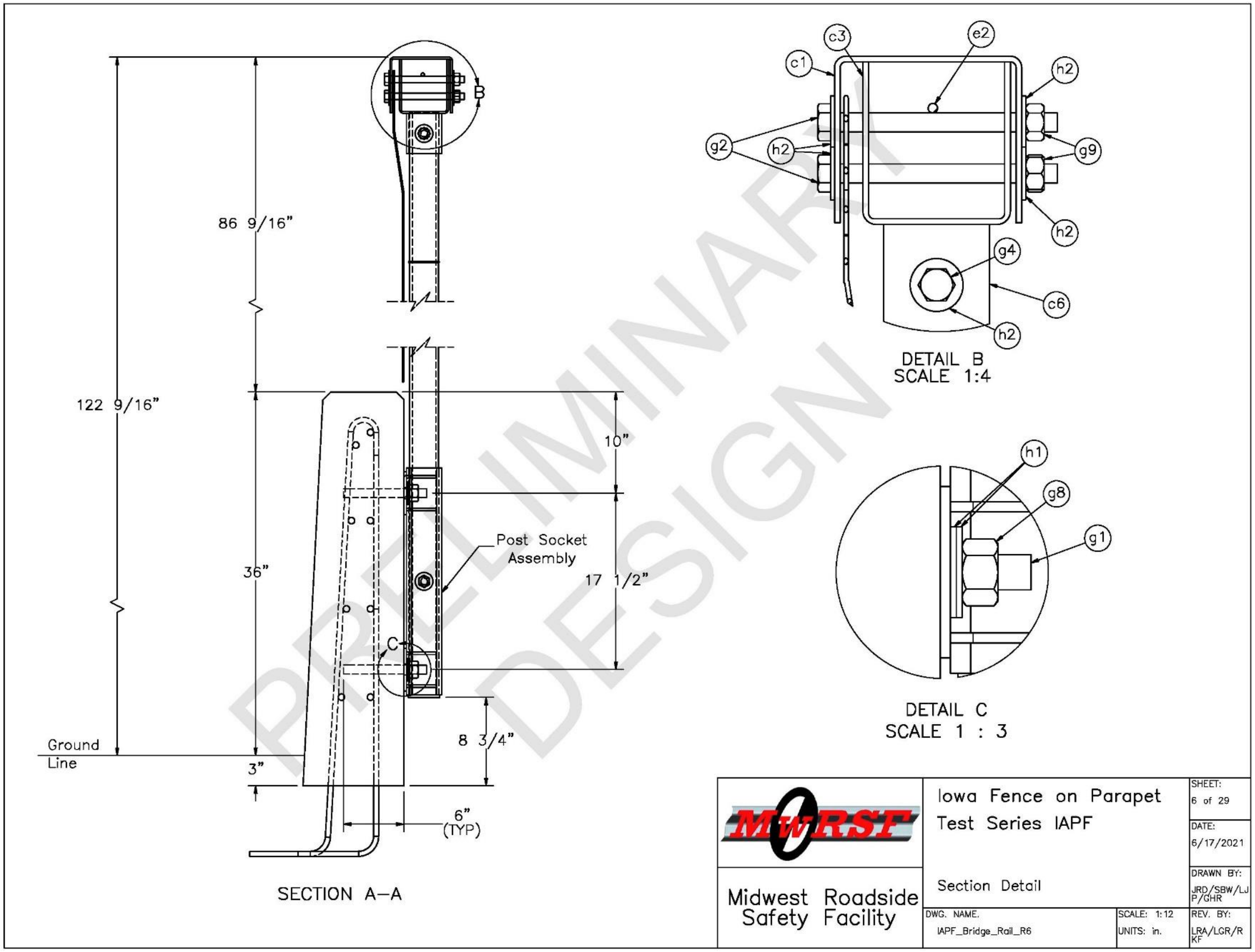

Figure 108. Preliminary Iowa Parapet Fence Design – System Cross Section

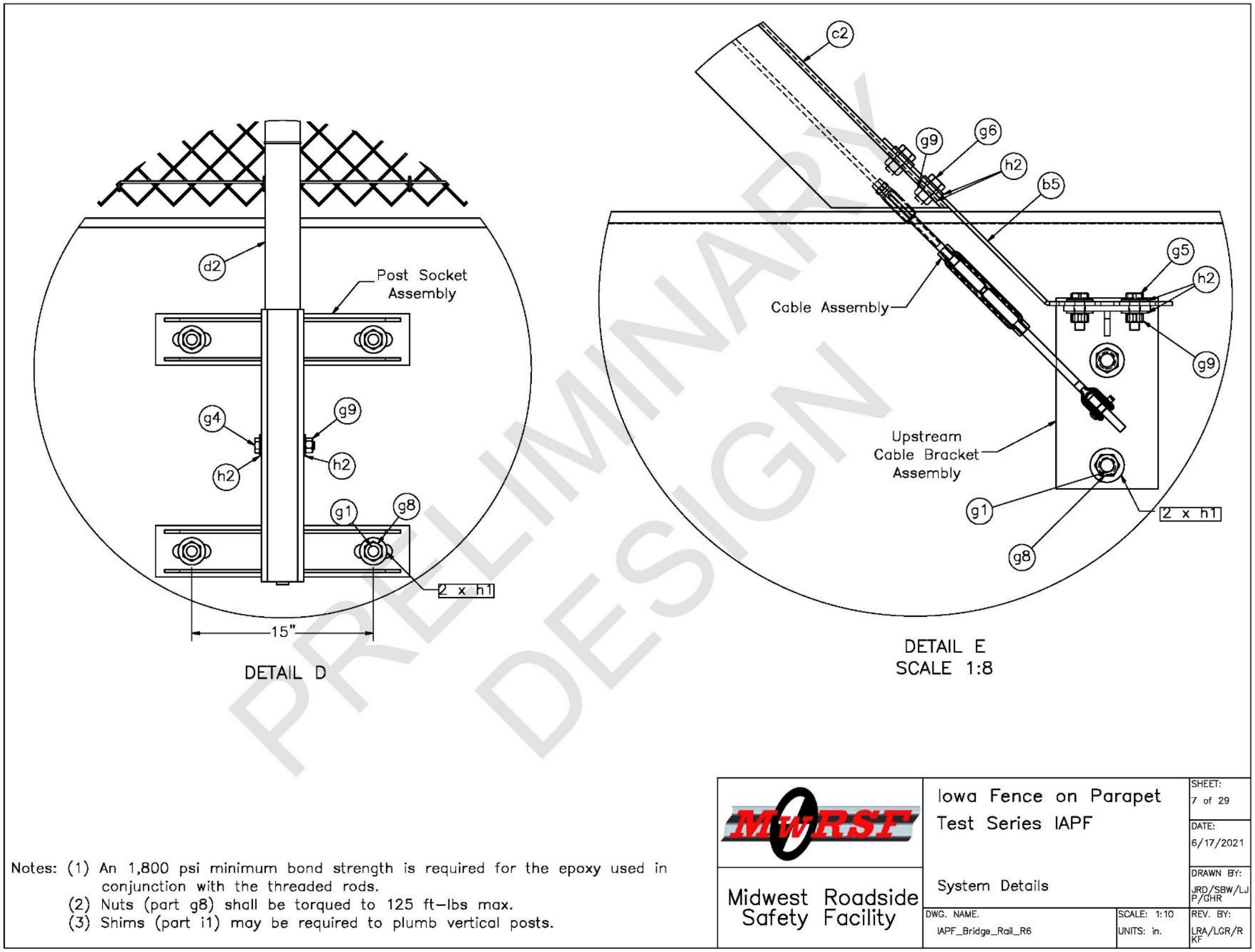

Figure 109. Preliminary Iowa Parapet Fence Design – Fence-to-Parapet Connection Details

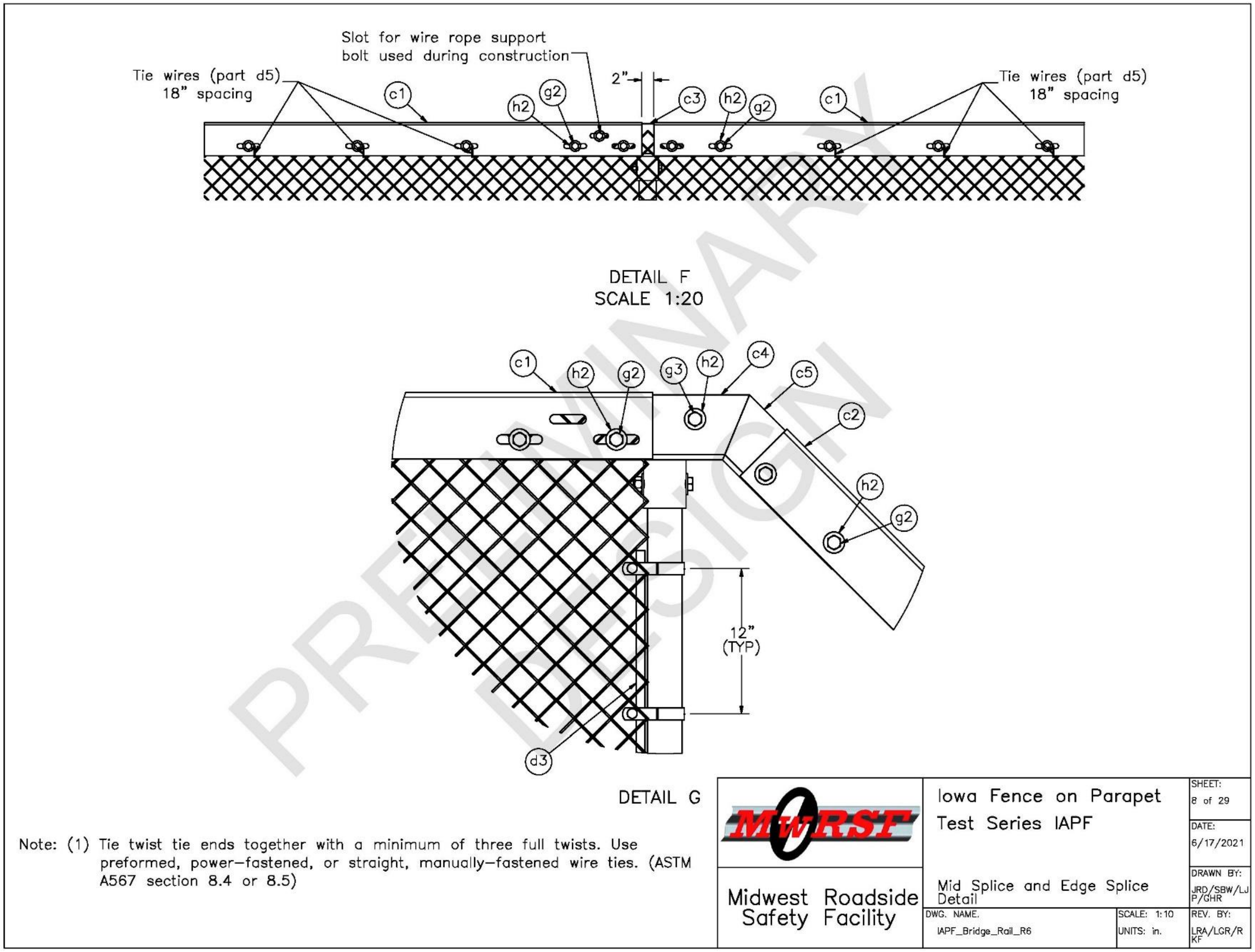

Figure 110. Preliminary Iowa Parapet Fence Design – Splice Rail Connection Details

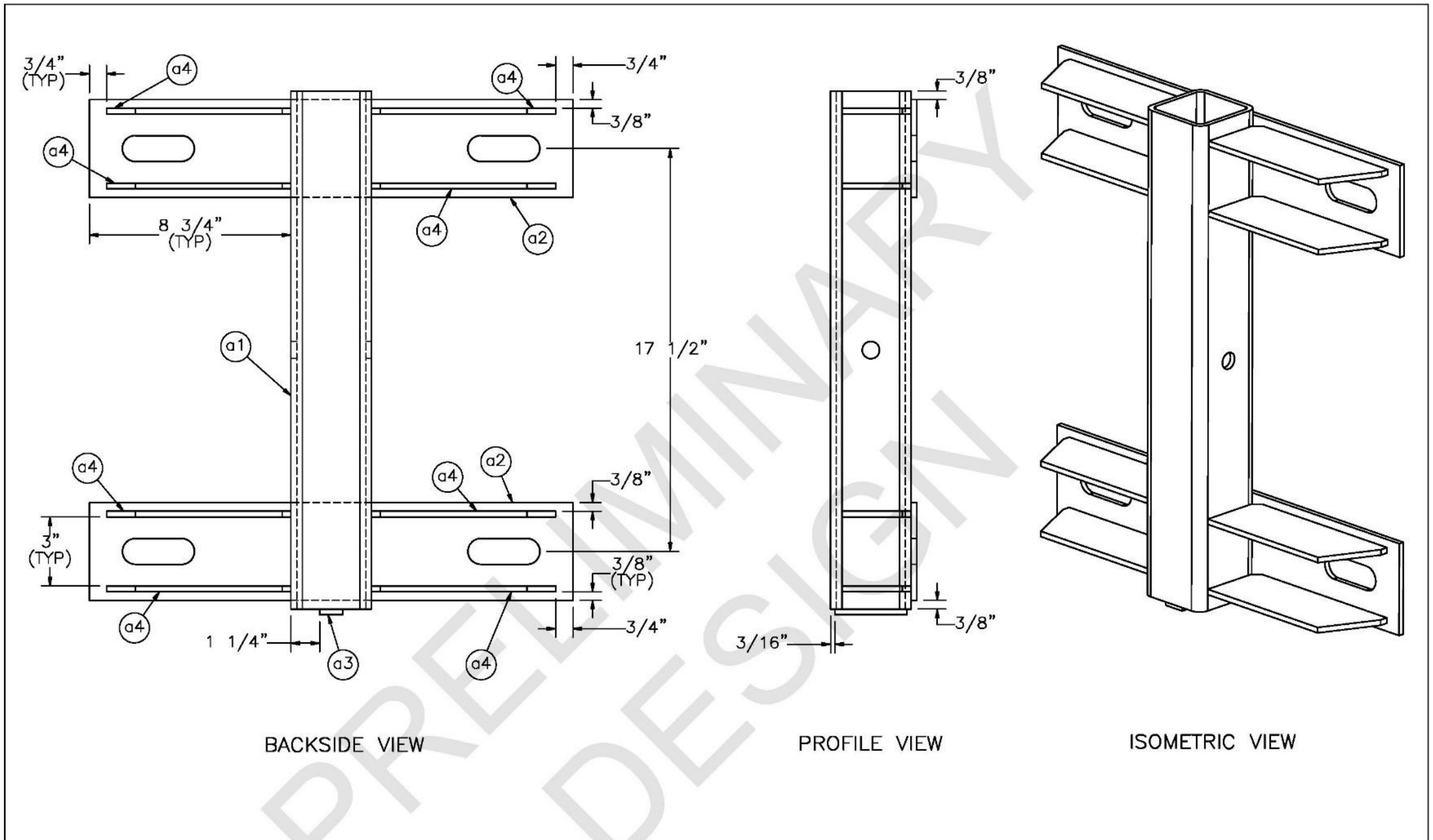

Item No.	QTY.	Description	Material Specification	Treatment Specification
–	14	Post Socket Assembly	–	ASTM A123
a1	1	HSS 3 1/2"x1/4", 22 1/2" Long Square Steel Tube	ASTM A500 Gr. B	–
a2	2	21"x4 1/4"x1/4" Steel Plate	ASTM A572 Gr. 50	–
a3	1	3 1/8"x1"x1/4" Steel Plate	ASTM A572 Gr. 50	–
a4	8	8"x3"x1/4" Steel Gusset	ASTM A572 Gr. 50	–

MwRSF
Midwest Roadside Safety Facility

Iowa Fence on Parapet
Test Series IAPF

Post Socket Assembly

SHEET: 9 of 29
DATE: 6/17/2021
DRAWN BY: JRD/SBW/LJP/GHR
REV. BY: LRA/LGR/RKF
DWG. NAME. IAPF_Bridge_Rail_R6
SCALE: 1:6
UNITS: in.

Figure 111. Preliminary Iowa Parapet Fence Design – Post Bracket Assembly

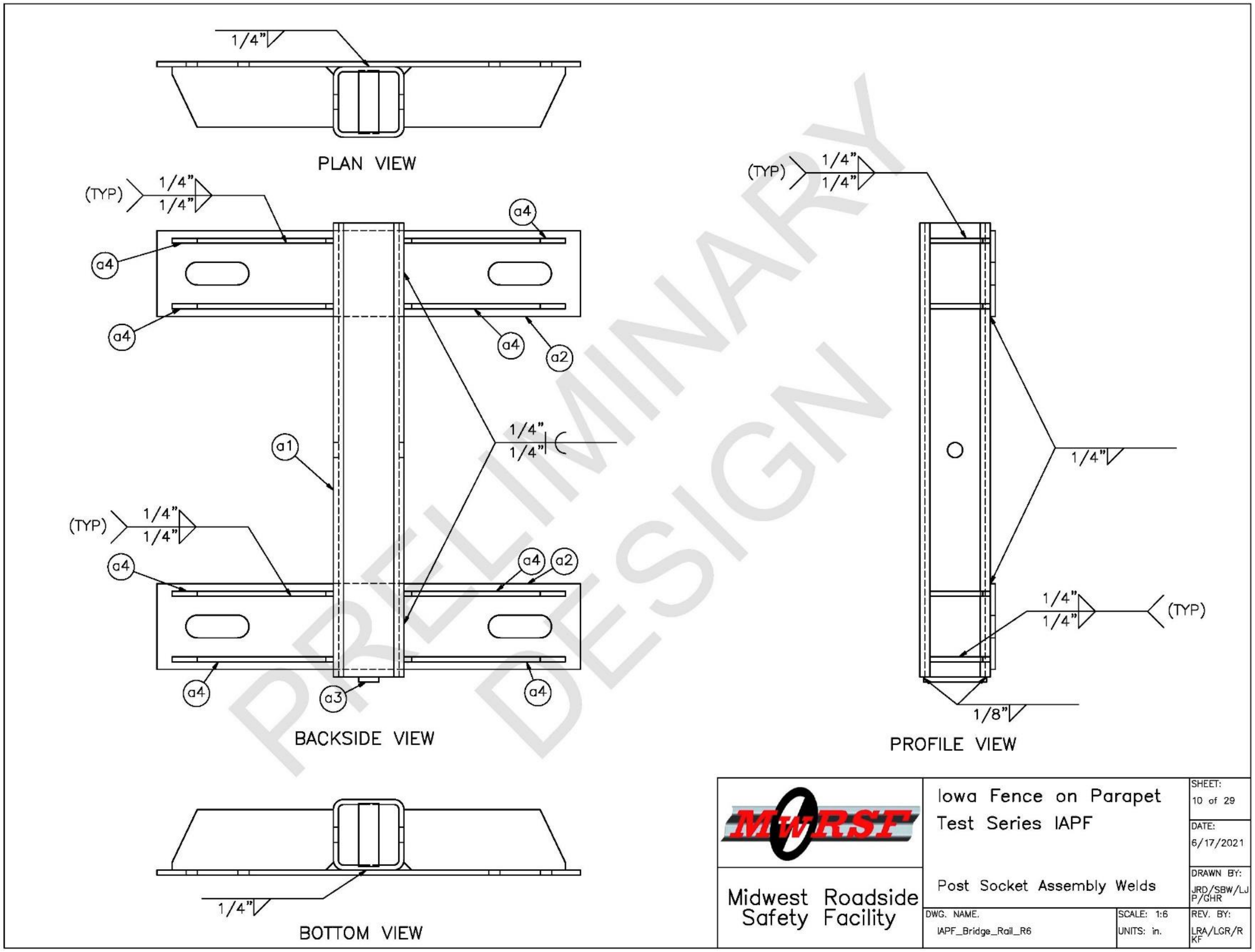

Figure 112. Preliminary Iowa Parapet Fence Design – Post Bracket Weldment Details

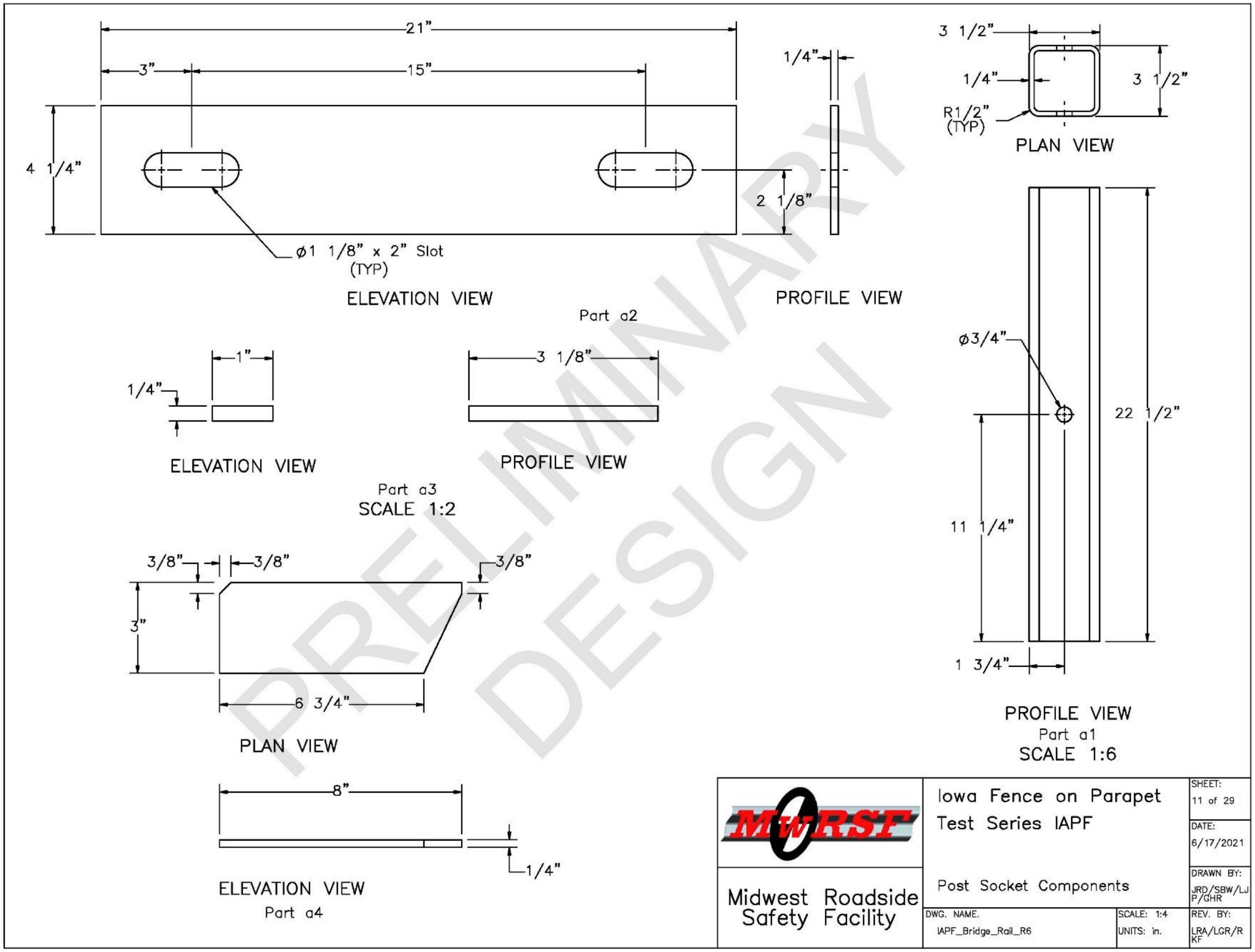

Figure 113.Preliminary Iowa Parapet Fence Design – Post Bracket Components

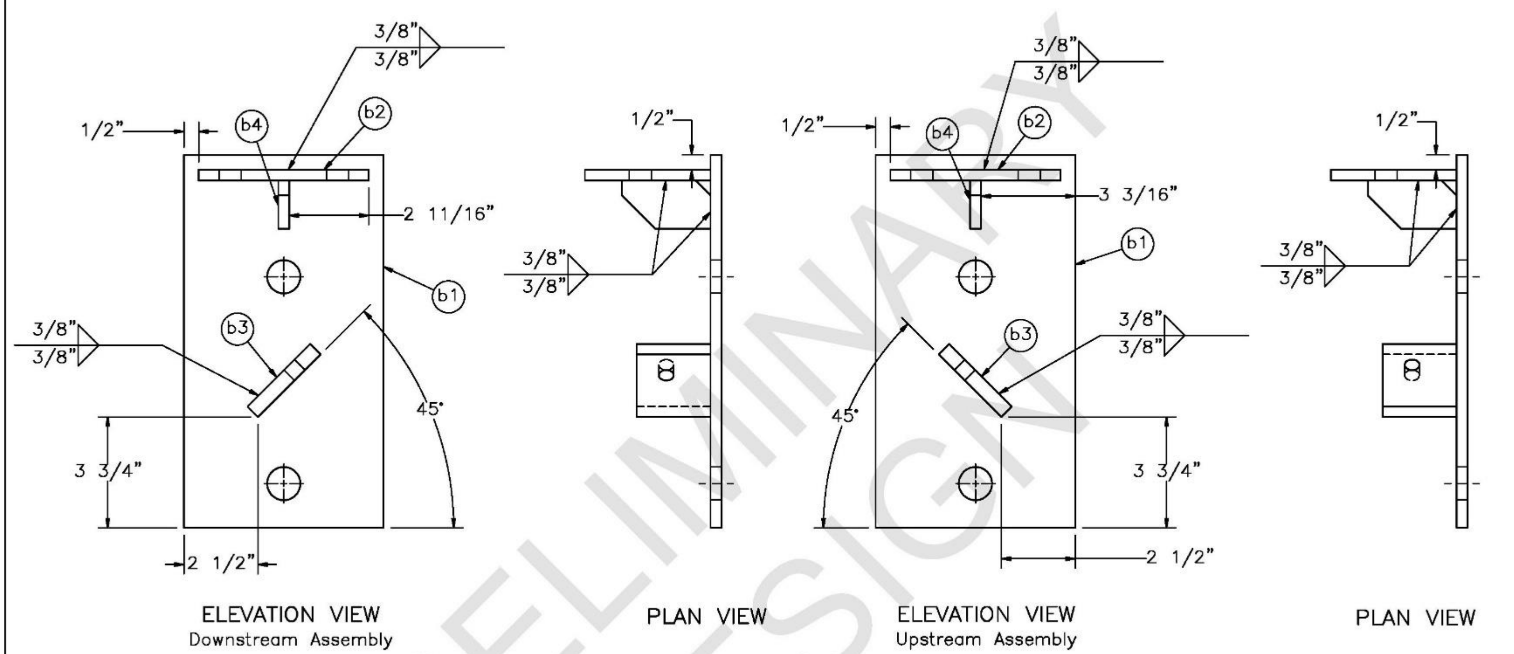

Item No.	QTY.	Description	Material Specification	Treatment Specification
–	1 ea.	Cable Bracket Assembly	–	ASTM A123
b1	1	12 5/8"x6 3/4"x 3/8" Steel Plate	ASTM A572 Gr. 50	–
b2	1	5 3/4"x4 1/4"x3/8" Steel Plate	ASTM A572 Gr. 50	–
b3	1	3"x2 1/2"x1/2" Steel Plate	ASTM A572 Gr. 50	–
b4	1	3"x1 5/8"x3/8" Steel Gusset	ASTM A572 Gr. 50	–

MwRSF
Midwest Roadside Safety Facility

Iowa Fence on Parapet
Test Series IAPF

Cable Bracket Assembly

SHEET: 12 of 29
DATE: 6/17/2021
DRAWN BY: JRD/SBW/LJP/GHR
DWG. NAME. IAPF_Bridge_Rail_R6
SCALE: 1:5
UNITS: in.
REV. BY: LRA/LGR/RKF

Figure 114. Preliminary Iowa Parapet Fence Design – Wire Rope Bracket Assembly and Weldment Details

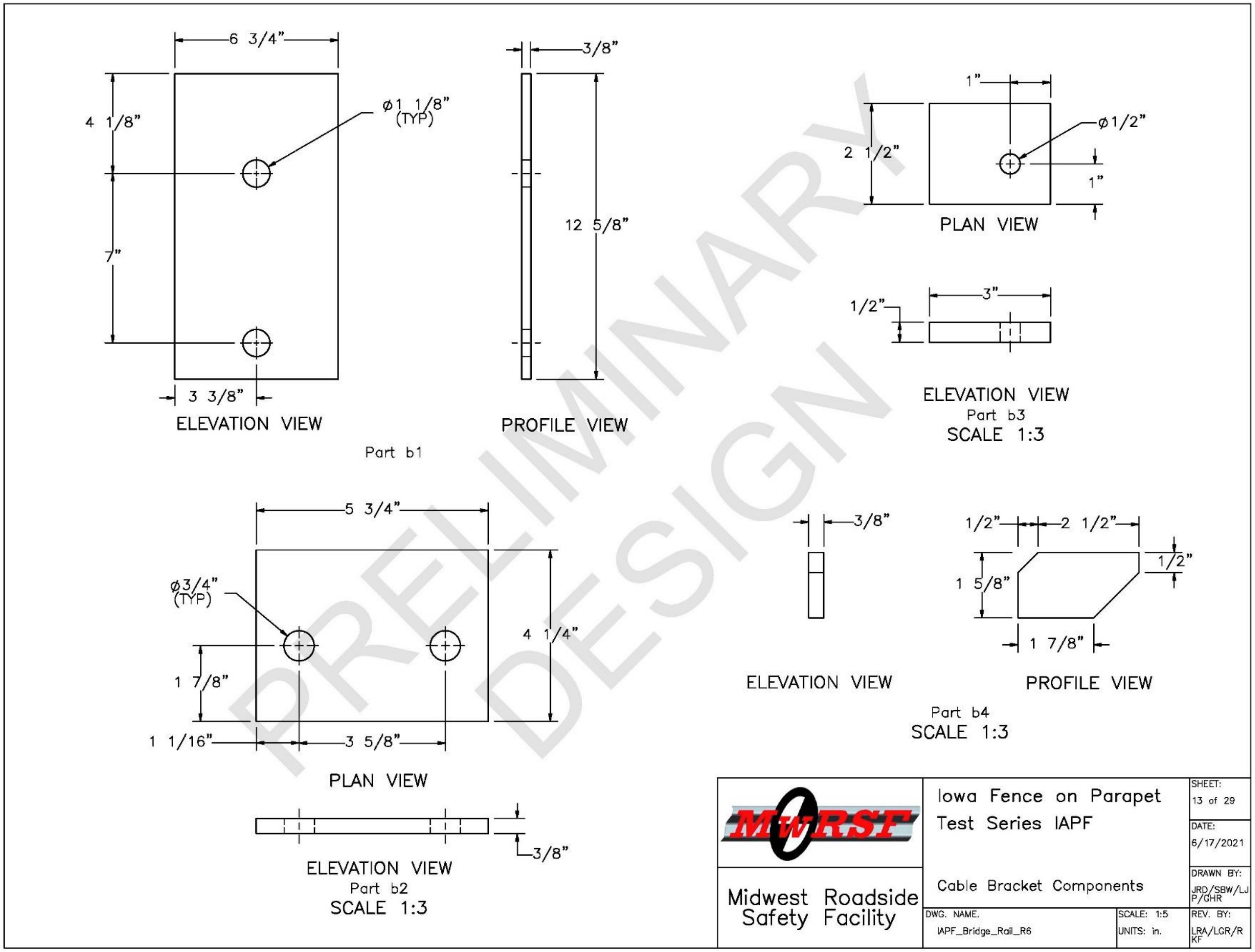

Figure 115. Preliminary Iowa Parapet Fence Design – Wire Rope Bracket Components

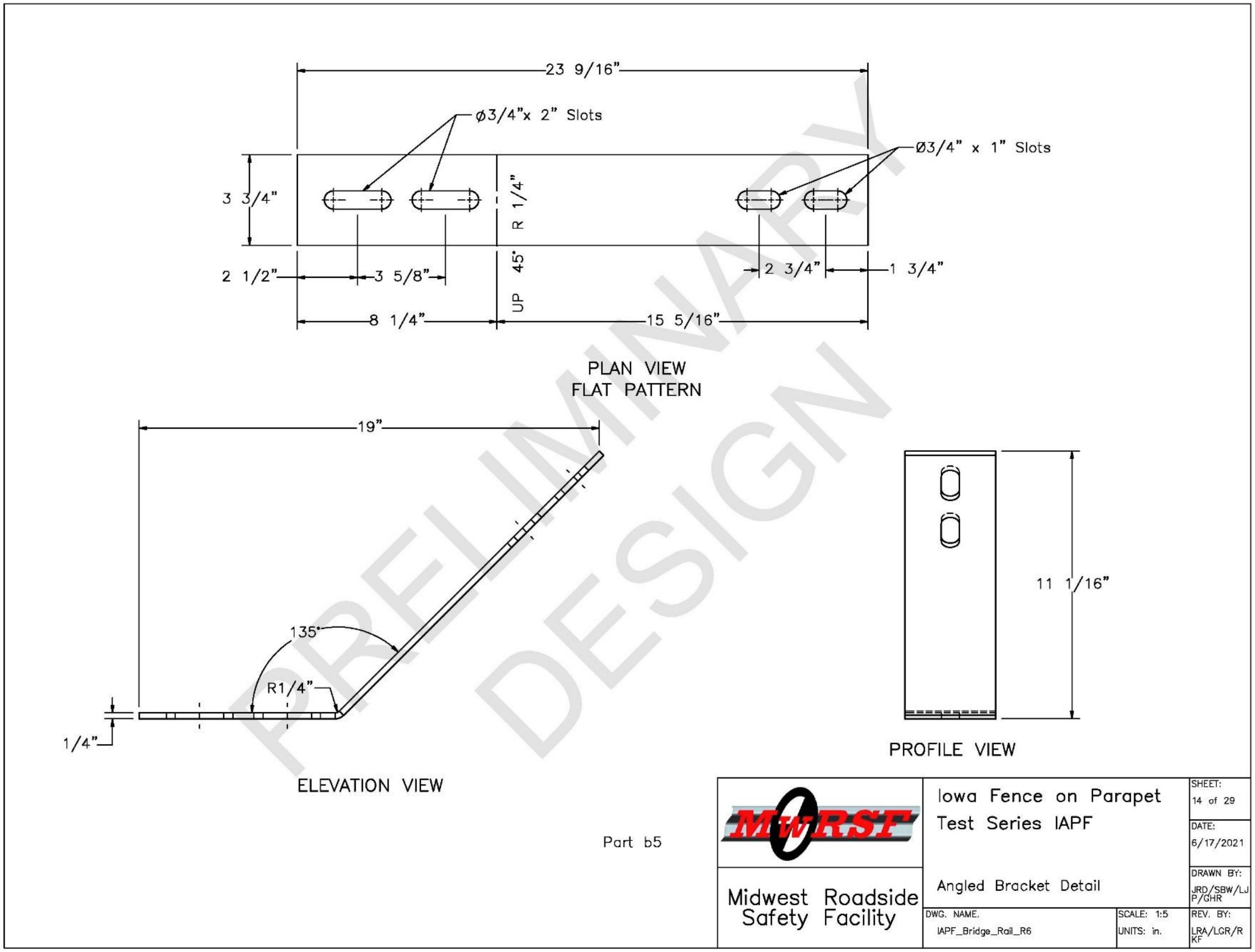

Figure 116. Preliminary Iowa Parapet Fence Design – Angled Bracket Details

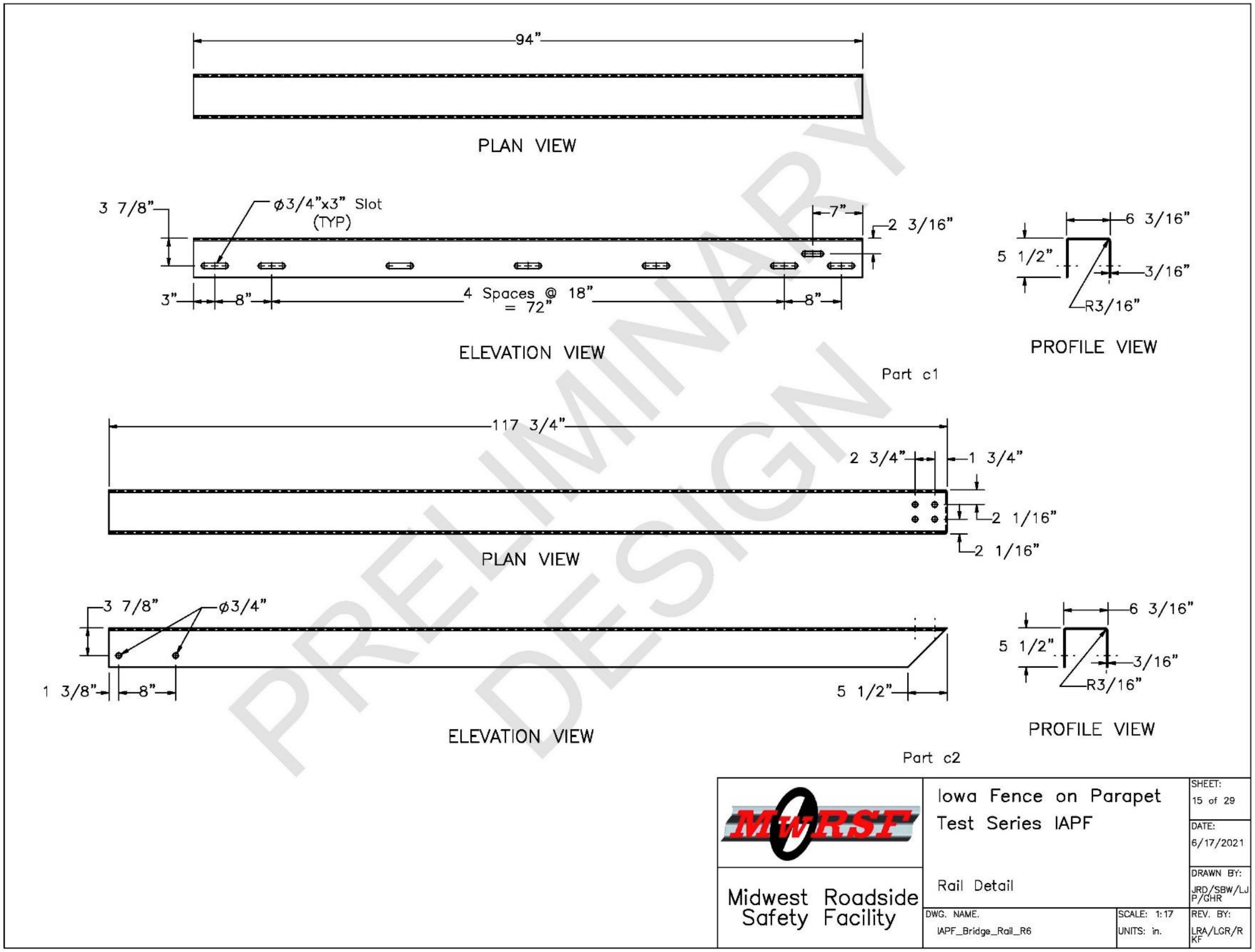

Figure 117. Preliminary Iowa Parapet Fence Design – Cap Rail Details

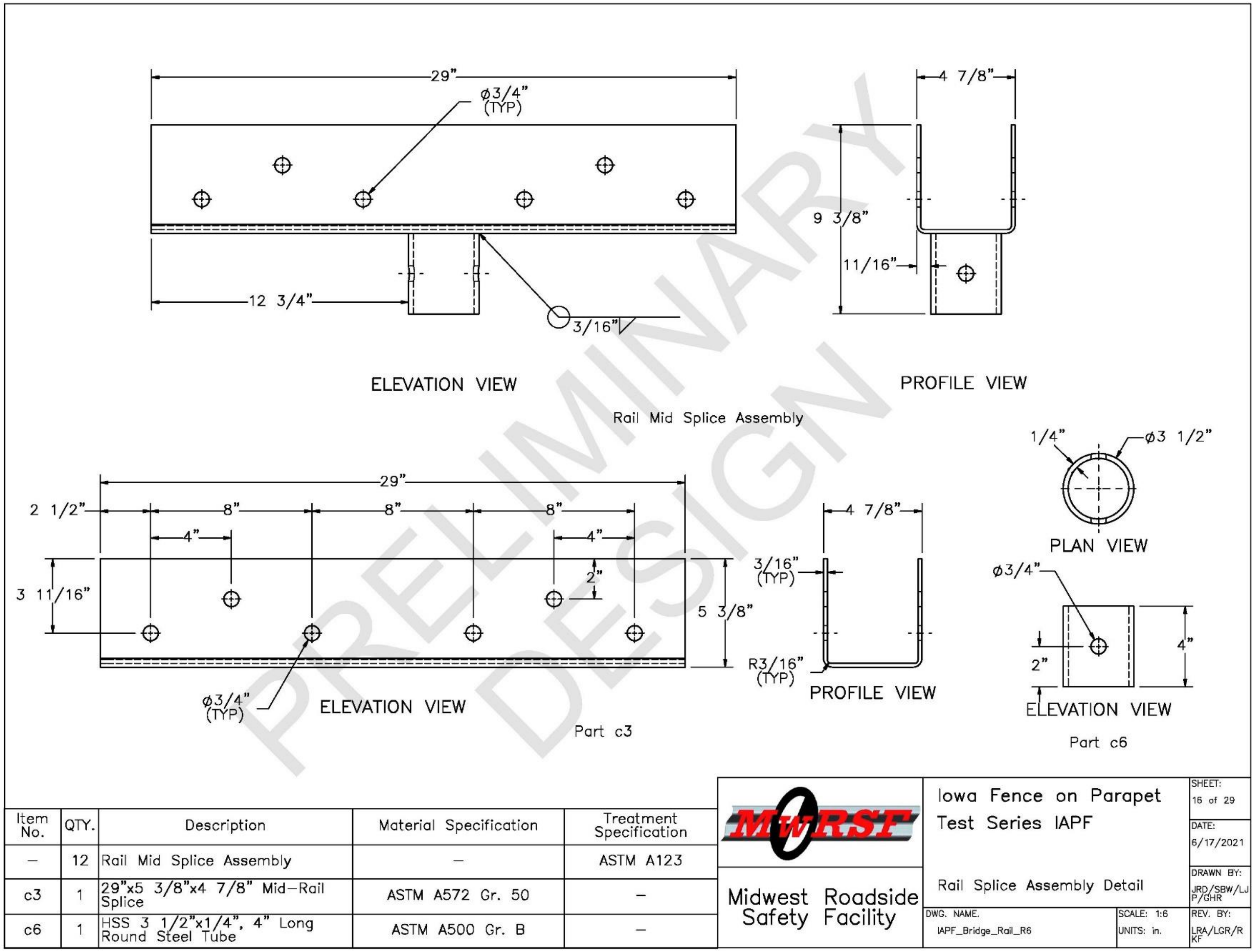

Figure 118. Preliminary Iowa Parapet Fence Design – Mid Span Rail Splice Assembly and Weldment Details

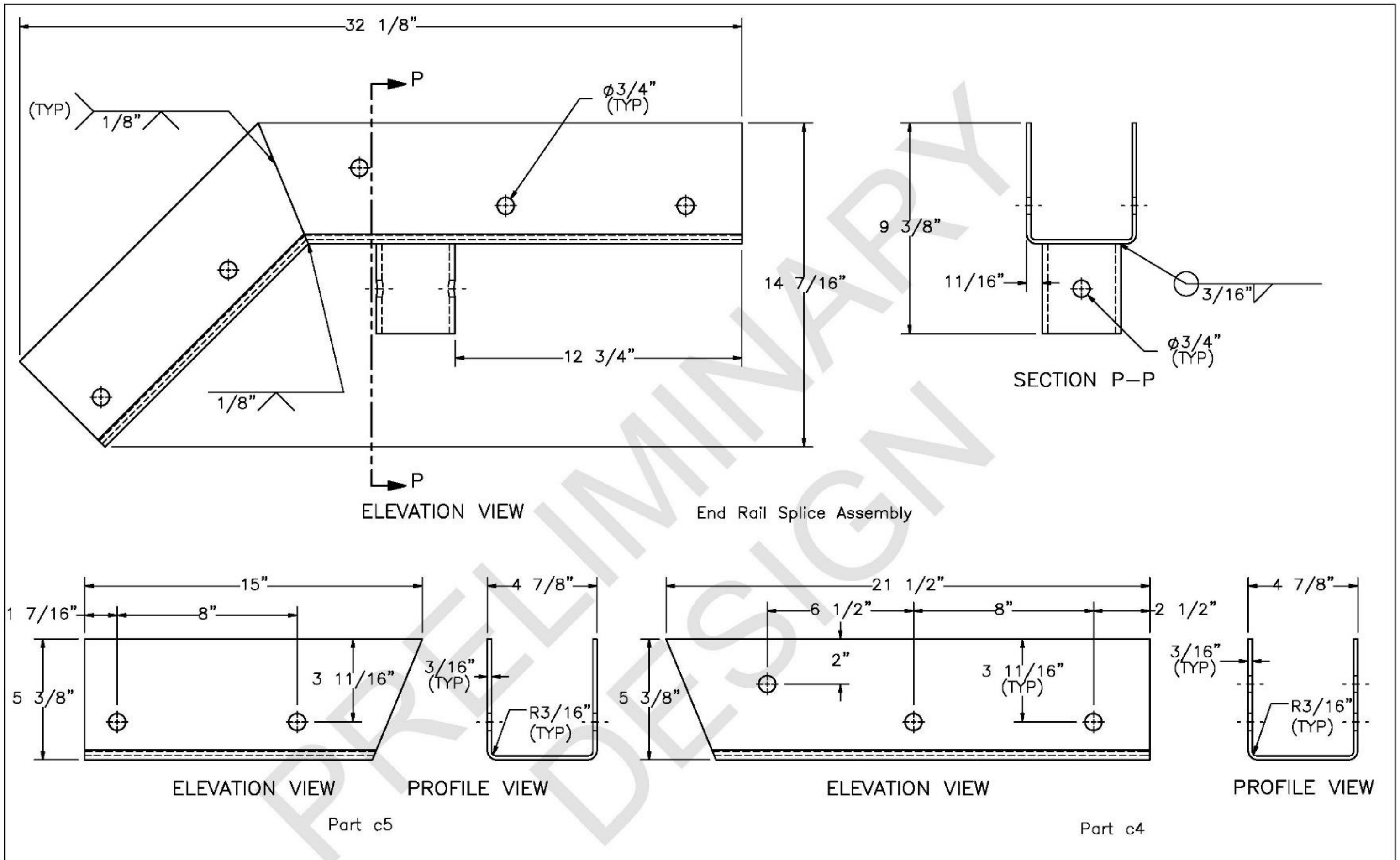

Item No.	QTY.	Description	Material Specification	Treatment Specification
–	2	Rail End Splice Assembly	–	ASTM A123
c4	1	21 1/2"x5 3/8"x4 7/8" Top Rail End Splice	ASTM A572 Gr. 50	–
c5	1	15"x5 3/8"x4 7/8" Angled End Splice	ASTM A572 Gr. 50	–
c6	1	HSS 3 1/2"x1/4", 4" Long Round Steel Tube	ASTM A500 Gr. B	–

MwRSF
Midwest Roadside Safety Facility

Iowa Fence on Parapet
Test Series IAPF

Rail Splice Detail

SHEET:	17 of 29
DATE:	6/17/2021
DRAWN BY:	JRD/SBW/LJ P/GHR
DWG. NAME.	IAPF_Bridge_Rail_R6
SCALE:	1:6
UNITS:	in.
REV. BY:	LRA/LGR/R KF

Figure 119. Preliminary Iowa Parapet Fence Design – End Rail Splice Assembly and Weldment Details

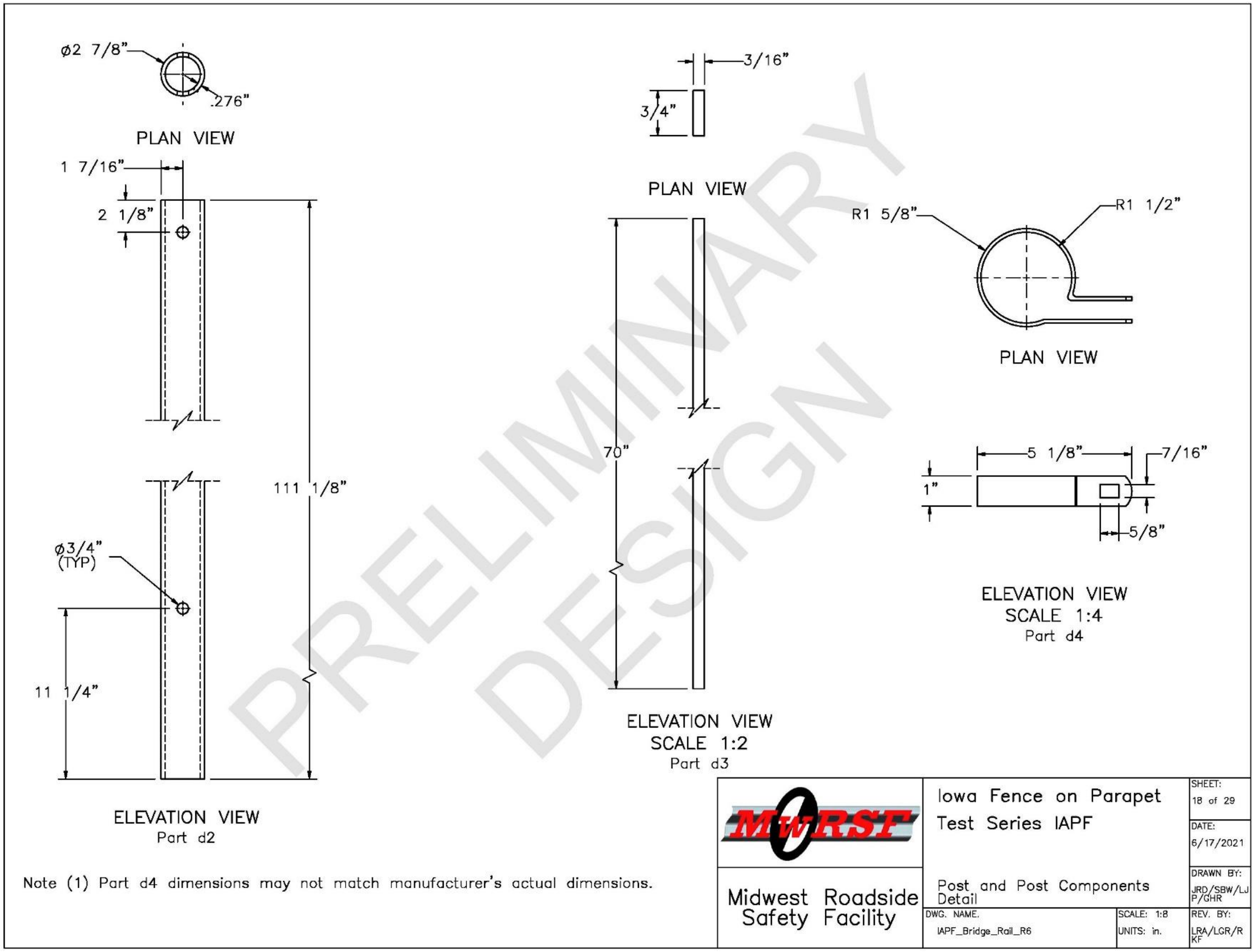

Figure 120. Preliminary Iowa Parapet Fence Design – Post, Tension Bar, and Tension Band Details

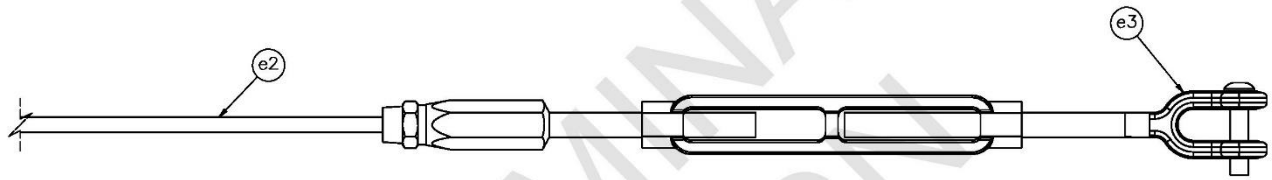

Item No.	QTY.	Description	Material Specification	Treatment Specification
–	2	Cable Assembly	–	–
e2	1	5/16" Dia. 7x19 FC Wire Rope	ASTM A1023 Table 7 EIP Min. Breaking Strength 9,800 lbs	ASTM A1007
e3	1	Electroline XD–4031–AX Forged Series Open Body Clevis and Socket Turnbuckle	ASTM F1145 Type 1 Gr. 1 Min. Breaking Strength 9,000 lbs	ASTM A153

MwRSF Midwest Roadside Safety Facility	Iowa Fence on Parapet Test Series IAPF		SHEET: 19 of 29
			DATE: 6/17/2021
	Cable Assembly		DRAWN BY: JRD/SBW/LJ P/GHR
	DWG. NAME. IAPF_Bridge_Rail_R6	SCALE: 1:3 UNITS: in.	REV. BY: LRA/LGR/R KF

Figure 121. Preliminary Iowa Parapet Fence Design – Wire Rope Assembly

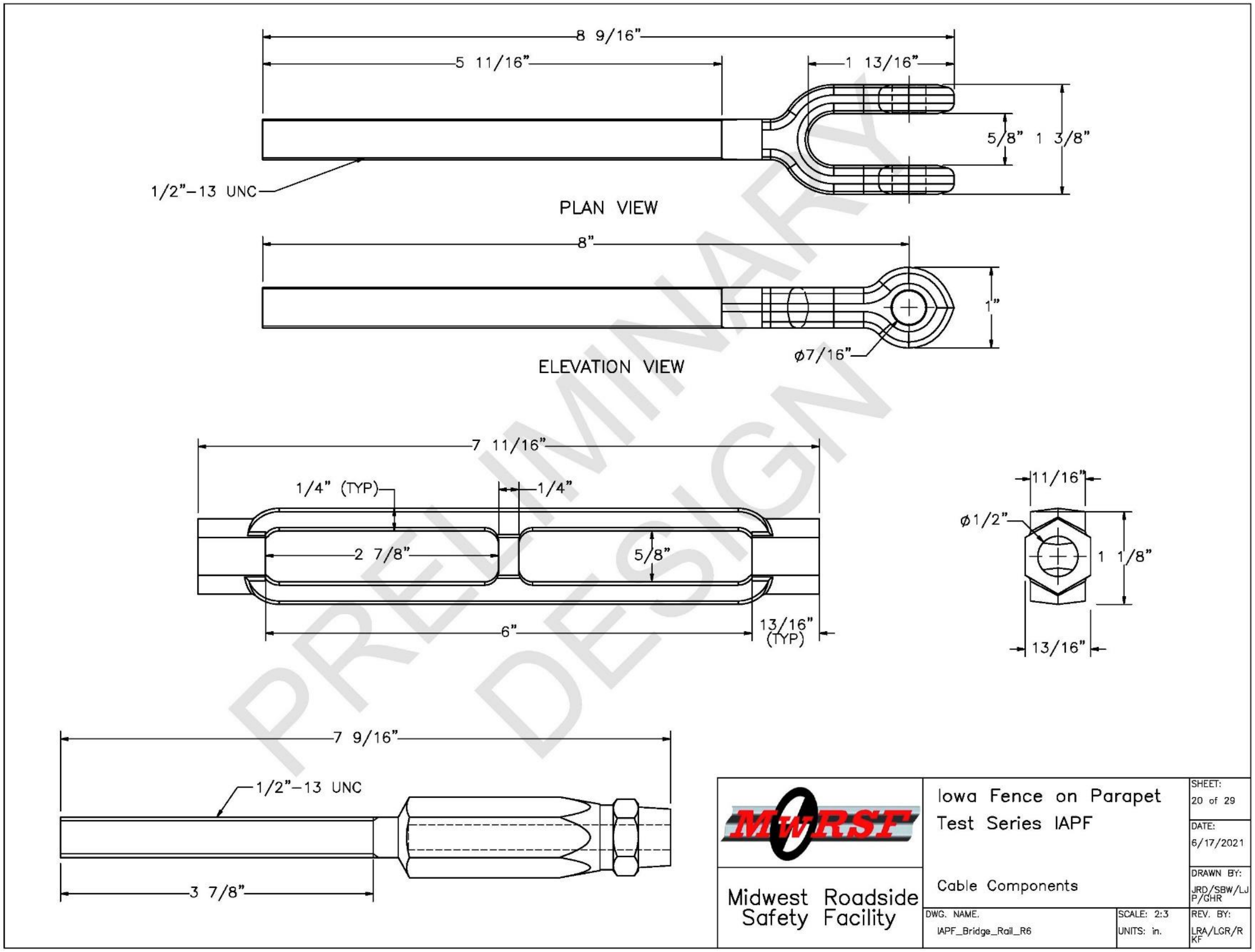

Figure 122. Preliminary Iowa Parapet Fence Design – Wire Rope and Connection Hardware

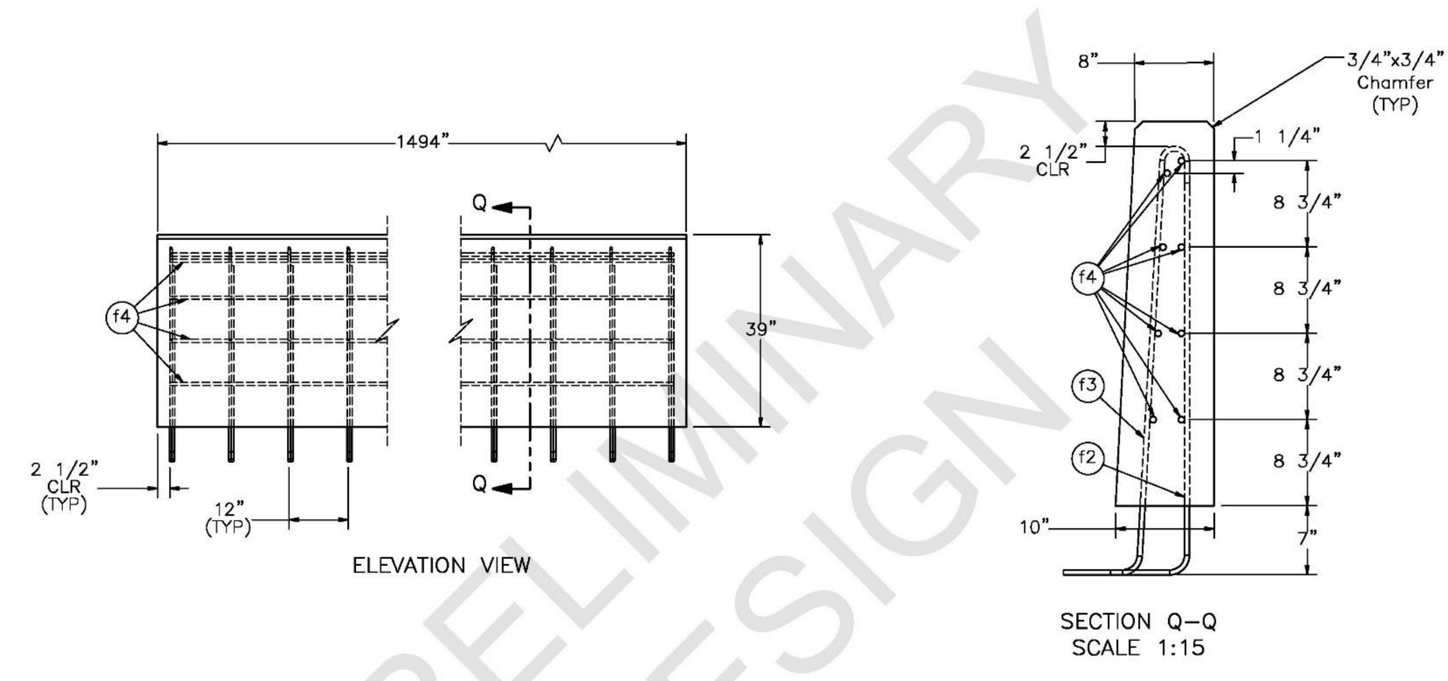

Item No.	QTY.	Description	Material Specification	Treatment Specification
–	1	Concrete Parapet Assmebly	–	–
f1	1	Bridge Rail Concrete	Min. f'c = 5,000 psi NE Mix L5500	–
f2	125	#4 Rebar, 46 1/2" Total Unbent Length	ASTM A615 Gr. 60	Epoxy–Coated (ASTM A775 or A934)
f3	125	#4 Rebar, 70 3/8" Total Unbent Length	ASTM A615 Gr. 60	Epoxy–Coated (ASTM A775 or A934)
f4	8	#5 Rebar, 1,489" Total Length	ASTM A615 Gr. 60	Epoxy–Coated (ASTM A775 or A934)

Midwest Roadside Safety Facility

Iowa Fence on Parapet
Test Series IAPF

Concrete Parapet Assembly

SHEET: 21 of 29
DATE: 6/17/2021
DRAWN BY: JRD/SBW/LJP/GHR
DWG. NAME. IAPF_Bridge_Rail_R6
SCALE: 1:30
UNITS: in.
REV. BY: LRA/LGR/RKF

Figure 123. Preliminary Iowa Parapet Fence Design – Concrete Parapet Assembly Details

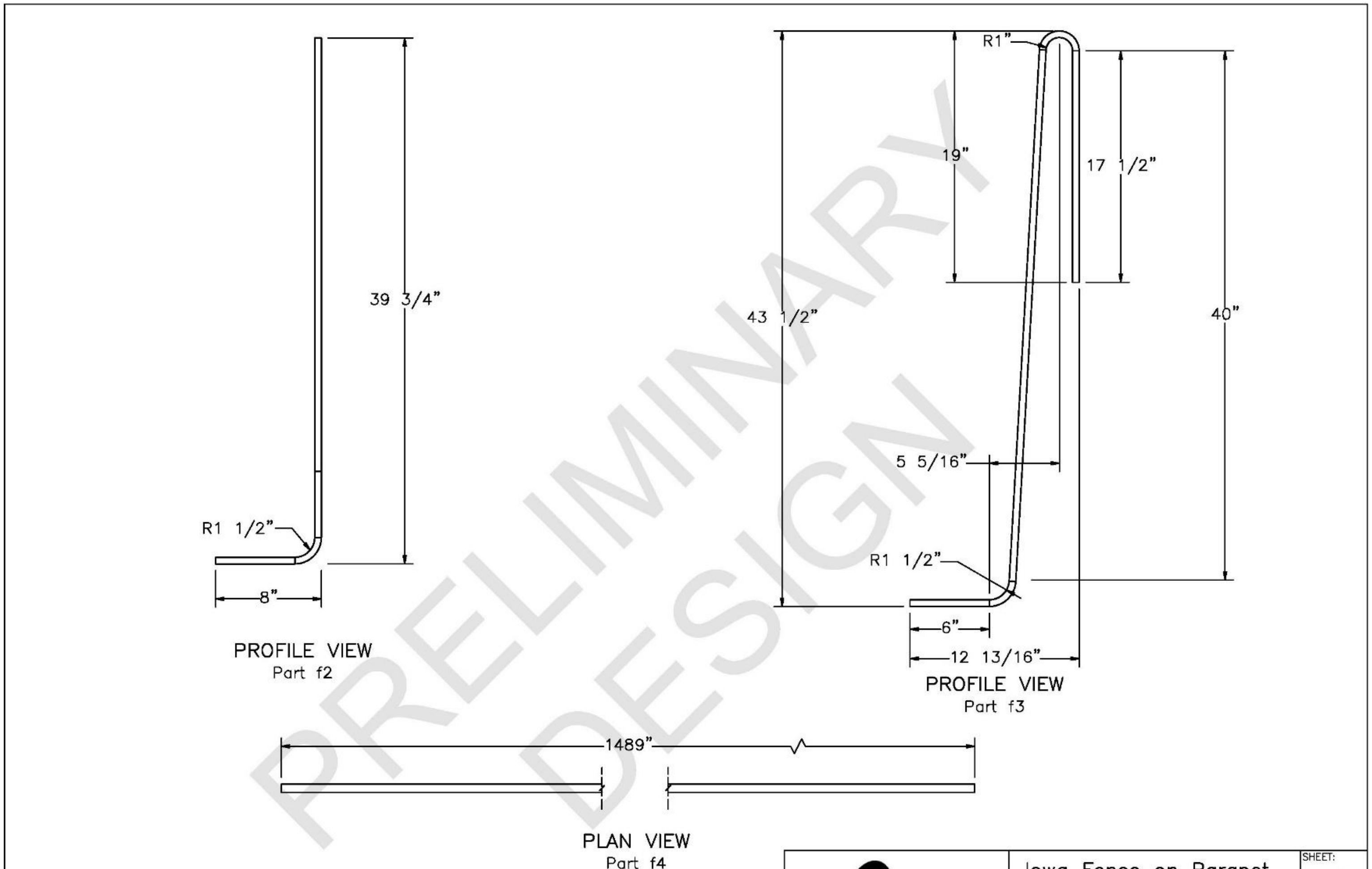

Bar	QTY.	Size	Unbent Length	Material Specification	Treatment Specification
f2	125	#4	46 1/2"	ASTM A615 Gr. 60	Epoxy-Coated (ASTM A775 or A934)
f3	125	#4	70 1/4"	ASTM A615 Gr. 60	Epoxy-Coated (ASTM A775 or A934)
f4	8	#5	1,489"	ASTM A615 Gr. 60	Epoxy-Coated (ASTM A775 or A934)

MwRSF Midwest Roadside Safety Facility	Iowa Fence on Parapet Test Series IAPF		SHEET: 22 of 29
			DATE: 6/17/2021
	System Rebar		DRAWN BY: JRD/SBW/LJP/GHR
	DWG. NAME. IAPF_Bridge_Rail_R6	SCALE: 1:10 UNITS: in.	REV. BY: LRA/LGR/RKF

Figure 124. Preliminary Iowa Parapet Fence Design – Concrete Parapet Reinforcement

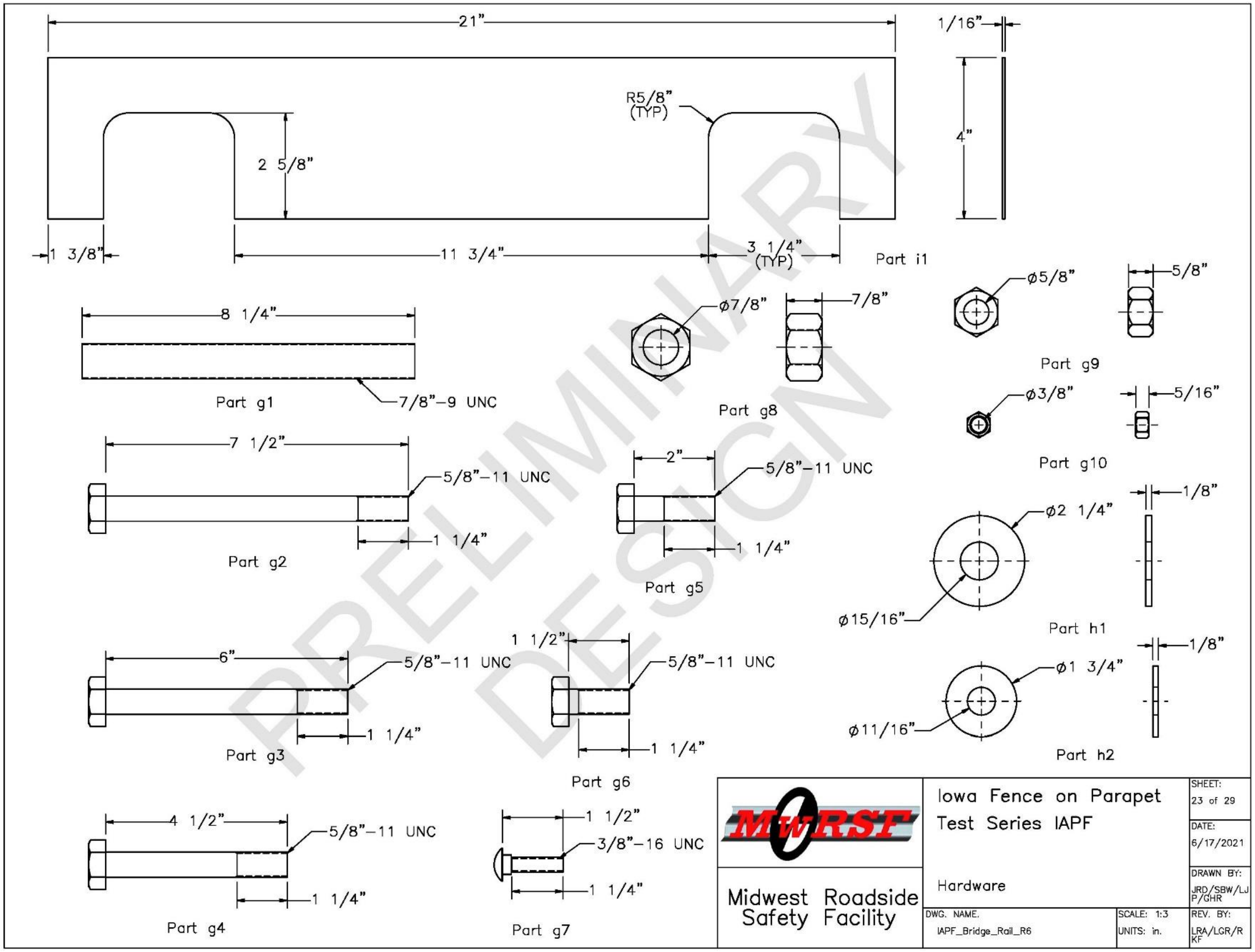

Figure 125. Preliminary Iowa Parapet Fence Design – Hardware

Item No.	QTY.	Description	Material Specification	Treatment Specification	Hardware Guide
a1	14	HSS 3 1/2"x1/4", 22 1/2" Long Square Steel Tube	ASTM A500 Gr. B	See Assembly	–
a2	28	21"x4 1/4"x1/4" Steel Plate	ASTM A572 Gr. 50	See Assembly	–
a3	14	3 1/8"x1"x1/4" Steel Plate	ASTM A572 Gr. 50	See Assembly	–
a4	112	8"x3"x1/4" Steel Gusset	ASTM A572 Gr. 50	See Assembly	–
b1	2	12 5/8"x6 3/4"x 3/8" Steel Plate	ASTM A572 Gr. 50	See Assembly	–
b2	2	5 3/4"x4 1/4"x3/8" Steel Plate	ASTM A572 Gr. 50	See Assembly	–
b3	2	3"x2 1/2"x1/2" Steel Plate	ASTM A572 Gr. 50	See Assembly	–
b4	2	3"x1 5/8"x3/8" Steel Gusset	ASTM A572 Gr. 50	See Assembly	–
b5	2	3 3/4"x1/4"x23 9/16" Long Unbent, Angled Bracket	ASTM A572 Gr. 50	ASTM A123	–
c1	13	94"x6 3/16"x5 1/2" Rail	ASTM A572 Gr. 50	ASTM A123	–
c2	2	117 3/4"x6 3/16"x5 1/2" End Rail	ASTM A572 Gr. 50	ASTM A123	–
c3	12	29"x5 3/8"x4 7/8" Mid–Rail Splice	ASTM A572 Gr. 50	See Assembly	–
c4	2	21 1/2"x5 3/8"x4 7/8" Top Rail End Splice	ASTM A572 Gr. 50	See Assembly	–
c5	2	15"x5 3/8"x4 7/8" Angled End Splice	ASTM A572 Gr. 50	See Assembly	–
c6	14	HSS 3 1/2"x1/4", 4" Long Round Steel Tube	ASTM A500 Gr. B	See Assembly	–
d1	3	9 Gauge, 2" Mesh, 7' Tall, Chain Link Fabric, 50' Rolls With Knucke Selvage Top and Bottom	ASTM A817	ASTM A392 Class 2	–
d2	14	2 1/2" NPS Schedule 80 Steel Pipe	ASTM A53 Gr. B	ASTM A123 Grade 80	–
d3	2	3/4"x3/16"x70" Galvanized Steel Tension Bar	ASTM F626	Hot–dip Galvanized, 1.2 oz/sqft. Min. Coating	–
d4	14	12 Gauge min, 3" Diameter x 1" Galvanized Steel Tension Band	ASTM F626	Hot–dip Galvanized, 1.2 oz/sqft. Min. Coating	TBBV3
d5	111	9 Gauge, Galvanized Steel Straight Wire Tie or Easy Twist, Power–Fastened Preformed Wire Tie	ASTM F626	ASTM 817, Type 2 Class 1 for Straight Wire Tie ASTM A641 Class B for Power–Fastened Wire Tie	–
d6	91	1 7/16", 9 Gauge Galvanized Steel Hog Ring	ASTM F626	ASTM A641 Class 3 or A Coating	–

MwRSF
Midwest Roadside Safety Facility

Iowa Fence on Parapet
Test Series IAPF

Bill of Materials

SHEET: 24 of 29
DATE: 6/17/2021
DRAWN BY: JRD/SBW/LJP/GHR
REV. BY: LRA/LGR/RKF
DWG. NAME. IAPF_Bridge_Rail_R6
SCALE: None
UNITS: in.

Figure 126. Preliminary Iowa Parapet Fence Design – Bill of Materials

Item No.	QTY.	Description	Material Specification	Treatment Specification	Hardware Guide
e1	1	7 Gauge Steel Wire – Length as Needed	ASTM A817	ASTM A824 or A817 Type II, Class 3 or ASTM A824 or A817 Type 1	–
e2	1	5/16" Diameter 7x19 Utility Wire Rope – Length as Needed	ASTM A1023 Table 7	ASTM A1007	–
e3	2	Electroline XD-4031-AX Forged Series Open Body Clevis and Socket Turnbuckle	ASTM F1145 Type 1 Gr. 1 Min. Breaking Strength 9,000 lbs	ASTM A153	–
f1	–	Bridge Rail Concrete	Min. f'c = 5,000 psi NE Mix L5500	–	–
f2	125	#4 Rebar, 46 1/2" Total Unbent Length	ASTM A615 Gr. 60	Epoxy-Coated (ASTM A775 or A934)	–
f3	125	#4 Rebar, 70 3/8" Total Unbent Length	ASTM A615 Gr. 60	Epoxy-Coated (ASTM A775 or A934)	–
f4	8	#5 Rebar, 1,489" Total Length	ASTM A615 Gr. 60	Epoxy-Coated (ASTM A775 or A934)	–
g1	60	7/8"- 9 UNC, 8 1/4" Long Fully Threaded Rod	ASTM A193 B7	ASTM A153 or F2329	FRR16b
g2	100	5/8"-11 UNC, 7 1/2" Long Heavy Hex Bolt	ASTM F3125 Gr. A325 Type 1 or Equivalent	ASTM F2329	FBX16b
g3	2	5/8"-11 UNC, 6" Long Heavy Hex Bolt	ASTM F3125 Gr. A325 Type 1 or Equivalent	ASTM F2329	FBX16b
g4	28	5/8"-11 UNC, 4 1/2" Long Heavy Hex Bolt	ASTM F3125 Gr. A325 Type 1 or Equivalent	ASTM F2329	FBX16b
g5	4	5/8"-11 UNC, 2" Long Heavy Hex Bolt	ASTM F3125 Gr. A325 Type 1 or Equivalent	ASTM F2329	FBX16b
g6	4	5/8"-11 UNC, 1 1/2" Long Heavy Hex Bolt	ASTM F3125 Gr. A325 Type 1 or Equivalent	ASTM F2329	FBX16b
g7	14	3/8"-16, 1 1/2" Long Square-Neck Carriage Bolt	ASTM A307 Grade A	ASTM F2329	Part no. g3604A669
g8	60	7/8"-9 UNC Heavy Hex Nut	ASTM A563DH or Equivalent	ASTM F2329	FNX22b
g9	138	5/8"-11 UNC Heavy Hex Nut	ASTM A563DH or Equivalent	ASTM F2329	FNX16b
g10	14	3/8"-16 UNC Hex Nut	ASTM A307 Grade A	ASTM F2329	FNX10a
h1	120	7/8" Diameter Plain USS Washer	ASTM F844	ASTM A123 or A153 or F2329	FWC20a
h2	276	5/8" Diameter Plain USS Washer	ASTM F844	ASTM A123 or A153 or F2329	FWC16a
i1	*	21"x4"x16 Gauge Shim	Minimum 25 ksi Yield Strength	ASTM A123	–

Note: * Quantity as needed

MwRSF

Midwest Roadside Safety Facility

Iowa Fence on Parapet Test Series IAPF

Bill Of Materials

SHEET: 25 of 29

DATE: 6/17/2021

DRAWN BY: JRD/SBW/LJP/GHR

REV. BY: LRA/LGR/RKF

DWG. NAME. IAPF_Bridge_Rail_R6

SCALE: None

UNITS: in.

Figure 127. Preliminary Iowa Parapet Fence Design – Bill of Materials, Continued

Online Resources

General installation guides:
America s Fence Store: https://americasfencestore.com/pages/how-to-guide-chain-link
Hoover Fence: https://www.hooverfence.com/chain-link-fence-installation-manual

How to install tension wire:
https://www.youtube.com/watch?v=74-GeS-Pjo4

How to splice chain-link fabric:
https://www.youtube.com/watch?v=btOwstKSjZA

How to install chain-link fabric: 6:45 minute time mark
https://www.youtube.com/watch?v=ODH_Xj3RrGQ&t=514s

Midwest Roadside Safety Facility	Iowa Fence on Parapet Test Series IAPF	SHEET: 26 of 29
		DATE: 6/17/2021
	Online Resources	DRAWN BY: JRD/SBW/LJP/GHR
	DWG. NAME. IAPF_Bridge_Rail_R6 / SCALE: 1:384 UNITS: in.	REV. BY: LRA/LGR/RKF

Figure 128. Preliminary Iowa Parapet Fence Design – Online Resources for Fence Installation

Fence Installation

1) Install anchors (g1) and post bracket assemblies onto backside of barrier. At this time, do not install anchors (g1) for the cable bracket assemblies.

2) Place posts (d2) inside of post socket assemblies and fasten g4 bolts.

3) Mount rail mid splice assemblies on posts (d2), for end post use rail end splice assemblies. Fasten g3 bolts on rail end splice assemblies.

4) Install chain–link fabric (d1) per typical fence construction practices (ASTM F567). Verify that the center of the second knuckle from the top of the chain–link fabric (d1) is not lower than 2 5/8" below the top of the rail end splice assemblies. The top of the chain–link fabric (d1) should also not extend past the top of the rail end splice assemblies, and the bottom of the chain–link fabric (d1) should not be higher than 3" above the top of the barrier. See Figure 1.

5) Attach angled brackets (b5) and cable bracket assemblies onto sloped cap rails (c2). Mount these assemblies onto rail end splice assemblies on both ends of the fence and use as a template for locating anchor (g1) placement used to attach cable bracket assemblies to the barrier.

6) Extend turnbuckles in the cable assemblies to introduce slack. Mount one of the cable assemblies to a cable bracket assembly on either side of the fence. Guide the cable (e2) through the sloped cap rail (c2) and over bolt g3.

7) Run cable (e2) to opposite end of fence, be sure cable is nested inside rail mid splice assemblies. At the opposite end, guide cable (e2) over bolt g3 and down through sloped cap rail (c2). Attach cable (e2) to cable assembly and mount it onto the cable bracket assembly, apply tension to cable (e2).

8) Once cable (e2) is tensioned, install cap rails (c1), do not install bolts (g2) in the bottom slots of cap rails (c1) at this time. Install bolts (g2) in cable support slots (shown in sheet 8) to hold up the cable (e2) whenever it sags below the slots at the bottom of cap rails (c1).

9) Install bolts (g2) in the bottom slots of cap rails (c1), in slot locations that capture the second knuckle from the top of the chain–link fabric (d1). See Figure 2.

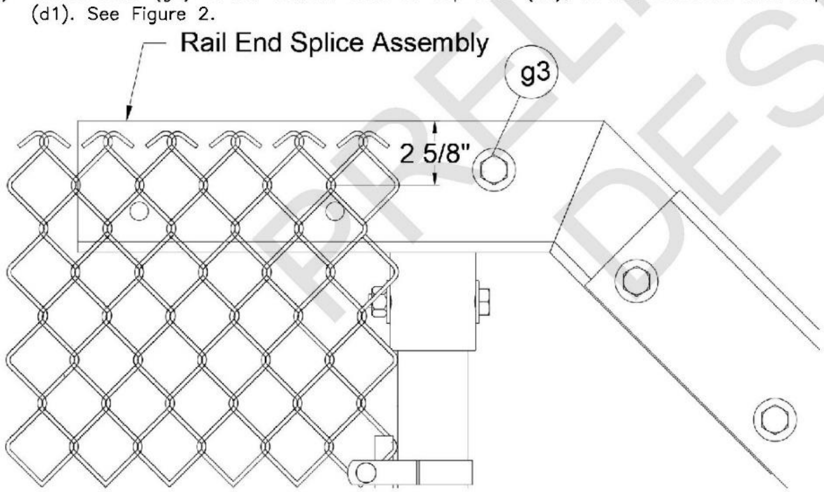

Figure 1: Chain–link fabric (d1) to rail end splice assembly

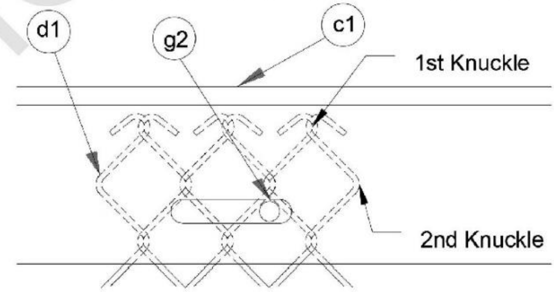

Figure 2: Chain–link Fence Connection to Cap Rail

Midwest Roadside Safety Facility

Iowa Fence on Parapet
Test Series IAPF

Construction Notes

SHEET: 27 of 29	DATE: 6/17/2021	DRAWN BY: JRD/SBW/LJP/GHR
DWG. NAME. IAPF_Bridge_Rail_R6	SCALE: 1:3 UNITS: in.	REV. BY: LRA/LGR/RKF

Figure 129. Preliminary Iowa Parapet Fence Design – Recommended Installation Procedure

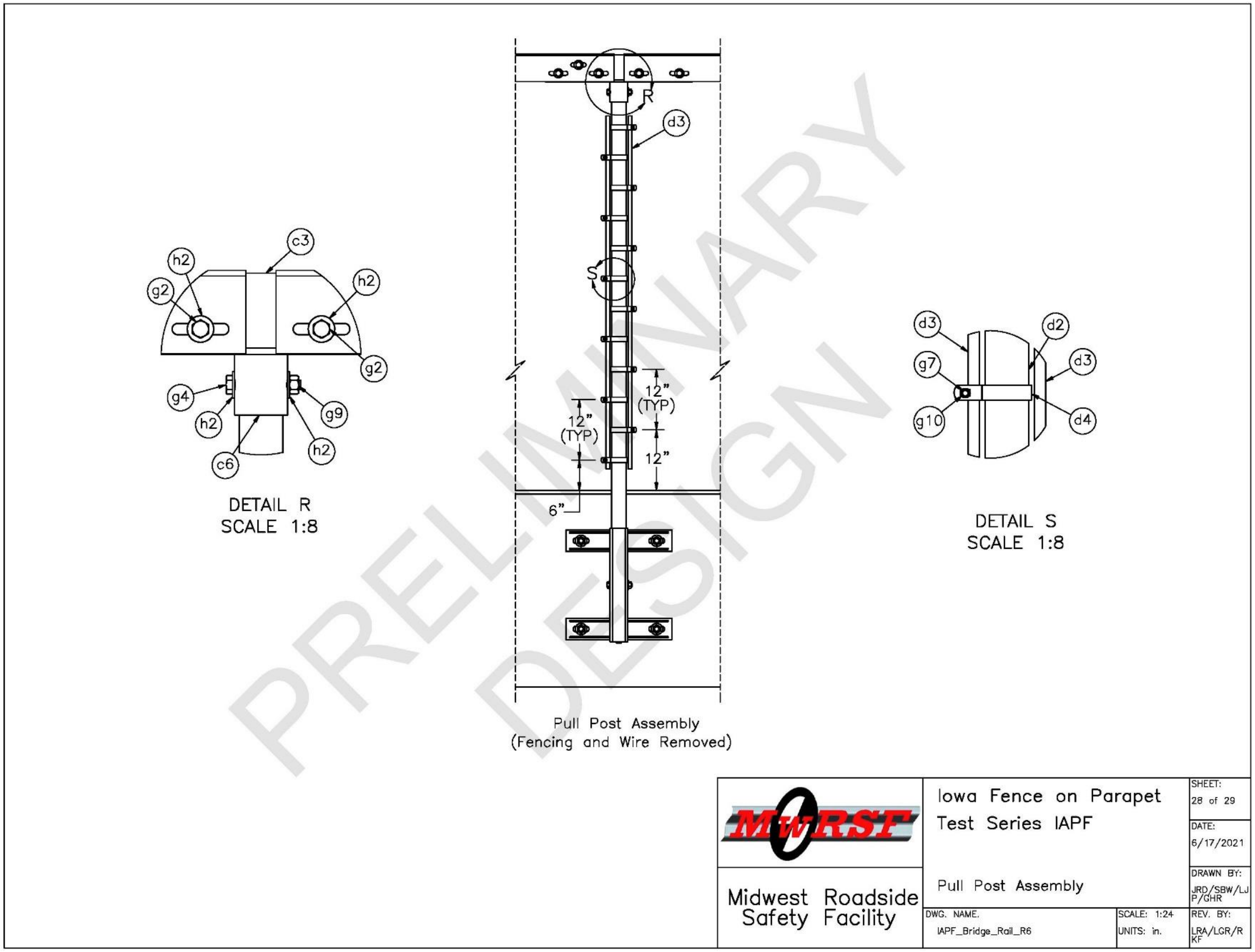

Figure 130. Preliminary Iowa Parapet Fence Design – Pull Post Assembly for Fence Mid Span

Item No.	QTY.	Description	Material Specification	Treatment Specification	Hardware Guide
a1	1	HSS 3 1/2"x1/4", 22 1/2" Long Square Steel Tube	ASTM A500 Gr. B	See Assembly	–
a2	2	21"x4 1/4"x1/4" Steel Plate	ASTM A572 Gr. 50	See Assembly	–
a3	1	3 1/8"x1"x1/4" Steel Plate	ASTM A572 Gr. 50	See Assembly	–
a4	8	8"x3"x1/4" Steel Gusset	ASTM A572 Gr. 50	See Assembly	–
c3	1	29"x5 3/8"x4 7/8" Mid–Rail Splice	ASTM A572 Gr. 50	See Assembly	–
c6	1	HSS 3 1/2"x1/4", 4" Long Round Steel Tube	ASTM A500 Gr. B	See Assembly	–
d2	1	2 1/2" NPS Schedule 80 Steel Pipe	ASTM A53 Gr. B	ASTM A123 Grade 80	–
d3	2	3/4"x3/16"x70" Galvanized Steel Tension Bar	ASTM F626	Hot–dip Galvanized, 1.2 oz/sqft. Min. Coating	–
d4	12	12 Gauge min, 3" Diameter x 1" Galvanized Steel Tension Band	ASTM F626	Hot–dip Galvanized, 1.2 oz/sqft. Min. Coating	TBBV3
g1	4	7/8"– 9 UNC, 8 1/4" Long Fully Threaded Rod	ASTM A193 B7	ASTM A153 or F2329	FRR16b
g2	5	5/8"–11 UNC, 7 1/2" Long Heavy Hex Bolt	ASTM F3125 Gr. A325 Type 1 or Equivalent	ASTM F2329	FBX16b
g4	2	5/8"–11 UNC, 4 1/2" Long Heavy Hex Bolt	ASTM F3125 Gr. A325 Type 1 or Equivalent	ASTM F2329	FBX16b
g7	12	3/8"–16, 1 1/2" Long Square–Neck Carriage Bolt	ASTM A307 Grade A	ASTM F2329	Part no. g3604A669
g8	4	7/8"–9 UNC Heavy Hex Nut	ASTM A563DH or Equivalent	ASTM F2329	FNX22b
g9	7	5/8"–11 UNC Heavy Hex Nut	ASTM A563DH or Equivalent	ASTM F2329	FNX16b
g10	12	3/8"–16 UNC Hex Nut	ASTM A307 Grade A	ASTM F2329	FNX10a
h1	8	7/8" Diameter Plain USS Washer	ASTM F844	ASTM A123 or A153 or F2329	FWC20a
h2	14	5/8" Diameter Plain USS Washer	ASTM F844	ASTM A123 or A153 or F2329	FWC16a

Note: This BOM is for the Pull Post Assembly only, not full system.

MwRSF
Midwest Roadside Safety Facility

Iowa Fence on Parapet Test Series IAPF

Pull Post Bill of Materials

SHEET: 29 of 29
DATE: 6/17/2021
DRAWN BY: JRD/SBW/LJP/GHR
REV. BY: LRA/LGR/RKF
DWG. NAME. IAPF_Bridge_Rail_R6
SCALE: 1:384
UNITS: in.

Figure 131. Preliminary Iowa Parapet Fence Design – Pull Post Assembly Bill of Materials

8.3 Discussion

8.3.1 Parapet Selection

Researchers at the MwRSF completed a study in March 2021 where an optimized MASH TL-4 bridge rail was developed and crash tested for the Midwest Pooled Fund Program. The authors of this report determined that the bridge railing met crashworthiness requirements as specified by MASH TL-4 criteria [49]. This barrier was selected as a baseline configuration used to develop fence-to-barrier attachments, adaptations to alternate barrier configurations are discussed in Section 9.3.

The selected railing consists of multiple longitudinal and vertical pieces of rebar with the top two longitudinal bars being 4 in. and 5¼ in. below the top of the railing. A design variation incorporating head ejection criteria is compared to the crash-tested design in Figure 132, which has the second piece of longitudinal rebar 6.62 in. below the top of the barrier. Thus, connections to the backside of the bridge railing were designed at 10 in. below the top of the railing to prevent any chance of the longitudinal rebar being struck when holes are drilled into other potential parapet options.

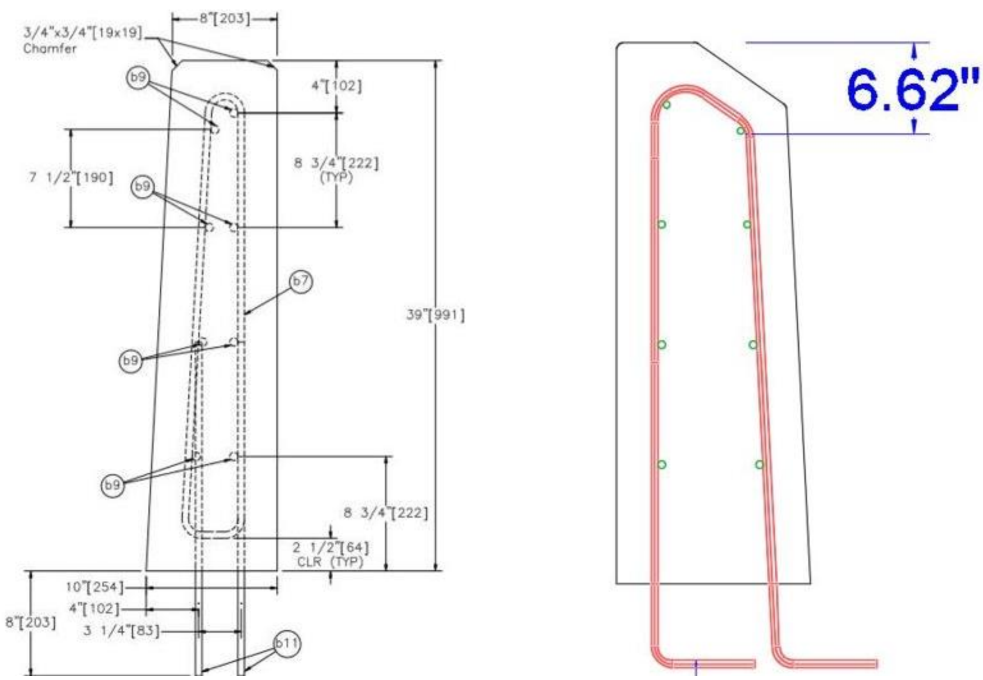

Figure 132. Comparison of TL-4 Barriers [49]

8.3.2 Chain-link Fence Fabric

The proposed chain-link fence was selected specifically to meet Iowa fence standards which is also a standard readily available chain-link size. Although Iowa DOT standards require a 6-ft fence, a 7-ft fence fabric was selected to meet UP-BNSF requirements for fences along railway overpasses. This specific height was selected since it was designed for installment on a railing at least 36-in. tall.

8.3.3 Vertical Post

8.3.3.1 Post Spacing

Prior to selecting a vertical post size, various post spacing arrangements were investigated. State DOT chain-link fence designs incorporate post spacing configurations that ranged from 5 ft to 10 ft intervals. Designs with large spacing between posts were evaluated because less fence sections would be necessary when installing a fence on any given railway overpass. As a result, the number of parts and connections would be reduced and the installation simplified.

Alternatively, decreasing the spacing between posts reduces wind loading applied on individual fence sections which transfer to vertical posts, requiring smaller post sizes to meet wind loading criteria. Adding to this, the demand on the concrete anchorage would decrease and may also reduce loads imposed on vehicles if contact with vertical posts occur during impact events. However, the cost would be increased and constructability would be more challenging for these configurations due to the added fence components and associated connections.

Researchers considered smaller post spacing options to reduce the required post stiffness but considered that it would result in a more labor-intensive, costly, and non-aesthetic installation. On the other hand, the benefits of increasing post spacing were not considered to counterbalance the complexity of the required concrete anchorage connection to develop the capacity of stiffer vertical posts. Considering these things, an 8-ft post spacing was selected as an optimized balance between cost, constructability, and crashworthiness.

8.3.3.2 Post Selection

Once the post spacing was selected, the procedure outlined in Section 6.4 was conducted in the selection of a post size. In this analysis, the post size was optimized by limiting it stiffness while meeting design criteria requirements. For a fence with 7-ft tall fabric and an 8-ft post spacing configuration, HSS2.875x0.188 round structural steel tube conforming to ASTM A1085 was selected as the preferred post option. The following list presents alternative post options that also meet design criteria and objectives:

- Round HSS2.875x0.203 ASTM A500 Grade C
- Pipe 2½ Schedule 40 ASTM F1083, High Strength (50 ksi)
- Pipe 2½ Schedule 80 ASTM A53 Grade B

Of these options, only the Schedule 40 pipe size meets Iowa DOT design requirements and, although it is not included Iowa DOT fence design standards, the post option conforming to ASTM A1085 is the primary recommendation. This is because ASTM tubes specifications typically have more stringent tolerances on allowed wall thickness and outer diameter variations then that of pipes [41]. Additionally, this specific ASTM designation has a specified minimum and maximum allowable yield stress. These two factors result in a more controlled post strength which will reduce the potential for the post capacity to exceed that of the post bracket and anchorage connections, and that will still meet the minimum strength requirements.

8.3.4 Post-to-parapet Attachment

Clamps incorporated in state DOT fence details require that the vertical post be held in place while the brackets are bolted to the back of the barrier. In the design shown in Figure 109, after fastening the bracket to the barrier, technicians can insert vertical post into the tube socket which holds the post in place via as strap welded to the bottom of the socket. This bracket includes slots, giving installers the option to drill a new hole if cutting through barrier reinforcements is not desired during anchor installation. The required anchor spacing and inclusion of these slots yielded an elongated bracket which decreased its bending capacity and, as a result, escalated the potential bracket deformation during vehicular impact events. This was counteracted by increasing the section of the bracket through the addition of gusset between the tube socket and steel flat stock.

8.3.5 Anchorage

Iowa DOT requested the use of post-installed epoxy anchors and preferred the anchors to be stainless steel threaded sleeves. Threaded sleeve inserts were not used in the design since they require a concrete embedment that cannot be achieved with the selected parapet. Standard readily-available stainless steel anchors do not have the mechanical properties needed to meet the requirements of impact loading conditions. Stainless steel anchors that meet impact loading requirements have a higher cost and limited availability and therefore were not used for anchoring the fence to the parapet.

The selected anchor size and material specification are commonly used in concrete anchorages due to their favorable material properties. The top anchorage location was selected to avoid concrete reinforcement, promote vertical post bending during impact events, and minimize the strength reduction effects of placing anchors near the free edge of the concrete parapet. The anchor longitudinal spacing and the distance below the top of the barrier of the second set of anchors was selected to maximize the concrete anchorage strength.

8.3.6 Wire Rope, Attachments, Termination

The proposed wire rope was selected since it has previously been used in a full-scale crash test of a bicycle bridge rail designed to satisfy MASH TL-4 crash test requirements [12]. Since it is imperative that the wire rope's connections and termination develop its capacity, the wire rope was attached to the concrete parapet, which has the potential to develop the wire rope's strength. The wire rope connection to the cable bracket, weld connections on the bracket, the bracket bending stiffness, and the concrete anchorage were designed to develop the capacity of the wire rope.

A tab was included on the cable brackets to attach end cap rails and prevent them from swaying during high wind loading events. As shown in Figure 104, the end cap rail is offset forward relative to the back barrier face. As such, the end cap rail cannot span downward towards the back of the barrier and reach the cable bracket where it attaches. This was resolved by incorporating a steel angled bracket that serves as a link between the cable bracket and cap rail. Slots were added to the angled bar bracket, shown in Figure 116, which account for installation tolerances.

8.3.7 Upper Horizontal Stiffener

Upper horizontal stiffeners, also referred to as cap rails, are shaped as channel geometries to create a removable part that encapsulates and allows access to the wire rope for future repairs. The thickness of the cap rail was selected to prevent twist warping and bending resulting from vertical loads applied to the cap rail via the chain-link fabric. Undesired distortion caused by the tightening of the chain-link connection bolts to the cap rail was also mitigated by increased cap rail thickness.

A 5½- in. flange height was selected to allow two chain-link fabric diamonds to nest inside the cap rails. This combined with the 3-in. long slots allow the installers to connect the fabric to the cap rail such that the second knuckle from the top of the fabric is captured by the bolts. Bearing the vertical loads imposed on the fence fabric on the top knuckle was not desired since it could cause the knuckle joint to untwine. To maximize the load capacity of these connections, bolt slots were designed to develop the capacity of wires that form the chain-link fabric. Calculations of bearing, shear and flexure strength of the bolt slots are detailed in Appendix F.

8.3.7.1 Horizontal Stiffeners at Fence Terminals

End cap rails were added at terminals to conceal the wire rope, giving a "clean", aesthetic appearance to the termination sections of the debris fence. The end cap rails had a similar geometry to that of the horizontal stiffeners with modifications that allowed its attachment to steel angled bracket used to connect it to the cable bracket.

Typical chain-link fences use bracing at the end posts used to stiffen the fence terminals. This bracing is necessary to distribute the lateral load applied to terminal posts during fence fabric tensioning and is achieved by connecting members such as horizontal pipes and diagonal truss rods between end posts and neighboring line posts. Furthermore, the Iowa fence standards also mention the use of bracing and truss rods and specifies sizing's and means of connections. The end cap rails also acts as end bracing for the fence framework, eliminating the need for bracing members that could dislodge during vehicle impacts with fence terminals.

8.3.7.2 Splice Connections

Splice rails, shown in Figure 118 and Figure 119, were incorporated as connections between vertical posts and cap rails. These splice rails have round tubes, functioning as sockets that seat on top of vertical posts. A single bolt was used in connecting splice rails to vertical post to prevent the splice rails from lifting up and detaching. Two bolts with slots were used to connect splice rails to cap rails. Slots allow for installation tolerances to accommodate variations in post spacing and alignment, while using two bolts assisted in the rotational alignment of cap rails. These connections also satisfy Iowa DOT fence standards that require posts and braces be connected such that they are held rigidly. In the case of the splice rails at fence ends, they are angled downward to match the slope of the wire rope at fence terminals.

Installation of the cap rail requires the wire rope be nested inside the cap rail and above the cap rail flange bolt slots. This can only be achieved if the wire rope is free of tension, allowing the installers to tuck the wire rope up above every bolt slot on the cap rail along the entire span of the fence. To further simplify the construction process, an "installation" bolt was added to end splice rails. The installation bolt is located above the bolt slots, thus as the wire rope is tensioned, it will rest on these bolts instead of resting on the cap rail flange bolts. This is beneficial since tensioning the wire rope will reduce interference with the cap and decrease difficulty of the fence installation and hanging process.

8.3.8 Lower Horizontal Stiffener

States commonly use small diameter pipes or tension wire to stiffen the bottom portion of the fence fabric. Critical failure points of pipes are within the ZOI at connection points between the pipes, where rail ends could disengage and spear an impacting vehicle. As such, MwRSF researchers believed that using tension wires may result in less vehicle damage during an impact and were used to stiffen the lower portion of the parapet-mounted fence. Tension wire is typically used in chain-link fence construction and uses hardware that is standard and readily available. Additionally, the proposed lower horizontal stiffener was selected to meet Iowa fence standards.

8.3.9 Additional Hardware

Hardware such as tension bars and tension bands are used to attach the chain-link fabric to each fence termination post. To prevent the fence fabric from “galloping” during wind gusts, wire ties are used to connect the fence fabric to line post and cap rails while hog rings serve as a connection between the fabric and lower horizontal stiffener. All mentioned hardware are standard components, which is typically used in chain-link fence constructions and conform to ASTM F626 as specified by Iowa DOT fence standards.

All bolts and nuts used within the debris fence, with the exception of carriage bolts used at tension bands, are structural and heavy hex to conform to Iowa DOT fence standards.

8.3.10 Pull Post Assemblies

Fence fabric is typically sold in 50-ft. rolls which may be spliced together to achieve the required chain-link fabric length for any given installation. Links to resources on how to splice these chain-link fabric rolls is provided in Figure 128. The number of 50-ft fabric sections that may be spliced together should not exceed 4; in other words, spliced chain link fabric shall not exceed 200 ft in length. If fence installations exceed 200 ft, then a mid-span pull post assembly is required, as shown in Figure 130. These pull post assemblies allow installers to divide the chain-link fabric sections into lengths shorter that the specified limit. A chain-link fabric continuous length limit of 200 ft was adopted from state DOT fence design details which specify similar requirements. MwRSF researchers also consulted with a local fence installer which mentioned that these limits are typically established to mitigate longitudinal deflection of terminal post during chain-link fabric tensioning. Setting these limits will reduce the length of chain-link fence being tensioned which will aid in reducing chain link fabric vertical sag during the installation process.

8.3.11 Recommended Installation Procedure

MwRSF researchers also developed a preliminary installation procedure to simplify fence installation onto any existing barrier using the proposed fence design. This procedure may later be refined in Phase II of this effort once this system is physically installed. The current proposed procedure will be presented and discussed in this section.

Construction shall start with the installation of epoxy anchor per manufacture's specifications followed by the attachment of post brackets onto the back side of the barrier. Next, slide vertical post into post brackets and fasten the lateral bolt at the center of the post socket. Mount the rail mid splices onto the top of vertical pots. For terminal post, install rail end splices and fasten "g3" bolt onto the rail end splices.

The fence termination should then be assembled by attaching the cable brackets to angled brackets, angled brackets to end cap rails, and end cap rails to ends splice rails. Mounting the end cap rails with the steel strap and cable bracket attached allows installers to use this assembly as a template for the drilling location of the cable bracket anchors on the concrete barrier.

Next, the wire rope assembly should be installed with the turnbuckles at maximum extension, which will allow the slack to be taken up during tightening. The cable assembly should then be attached to one cable bracket, guided up to the end splice rail and over the "g3" bolt. The cable should be run to the opposite end of the fence and over bolt "g3" on that end splice rail and attached to the opposite cable bracket, ensuring that the cable is nested inside of each mid rail splice. Tension the cable and install the tension wire at the bottom of the fence framework.

Next, commence the installation the chain-link fabric per typical fence construction practices as described in ASTM F567 [39]. Verify that the fabric is does not extend above the top of splice rails. The second knuckle from the top of the chain-link fabric should also not be lower than 2⅝ in. below the top of splice rails and the fence fabric should not be higher than 3 in. above the barrier top surface.

Once the fabric is positioned and the cable is tensioned, place the cap rails onto the splice rails. Prior to installment of the lower bolts "g2" between the splice rails and cap rails, verify that the cable does not sag below the slots near the bottom edge of cap rail flanges. If this occurs, install bolts in the cable supports slots, shown in Figure 110, while the wire rope is manually lifted above these bolts. Next, bolts "g2" can be installed between the lower slots on the cap rail flanges, the splice rails, and the chain-link fence. Technicians should ensure that these bolts be positioned in slots locations that capture the second knuckle form the top of the chain link fabric, as shown in Figure 129.

In this procedure, the cable is positioned at terminations over bolts "g3" on end splice rails and additional installation of cable support bolts along the mid-span of the fence is recommended whenever the cable sags down below the lower flange slots on the cap rail. These steps were incorporated to prevent the interference of the wire rope during cap rail installation. If the wire rope sagged below the mentioned slots, installers may raise the wire rope at each slot which could be cumbersome. It is also recommended that these lower cap rail flange bolts be positioned such that they capture the second knuckle from the top of the chain link fabric to increase this connection's strength, since the top knuckle could untwine during severe loading scenarios. As previously mentioned, the proposed installation procedure is preliminary and will be further refined when physical construct is conducted in a future Phase II of this design effort.

8.3.12 Expected Vehicle and Barrier-Mounted Fence Interaction

The full-scale crash test conducted by Caltrans, outlined in the literature review, consisted of a pickup truck impacting a 36-in. tall single-slope barrier with a top-mounted post installed 4¼ in. behind the top barrier face. This test failed due to occupant compartment deformation and snag that occurred between the post and vehicle hood, showing the importance of not placing structural elements within the ZOI. The TTI sign support study included four full-scale crash test of different sign configurations designed to mitigate snag. All four tests included posts mounted 2½ in. behind the top front corner of a 32-in. tall New Jersey barrier. Two of the four crash test resulted in sign systems that behaved similar to stiff posts configurations, and all four were deemed crashworthy per MASH TL-3 criteria [7]. Results of the mentioned full-scale crash tests could be attributed to the barrier size and shape, the impact conditions and potentially the test vehicle. Considering these things, MwRSF researchers believed that the 8-in. offset achieved by attaching vertical post to the back of the 36-in. tall TL-4 optimized bridge rail would be sufficient for reducing the potential for vehicle snag and the potential for serious occupant compartment deformation and excessive occupant risk. This will be discussed in further detail in this section.

MwRSF's ZOI study noted that one crash test has shown that the risk of snagging is greatly reduced when structurally-stiff posts are mounted on top of stiff bridge railings with a 7-in. lateral offset [3]. However, these findings were from a crash test conducted under NCHRP Report 350 requirements and vertical posts consisted of rectangular tubes mounted on top of a 20-in. tall bridge rail [50]. A longitudinal railing was also situated on top of the posts, creating a 12 in. opening where the bumper could snag on vertical posts. The recommendations on posts lateral offset are not directly applicable to the debris fence designed in this effort since the selected 36-in. tall bridge rail with a fence installation poses snag concerns between the errant vehicle's fender and hood whereas there is no concern that bumper snag could occur.

The TTI sign support study where crash testing was conducted on a test article with round vertical posts mounted 2½-in. from the front face of a 32-in. tall barrier resulted in snagging between the vehicle's fender and these vertical members however, this did not violate MASH TL-3 requirements. Researchers considered two attributes of the vehicles used in this testing series when reviewing these results: (1) the hoods do not extend to the lateral extremities of the vehicle's front end and (2) the hoods connect to the front grill. As such, the front grill-to-hood connection may have restricted the hood's ability to extend past the front barrier face. Considering these things, this vehicle may not have produced the worst-case snag scenario.

Full-scale crash tests nos. MNPD-1 and MNPD-3 had test articles consisting of 32-in. tall J-shape barriers with pedestrian railing mounted 9½ in. and 9¾ in. from the front barrier face and were conducted under NCHRP Report 350 and MASH 2016 requirements, respectively. In both of these full-scale crash tests the pickup truck protruded past the front barrier face and interacted with the back-mounted pedestrian railing. However, neither test produced significant snag concerns [12, 13]. Furthermore, in MNPD-3, a 12 ¾ in. ZOI was reported for the 32-in. tall barrier. Both of these tests used vehicles where the hoods extended near the lateral extremities of the vehicle's front end and did not attach to the grill.

Considering the interactions between the vehicle and pedestrian rails in MNPD-1 and MNPD-3, researchers believed that the 1¾-in. lateral offset difference between the 8-in. offset achieved by mounting the fence to the barrier back side compared to the 9¾-in. lateral offset from the test article from MNPD-3, will not result in a significant snag increase to a degree that causes concern for occupant safety. It is expected however that for MASH TL-3 conditions, the pickup truck will extend past the front barrier face where contact between the vehicle's hood and fender and the fence system may occur.

9 CONSIDERATIONS FOR MODIFYING OR ADAPTING IOWA DOT DEBRIS FENCE DESIGN

The debris fence developed in this research effort was specifically designed to attach to the TL-4 optimized bridge rail and to be installed in the state of Iowa. Design adjustments may be necessary if the fence will be constructed in other geographic locations with alternative design loading conditions. All local design codes should be followed when designing a debris fence for alternative locations. Attaching the debris fence to a different barrier may also be desired and may require a modified anchorage configuration. Some of the modifications and adjustments to design parameters that may need to be considered are discussed in the following sections.

9.1 Importance of the Debris Fence

According to ASCE 7-16 provisions, a structure must be categorized depending on the risk to human life posed in the event of failure. This categorization applies to the determination of wind, snow, and ice loading by adjusting the severity of these loading effects. Researchers believed that failure of the debris-containment fence caused by severe loading events represented a minimal threat to human life, defined in ASCE 7-16 as Risk Category I.

If the fence will be constructed on a structure or near an area where it is deemed that failure could pose significant risk to human life, the design must be re-evaluated to account for the increased risk category and subsequent design loads. Re-designing the debris fence to a higher Risk Category will increase the expected wind velocity, the weight of snow and thickness of ice that can accumulate on the debris fence structure. As a result, a vertical post option with a higher capacity may be required to withstand these loads. Since the barrier attachment is designed to develop the capacity of vertical posts, anchorage and attachments may also require design modifications. It should be noted that the proposed fence configuration was not design for this kind of stringent requirements.

9.2 Accommodations for Geographic Location

Design of the debris fence accounted for multiple loading scenarios such as high wind events and severe ice storms. The severity of these events is dependent on the geographic location, shown in Figure 26.5-1A in Section 26.5.3 and in Figure 10.4-2 in Section 10.4.2 of ASCE 7-16, where higher wind velocities are expected in states sharing coasts with the Atlantic Ocean and ice thickness accumulation is more severe in Midwest regions. If other state DOTs intend to utilize the debris fence design proposed for the Iowa DOT, designers should review the design for the typical loading conditions expected in the region of use.

Topographic effects should also be considered if a structure is constructed on an unobstructed hill or ridge due to the increased speeds and subsequent increased icing effects as the wind passes over these features. The severity of the elevated wind speeds and icing effects are dependent on type of topographic feature and the construction location of the debris fence on this feature. If the debris-containment fence is to be constructed on a topographic feature where analysis indicates that wind rise up effects will occur, provisions in Section 26.8 of ASCE 7-16 should be followed.

Constructing the fence structure at an elevated height above ground level also produces increased wind speeds. The debris fence was designed to withstand wind and ice loading effects at 100 ft. above ground level. Variations from this design height may affect fence design and therefore the procedures presented in ASCE 7-16 should be utilized to determine system's load demand. In this case, wind load and ice loading should be calculated including these topographic and height above ground level effects.

9.3 Accommodations for Barrier Selection

To meet UP-BNSF requirements, a 7-ft tall fence was designed to attach onto the selected 39-in. tall barrier with a 3-in. overlay. Other rail companies may also have alternate requirements for structures located near railways. Note that if installment of this fence design on a shorter barrier is desired, a taller fence is required to meet UP-BNSF height requirements. For barrier heights shorter than 36-in., an 8-ft fence will be required which will increase the loading demand followed by the required post strength and subsequently the post bracket and anchorage to the barrier. In the case of installment on a shorter barrier with an 8-ft fence, the debris fence should be evaluated to validate the capacity of the major fence components.

The concrete anchorage was designed to develop the capacity of vertical posts by ensuring that tensile and shear forces on anchors during vertical post failure do not exceed the strength of concrete breakout in tension and shear and anchor pullout and pryout. These concrete failure modes have a dependency on the strength of concrete mix used to construct the barrier, the presence of cracks on the barrier, and the barrier reinforcement configuration.

The anchorage design in this research effort was developed on the condition that it would be installed on a recently-constructed TL-4 Optimized bridge rail [49] using 5,000-psi concrete mix, and it was assumed that major and minor cracking, other than shrinkage cracks, would not be present. On this bridge rail, shear reinforcement was spaced 12-in. apart which could help prevent concrete from splitting before the capacity of the anchorage is developed during vehicle impacts. If the fence is installed on a barrier with reduced reinforcement, constructed with a lower strength concrete mix, or on a barrier with cracks, the anchorage capacity should be re-evaluated to ensure that it can develop the capacity of the vertical posts.

Barrier geometry and changes to the anchorage will also affect the strength of the concrete connection. The anchorage embedment depth may be shallower for barriers with limited thicknesses, and the corresponding anchorage connection strength will be reduced in these instances. Anchor location and spacing may also require modifications to avoid concrete reinforcement for other barrier configurations.

Modifications to vertical anchor distances relative to the barriers top edge will also alter the system's loading conditions. Raising the top anchorage location will increase shear loading on the post during impact events which transfers to the anchor connection, increasing anchorage demand. Lowering the top anchorage location could lengthen the lever arm which the lateral wind loads act on, magnifying the moment on vertical posts. A concrete anchorage strength analysis must be conducted if installation on an alternative barrier configuration alter the mentioned anchorage parameters. The vertical posts flexure demand should also be re-evaluated through a loading analysis if adaptation to a different barrier changes the post's cantilever length.

9.4 Accommodations for Test Level-4 Conditions

The debris fence was designed meet MASH TL-3 test conditions with added features used to retain fence components during impacts scenarios which could be consistent with MASH TL-4 impact conditions. Nonetheless, the debris fence was not designed to meet MASH TL-4 test conditions. The ZOI envelope of TL-4 vehicles is much taller and extends farther past the front barrier face when comparted to TL-3 vehicles [3]. Modifications to the current design may be necessary to improve resistance to fracture or release during heavy truck impacts.

If it is deemed necessary to increase the retention of fence components when failures occur, additional retention elements such as wire rope may be added to the middle and bottom portion of the fence. This will distribute the forces caused by the displaced fence component to multiple wire rope segments, reducing the potential for wire rope breakage. It is also recommended that a larger wire rope size be used to further reduce the potential for wire rope breakage. As such, the wire rope termination will need to be re-evaluated to accommodate for a larger wire rope size with a higher capacity and to accommodate for multiple wire rope connections. Any added wire rope elements should also comply with design objectives of the wire rope incorporated to the top portion of the current fence design. These objectives require that termination must develop the capacity of the wire rope and that connection points along the span of the fence allow longitudinal displacement.

10 SUMMARY, CONCLUSIONS, AND RECOMMENDATIONS

10.1 Summary

The objective of this research was to design a MASH TL-3 compliant debris fence system with attachment to a crashworthy concrete bridge parapet design. In this design effort, a literature review was completed and included state DOT debris fence designs. The aim of this effort was to gather key information on parapet-mounted fence attributes. These state designs were then ranked based on these attributes and the highest-ranking designs were adopted as the groundwork for the fence designed in this effort. Real-world crashes, crash tests related to debris fences, and ZOI information were also reviewed to gain an understanding of the interactions that may occur between an impacting vehicle and a parapet-mounted fence during MASH TL-3 test level conditions. Information on standards, such as Iowa DOT design standards and UP-BNSF standards, were also collected to ensure that the debris fence was designed to satisfy necessary requirements.

The design portion of this research effort consisted of the establishment of design criteria derived from information collected in the literature review. The key criteria pertaining to the design of parapet-mounted debris fences for roadside safety purposes is summarized below:

- If possible, fences should be back-mounted to minimize the potential for vehicle snag
- Structurally-stiff horizontal members should be positioned within passenger vehicle ZOI should be avoided
- Robust connections throughout the fence structure should be prioritized to reduce the potential for component detachment

The effects of wind, ice, snow, and the combination of these severe loading events imposed on the debris-containment fence were investigated to determine design loads. These design loads were then applied to the debris fence structure though a structural analysis used to select an optimized vertical post size and spacing configuration. Other fence components were designed to withstand these loading scenarios, while also satisfying design standards and established objectives.

The proposed Iowa parapet fence included the design of components, such as the post-to-barrier bracket, concrete anchorage, horizontal stiffeners, and fence terminations, and included the selection of hardware for vertical posts, fence fabric, tension wire, and wire rope. Parts were designed and selected considering crashworthiness, cost, constructability, and aesthetics. As such, standard and readily available options were designated for components and hardware used for fabrication while minimizing the different number of parts and types of materials used. Components were also designed for ease of fabrication and considered features to simplify fence installation.

Lastly, accommodations for design parameter alterations, such as construction location and fence installation on alternative barrier configurations, were discussed. Recommendations of system modifications were also presented to accommodate for TL-4 impact conditions.

10.2 Conclusions

Based on the results of various crash tests presented in the literature review, during impact events consistent with MASH TL-3 conditions, a pickup truck's fender and hood may interact with the parapet-mounted debris fence designed in this effort. However, it is believed that this interaction will not cause significant snag or occupant safety concerns. During impact events involving 1100C vehicles with conditions consistent with MASH TL-3 conditions, interactions between the vehicle and back-mounted fence are not expected. This was concluded from the results of multiple crash tests with "rigid" barriers near the 36-in. height, where the lateral extent of structural components of the small car past the front barrier face was minimal [51, 52].

10.3 Recommendations

In the debris fence design, attributes which could improve the crashworthiness of the system were incorporated, such as mounting the post on the back face of the barrier and the reduction of horizontally stiff elements within the vehicle's ZOI to reduce the potential for spearing hazards. However, a full-scale crash test is recommended for a future Phase II of this research effort to evaluate the crashworthiness of the proposed parapet-mounted debris fence design. At this time, none of the existing debris fence designs have been full-scale crash tested to assess the crashworthiness of these systems. This full-scale crash test should comply with MASH test designation 3-11 and will serve to examine the parapet and fence structure's ability to safely contain and redirect pick-up trucks impacting within system's the length-of-need. For this test, researchers should select a critical impact point that maximizes the potential for vehicle snag on vertical fence posts. MASH 2016 test designation 3-10, which involves the 1100C small car vehicle, was not deemed necessary or critical due to the reduced lateral extent of the vehicle past the front barrier face which will most likely not interact with the back-mounted debris fence.

Impact events between TL-4 vehicles and barrier-mounted, chain-link fences has not been studied or full-scale crash tested and could result in vehicle stability concerns if the vehicle's box interacts with fence elements. Occupant safety is also a concern; since, the cab could interact with vertical posts, potentially resulting in occupant compartment deformations that exceed MASH limits. Thus, it is recommended that two impact scenarios be investigated, a length-of-need and a fence terminal impact event. The length-of-need impact scenario should be studied to examine the system's ability to safely contain and redirect errant vehicles. Large vehicle impact with fence terminals is also a concern; since, the vehicle's box and/or cab could potentially snag on terminal posts and end cap rails. These studies will also serve to assess the proposed fence design's ability to retain fence elements during impact conditions with large vehicles. This is a concern since the ejection of large fence components potentially caused by these impact scenarios could acts as hazards for railroad operations.

Studying the effects of debris impacts with parapet-mounted fences was not in the scope of this research effort. However, investigating and designing a debris fence capable of containing large projectile impacts is recommended; since, it will further improve the safety of railroad operations and employees.

11 REFERENCES

1. *Manual for Assessing Safety Hardware (MASH), Second Edition*, American Association of State Highway and Transportation Officials (AASHTO), Washington, D.C., 2016.

2. *Roadside Design Guide*, *Fourth Edition*, American Association of State Highway and Transportation Officials (AASHTO), Washington, D.C., 2011.

3. Keller E.A., Sicking, D.L., Faller, R.K., Polivka, K.A., and Rohde, J.R., *Guidelines for Attachments to Bridge Rails and Median Barriers,* Final Report to the Midwest States' Regional Pooled Fund Program, Transportation Research Report No. TRP-03-98-03, Project No. SPR-3(17), Midwest Roadside Safety Facility, University of Nebraska-Lincoln, Lincoln, Nebraska, February 26, 2003.

4. Reid, J.D., and Sicking, D.L., *Zone of Intrusion Study,* Final Report to the Midwest States' Regional Pooled Fund Program, Transportation Research Report No. TRP-03-242-10, Midwest Roadside Safety Facility, University of Nebraska-Lincoln, Lincoln, Nebraska, October 15, 2010.

5. Ross, H.E., Sicking, D.L., Zimmer, R.A., and Michie, J.D., *Recommended Procedures for the Safety Performance Evaluation of Highway Features*, National Cooperative Highway Research Program (NCHRP) Report No. 350, Transportation Research Board, Washington, D.C., 1993.

6. Stolle, C.J., Reid, J.D., and Faller, R.K., *Zone of Intrusion for Permanent 9.1-Degree Single-Slope Concrete barriers,* Final Report to the Wisconsin Department of Transportation, Transportation Research Report No. TRP-03-292-13, Midwest Roadside Safety Facility, University of Nebraska-Lincoln, Lincoln, Nebraska, March 14, 2014.

7. Abu-Odeh, A., Williams, W., Ferdous, R., Spencer, M., Bligh, R., and Menges, W., *Signs on Concrete Median Barriers*, Texas Transportation Institute, University of Texas A&M, College Station, Texas, April, 2013.

8. Hirsch, T.J., Post, E. R., Hayes, G. G., *Vehicle Crash Test and Evaluation of Median Barriers for Texas Highways*, Research Report Number 146-4, Texas Transportation Institute, Texas A&M University, College Station, Texas, 1972.

9. Buth, E., and Menges, W., *Crash Testing and Evaluation of Retrofit Bridge Railings and Transition,* Texas Transportation Institute, Texas A&M University, College Station, Texas, 1995.

10. *Guide Specifications for Bridge Railings*, American Association of State Highway and Transportation Officials (AASHTO), Washington, D.C., 1989

11. Dobrovolny, C.S., Shi, S., Kovar, J.C., *Development and Evaluation of Concrete Barrier Containment Options for Errant Motorcycle Riders,* Report No. FHWA/TX-18/0-6968-R6, Texas Transportation Institute, Texas A&M University, College Station, Texas, June 2019.

12. Polivka, K.A., Faller, R.K., Keller, E.A., Sicking, D.L., Rohde, J.R., and Holloway, J.C., *Design and Evaluation of the TL-4 Minnesota Combination Traffic/Bicycle Bridge Rail*, Final Report to the Midwest States' Regional Pooled Fund Program, Transportation Research Report No. TRP-03-74-98, Project No. SPR-3(17), Midwest Roadside Safety Facility, University of Nebraska-Lincoln, Lincoln, Nebraska, November 1998.

13. Hinojosa, M.A., Faller, R.K., Rosenbaugh, S.K., *MASH 2016 Test Level 3 Evaluation of MnDOT Bicycle and Pedestrian Rail,* MwRSF Research Report No. TRP-03-443-20, Midwest Roadside Safety Facility, Lincoln, December 2020.

14. Caldwell, C. *Investigation of the Crashworthiness of Barrier Mounted Hardware: Barrier Mounted Sign and Signpost,* Final Report to the Roadside Safety Research Group of the California Department of Transportation. Caltrans, Sacramento, California, June 2011.

15. Alberson, D.C., Menges, W.L., Bligh, R.P., Abu-Odeh, A.Y., Buth, E., and Haug, R.R., *Thrie Beam Transition Crash Tests*, Report No. FHWA-RD-04-115, Texas A&M Transportation Institute, Texas A&M University, January 2005.

16. Miller, S., *Fencing Saves Driver from Plunging off Valley View Bridge*, Cleveland Channel 19 News, Cleveland Ohio, April 5, 2018. < http://www.cleveland19.com/story/37892707/fencing-saves-driver-from-plunging-off-valley-view-bridge> Last accessed July 13, 2018

17. *Crash Viewer NASS CDS (2004-2015)*, National Highway Traffic Safety Administration https://crashviewer.nhtsa.dot.gov/LegacyCDS/Search > Last accessed February 24, 2020.

18. *NASS CASE Viewer CASE ID: 828018044*, April, 2014. https://crashviewer.nhtsa.dot.gov/nass-cds/CaseForm.aspx?xsl=main.xsl&CaseID=828018044 > Last accessed February 24, 2020.

19. *NASS CASE Viewer CASE ID: 727019493*, September, 2015. https://crashviewer.nhtsa.dot.gov/nass-cds/CaseForm.aspx?xsl=main.xsl&CaseID=727019493> Last accessed July 16, 2018.

20. *Bridge Deck Rail Bridge Standards*, Iowa Department of Transportation (IowaDot), Iowa, August. 29, 2016.

21. *Standard Plans*, California State Transportation Agency (Caltrans), California, 2015.

22. *Standard Construction Drawings*, Delaware Department of Transportation (DelDOT), Delaware, Dec. 30, 2014.

23. *Standard Plans for Bridge Construction*, Florida Department of Transportation (FDOT), Florida, Nov. 11, 2017.

24. *Standard Drawings*, Idaho Transportation Department (ITD), Idaho, October. 2017.

25. *Standard Plans*, Indiana Department of Transportation (INDOT), Indiana, September. 4, 2012.

26. *Standard Plans, Standard Drawing No. E706-BRSF*, Indiana Department of Transportation (INDOT), Indiana, September. 4, 2012.

27. *Standard Drawings*, Kansas Department of Transportation (KDOT), Kansas, May 2, 2015.

28. *Book of Standards – For Highway & Incidental Structures*, Maryland Department of Transportation (MDOT), Maryland, September. 24, 2013.

29. *Standard Plates*, Minnesota Department of Transportation (MnDOT), Minnesota, August. 28, 2017.

30. *Bridge Office Policies and Procedures*, Nebraska Department of Roads Bridge Divison, Nebraska, 2016.

31. *Bridge Construction Details*, New Jersey Department of Transportation (NJDOT), New Jersey, July 19, 2017.

32. *Standard Sheets – English – USC*, New York Department of Transportation (NYSDOT), New York, July 14, 2016.

33. *Standard Details*, Oregon Department of Transportation (ODOT), Oregon, 2018.

34. *CAD Standards*, Texas Department of Transportation (TxDOT), Texas, March, 2018.

35. *Bridge Manual Standard Drawings*, Wisconsin Department of Transportation, Wisconsin, July 7, 2017.

36. *IOWA DOT GS-15006 – General Supplemental Specifications for Highway and Bridge Construction.*, Iowa DOT, April 17, 2018. <https://iowadot.gov/specifications/new_docs/GS-15004.pdf> Last accessed July 25, 2018.

37. Friensen R., Hurst A., *Guidelines for Railroad Grade Separation Projects*, Union Pacific Railroad, January 5, 2016.

38. *IOWA DOT* – Office of Bridges and Structures – *LRFD Bridge Design Manual*, Iowa DOT, January 2019

39. ASTM International. *F567-14a(2019) Standard Practice for Installation of Chain-Link Fence*. West Conshohocken, PA, 2019. doi: https://doi.org/10.1520/F0567-14AR19

40. *Minimum Design Loads and Associated Criteria for Buildings and Other Structures.* American Society of Civil Engineers ASCE/SEI, 2017.

41. *Steel Construction Manual*, American Institute of Steel Construction (AISC), Fifteenth Edition, First Printing, 2017.

42. *Building Code Requirements for Structural Concrete (ACI 318-14)*, American Concrete Institute (ACI), September, 2014.

43. *Steel Design Guide 9: Torsional Analysis of Structural Steel Members*, American Institute of Steel Construction (AISC), Second Printing, October, 2003

44. *Chain Link Fence Wind Load Guide for the Selection of Line Post and Line Post Spacing*, Chain Link Manufactures Institute, June, 2016.

45. *AASHTO LRFD Bridge Design Specifications*, Seventh Edition, American Association of State Highway and Transportation Officials (AASHTO), Washington, D.C., 2014.

46. *Transverse Shear Loading of Beams With Solid or Open Cross Sections - Flexural Shear Stress and Shear Flow*, Mississippi State University Tutorial Page of Aerospace Structures(TuPAS), <https://www.ae.msstate.edu/tupas/SA2/chA14.6_text.html> Last accessed June 6, 2021

47. *Chain Link Fence Manufacturers Institute Product Manual (CLF-PM0610)*, Chain Link Manufactures Institute (CLMFI), Updated March, 2017

48. Stolle, C.S., Reid, J.D., Polivka, K.A., *Development of Advanced Finite Element Material Models for Cable Barrier Wire Rope,* MwRSF Research Report No. TRP-03-233-10, Midwest Roadside Safety Facility, Lincoln, August 2010.

49. Rosenbaugh, S.K., Faller, R.K., Dixon, J.D., *Development and Testing of an Optimized MASH TL-4 Concrete Bridge Rail*, MwRSF Research Report No. TRP-03-415-21, Midwest Roadside Safety Facility, Lincoln, March 2021.

50. Pfeifer B.G., Holloway J.C., Faller R.K, and Rosson B.T., *TL-4 Evaluation of the Minnesota Combination Bridge Rail*, Research Report No. TRP-03-53-96, Midwest Roadside Safety Facility, University of Nebraska-Lincoln, Lincoln, Nebraska, 1995.

51. Bielenberg, R.W., Yoo, S.H., Faller, R.K., *Crash Testing and Evaluation of the Hdot 34-In. Tall Aesthetic Concrete Bridge Rail: Mash Test Designation Nos. 3-10 and 3-11*, Research Report No. TRP-03-420-19, Midwest Roadside Safety Facility, University of Nebraska-Lincoln, Lincoln, Nebraska, 2019.

52. Hinojosa, M.A., Faller, R.K., Rosenbaugh, S.K., *MASH 2016 Test Level 4 Evaluation of MnDOT Concrete Parapet with Brush Curb and Upper Beam and Post Rail with New Tapered End Section*, MwRSF Research Report No. TRP-03-403-21, Midwest Roadside Safety Facility, Lincoln, March 2021.

53. *Full-weight Hot-dip Galvanized ASTM F1083 Schedule 40 Pipe*, Wheatland Tube, <https://www.wheatland.com/wp-content/uploads/2017/12/F1083-Schedule-40-Specifications.pdf> Last accessed November 30, 2018

54. *Chain Link Galvanized Fence*, Your Fence Store, <http://www.yourfencestore.com/cl/clgal.htm> Last accessed December 1, 2018.

12 APPENDICES

Appendix A. ASCE Design Loads

A.1. Dead and Live Loads

ASCE 7-16 DEAD & LIVE LOADS

DEAD LOAD IN 8-ft FENCE SECTION, 7-ft TALL

→ 9 ga, 2-in. MESH = 0.71 lb/ft² (WHEATLAND.COM)

MESH WEIGHT = $0.71\ \text{lb/ft}^2\ (8\text{ft} \cdot 7\text{ft}) = \boxed{39.8\ \text{lb}}$

– POST: 2 7/8-in. SCHEDULE 80 PIPE

7.67 lb/ft (WHEATLAND.COM)

POST WEIGHT = $\frac{112\ \text{in.}}{12\ \text{ft}}\ (7.67\ \text{lb/ft}) = \boxed{71.6\ \text{lb}}$

– CAP RAIL: 3/16-in. THICK, 5 1/2-in. x 6 3/16-in. CHANNEL

7.65 lb/ft² (ENGINEERINGTOOLBOX.COM)

CAP RAIL AREA = $(2 \cdot 5\tfrac{1}{2}\ \text{in.} + 6\tfrac{3}{16}\ \text{in.})(96\ \text{in})$
$= 1650\ \text{in.}^2$

CAP RAIL WEIGHT = $\frac{1650\ \text{in.}^2}{144\ \text{ft}^2}\ (7.65\ \text{lb/ft}^2) = \boxed{87.7\ \text{lb}}$

– SPLICES: 29-in. LONG, 5 3/8-in. x 4 7/8-in. CHANNEL
3/16-in. THICK

AREA = $(2 \cdot 5\tfrac{3}{8}\ \text{in.} + 4\tfrac{7}{8}\ \text{in.})(29\ \text{in.})$
$= 453.1\ \text{in.}^2$

SPLICE WEIGHT = $\frac{453.1\ \text{in.}^2}{122\ \text{in.}^2}\ (7.65\ \text{lb/ft}^2) = 28.4\ \text{lb}$

SPLICE TOTAL WEIGHT (WITH TUBE) = $\boxed{31.3\ \text{lb}}$

Figure A-1. Design Loads: Dead Loads

ASCE 7-16 DEAD & LIVE LOADS

- POST BRACKET WEIGHT: 1/4-in. THICK PLATE

$10.2\ lb/ft^2$ (ENGINEERING TOOLBOX.COM)

- X2 BASE PLATES: 21 in. X 4 1/4 in.
- X4 GUSSETS : 8 in. X 3 in.

FLAT STOCK AREA = 274.5 in.^{2}

$$\text{WEIGHT} = \frac{274.5\ in.^2}{122\ ft^2}\left(10.2\ lb/ft^2\right) = 19.4\ lb$$

- TUBE SOCKET: 22 1/2-in. LONG, 3 1/2-in. X 1/4 in. SQUARE HSS

10.51 lb/ft (AISC STEEL MANUAL)

$$\text{WEIGHT} = \frac{22.5\ in.}{12\ in.}\left(10.51\ lb/ft\right) = 19.7\ lb$$

POST BRACKET WEIGHT = $\boxed{39.1\ lb}$

TOTAL WEIGHT IN 8-FT SECTION: $\boxed{279.5\ lb}$
- ESTIMATE 10-lb OF HARDWARE

LIVE LOAD:

THREE - 250-lb PERSONS

LIVE LOAD = $\boxed{750\ lb}$

Figure A-2. Design Loads: Dead (Continued) and Live Loads

A.2. Snow Load

ASCE 7-16 SNOW LOAD

FLAT ROOF SNOW LOAD

$P_f = 0.7 C_e C_t I_s P_g$ (Eq 7.3-1)

$C_e = 0.9$, FULLY EXPOSED, ROUGHNESS C (WORST CASE)
$C_t = 1.2$, UNHEATED, OPEN AIR STRUCTURE
$I_s = 0.8$, SNOW IMPORTANCE FACTOR (RISK CAT. I)
$P_g = 40$ lb/ft², IOWA GROUND SNOW LOAD (FIG 7.2-1)

$\boxed{P_f = 24.19 \text{ lb/ft}^2}$

SNOW LOADS ON PIPES & CABLE TRAYS

$0.73\, P_f/\gamma$ (SECTION 7.13.3)

$\gamma = 0.13\, P_g + 14$ (Eq 7.7-1)
- BUT NOT MORE THAN 30 lb/ft³

$\boxed{\gamma = 19.2 \text{ lb/ft}^3}$

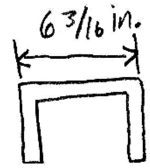

$0.73\, P_f/\gamma = 0.92 \text{ ft} = 11.04 \text{ in.}$

- CAP RAIL WIDTH = 6.19 in. < 11.04 in.

TRIANGLE SNOW LOAD

LOAD = $1.37\, D\, \gamma$ (FIG. 7.13-2A)

LOAD = $1.37 \left(\frac{6.19 \text{ in.}}{12 \text{ in./ft}} \right) 19.2 \text{ lb/ft}^3 = 13.56 \text{ lb/ft}^2$

$P_s = 13.56 \text{ lb/ft}^2 (6.19 \text{ in.})(96 \text{ in.}) = 55.94 \text{ lb}$

$\boxed{\text{SNOW LOAD} = 55.9 \text{ lb}}$

Figure A-3. Design Loads: Snow Load

A.3. Ice Load

ASCE 7-16 ICE LOADS

- DESIGN ICE THICKNESS (SECTION 10.4.6)

$t_d = t\, I_i\, f_z (K_{zt})^{0.35}$ (EQ 10.4-5)

$t = 1.5$ in., IOWA ICE THICKNESS (FIG 10.4-2)
$I_i = 0.8$, ICE IMPORTANCE FACTOR (RISK CAT. I)
$f_z = 1.12$, BRIDGE 100 FT ABOVE GROUND
$K_{zt} = 1$, ASSUME NO TOPOGRAPHIC EFFECTS

- ASSUME ROAD SURFACE 100 FT ABOVE GROUN(D)
(100 FT + 5 FT TO CENTER OF FENCE)

$F_z = (Z/33)^{0.10}$ (EQ 10.4-4)

$F_z = (105/33)^{0.10} = 1.12$

$\boxed{t_d = 1.35 \text{ in.}}$

- ICE ON FENCE FABRIC

— ICE LOAD DETERMINED FROM GLAZE OF ICE ON ALL EXPOSED SURFACES (SECTION 10.4.1)

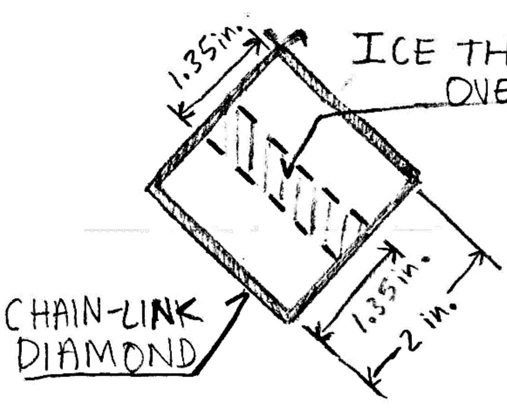

- FOLLOWING THIS PROCEDURE WILL OVER-COMPENSATE ICE WEIGHT ON FABRIC DUE TO ICE THICKNESS OVERLAP

Figure A-4. Design Loads: Design Ice Thickness

ASCE 7-16 ICE LOADS

FENCE FABRIC ICE WEIGHT - SHEET METHOD

- CONSIDERED FENCE FABRIC A SHEET

$V_i = \pi t_d A_s$ (EQ 10.4-2)

- VOLUME OF ICE (V_i) MAY BE MULTIPLIED BY 0.8 FOR VERTICAL PLATES

A_s = EXPOSED MESH AREA

$$A_s = \frac{81 \text{ in.} \cdot 96 \text{ in.}}{144 \text{ in.}^2/\text{ft}^2} = \boxed{54 \text{ ft}^2}$$

- CAP RAIL COVERS 3 in. OF 7-ft MESH

$$V_i = \pi \left(\frac{1.35 \text{ in.}}{12 \text{ in/ft}}\right) 54 \text{ft}^2 (0.8) = 15.27 \text{ ft}^3$$

$W_i = \rho \cdot V_i$

$\rho = 56$ lb/ft³, ICE DENSITY

$$\boxed{W_i = 855.1 \text{ lb}}$$

Figure A-5. Design Loads: Ice Loads on Fence Fabric

ASCE 7-16 ICE LOADS

ICE WEIGHT ON CAP RAIL

$A_i = \pi t_d (D_c + t_d)$ (EQ 10.4-1)

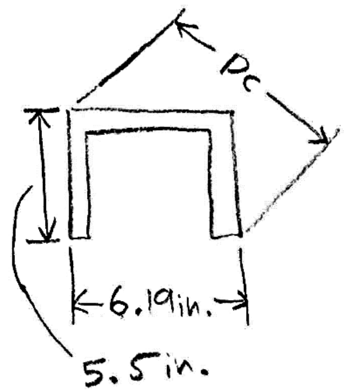

$D_c = \sqrt{(5.5 \text{ in.})^2 + (6.19 \text{ in.})^2} = 8.28 \text{ in.}$

$t_d = 1.35 \text{ in}$

$A_i = 40.63 \text{ in.}^2$

$V_i = \left(\frac{40.84 \text{ in.}^2}{144 \text{ in.}^2/\text{ft}^2}\right) 8 \text{ ft}$

$V_i = 2.26 \text{ ft}^3$

$W_i = 2.27 \text{ ft}^3 (56 \text{ lb}/\text{ft}^3)$

$\boxed{W_i = 127.1 \text{ lb}}$

TOTAL ICE WEIGHT

$W_i = W_{i\,MESH} + W_{i\,CAP\,RAIL}$

$\boxed{W_i = 982.2 \text{ lb}}$

Figure A-6. Design Loads: Ice Load on Cap Rail

A.4. Minimum Design for Wind Loading

ASCE 7-16 WIND LOADS

VELOCITY PRESSURE (SECTION 26.10)

$q_z = 0.00256 K_z K_{zt} K_d K_e V^2$ (EQ 26.10-1)

$K_z = 1.44$, EXPOSURE D, FENCE 105 ft ABOVE GROUND
$K_{zt} = 1$, ASSUME NO TOPOGRAPHIC EFFECT
$K_d = 0.85$, DIRECTIONALITY FOR SINGLE-PLANE OPEN FRAME
$K_e = 1$, ELEVATION FACTOR FOR ALL ELEVATIONS
$V = 105$ MPH, WIND SPEED, IOWA (FIG 26.5-1A)

$\boxed{q_z = 34.55 \text{ lb/ft}^2}$

GUST EFFECT FACTOR (SECTION 26.11)

- DETERMINE IF STRUCTURE IS RIGID ($n_1 > 1$ Hz)

- NATURAL FREQUENCY (n_1) IS TAKEN AS THAT OF THE VERTICAL POST

$n_1 = 0.56 \sqrt{\frac{EI}{m h^4}}$ (EQ C26.11-11)

$E = 29{,}000$ ksi, STEEL YOUNG'S MODULUS (200 GPa)
$h = 94$ in. (2.388 m), FENCE HEIGHT + 10 in. TO TOP ANCHORS
$I = 1.35 \text{ in.}^4 (5.619 \times 10^{-7} \text{ m}^4)$, HSS 2.875 X 0.188 TUBE
$m = 5.4$ lb/ft (8.036 kg/m), HSS 2.875 X 0.188 TUBE

$n_1 = 0.56 \sqrt{\frac{200 \times 10^9 (5.619 \times 10^{-7})}{8.036 (2.388)^4}}$ $\left[\sqrt{\frac{\frac{kg}{m s^2} m^4}{\frac{kg}{m} \cdot m^4}}\right] = \sqrt{\frac{1}{s^2}} = \text{Hz}$

$\boxed{n_1 = 11.6 \text{ Hz}} > 1 \text{Hz}$

SINCE SYSTEM IS RIGID, GUST EFFECT FACTOR = 0.85 (ASCE)

Figure A-7. Design Loads: Wind Loading, Velocity Pressure and Gust Effect Factor

ASCE 7-16 WIND LOADS

FORCE COEFFICIENT (C_f) : FENCE FABRIC
- FIGURE 29.4-2, FOR OPEN SIGNS & SINGLE-PLANE OPEN FRAMES

- SOLIDITY RATIO (ε) DETERMINATION

• 2-in. FENCE MESH WITH 9ga. (0.148in.) WIRE
D = 0.148 in.
S = 2.0 in.

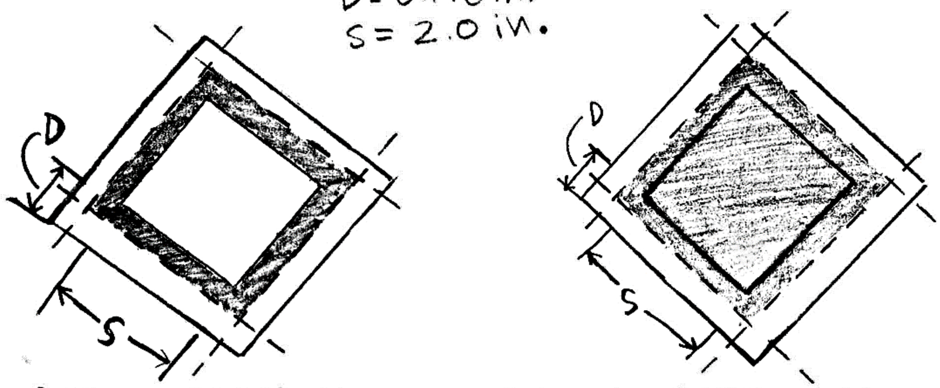

SOLID AREA IN ONE DIAMOND

GROSS AREA IN ONE DIAMOND

- GROSS AREA, A_g

$$A_g = (S+D)^2 = (2.148)^2 = 4.614 \text{ in.}^2$$

- SOLID AREA

$$A_s = [(S+D) \cdot D/2] \cdot 4 = (S+D)2D$$
$$A_s = (2.148 \text{ in.})2(0.148 \text{ in.}) = 0.636 \text{ in.}^2$$

- SOLIDITY RATIO: $\varepsilon = \frac{A_s}{A_g} = \boxed{0.138}$

$$\boxed{\varepsilon = 0.138}$$

Figure A-8. Design Loads: Wind Loading, Force Coefficient for Fence Fabric

ASCE 7-16 WIND LOADS

FORCE COEFFICIENT (C_f): FENCE FABRIC (CONT.)

- FIGURE 29.4-2, OPEN SIGNS

• $D\sqrt{q_z} \leq 2.5$ OR > 2.5 ?

$D = 0.148$ in. (0.0123 ft), FABRIC WIRE DIAMETER
$q_z = 34.55$ lb/ft², VELOCITY PRESSURE

$\boxed{D\sqrt{q_z} = 0.072 < 2.5}$

$\boxed{C_f = 1.3}$ (FIGURE 29.4-2)

PROJECTED AREA (A_f): FENCE FABRIC

$A_f = L \cdot H \cdot \epsilon$

$L = 96$ in., 8-ft POST SPACING
$H = 81$ in., EXPOSED FENCE FABRIC (TOP OF FABRIC COVERED BY CAP RAIL)
$\epsilon = 0.138$, SOLIDITY RATIO

$\boxed{A_f = 7.45 \text{ ft}}$

WIND LOAD ON FABRIC

$F = q_z G C_f A_f$ (EQ 29.4-1)

$q_z = 34.55$ lb/ft²; $G = 0.85$; $C_f = 1.3$; $A_f = 7.45$ ft

$\boxed{F = 284.4 \text{ lb}}$

Figure A-9. Design Loads: Wind Loading, Projected Area and Wind Load on Fabric

ASCE 7-16 WIND LOADS

VELOCITY PRESSURE (q_z): VERTICAL POST

$q_z = 0.00256\, K_z K_{zt} K_d K_e V^2$ (EQ 26.10-1)

$K_z = 1.44$
$K_{zt} = 1$
$K_d = 0.95$, ROUND MEMBER USED WITH NONAXIS SYMMETRIC SYSTEM, (NOTE "A" TABLE 26.6-1)
$K_e = 1$
$V = 105$ MPH

FORCE COEFFICIENT (C_f): VERTICAL POST

– FIGURE 29.3-1, SOLID FREESTANDING SIGN

– POST TREATED AS SIGN, CASE A, FORCE ACTING NORMAL TO SIGN FACE ON CENTER

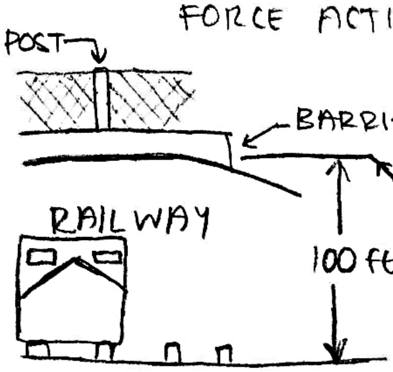

PARAMETERS

$B = 2.875 \text{ in.} = 0.240 \text{ ft}$
$S = 7 \text{ ft}$
$h = 110 \text{ ft}$

$\boxed{C_f = 1.95}$ $B/s = 0.03$, $s/h = 0.06$

WIND LOAD ON POST

$F = q_z G C_f A_s$ (EQ 29.3-1)

$q_z = 38.61 \text{ lb/ft}^2$; $G = 0.85$; $C_f = 1.95$; $A_s = 1.68 \text{ ft}$

$\boxed{F = 107.3 \text{ lb}}$

Figure A-10. Design Loads: Wind Loading on Vertical Post

ASCE 7-16 WIND LOADS

VELOCITY PRESSURE (q_z): CAP RAIL

$q_z = 0.00256\ K_z K_{zt} K_d K_e V^2$ (EQ 26.10-1)

$K_z = 1.46$, EXPOSURE D, RAIL 110 ft ABOVE GROUND
$K_{zt} = 1$,
$K_d = 0.85$, SOLID FREESTANDING SIGN
$K_e = 1$,
$V = 105$ MPH

$\boxed{q_z = 35.03\ lb/ft^2}$

FORCE COEFFICENT (C_f): CAP RAIL

– FIGURE 29.3-1, SOLID FREE STANDING SIGN

CHANNEL DIMENSIONS:

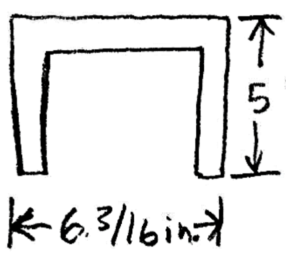

PARAMETERS

$B = 200$ ft
$s = 5.5$ in. $= 0.458$ ft
$h = 110$ ft

– ASSUMED 200-ft FENCE INSTALLATION LENGTH, WHICH WILL BE THE "SIGN" DIMENSION B

- FOR CASE A: FORCE ACTING NORMAL TO SIGN FACE, ON CENTER

$\boxed{C_f = 1.95}$ $B/s = 437$ $s/h = 0.004$

Figure A-11. Design Loads: Wind Loading on Cap Rail

ASCE 7-16 WIND LOADS

GROSS AREA (A_s): CAP RAIL

CAP RAIL DIMENSIONS, 8-ft FENCE SECTION:

$$A_s = L \cdot H = 8\,ft \cdot \frac{5.5\,in.}{12\,in./ft} = \boxed{3.67\,ft}$$

WIND LOAD ON CAP RAIL

$F = q_z G C_f A_s$ (EQ 29.3-1)

$q_z = 35.03$ lb/ft²; $G = 0.85$; $C_f = 1.95$, $A_s = 3.67$ ft

$\boxed{F = 212.9\ lb}$

WIND LOADING SUMMARY

$W_{MESH} = 284.9$ lb

$W_{POST} = 107.3$ lb

$W_{CAP\ RAIL} = 212.9$ lb

Figure A-12. Design Loads: Wind Loading on Cap Rail (Continued) and Summary

A.5. Minimum Design for Wind Loading on Ice Covered Structures

ASCE 7-16 WIND ON ICE LOAD

— SECTION 10.5:

"THE PROJECTED AREA SHALL BE INCREASED BY ADDING t_d (DESIGN ICE THICKNESS) TO ALL FREE EDGES OF THE PROJECTED AREA"

- ADDING $t_d = 1.35$ in. TO WIRE FROM 2-in. MESH DIAMONDS PRODUCES A SOLID ICE WALL

- SOLID ICE COVERED FENCE TREATED AS A SOLID FREE STANDING SIGN

VELOCITY PRESSURE (q_z): ICE WALL

$q_z = 0.00256\ K_z K_{zt} K_d K_e V^2$ (EQ 26.10-1)

$K_z = 1.44$,
$K_{zt} = 1$
$K_d = 0.85$
$K_e = 1$
$V = 50$ MPH, IOWA WIND SPEED DURING ICEING (FIGURE 10.4-2)

$\boxed{q_z = 7.83\ lb/ft^2}$

FORCE COEFFICIENT (C_f): ICE WALL
— FIGURE 29.3-1, SOLID FREE STANDING SIGN

- FOR 7-ft TALL, 200 ft LONG FENCE

PARAMETERS:
$B = 200$ ft
$s = 7$ ft
$h = 110$ ft

- FOR CASE A:

$\boxed{C_f = 1.90}$ $B/s = 28.6$, $s/h = 0.06$

Figure A-13. Design Loads: Wind on Ice Loading

ASCE 7-16 WIND ON ICE LOAD

GROSS AREA (A_s): ICE-COVERED FENCE

- AREA IN 8-ft FENCE SECTION

- 7-ft TALL FENCE FABRIC
- 3-in. OF CAP RAIL ABOVE FENCE
- 1.35-in. OF ICE ON TOP OF FENCE

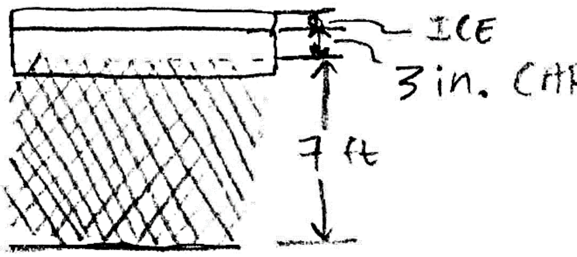

TOTAL HEIGHT = 7.36 ft

$A_s = 8\text{ ft} \cdot 7.36\text{ ft} = 58.88\text{ ft}$

WIND LOAD ON ICE WALL

$F = q_z G C_f A_s$ (EQ 29.3-1)

$q_z = 7.83$
$G = 0.85$
$C_f = 1.90$
$A_s = 58.88\text{ ft}$

$\boxed{F = 744.6\ lb}$

Figure A-14. Design Loads: Wind on Ice Loading (Continued)

A.6. LRFD Load Combinations

ASCE 7-16 LRFD LOAD COMBINATIONS

DESIGN LOAD SUMMARY

LOAD TYPE	MESH (lb)	POST (lb)	CAP RAIL (lb)
DEAD	39.8	112.9	87.7
ICE DEAD	855.1	N/A	127.1
LIVE	750	N/A	N/A
SNOW	N/A	N/A	55.9
WIND	284.4	107.3	212.9
WIND ON ICE	744.6 lb		

- NOTE: POST DEAD WEIGHT INCLUDES:
  - POST WEIGHT = 71.6 lb
  - RAIL SPLICES = 31.3 lb
  - ADDITIONAL HARDWARE = 10 lb

BASIC LOAD COMBINATIONS (SECTION 2.3.1)

1. 1.4 DEAD

	MESH	POST	CAP RAIL	TOTAL
DEAD:	55.7 lb	158 lb	122.8 lb	$\boxed{336.5 \text{ lb}}$

2. 1.2 DEAD + 1.6 LIVE + 0.5 SNOW

	MESH (lb)	POST (lb)	CAP RAIL (lb)	TOTAL (lb)
DEAD	47.8	135.5	105.2	288.5
LIVE	1200	N/A	N/A	1200
SNOW	N/A	N/A	28	28
TOTAL	1247.8	135.5	133.2	$\boxed{1516.5 \text{ lb}}$

3A: 1.2 DEAD + 1.6 SNOW + LIVE

	MESH (lb)	POST (lb)	CAP RAIL (lb)	TOTAL (lb)
DEAD	47.8	135.5	105.2	288.5
LIVE	750	N/A	N/A	750
SNOW	N/A	N/A	89.4	89.4
TOTAL	797.8	135.5	194.6	$\boxed{1127.9 \text{ lb}}$

Figure A-15. Design Loads: LRFD Basic Load Combinations

ASCE 7-16 LRFD LOAD COMBINATIONS

BASIC LOAD COMBINATIONS (SECTION 2.3.1)

3B: 1.2 DEAD + 1.6 SNOW + 0.5 WIND

	MESH (lb)	POST (lb)	CAPRAIL (lb)	TOTAL (lb)
DEAD	47.8	135.5	105.2	228.5
SNOW	N/A	N/A	89.4	89.4
WIND	142.2	53.7	106.5	306
TOTAL VERTICAL	47.8	135.5	194.6	377.9

4: 1.2 DEAD + 1 WIND + L + 0.5 SNOW

	MESH (lb)	POST (lb)	CAPRAIL (lb)	TOTAL (lb)
DEAD	47.8	135.5	105.2	288.5
LIVE	750	N/A	N/A	750
SNOW	N/A	N/A	28	28
WIND	284.4	107.3	212.9	604.6
TOTAL VERTICAL	797.8	135.5	133.2	$\boxed{1066.5\text{ lb}}$ (VERTICAL ONLY)

5: 0.9 D + 1.0 WIND

	MESH (lb)	POST (lb)	CAPRAIL (lb)	TOTAL (lb)
DEAD	35.8	101.6	78.9	216.3
WIND	284.4	107.3	212.9.	604.6

SUMMARY

- WORST-CASE COMBINED WIND & VERTICAL LOAD
  → CASE 4
- WORST-CASE VERTICAL POST AXIAL LOAD
  → CASE 2, MAX TOTAL VERTICAL LOAD
- WORST-CASE CAP RAIL VERTICAL LOAD
  → CASE 2, MESH + CAP RAIL VERTICAL LOAD

Figure A-16. Design Loads: LRFD Basic Load Combinations (Continued)

ASCE 7-16 LRFD LOAD COMBINATIONS WITH ICE

CASE 1: 1.2DEAD + 1.6LIVE + 0.2 DEAD-ICE + 0.5 SNOW

	MESH (lb)	POST (lb)	CAP RAIL (lb)	TOTAL (lb)
DEAD	47.8	135.5	105.2	288.5
LIVE	1200	N/A	N/A	1200
DEAD-ICE	171.	N/A	25.4	196.4
SNOW	N/A	N/A	28	28
TOTAL	1418.8	135.5	158.6	$\boxed{1712.9\text{ lb}}$

CASE 2: 1.2DEAD + LIVE + DEAD-ICE + WIND-ICE + 0.5SNOW

	MESH (lb)	POST (lb)	CAP RAIL (lb)	TOTAL (lb)
DEAD	47.8	135.5	105.2	288.5
LIVE	750	N/A	N/A	750
DEAD-ICE	855.1	N/A	127.1	982.2
SNOW	N/A	N/A	28	28
WIND-ICE	→	→	→	744.6
TOTAL VERTICAL	1652.9	135.5	260.3	$\boxed{2048.5\text{ lb}}$

*(VERTICAL ONLY)

CASE 3: 0.9DEAD + DEAD-ICE + WIND-ICE

	MESH (lb)	POST (lb)	CAP RAIL (lb)	TOTAL (lb)
DEAD	35.8	101.6	78.9	216.3
DEAD-ICE	855.1	N/A	127.1	982.2
WIND-ICE	→	→	→	744.6
TOTAL VERTICAL	890.9	101.6	206	$\boxed{1198.5\text{ lb}}$

*(VERTICAL ONLY)

CASE 4: 1.2 DEAD + DEAD-ICE

	MESH (lb)	POST (lb)	CAP RAIL (lb)	TOTAL (lb)
DEAD	47.8	135.5	105.2	288.5
DEAD-ICE	855.1	N/A	127.1	982.2
TOTAL	902.9	135.5	232.3	$\boxed{1270.7\text{ lb}}$

WORST CASE LOADING FOR LATERAL & VERTICAL: CASE 2

Figure A-17. Design Loads: LRFD Load Combinations Including Ice Effects

A.7. LRFD Static Load Analysis

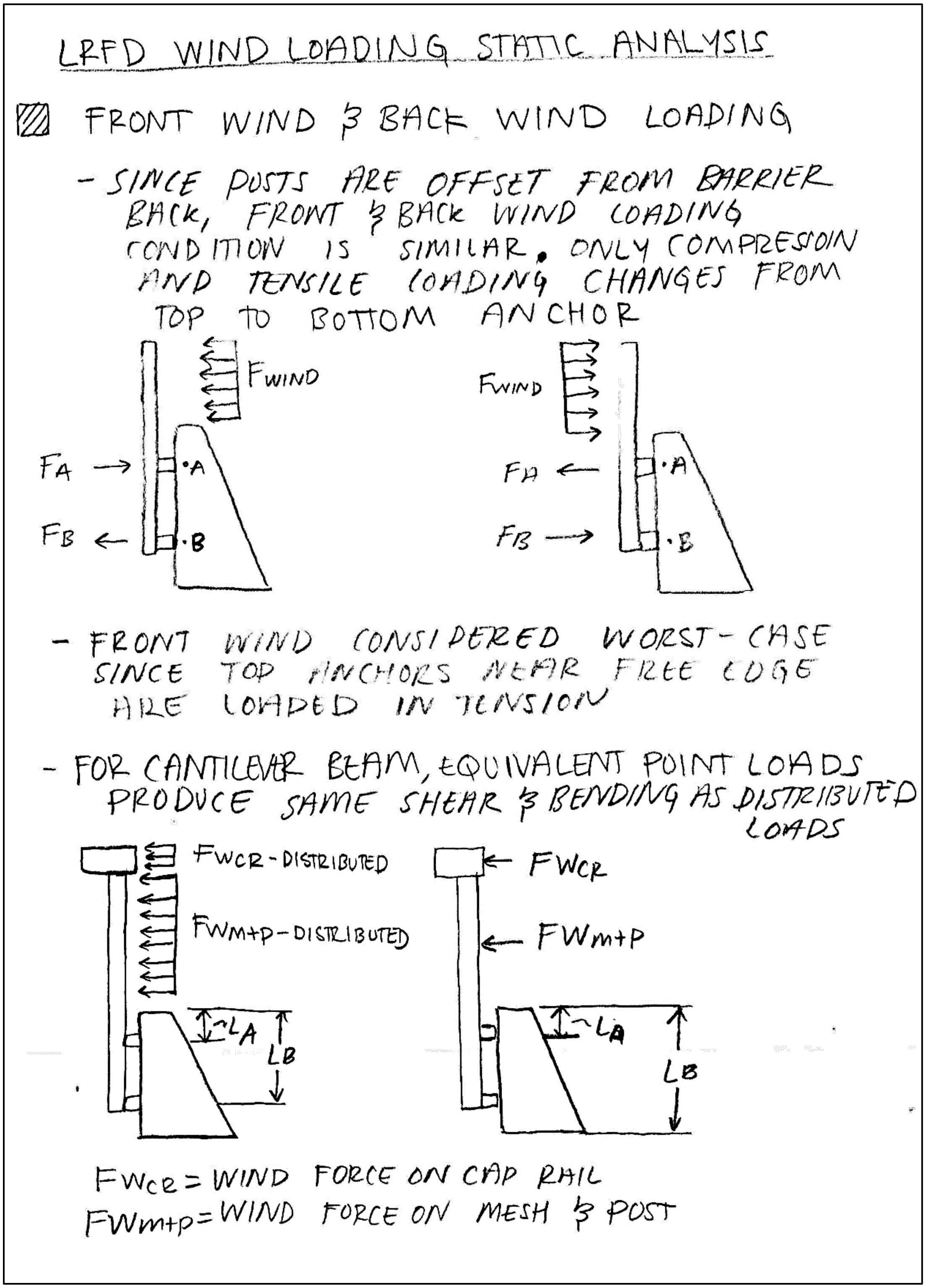

Figure A-18. Static Load Analysis: Wind Loading

LRFD WIND LOADING STATIC ANALYSIS

FRONT WIND LOADING (CONT.)

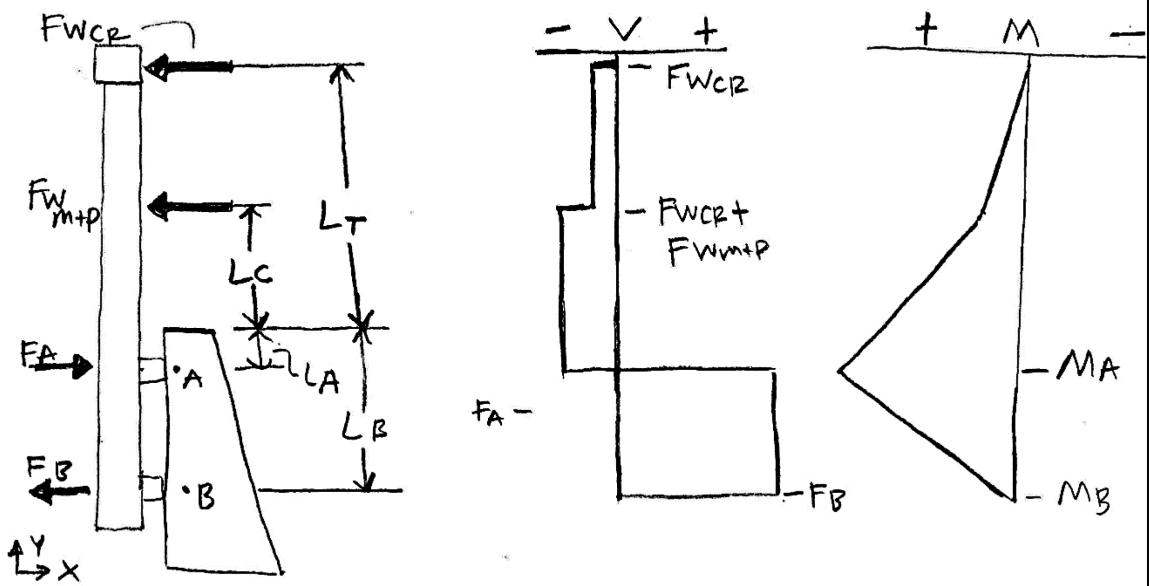

• $\sum M_B = 0 \quad +\circlearrowleft$

$$FW_{CR}(L_T + L_B) + FW_{m+p}(L_C + L_B) - F_A(L_B - L_A)$$

$$F_A = \frac{FW_{CR}(L_T + L_B) + FW_{m+p}(L_C + L_B)}{(L_B - L_A)} \qquad \text{(EQ W1)}$$

• $\sum F_X = 0$

$$F_B = F_A - FW_{CR} - FW_{m+p} \qquad \text{(EQ W2)}$$

• $M_A = F_B(L_B - L_A) \qquad \text{(EQ W3)}$

Figure A-19. Static Load Analysis: Wind Loading, Shear and Bending Moment Diagrams

LRFD WIND LOADING STATIC ANALYSIS

FRONT WIND LOADING (CONT.)

- USING THE FOLLOWING PARAMETERS:

VARIABLE	VALUE	DEFINITION
FW_{CR}	212.9 lb	WIND FORCE ON CAP RAIL
FW_{M+P}	391.7 lb	WIND FORCE ON MESH & POST
LA	10 in.	BARRIER TOP-TO-TOP ANCHOR DISTANCE
LB	27.5 in.	BARRIER TOP-TO-BOTTOM ANCHOR DISTANCE
LC	40.5 in.	BARRIER TOP-TO-MESH CENTER DISTANCE
LT	84 in.	BARRIER TOP-TO-CAP RAIL DISTANCE

- USING EQ W1:

$$F_A = \frac{212.9\text{ lb}\,(84+27.5)\text{in.} + 391.7\text{ lb}\,(40.5+27.5)\text{in.}}{(27.5-10)\text{in.}}$$

$F_A = 2878.5$ lb $\boxed{F_A = 2.88 \text{ kips}}$

- USING EQ W2:

$F_B = 2878.5\text{ lb} - 212.9\text{ lb} - 391.7\text{ lb} = 2273.9\text{ lb}$

$\boxed{F_B = 2.27 \text{ kips}}$

- NOW WITH EQ W3:

$M_A = 2273.9\text{ lb}\,(27.5-10)\text{in} = 39793.3\text{ lb-in.}$

$\boxed{M_A = 39.79 \text{ kip-in.}}$

CRITICAL LOAD DEMAND:

ANCHORAGE = 2.88 kips

VERTICAL POST = 39.79 kip-in.

Figure A-20. Static Load Analysis: Wind Loading (Continued)

LRFD WIND ON ICE LOADING STATIC ANALYSIS

- SIMILAR TO BASIC WIND LOADING, FRONT & BACK WIND ON ICE LOADING ARE ALIKE, WITH ONLY COMPRESSION & TENSILE LOADING CHANGING FROM BOTTOM TO TOP ANCHORAGE
- ADDITIONALLY, DISTRIBUTED WIND ON ICE LOAD CAN BE SIMPLIFIED TO EQUIVALENT POINT LOAD.

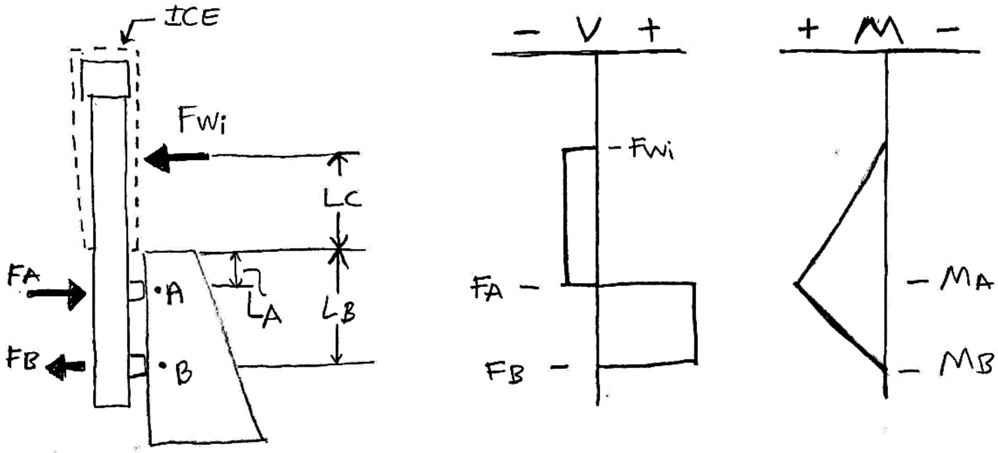

- $\Sigma M_B = 0$ ↺+

$$F_{W_i}(L_C+L_B) - F_A(L_B-L_C) = 0$$

$$F_A = \frac{F_{W_i}(L_C+L_B)}{(L_B-L_C)} \qquad \text{(EQ W4)}$$

- $\Sigma F_X = 0$

$$F_B = F_A - F_{W_i} \qquad \text{(EQ W5)}$$

- $$M_A = F_{W_i}(L_C+L_A) \qquad \text{(EQW6)}$$

Figure A-21. Static Load Analysis: Wind on Ice Loading

LRFD WIND ON ICE LOADING STATIC ANALYSIS

– USING THE FOLLOWING PARAMETERS:

VARIABLE	VALUE	DEFINITION
F_{Wi}	744.6 lb	WIND FORCE ON ICE-COVERED FENCE
L_A	10 in.	BARRIER TOP-TO-TOP ANCHORAGE DISTANCE
L_B	27.5 in.	BARRIER TOP-TO-BOTTOM ANCHORAGE DISTANCE
L_C	44 in.	BARRIER TOP-TO-ICE-COVERED FENCE CENTER

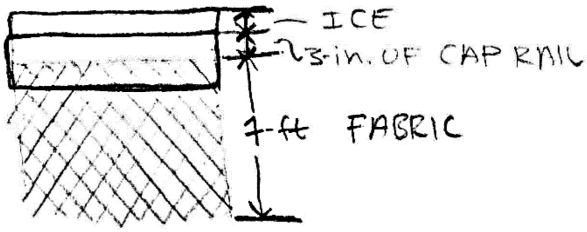

TOTAL HEIGH ≈ 88 in.

CENTER OF ICE-COVERED FENCE ≈ 44 in.

– USING EQ W4:

$$F_A = \frac{744.6\ lb\ (44 + 27.5)\ in.}{(27.5 - 10)\ in.} = 3042.2\ lb$$

$$\boxed{F_A = 3.04\ kips}$$

– WITH EQ W5:

$$F_B = 3042.2\ lb - 744.6\ lb = 2297.6\ lb$$

– USING EQ W6:

$$M_A = 744.6\ lb\ (44 + 10)\ in. = 40208.4\ lb\text{-}in.$$

$$\boxed{M_A = 40.21\ kip\text{-}in.}$$

CRITICAL LOAD DEMAND:

TENSILE FORCE ON TOP ANCHORAG = 3.04 kips

MOMENT ON VERTICAL POST = 40.21 kip-in.

Figure A-22. Static Load Analysis: Wind on Ice Loading (Continued)

Appendix B. Vertical Post Design

B.1. Design of Members for Flexure, Shear Compression and Combined Forces

VERTICAL POST DESIGN

SELECTED POST SIZE

HSS 2.875 X 0.188 – ASTM A1085 (F_y = 50 ksi)

t_d	AREA	D/t	I	S	Z
0.174 in.	1.48 in.^{2}	16.5	1.35 in.^{4}	0.941 in.^{3}	1.27 in.^{2}

DESIGN FOR FLEXURE

– SECTION CLASSIFICATION FOR LOCAL BUCKLING: TABLE B4.1b,20

$\lambda_p = 0.07 \dfrac{E}{F_y} = 40.6$, $D/t = 16.5$

$E = 29{,}000$ ksi
$F_y = 50$ ksi

$40.6 > 16.5$ $\quad \lambda_p > D/t \rightarrow \boxed{\text{COMPACT}}$

$\phi M_n = \phi F_y Z$ (AISC F8-1)

$F_y = 50$ ksi
$Z = 1.27$ in.^{2}
$\phi = 0.9$

$\boxed{\phi M_n = 57.15 \text{ kip-in.}}$ //

DESIGN FLEXURAL LOAD: ICE LOADING:

$M_{ua} = 40.21$ kip-in.

$\phi M_n > M_{ua}$

Figure B-1. Vertical Post Design: Design for Flexure

VERTICAL POST DESIGN

☒ DESIGN FOR SHEAR

$\phi_v V_n = F_{cr} A_g / 2$ (AISC G5-1)

$A_g = 1.48 \text{ in.}^2$, GROSS AREA (HSS 2.875 X .0.188)
$\phi_v = 0.9$, SHEAR REDUCTION FACTOR

- F_{cr} ARE CALCULATED USING (G5-2) & (G6-2) AND SHOULD BE TAKEN AS LARGEST BUT SHOULD NOT EXCEED $0.6 F_y$
- $\phi_v V_n = 0.6 F_y A_g / 2$

$\boxed{\phi_v V_n = 19.98 \text{ kips}}$

- DESIGN SHEAR LOAD: SHEAR FORCE @ TOP ANCHORAGE DURING WIND ON ICE LOADING

$V_{ua} = 3.04$ kips

$\underline{\phi_v V_n > V_{ua}}$

☒ DESIGN FOR COMPRESSION

- SECTION CLASSIFICATION: TABLE B4.1a, 9

$\lambda_r = 0.11 \frac{E}{F_y} = 63.8$, $D/t = 16.5$

$E = 29{,}000$ ksi
$F_y = 50$ ksi

$\lambda_r > D/t \rightarrow \boxed{\text{NON-SLENDER}}$

Figure B-2. Vertical Post Design: Design for Shear and Compression

VERTICAL POST DESIGN

DESIGN FOR COMPRESSION (CONT.)

$\phi_n P_n = \phi_n F_{cr} A_g$ (AISC E3-1)

$A_g = 1.48 \text{ in.}^2$, GROSS AREA,
F_{cr} = CRITICAL STRESS DETERMINED BELOW:
$\phi_n = 0.9$

- DETERMINE $\frac{KL}{r} \gtrless 4.71\sqrt{\frac{E}{F_y}}$

K = 2.1, EFFECTIVE LENGTH FACTOR (TABLE C-A-7.1)
ROTATION FIXED, TRANSLATION FREE
L = 94 in., LATERALLY-UNBRACED LENGTH
(84-in. FENCE + 10-in. TO BOTTOM ANCHORAGE
r = 0.957 in., RADIUS OF GYRATION (HSS 2.875 X 0.188)

$\frac{KL}{r} = 206.27$, $4.71\sqrt{\frac{E}{F_y}} = 113.43$

$\frac{KL}{r} > 4.71\sqrt{\frac{E}{F_y}}$ → USE EQ E3-3

$F_{cr} = 0.877 F_e$ (AISC E3-3)

where:

$F_e = \frac{\pi^2 E}{\left(\frac{KL}{r}\right)^2}$ (AISC E3-4)

$F_e = 6.73$ ksi
$F_{cr} = 5.90$ ksi

Figure B-3. Vertical Post Design: Design for Compression (Continued)

VERTICAL POST DESIGN

DESIGN FOR COMPRESSION (CONT.)

$$\phi_n P_n = 0.9 \cdot 5.90\,ksi \cdot 1.48\,in.^2$$

$$\boxed{\phi_n P_n = 7.86\ kips}$$

- DESIGN VERTICAL LOAD: ICE LOADING
  LRFD LOAD COMBINATION H2,
  TOTAL VERTICAL LOAD

$$P_{ua} = 2.05\ kips$$

$$\underline{\phi_n P_n > P_{ua}}$$

DESIGN FOR COMBINED FORCES

$$\left(\frac{P_r}{P_c} + \frac{M_r}{M_c}\right) + \left(\frac{V_r}{V_c} + \frac{T_r}{T_c}\right)^2 \leq 1.0 \quad \text{(AISC H3-6)}$$

P_r = 2.05 kips, LRFD LOAD COMBINATIONS REQ. AXIAL STRENGTH
P_c = 7.86 kips, DESIGN COMPRESSION STRENGTH
M_r = 40.21 kip-in., LRFD LOAD COMBINATIONS REQ. FLEXURAL STRENGTH
M_c = 57.15 kip-in., DESIGN FLEXURAL STRENGTH
V_r = 3.04 kips, LRFD LOAD COMBINATIONS REQ. SHEAR STRENGTH
V_c = 19.98 kips, DESIGN SHEAR STRENGTH
T_r = 0 kip-in., ASSUME NO TORSION
T_c = ... ASSUME NO TORSION

$$\left(\frac{P_r}{P_c} + \frac{M_r}{M_c}\right) + \left(\frac{V_r}{V_c}\right)^2 = \boxed{0.988 < 1.0}$$

Figure B-4. Vertical Post Design: Design for Combined Forces

B.2. Approximate Second Order Analysis

VERTICAL POST DESIGN

APPROXIMATE SECOND-ORDER ANALYSIS
AISC APPENDIX 8

$$M_r = B_1 M_{nt} + B_2 M_{lt} \quad \text{(AISC A-8-1)}$$

M_r = REQ 2^{nd} ORDER FLEXURAL STRENGTH
B_1 = IGNORED, P-δ MULTIPLIER
M_{nt} = FIRST-ORDER MOMENT USING LRFD, LATERAL RESTRAINED
B_2 = P-Δ MULTIPLIER
M_{lt} = 40.21 kip-in., LRFD MOMENT DUE TO LATERAL TRANSLATION

- P-δ IGNORED SINCE FENCE WILL MOST LIKELY TRANSLATE LATERALLY. CAP RAIL WILL NOT CONTRIBUTE TO LATERAL RESTRAINT AND INSTEAD, FENCE WILL TRANSLATE LATERALLY ACROSS SEVERAL FENCE SECTIONS.

$$B_2 = \frac{1}{1 - \frac{\alpha P_{story}}{P_{e\,story}}} \geq 1 \quad \text{(AISC A-8-6)}$$

α = 1.0, LRFD DESIGN
P_{story} = 2.05 kips, VERTICAL LOAD SUPPORTED BY POST
$P_{e\,story}$ = ELASTIC CRITICAL BUCKLING STRENGTH

$$P_{e\,story} = R_M \frac{HL}{\Delta_H} \quad \text{(AISC A-8-7)}$$

R_M = 0.85, LOWER BOUND VAL. FOR MOMENT FRAMES (USER NOTE, PAGE 16.1-251)

H = 1 kip, TOTAL STORY SHEAR, PRODUCED BY LATERAL FORCES USED TO COMPUTE Δ_H

Figure B-5. Vertical Post Design: Approximate Second Order Analysis

VERTICAL POST DESIGN

APPROXIMATE SECOND-ORDER ANALYSIS CONT.

$$\Delta H = \frac{HL^3}{3EI(0.8)}$$

(MECHANICAL ENGINEERING DESIG, 10TH EDITION, SHIGLEY'S TABLE A-9 CASE 1)

H = 1 Kip,
L = 94 in., 7 ft TALL FENCE ANCHORED 10 in. BELOW BARRIER TOP
E = 29,000 ksi, STEEL MODULUS OF ELASTICITY
I = 1.35 in.^{4}, HSS 2.875X0.188 ROUND TUE

*NOTE: STIFFNESS REDUCTION (EI0.8) DONE IN ACCORDANCE WITH AISC SECTION C 2.3

$$\boxed{\Delta H = 8.84 \text{ in.}}$$

$$P_{e\ STORY} = (0.85)\frac{1 \text{ kip} \cdot 94 \text{ in.}}{8.84 \text{ in.}} = \boxed{9.04 \text{ kips}}$$

$$B_2 = \frac{1}{1 - \frac{\alpha P_{STORY}}{P_{e\ STORY}}} = \frac{1}{1 - \frac{2.05 \text{ kips}}{9.04 \text{ kips}}} = \boxed{1.293 = B_2}$$

$$M_r = \cancel{B_1 M_{nt}} + B_2 M_{lt} = 1.293(40.20 \text{ kip-in.})$$

$$\boxed{M_r = 51.98 \text{ kip-in.}}$$

– REQUIRED FLEXURAL STRENGTH FOR ICE LOADING

51.98 kip-in. < 57.15 kip-in.
(DEMAND) (CAPACITY)

Figure B-6. Vertical Post Design: Approximate Second Order Analysis (Continued)

B.3. Second Order Effects Using Deflection Method

VERTICAL POST DESIGN

SECOND ORDER ANALYSIS: WIND LOADING

- ANALYSIS CONDUCTED ON WORST-CASE BASIC LOAD COMBINATIONS: CASE 4
- APPROACH: DETERMINE DEFLECTION @ FENCE VERTICAL C.G. & MULTIPLY IT BY THE VERTICAL LOAD TO IDENTIFY SECONDARY MOMENT
- DEFLECTION @ VERTICAL C.G. DETERMINED BY SUPERPOSITION OF DEFLECTIONS CAUSED BY MESH, VERTICAL POSTS & CAP RAIL

- VERTICAL C.G. DETERMINATION

- TOTAL VERTICAL LOAD & LOCATION PER PART (FROM LRFD LOAD COMBINATION NO. 4)

PART	TOTAL LOAD	VERTICAL LOCATION
MESH	797.8 lb	52 in.
POST	97.9 lb	52 in.
CAP RAIL	170.8 lb	94 in. (CONSERVATIVE)

$$\bar{Y} = \frac{W_{CR} \cdot Y_{CR} + (W_m + W_P) \cdot Y_m}{W_{CR} + W_m + W_P}$$

$$\boxed{\bar{Y} = 58.73 \text{ in.}}$$

*NOTE: SPLICE RAIL WEIGHT COMBINED WITH CAP RAIL WEIGHT

Figure B-7. Vertical Post Design: Second Order Analysis

VERTICAL POST DESIGN

SECOND ORDER ANALYSIS: WIND LOADING CONT.

- DEFLECTION FROM WIND LOAD ON CAP RAIL

$$Y = \frac{Fx^2}{6EI(0.8)}(x - 3L) \quad \left(\begin{array}{c}\text{SHIGLEY'S TABLE A-9} \\ \text{CASE 1}\end{array}\right)$$

Y = LATERAL DEFLECTION
X = 58.73 in., LOCATION WHERE Y IS DETERMINED
E = 29X10^6 Psi, STEEL MODULUS OF ELASTICITY
I = 1.35 in.^4, HSS 2.875X0.188 ROUND TUBE
F = 212.9 lb, WIND LOAD ON CAP RAIL (LRFD CASE 4)
L = 94 in., HEIGHT OF CANTILEVER BEAM

$\boxed{Y = 0.872 \text{ in.}}$ DEFLECTION FROM CAP RAIL WIND LOAD

- DEFLECTION FROM WIND LOAD ON MESH & POST

$$Y = \frac{Fa^2}{6EI(0.8)}(a - 3x) \quad \left(\begin{array}{c}\text{SHIGLEY'S TABLE A-9} \\ \text{CASE 2}\end{array}\right)$$

a = 52 in., LOCATION OF WIND FORCE
F = 391.7 lb, WIND LOAD ON MESH & ON POST

$\boxed{Y = 0.700 \text{ in.}}$

SECONDARY MOMENT = (1.572 in.)(1066.5 lb) = 1676.5 lb-in.

$\boxed{M_r = 41.40 \text{ kip-in}}$

41.40 kip-in. < 57.15 kip-in.
(DEMAND) (CAPACITY)

Figure B-8. Vertical Post Design: Second Order Analysis (Continued)

VERTICAL POST DESIGN

SECOND ORDER ANALYSIS: WIND ON ICE LOADING

- VERTICAL C.G. DETERMINATION

– TOTAL VERTICAL LOAD PER PART & LOCATION
(FROM LRFD ICE COMBINATION NO. 2)

PART	TOTAL LOAD	VERTICAL LOCATION
MESH	1652.9 lb	52 in.
POST	97.9 lb	52 in.
CAP RAIL	297.7 lb	94 in.

* NOTE: CAP RAIL DEAD LOAD COMBINED WITH SPLICE RAIL DEAD LOAD

$$\bar{y} = \frac{W_{CR} \cdot Y_{CR} + (W_m + W_P)\, Y_m}{W_{CR} + Y_{CR} + W_P} = 58.54 \text{ in.}$$

- DEFLECTION

$$y = \frac{Fa^2}{6EI(0.8)}(a - 3x) \quad \left(\text{SHIGLEY'S TABLE A-9 CASE 2}\right)$$

F = 744.5 lb, WIND ON ICE LOAD
a = 54 in., LOCATION OF WIND ON ICE LOAD
x = 58.54 in, LOCATION WHERE Y IS DETERMINED

$\boxed{Y = 1.405 \text{ in.}}$ SECONDARY MOMENT = 2878.1 lb-in.

M_r = 40.21 kip-in. + 2.88 kip-in = $\boxed{43.09 \text{ kip-in.}}$ //

43.09 kip-in. < 57.15 kip-in.
(DEMAND) (CAPACITY)

Figure B-9. Vertical Post Design: Second order Analysis (Continued)

Appendix C. Design Impact Loading

DESIGN IMPACT LOADING

DESIGN METHODOLOGY

- DETERMINE "IMPACT" LOAD THAT CAUSES POST TO FAIL IN BENDING
  - USE THIS "IMPACT" LOAD TO DETERMINE POST BRACKET & ANCHORAGE DEMAND

ASSUMPTIONS

- IMPACT FORCE APPLIED **3 in.** ABOVE BARRIER TOP
  - FORCE CONCENTRATIONS BELOW THIS VALUE ARE NOT EXPECTED
- POST WILL HINGE AT THE TOP SURFACE OF THE POST BRACKET, **7.5 in.** BELOW BARRIER TOP
- TOP & BOTTOM ANCHORS LOCATED 10 in. & 27 1/2 in. BELOW BARRIER TOP SURFACE

SCHEMATIC:

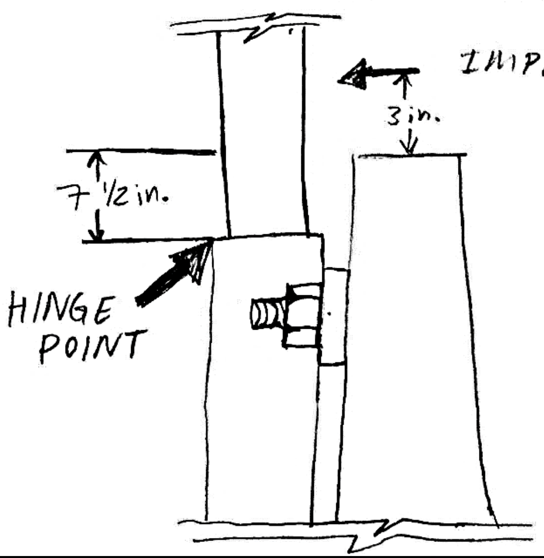

Figure C-1. Design Impact Loading: Methodology and Assumptions

DESIGN IMPACT LOADING

LATERAL IMPACT FORCE

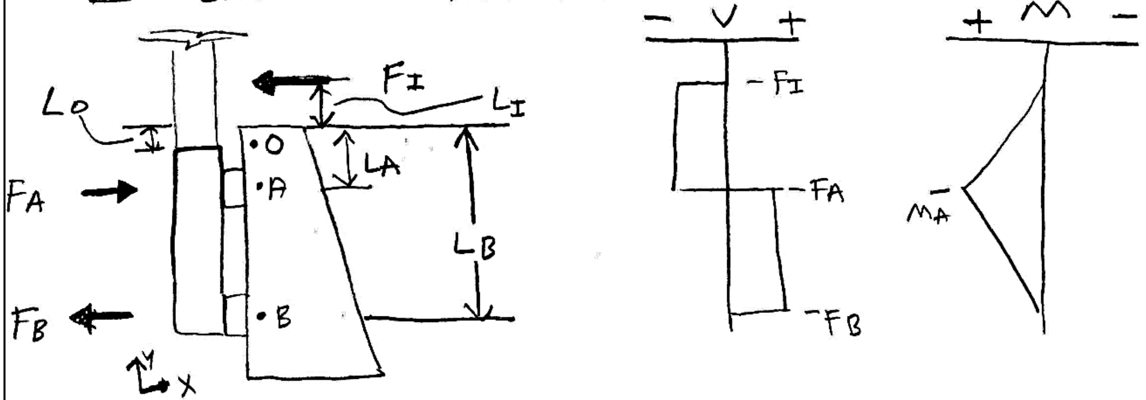

• IMPACT FORCE ESTIMATION

$$F_I = M_o / (L_I + L_o)$$

M_o = POST CAPACITY
$L_I = 3 \text{ in.}$
$L_o = 7.5 \text{ in.}$

– FOR PIPE 2 1/2 SCH 80 ASTM A53 GR. B:
$Z = 1.77 \text{ in.}^3$
$F_y = 35 \text{ ksi}$

– 20 ksi ADDED TO SPECIFIED F_y TO ACCOUNT FOR STRENGTH VARIATIONS FROM MANUFACTURING PROCESS.

$$M_o = F_y Z = 55 \text{ ksi} + 1.77 \text{ in.}^3 = 97.35 \text{ kip-in.}$$

$$F_I = 97.35 \text{ kip-in.} / (3 + 7.5 \text{ in.})$$

$$\boxed{F_I = 9.27 \text{ kips}}$$

Figure C-2. Design Impact Loading: Impact force Derivation

DESIGN IMPACT LOADING

LATERAL IMPACT LOAD CONT.
- FROM SCHEMATIC

- $\Sigma M_B = 0 +\circlearrowright$

$$F_I(L_I + L_B) - F_A(L_B - L_A)$$

$$F_A = \frac{F_I(L_I + L_B)}{(L_B - L_A)} \qquad \text{(EQ I1)}$$

- $\Sigma F_X = 0$

$$F_B = F_A - F_I \qquad \text{(EQ I2)}$$

- USING THE FOLLOWING PARAMETERS

VARIABLES	VALUE	DEFINITION
F_I	9.27 kips	ESTIMATED IMPACT FORCE
L_I	3 in.	IMPACT FORCE-TO-BARRIER TOP DISTANCE
L_A	10 in.	BARRIER TOP-TO-TOP ANCHOR DISTANCE
L_B	27.5 in	BARRIER TOP-TO-BOTTOM ANCHOR DISTANCE

USING EQ I1:

$$F_A = 9.27 \text{ kips} (3+27.5)\text{in.} / (27.5-10)\text{in}$$

$$\boxed{F_A = 16.16 \text{ kips}}$$

USING EQ I2: $\boxed{F_B = 6.89 \text{ kips}}$

ANCHOR TENSILE DEMAND: 16.16 KIPS

LONGITUDINAL IMPACT LOAD:
- POST IS ROUND & THEREFORE OMNIDIRECTIONAL

ANCHOR SHEAR DEMAND: 16.16 kips

Figure C-3. Design Impact Loading: Critical Load Determination

Appendix D. Concrete Anchorage Design

ANCHORAGE DESIGN

DESIGN LOADS

- LONGITUDINAL IMPACT LOAD + VERTICAL FORCE = SHEAR
- LATERAL IMPACT LOAD = TENSILE LOAD

• SHEAR DEMAND (F_s)

$$F_s = \sqrt{\left(\frac{F_a}{2}\right)^2 + \left(\frac{F_v}{4}\right)^2}$$

F_a = 16.16 kips, LONG. IMPACT FORCE ON TOP ANCHORS
F_v = 2.10 kips, LRFD MAXIMUM VERTICAL LOAD
(INCLUDES POST BRACKET DEAD LOAD)

$\boxed{F_s = 8.10 \text{ kips}}$

• TENSILE DEMAND (F_T) FROM ECCENTRICITY

ASSUMPTIONS:
- ANCHORS WILL ACT AS "RIGID" (NO ROTATION)
- ANCHOR LONG. SPACING OF 15 in.
- POST BRACKET WILL HAVE 2-in. SLOTS

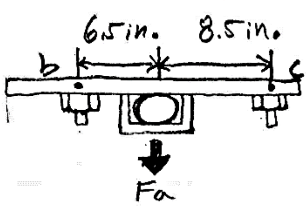

$\Sigma M_c = 0$

$F_b(15\text{in.}) - F_a(8.5\text{in.}) = 0$

$\boxed{F_b = 9.16 \text{ kips}}$

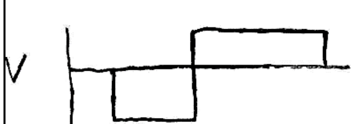

$F_c = F_b - F_c$ $\boxed{F_c = 7 \text{ kips}}$

$\boxed{F_T = 9.16 \text{ kips}}$

Figure D-1. Anchorage Design: Design Loads

D.1. Tensile Loading

ANCHORAGE DESIGN

TENSILE LOADING: STEEL STRENGTH

$\phi N_{sa} = \phi A_{se,N} f_{uta}$ (ACI 318-14 EQ 17.4.1.2)

$A_{se,N} = 0.462 \text{ in}^2$, 7/8 in. DIAMETER UNC BOLT
$f_{uta} = 125$ ksi, ASTM A193 GRADE B7
$\phi = 0.75$, REDUCTION FACTOR FOR DUCTILE STEEL IN TENSILE LOADING

$\boxed{\phi N_{sa} = 43.31 \text{ kips}}$

TENSILE LOADING: CONCRETE BREAKOUT STRENGHT

$\phi N_{cb} = \phi \frac{A_{Nc}}{A_{Nco}} \psi_{ed,N} \psi_{c,N} \psi_{cp,N} N_b$ (ACI 17.4.2.1)

N_b = BASIC CONCRETE BREAKOUT STRENGTH IN TENSION
A_{Nc} = PROJECTED CONCRETE FAILURE AREA
A_{Nco} = PROJECTED CONCRETE FAILURE AREA OF SINGLE ANCHOR
$\psi_{ed,N} = 1.0$, SINCE $C_{a,min} \geq 1.5 h_{ef}$
$\psi_{cp,N} = 1.0$, SINCE SUPPLEMENTARY REINFORCEMENT TO CONTROL SPLITTING IS PRESENT (SECTION R 17.4.2.7)
$\psi_{c,N} = 1.4$, FOR POST-INSTALLED ANCHORS (SECTION 17.4.2.6)
$\phi = 0.55$, FROM SECTION 17.3.3, CATEGORY 2, CONDITION B

- REDUCTION FACTOR SELECTED FOR MEDIUM SENSITIVITY TO INSTALLATION & MEDIUM RELIABILITY

- CONDITION B, NO SUPPLEMENTARY RIENFORCEMENT SELECTED SINCE RIENFORCEMENTS SHOULD GENERALLY CONFORM TO FIGURE R17.4.2.9

  - NO REINFORCEMENTS ARE PRESENT THAT RUN PARALLEL TO ANCHORS

Figure D-2. Anchorage Design: Tensile Loading, Steel Strength and Concrete Breakout

ANCHORAGE DESIGN

TENSILE LOADING: CONCRETE BREAKOUT STRENGTH CONT.

$A_{Nco} = 9\, h_{ef}^2$ (17.4.2.1c)

$h_{ef} = 6$ in., ANCHOR EMBEDMENT

$\boxed{A_{Nco} = 324 \text{ in.}^2}$

$A_{Nc} = (S/2 + 1.5 h_{ef})(3 h_{ef})$

S = 15 in., ANCHOR LONGITUDINAL SPACING

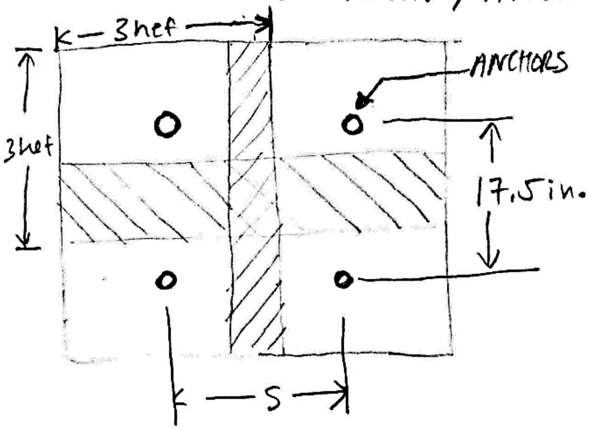

- BOTTOM ANCHORS IN COMPRESSION, SO VERTICAL OVERLAP NEGLECTED
- A_{Nc} TAKEN AS AREA OF ONE ANCHOR ACCOUNTING FOR GROUP ACTION

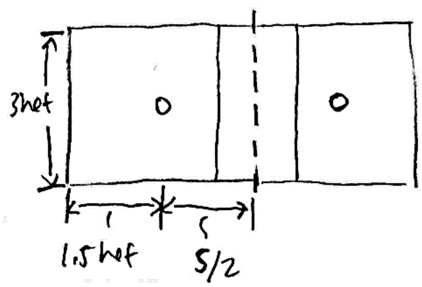

$A_{Nc} = \left(\frac{15 \text{ in.}}{2} + 1.5(6 \text{ in.})\right)(3(6 \text{ in.}))$

$A_{Nc} = 297 \text{ in.}^2$

$\frac{A_{Nc}}{A_{Nco}} = \frac{297}{324} = 0.917$

$\boxed{\frac{A_{Nc}}{A_{Nco}} = 0.917}$

Figure D-3. Anchorage Design: Tensile Loading, Breakout Strength (Continued)

ANCHOR DESIGN

☒ TENSILE LOADING: BREAKOUT STRENGTH CONT.

$N_b = k_c \lambda_a \sqrt{f'_c}\, h_{ef}^{1.5}$ (ACI 17.4.2.2a)

$k_c = 17$, FOR POST INSTALLED ANCHORS
$\lambda_a = 1$, NORMAL WEIGHT CONCRETE (TABLE 19.2.4.2 ACI)
$f'_c = 5000\,psi$, CONCRETE STRENGTH (4CBR-1 BRIDGERAIL)
$h_{ef} = 6\,in.$, ANCHOR EMBEDMENT

$N_b = 17666.9\,lb$ $\boxed{N_b = 17.67\ kips}$

$\phi N_{cb} = 0.55\left(\frac{297}{324}\right)(1.0)(1.4)(1.0)(17.67\ kips)$

$\boxed{\phi N_{cb} = 12.47\ kips}$

9.16 kips < 12.47 kips
(DEMAND) (CAPACITY)

☒ TENSILE LOADING: BOND STRENGHT

$\phi N_a = \phi \frac{A_{Na}}{A_{Nao}} \Psi_{ed,Na} \Psi_{cp,Na} N_{ba}$ (ACI 17.4.5.1a)

A_{Nao} = PROJECTED INFLUENCE AREA OF SINGLE ANCHOR
A_{Na} = PROJ. INFLUENCE AREA OF ANCHOR IN GROUP ACTION
$\Psi_{ed,Na} = 0.968$, EDGE EFFECT FACTOR
$\Psi_{cp,Na} = 1.0$, SUPPLEMENTARY RIENFORCEMENT TO CONTROL SPLITTING

$A_{Nao} = (2 C_{Na})^2$ (ACI 17.4.5.1c)

$C_{Na} = 10\, d_a \sqrt{\frac{\tau_{uncr}}{1100}}$ (ACI 17.4.5.1d)

Figure D-4. Anchorage Design: Tensile Loading, Breakout Strength (Continued) and Bond Strength

ANCHOR DESIGN

VII TENSILE LOADING: BOND STRENGTH CONT.

$d_a = 7/8$ in., ANCHOR DIAMETER
$\tau_{uncr} = 1800$ psi, CHARACTERISTIC BOND STRESS OF EPOXY IN UNCRACKED CONCRETE

$\boxed{C_{Na} = 11.19 \text{ in.}}$

$\boxed{A_{Na0} = 501.14 \text{ in.}^2}$

$A_{Na} = (S/2 + C_{Na})(C_{Na} + C_a)$
- $C_a = 10$in., DISTANCE FROM ANCHOR TO BARRIER TOP
- DERIVED FROM ACI FIGURE R 17.4.5.1
- BOTTOM ANCHORS IN COMPRESSION AND THEREFORE GROUP ACTION BETWEEN TOP & BOTTOM ANCHORS WAS NEGLECTED

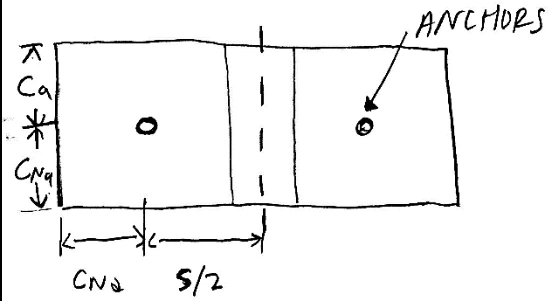

$\boxed{A_{Na} = 396.04 \text{ in.}^2}$

$$\psi_{ed,Na} = 0.7 + 0.3\,\frac{C_{a,min}}{C_{Na}}$$

$C_{a,min} = 10$in., DISTANCE FROM TOP ANCHOR TO BARRIER TOP
$C_{Na} = 11.19$in., FROM ABOVE

$\psi_{ed,Na} = 0.968$

Figure D-5. Anchorage Design: Tensile Loading, Bond Strength (Continued)

ANCHOR DESIGN

TENSILE LOADING: BOND STRENGTH CONT.

$N_{ba} = \lambda_a \tau_{uncr} \pi d_a h_{ef}$ (ACI 17.4.5.2)

$\lambda_a = 1$, NORMAL WEIGHT CONCRETE
$\tau_{uncr} = 1800psi$, EPOXY BOND STRESS, UNCRACKED CONCRETE
$d_a = 7/8 in.$, ANCHOR DIAMETER
$h_{ef} = 6 in.$, ANCHOR EMBEDMENT

$N_{ba} = 29688.05 \text{ lb} = \boxed{29.69 \text{ kips}}$

$\phi N_a = 0.55 \left(\frac{396.04}{501.14} \right) (0.968)(1.0)(29.69 \text{ kips})$

$\boxed{\phi N_a = 12.49 \text{ kips}}$

9.16 kips < 12.49 kips
(DEMAND) (CAPACITY)

Figure D-6. Anchorage Design: Tensile Loading, Bond Strength (Continued)

D.2. Shear Loading

ANCHOR DESIGN

SHEAR LOADING: STEEL STRENGTH

$\phi V_{sa} = 0.6 A_{se,V} f_{uta}$ (ACI 17.5.1.2 b)

$A_{se,V} = 0.462$ in.^{2} , 7/8 in. DIAMETER BOLT
$f_{uta} = 125$ ksi, ASTM A193 B7
$\phi = 0.65$; REDUCTION FACTOR FOR DUCTILE STEEL IN SHEAR

$\boxed{\phi V_{sa} = 22.52 \text{ Kips}}$

SHEAR LOADING: CONCRETE BREAKOUT STRENGTH

$\phi V_{cb} = \phi \frac{A_{vc}}{A_{vco}} \psi_{ed,V} \psi_{cV} \psi_{h,V} V_b (2)$ (ACI 17.5.2.1a)

A_{vc_o} = PROJECTED AREA OF SINGLE ANCHOR
A_{vc} = PROJECTED AREA OF FAILURE OF ANCHOR IN GROUP ACTION
$\psi_{ed,V} = 1.0$, EDGE EFFECT FACTOR NEGLECTED
$\psi_{cV} = 1.4$, NO CRACKING AT SERVICE LOADS
$\psi_{h,V} = 1.37$, MODIFICATION WHEN $h_a < 1.5 C_{a1}$
V_b = BASIC CONCRETE BREAKOUT STRENGTH
$\phi = 0.55$, SECTION 17.3.3, CATEGORY 2, CONDITION B
*NOTE: V_{cb} DOUBLED WHEN LOAD PARALLEL TO BARRIER EDGE

$A_{vco} = 4.5 (C_{a1})^2$ (ACI 17.5.2.1c)

$C_{a1} = 10$ in., DISTANCE FROM TOP ANCHORS TO BARRIER TOP

$\boxed{A_{vco} = 450.0 \text{ in.}^2}$

$A_{vc} = [2(1.5 C_{a1}) + s] h_a$ (ACI FIG. R17.5.2.1b)

$h_a = 8.5$ in., BARRIER THICKNESS @ ANCHOR

$\boxed{A_{vc} = 382.5 \text{in.}^2}$

*NOTE: A_{vc} FOR BOTH TOP ANCHORS

Figure D-7. Anchorage Design: Shear Loading, Steel and Concrete Breakout Strength

ANCHOR DESIGN

SHEAR LOADING: CONCRETE BREAKOUT STRENGTH

- BASIC CONCRETE BREAKOUT STREGTH DETERMINED FROM THE LOWEST VALUE OBTAINED FROM FOLLOWING EQUATIONS:

$$V_b = \left[7\left(\frac{l_e}{d_a}\right)^{0.2}\sqrt{d_a}\right]\lambda_a\sqrt{f'_c}\,(C_{a1})^{1.5} \quad \text{(ACI 17.5.2.2a)}$$

$l_e = h_{ef} = 6$ in., FOR POST INSTALLED ANCHORS
$d_a = 7/8$ in., ANCHOR DIAMETER
$\lambda_a = 1.0$, NORMAL WEIGHT CONCRETE
$f'_c = 5000$ psi, CONCRETE STRENGTH
$C_{a1} = 10$ in., DISTANCE FROM ANCHOR TO EDGE

$V_b = 21518.68$ lb $\quad \boxed{V_b = 21.52 \text{ kips}}$

$$V_b = 9\lambda_a\sqrt{f'_c}\,(C_{a1})^{1.5} \quad \text{(ACI 17.5.2.2b)}$$

$V_b = 20124.61 \quad \boxed{V_b = 20.12 \text{ kips}}$ ←

$$\Psi_{h,V} = \sqrt{\frac{1.5C_{a1}}{h_a}} \quad \text{(ACI 17.5.2.8)}$$

$$\boxed{\Psi_{h,V} = 1.33}$$

$$\phi V_{cb} = 0.55\left(\frac{382.5}{450}\right)(1)(1.4)(1.33)(20.12\text{kips})(2)$$

$$\boxed{\phi V_{cb} = 35.03 \text{ kips}}$$

16.19 kips < 35.03 kips
(DEMAND) (CAPACITY)

Figure D-8. Anchorage Design: Shear Loading, Concrete Breakout Strength (Continued)

ANCHOR DESIGN

SHEAR LOADING: CONCRETE PRYOUT STRENGTH

$V_{cp} = K_{cp} N_{cp}$ (ACI 17.5.3.1a)

$K_{cp} = 2.0$, SINCE $h_{ef} \geq 2.5$ in.
$N_{cp} = 12.47$ kips, LOWER OF BOND & BREAKOUT

$\boxed{V_{cp} = 24.94 \text{ kips}}$ //

COMBINED LOADING REQUIREMENT

MODE	TENSION (kips) STEEL	BREAKOUT	BOND	SHEAR (kips) STEEL	BREAKOUT	PRYOUT
DEMAND	9.16	9.16	9.16	8.10	16.19	8.10
CAPACITY	43.31	12.47	12.49	22.52	35.03	24.94
RATIO	0.211	0.735	0.733	0.360	0.461	0.325

$$\frac{N_{ua}}{\phi N_n} + \frac{V_{ua}}{\phi V_n} \leq 1.2$$ (ACI 17.6.3)

$N_{ua} = 9.16$ kips, TENSILE DEMAND
$\phi N_n = 12.47$ kips, GOVERNING STRENGTH - TENSILE
$V_{ua} = 16.19$ kips, SHEAR DEMAND (TWO ANCHORS)
$\phi V_n = 35.03$ kips, GOVERNING STRENGTH - SHEAR (TWO ANCHORS)

$0.735 + 0.461 = 1.196$

$\boxed{1.196 < 1.2}$ //

Figure D-9. Anchorage Design: Shear Loading, Pryout Strength and Combined Loading

Appendix E. Post-to-Parapet Bracket Design

E.1. Design of Bolted and Welded Connections

POST BRACKET DESIGN

LOADING

- FROM DESIGN IMPACT LOADING:

TENSILE DEMAND: 16.16 kips
SHEAR DEMAND: 16.19 kips
- INCLUDES LRFD VERTICAL LOAD

DESIGN OF BOLTED CONNECTIONS

$\phi R_n = \phi 2.4\, d\, t\, F_u$ (AISC J3-6a)

ϕR_n = DESIGN BEARING STRENGTH, (kips)
d = 7/8 in., 7/8 UNC ANCHOR DIAMETER
t = 1/4 in., BRACKET THICKNESS
F_u = 65 ksi, ASTM A572 GRADE 50
ϕ = 0.75, RESISTANCE FACTOR (LRFD)

$\boxed{\phi R_n = 25.59 \text{ kips}}$

$\phi R_n = \phi 1.2\, l_c\, t\, F_u$ (AISC J3-6c)

ϕR_n = DESIGN TEAROUT STRENGTH, (kips)
l_c = 1.44 in., CLEAR DISTANCE
t = 1/4 in., BRACKET THICKNESS
F_u = 65 ksi, ASTM A572 GRADE 50
ϕ = 0.75, RESISTANCE FACTOR (LRFD)

$\boxed{\phi R_n = 21.06 \text{ kips}}$

Figure E-1. Post Bracket Design: Bolted Connection Strength

POST BRACKET DESIGN

TENSILE FAILURE FROM LONGITUDINAL FORCE

- YIELDING

$\phi R_n = F_y A_g$, $\phi = 0.9$ (AISC J4-1)

- RUPTURE

$\phi R_n = F_u A_e$, $\phi = 0.75$ (AISC J4-2)

ϕR_n = DESIGN STRENGTH, (KIPS)
F_y = 50 ksi, ASTM A572 GRADE 50
F_u = 65 ksi, ASTM A572 GRADE 50
$A_g = W \cdot t$, GROSS AREA (in.^{2})
$A_e = (W - D) \cdot t$, NET AREA (in.^{2})
W = 4.25 in., WIDTH OF BRACKET @ BOLT LOCATION
t = 0.25 in., THICKNESS OF BRACKET
D = 1.125 in., DIAMETER OF SLOT FOR BOLT

YIELDING: $\phi R_n = \boxed{47.81 \text{ kips}}$

RUPTURE: $\boxed{\phi R_n = 38.09 \text{ kips}}$

- NOTE* = CALCULATIONS DO NOT INCLUDE AREA OF GUSSETS

DESIGN OF WELDED CONNECTIONS

- WELDS LOADED IN TENSION & IN SHEAR

- ASSUME WELD A & WELD B MUST DEVELOPE TENSILE & SHEAR DEMAND, VERY CONSERVATIVE

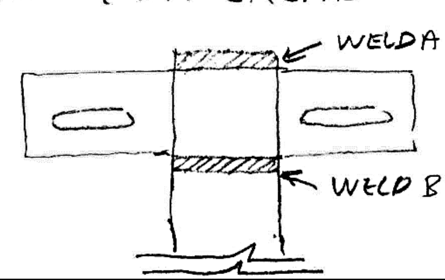

Figure E-2. Post Bracket Design: Bolted (Continued) and Welded Connection Strength

POST BRACKET DESIGN

DESIGN OF WELDED CONNECTIONS CONT.

$\phi R_n = \phi F_{nw} A_{we}$ (AISC J2-4)

$F_{nw} = 0.60 F_{EXX}(1.0 + 0.50 \sin^{1.5}\theta)$ (AISC J2-5)

ϕR_n = DESIGN WELD STRENGTH
$A_{we} = t_e \ell$, EFFECTIVE WELD AREA
$t_e = 0.707t$, EFFECTIVE THROAT THICKNESS
t = 0.25 in., WELD THICKNESS
ℓ = 3.5 in., WELD LENGTH
F_{EXX} = 60 ksi, WELD MATERIAL CLASSIFICATION STRENGTH
θ = ANGLE BETWEEN FORCE DIRECTION & WELD LONG. AXIS
ϕ = 0.75, RESISTANCE FACTOR

- TENSILE LOADING, $\theta = 90°$

F_{nw} = 54 ksi

ϕR_n = 25.06 kips

– TWO WELDS

$\boxed{\phi R_n = 50.1 \text{ kips}}$

- SHEAR LOADING, $\theta = 0°$

F_{nw} = 36 ksi

ϕR_n = 16.71 kips

– TWO WELDS

$\boxed{\phi R_n = 33.41 \text{ kips}}$

- OBLIQUE IMPACT LOADING, $\theta = 25°$

F_{nw} = 40.95 ksi

ϕR_n = 19.00 kips

– TWO WELDS

$\boxed{\phi R_n = 38 \text{ kips}}$

Figure E-3. Post Bracket Design: Welded Connection Strength (Continued)

E.2. Design of Members for Flexure

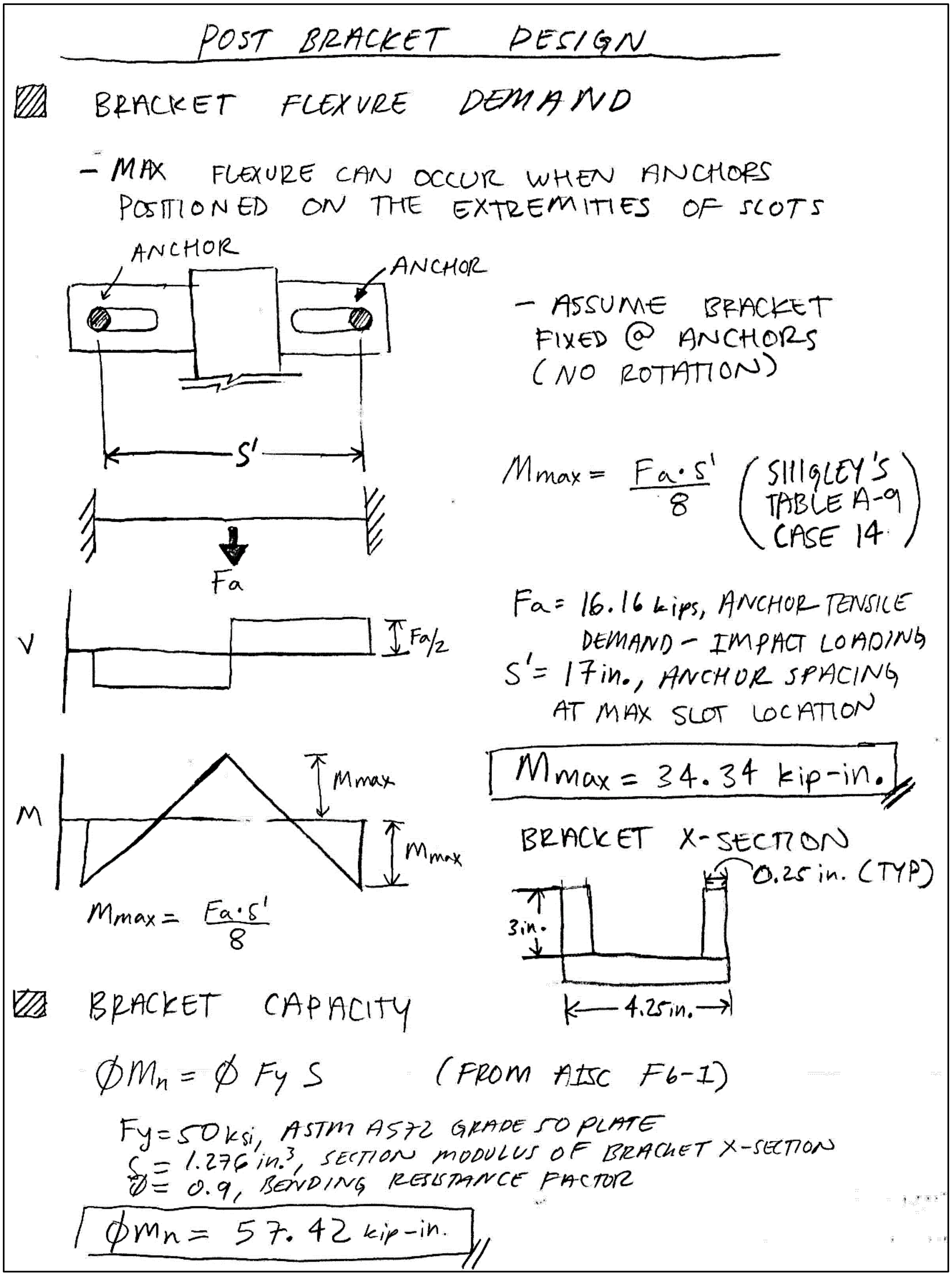

Figure E-4. Post Bracket Design: Flexure Design

POST BRACKET DESIGN

FLEXURE CAPACITY

- IF FLANGES ARE NON-COMPACR OR SLENDER, FLANGE LOCAL BUCKLING APPLIES

• AISC TABLE B4.1b, CASE 13

$\frac{b}{t}$

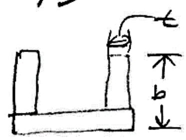

FROM BEFORE:
$E = 29{,}000$ ksi
$F_y = 50$ ksi
$b = 3.25$ in.
$t = 0.25$ in

$$\lambda_p = 0.38\sqrt{\frac{E}{F_y}}$$

$$\lambda_r = \sqrt{\frac{E}{F_y}}$$

$b/t = 13 \qquad \lambda_p = 9.15 \qquad \lambda_r = 24.08$

$$\boxed{\lambda_p < b/t < \lambda_r \qquad \text{NON-COMPACT}}$$

$$M_p = F_y Z_y \qquad \text{(AISC F6-1)}$$

$$M_n = M_p - (M_p - 0.7 F_y S_y)\left(\frac{\lambda - \lambda_p}{\lambda_r - \lambda_p}\right) \qquad \text{(AISC F6-2)}$$

$Z_y = 2.287$, PLASTIC SECTION MODULUS OF BRACKET X-SEC

$M_p = 114.35$ kip-in.

$$\boxed{M_n = 96.37 \text{ kip-in.}}$$

- FLEXURE YIELDING & FLANGE LOCAL BUCKLING CAPACITY DOES NOT EXCEED FLEXURE DEMAND

Figure E-5. Post Bracket Design: Flange Local Buckling Strength

Appendix F. Horizontal Fence Stiffener Design

F.1. Design of Members for Flexure

CAP RAIL DESIGN

FLEXURE DESIGN : DEMAND (LRFD ICE COMBO. #2)

1.2 DEAD = 1.2 (MESH + CAP RAIL WEIGHT)
LIVE = THREE 250-lb Persons
ICE WEIGHT = MESH + CAPRAIL ICE LOAD
SNOW = CAP RAIL SNOW LOAD

- LOADS DIRECTLY ON CAP RAIL ARE DISTRIBUTED, SIMPLIFY PROBLEM and assume LOADS ON MESH TRANSFERED TO CAP RAIL ARE DISTRIBUTED

CAP RAIL TOTAL LOAD : 260.3 lb

MESH TOTAL LOAD : 1652.9 lb

TOTAL LOAD ON CAP RAIL = 1913.2 lb

- ASSUME CAP RAIL CONNECTIONS ARE PINNED

8-FT POST SPACING WITH "PINNED" CONNECTION LOCATED 6 1/2 -IN. FROM EACH POST

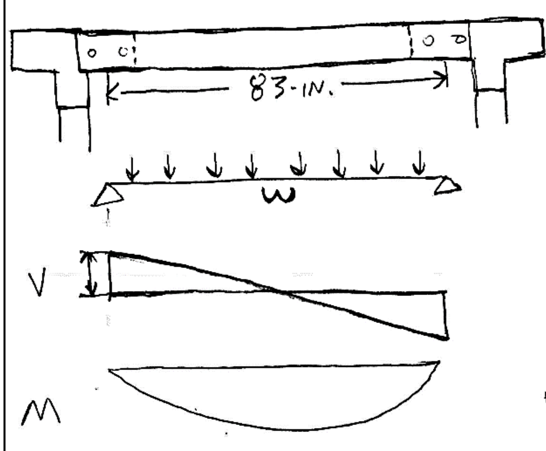

$$w = \frac{1913.2\text{ lb}}{83\text{ in}} = 23.05\text{ lb/in.}$$

$$V = \frac{w \cdot L}{2} = \frac{1913.2\text{ lb}}{2} = 956.6\text{ lb}$$

$$M = \frac{1}{2} V\left(\frac{L}{2}\right) = \frac{VL}{4} = 19849.5\text{ lb-in.}$$

$$\boxed{M_u = 19.85\text{ kip-in.}}$$

1

Figure F-1. Cap Rail Design: Flexural Demand

CAP RAIL DESIGN

CAPACITY

- FLANGE LOCAL BUCKLING NOT CONSIDERED SINCE BOLTS WILL PREVENT FLANGE OUTWARD BUCKLING

- YIELDING LIMIT CALCULATION:

$\phi M_n = \phi F_y Z_y$ (AISC F6-1)

USED S_y FOR CONSERVATIVE APPROACH

FOR 5 1/2-IN. X 6 3/16-IN., 3/16-IN. THICK CHANNEL
- ASTM A572 Gr. 50
  - $F_y = 50$ ksi

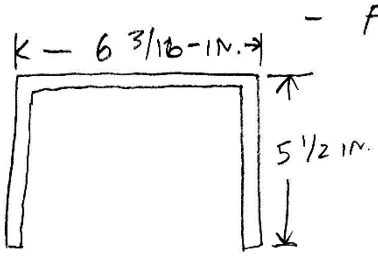

$S_y = 2.79 \text{ in.}^3$

$\phi = 0.9$ (AISC F1)

$\phi M_n = 0.9(50 \text{ ksi})(2.79 \text{ in.}^3)$

$\boxed{\phi M_n = 125.5 \text{ kip-in.}}$

$M_u = 19.85 \text{ kip-in.} < 125.5 \text{ kip-in.}$

Figure F-2. Cap Rail Design: Flexural Strength

F.2. Design of Members for Torsion

CAP RAIL DESIGN

TORSION LOADING: DEMAND

- TORSION APPLIED BY LOADS ON MESH TRANSFERED TO CAP RAIL

- MAX VERTICAL LOAD ON MESH: FROM LRFD ICE COMB. #2

$P = 1652.9 \text{ lb}$

- CONSERVATIVE ASSUMPTION THAT THIS LOAD IS TRANSFERED TO CAP RAIL BY THE 3 BOLTS ON CAP RAIL FLANGE IN BETWEEN CAP RAIL SUPPORTS:

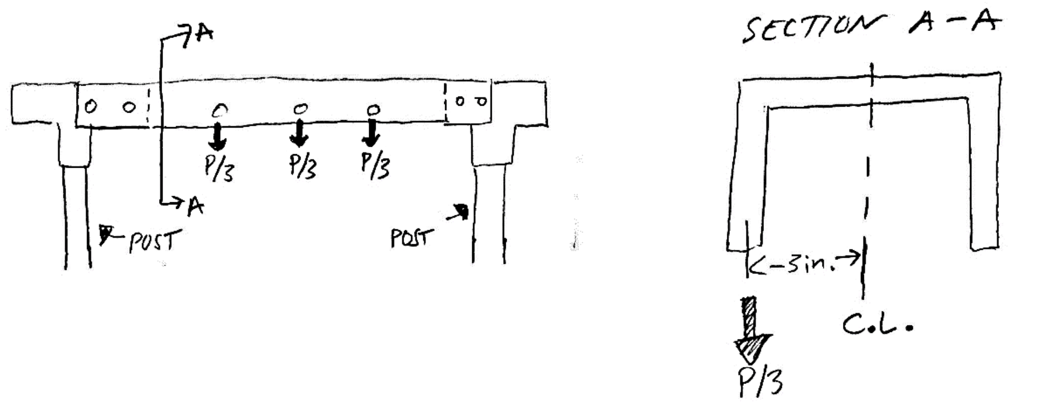

- TORSIONAL LOAD PER BOLT:

$T = F \cdot l$ (TORQUE)

$F = P/3 = 1652.9 \text{ lb}/3$

$l = 3 \text{ in.}$

$T = 1652.9 \text{ lb}$

$\boxed{T = 1.653 \text{ Kips}}$

Figure F-3. Cap Rail Design: Torsion Design, Torsion Demand

CAP RAIL DESIGN

TORSION DESIGN: CAP RAIL PROPERTIES

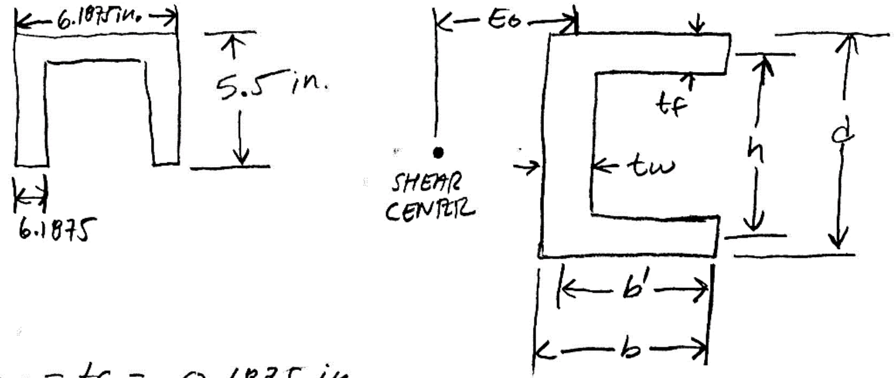

$t_w = t_f = 0.1875$ in.
$d = 6.1875$ in.
$h = 6.0$ in.
$b = 5.5$ in.

$b' = 5.406$ in.
$I_x = 21.637$ in.^{4}

FROM STEEL DESIGN GUIDE (DSG9) SECTION 3.2

$$E_o = \frac{t_f b'^2}{2b't_f + \frac{h t_w}{3}} \qquad (\text{DSG9 } 3.19)$$

$$\boxed{E_o = 2.281 \text{ in.}}$$

$$u = b' - E_o \qquad (\text{DSG9 } 3.22)$$

$$\boxed{u = 3.125 \text{ in.}}$$

$$C_w = \frac{h^2 (b')^2 t_f (b' - 3E_o)}{6} + E_o^2 I_x \qquad (\text{DSG9 } 3.18)$$

$$\boxed{C_w = 65.331 \text{ in.}^6}$$

Figure F-4. Cap Rail Design: Torsion Design, Cap Rail Torsional Properties

CAP RAIL DESIGN

TORSION DESIGN: CAP RAIL PROPERTIES CONT.

$$S_{w1} = \frac{u^2 h t_f}{4} \qquad (DSG\,9\ \ 3.15)$$

$$\boxed{S_{w1} = 2.747 \text{ in.}^4}$$

$$S_{w2} = \frac{h b' t_f (b' - 2E_0)}{4} \qquad (DSG\,9\ \ 3.16)$$

$$\boxed{S_{w2} = 1.283 \text{ in.}^4}$$

$$S_{w3} = S_{w2} - \frac{E_0 h^2 t_w}{8} \qquad (DSG\,9\ \ 3.17)$$

$$\boxed{S_{w3} = -0.641 \text{ in.}^4}$$

$$J = \sum \left(\frac{bt^3}{3} \right) \qquad (DSG\,9\ \ 3.4)$$

$$J = \left(\frac{t^3}{3} \right) (2b + (h - t))$$

$$\boxed{J = 0.0369 \text{ in.}^4}$$

$$a = \sqrt{\frac{E C_w}{G J}} \qquad (DSG\,9\ \ 3.12)$$

$E = 29{,}000$ ksi
$G = 11{,}200$ ksi

$$\boxed{a = 67.707 \text{ in.}}$$

Figure F-5. Cap Rail Design: Torsion Design ,Cap Rail Torsional Properties (Continued)

CAP RAIL DESIGN

TORSION DESIGN : DETERMINATION OF MAX TWIST (θ)

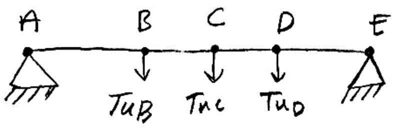

- CAP RAIL CONSIDERED TORSIONALLY- PINNED

- MAX SHEAR IDENTIFIED @ SUPPORT (A)
- MAX TWIST ANGLE IDENTIFIED @ MID SPAN (C)

- APPENDIX B CASE 3 PAGES 58 TO 63 (DSG 9)

TORQUE	T_{uB}	T_{uC}	T_{uD}
z/ℓ	0.5	0.5	0.5
α	~0.3	0.5	~0.3*
$\theta\left(\frac{GJ}{T\ell}\right)=$	0.025	0.033	0.025

* REFERENCE POINT FLIPPED

$\ell = \overline{AE} = 83$ in.
$\overline{AB} = 23.5$ in.
$\overline{AC} = 41.5$ in.
$\overline{AD} = 59.5$ in.
$\ell/a = 83/67.707$
$\boxed{\ell/a = 1.226}$

- TORQUE EFFECTS (T_{uB}, T_{uC}, T_{uD}) COMBINED BY SUPERPOSITION

$$T_{uB} = T_{uC} = T_{uD} = T_u$$

$$\theta = \frac{T_u \ell}{GJ}(0.025 + 0.033 + 0.025)$$

$T_u = 1.653$ kips
$\ell = 83$ in.
$G = 11{,}200$ ksi
$J = 0.0369$ in.^{4}

$$\theta = 0.276 \text{ RAD}$$

$\boxed{\theta = \mathbf{1.58} \text{ degrees}}$ AT MIDSPAN

Figure F-6. Cap Rail Design: Torsion Design, Maximum Twist Angle Determination

CAP RAIL DESIGN

TORSION DESIGN: DETERMINATION OF MAX SHEAR

• DSG 9 – APPENDIX B CASE 3 PAGES 58 – 63

TORQUE	T_{uB}	T_{uC}	T_{uD}
z/ℓ	0	0	0
α	~0.3	0.5	~0.3*
$\theta\left(\frac{GJ}{T\ell}\right)$	0	0	0
$\theta'\left(GJ/T\right)$	0.1	0.1	0.1
$\theta''\left(GJa/T\right)$	0	0	0
$\theta'''\left(GJa^2/T\right)$	−0.625	−0.4	−0.1875

$z/\ell = 0$, SHEAR DETERMINED AT SUPPORT

*NOTE: REFERENCE POINT FLIPPED

– TORQUE EFFECTS ($T_u = T_{uB} = T_{uC} = T_{uD}$) COMBINED BY SUPERPOSITION

$$\theta' = \frac{T_u}{GJ}(0.1 + 0.1 + 0.1)$$

$$\boxed{\theta' = 1.200 \times 10^{-3} \text{ rad/in.}}$$

$$\theta''' = \frac{T_u}{GJa^2}(-0.625 - 0.4 - 0.1875)$$

$$\boxed{\theta''' = -1.057 \times 10^{-6}}$$

$$\tau_t = Gt\theta' \quad \text{(AISC DSG9 4.1)}$$

$G = 11{,}200$ ksi
$t = 0.1875$ in.
$\theta' = 1.200 \times 10^{-3}$ rad/in.

$$\boxed{\tau_t = 2.520 \text{ ksi}}$$

Figure F-7. Cap Rail Design: Torsion Loading, Shear Determination

CAP RAIL DESIGN

TORSION DESIGN: DETERMINATION OF MAX SHEAR

$$\tau_{ws} = \frac{-E\, S_{ws}\, \theta'''}{t} \qquad \text{(AISC DG9 4-2a)}$$

$E = 29{,}000$ ksi
$t = 0.1875$ in.
$\theta''' = -1.057 \times 10^{-6}$
$S_{w1} = 2.747$ in.^{4}
$S_{w2} = 1.283$ in.^{4}
$S_{w3} = -0.641$ in.^{4}

$\tau_{w1} = 0.499$ ksi
$\tau_{w2} = 0.210$ ksi
$\tau_{w3} = -0.105$ ksi

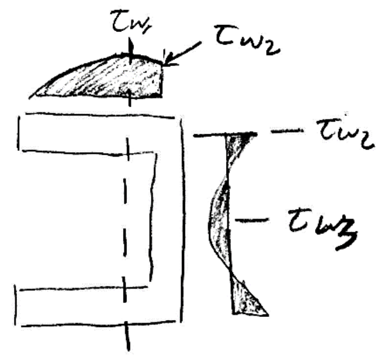

SHEAR FROM WARPING

- SHEAR DUE TO APPLIED SHEAR

$$\tau_{b_s} = \frac{V Q_s}{I t} \qquad \text{(AISC DG9 4.6)}$$

$V = 956.6$ lb, SHEAR AT SUPPORTS, FROM FLEXURE DESIGN
$Q_1 = 2.524$ in.^{3}
$Q_2 = 2.016$ in.^{3}
$I = 10.233$ in.^{4}
$t = 0.1875$ in.
s = POINT OF INTEREST

$\tau_{b1} = 1.258$ ksi
$\tau_{b2} = 1.005$ ksi

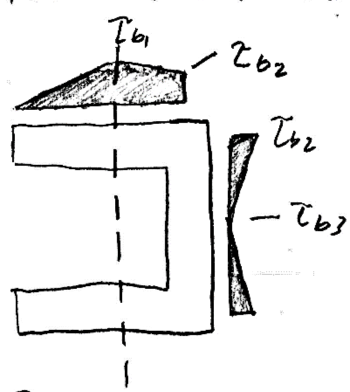

SHEAR FROM APPLIED SHEAR

Figure F-8. Cap Rail Design: Torsion Design, Shear Determination (Continued)

CAP RAIL DESIGN

TORSIONAL DESIGN: SHEAR STRESS AT SUPPORT

LOCATION	τ_t (ksi)	τ_w (ksi)	τ_b (ksi)	TOTAL (ksi)
1	2.52	0.45	1.26	4.23
2	2.52	0.21	1.01	3.74
3	2.52	-0.11	0	2.41

$\boxed{\tau_{max} = 4.23 \text{ ksi}}$

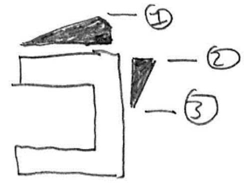

$f_{uv} \leq \phi\, 0.6\, F_y$ (AISC DS99 4.13)

f_{uv} = 4.23 ksi, SHEAR DEMAND
F_y = 50 ksi, ASTM A572 GRADE 50 PLATE
ϕ = 0.9, RESISTANCE FACTOR

$\boxed{4.23 \text{ ksi} < 27 \text{ ksi}}$

Figure F-9. Cap Rail Design: Torsion Design, Shear Determination (Continued)

F.3. Design of Bolted Connections

BOLTED CONNECTION DESIGN

- GOAL: DEVELOP CHAIN-LINK MESH CAPACITY (1290 lb)

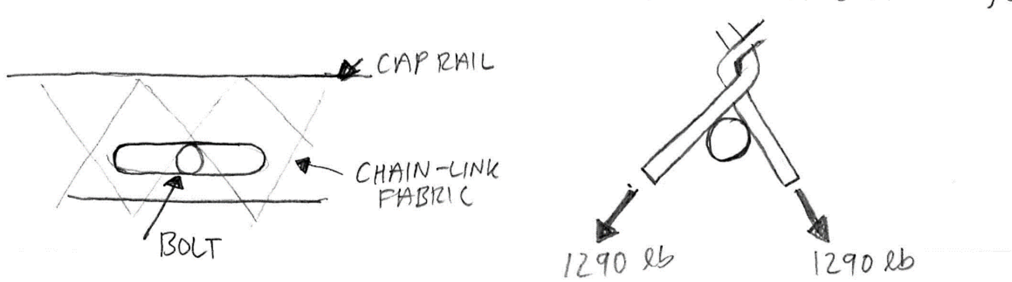

- UNDER SEVERE MESH LOADING, DEMAND ON BOLTED CONNECTION = 2580 lb

Figure F-10. Cap Rail Design: Bolted Connection Design

CAP RAIL DESIGN

BOLTED CONNECTION DESIGN : BEARING

- FORCE PERPANDICULAR TO LONG SLOTS : BEARING

$\phi R_n = \phi\, 2\, d t F_u$ (AISC J3-6e)

$d = 0.625$ in., BOLT DIAMETER
$t = 0.1875$ in., MATERIAL THICKNESS
$F_u = 65$ ksi, ASTM A572 GRADE 50
$\phi = 0.75$, RESISTANCE FACTOR

$\boxed{\phi R_n = 11.43 \text{ kips}}$ > 2.58 kips (DEMAND)

- FORCE PERPANDICULAR TO LONG SLOTS : TEAROUT

$\phi R_n = \phi\, l_c t F_u$ (AISC J3-6f)

$l_c = 1.25$ in., CLEAR DISTANCE

$\boxed{\phi R_n = 11.43 \text{ kips}}$ > 2.58 kips (DEMAND)

- BENDING OF BOLT SLOT

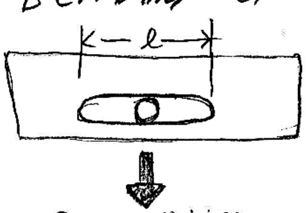

P = 2.58 kips

$M_u = \frac{P l}{4}$ (SIMPLY SUPPORTED BEAM)

$l = 3$ in, $P = 2.58$ kips

$\boxed{M_u = 1.94 \text{ kip-in.}}$

$\phi M_n = \phi F_y Z$ (AISC F11-1)

$F_y = 50$ ksi, ASTM A572 GR. 50
$Z = 0.0732$ in.^{3}, 1.25 in. TALL, 0.1875 THICK SQUARE
$\phi = 0.9$, RESISTANCE FACTOR FOR BENDING

$\boxed{\phi M_n = 3.29 \text{ kip-in.}}$ > 1.94 kip-in. (DEMAND)

Figure F-11. Cap Rail Design: Bolted Connection Design (Continued)

Appendix G. Wire Rope-to-Parapet Bracket Design

G.1. Connection and Flexure Design

CABLE BRACKET DESIGN

DESIGN LOAD

- 5/16 in. DIAMETER 7X19 WIRE ROPE
  CONFORMING TO ASTM A1023

  → 9.80 kip MINIMUM BREAKING STRENGTH

  DEMAND = 9.80 kips • 1.6 = 15.68 kips

  - 1.6 FACTOR DISCUSSED IN DESIGN CHAPTER

PIN BEARING

$\phi R_n = \phi 1.8 F_y A_{pb}$ (AISC J7-1)

$F_y = 50$ ksi, ASTM A572 GR. 50 PLATE
$A_{pb} = t \cdot d$, PROJECTED AREA IN BEARING
$\phi = 0.75$, RESISTANCE FACTOR
$t = 0.5625$ in., 9/16 in. thick PLATE
$d = 0.4375$ in., 7/16 in. DIAMETER PIN FROM TURNBUCKLE

$\boxed{\phi R_n = 16.61 \text{ kips}}$ > 15.68 kip DEMAND

WELD DESIGN

- WELD LOADED IN SHEAR & COULD BE
  LOADED IN SHEAR

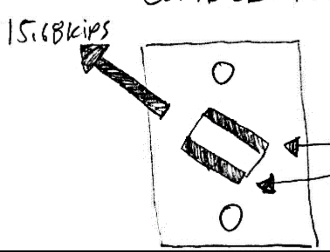

- SHEAR IS WORST
  CASE SCENARIO
  FOR WELD LOADING

Figure G-1. Cable Bracket Design: Design Load, Pin and Weld Connection Design

CABLE BRACKET DESIGN

WELD DESIGN CONTINUED

$\phi R_n = \phi F_{nw} A_{we}$ (AISC J2-4)

$F_{nw} = 0.60\ F_{exx}$ – SHEAR ONLY (AISC J2-5)

$A_{we} = t_e \ell$, EFFECTIVE WELD AREA
$t_e = 0.707t$, EFFECTIVE THROAT THICKNESS
$t = 0.375$ in., WELD THICKNESS
$\ell = 3$ in., WELD LENGTH
$F_{exx} = 60$ ksi, WELD MATERIAL CLASSIFICATION STRENGTH
$\phi = 0.75$, RESISTANCE FACTOR

$F_{nw} = 36$ ksi – FOR TWO WELDS

$\phi R_n = 21.48$ kips $\boxed{\phi R_n = 42.95 \text{ kips}}$

FLEXURE DESIGN

- DESIGN LOAD ON BRACKET: 15.68 kips

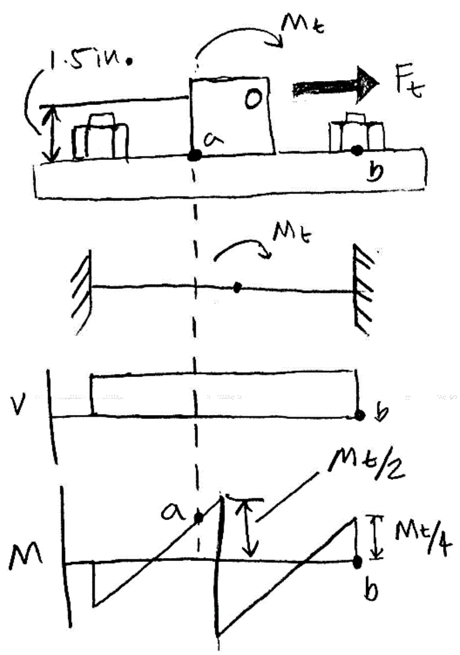

$M_t = F_t \cdot 1.5$ in.
$F_t = 15.68$ kips

$M_t = 23.52$ kips

$M_b = \dfrac{M_t}{4} = 5.88$ kip-in.

$\boxed{M_a = 7.35 \text{ kips}}$

Figure G-2. Cable Bracket Design: Weld Connection (Continued) and Flexure Design

CABLE BRACKET DESIGN

FLEXURE DESIGN

$$\phi M_n = \phi F_y Z \leq 1.6 F_y S \phi \quad \text{(AISC F11-1)}$$

F_y = 50ksi, ASTM A572 GR.50
Z = 0.237 in.^{3}, PLASTIC SECTION MODULUS
S = 0.158 in.^{3}, SECTION MODULUS
ϕ = 0.9, FLEXURE RESISTANCE FACTOR

- PROPERTIES FOR 3/8-in. THICK, 6 3/4-in. WIDE PLATE

$\boxed{\phi M_n = 10.67 \text{ kip-in.}}$ > 7.35 kip-in. DEMAND

Figure G-3. Cable Bracket Design : Flexure Design (Continued)

G.2. Concrete Anchorage Design

ANCHOR LOADING

- TO MITIGATE POSSIBILITY OF ANCHOR FAILURE, ASSUME CABLE DESIGN IS APPLIED IN TENSION & IN SHEAR (VERY CONSERVATIVE)

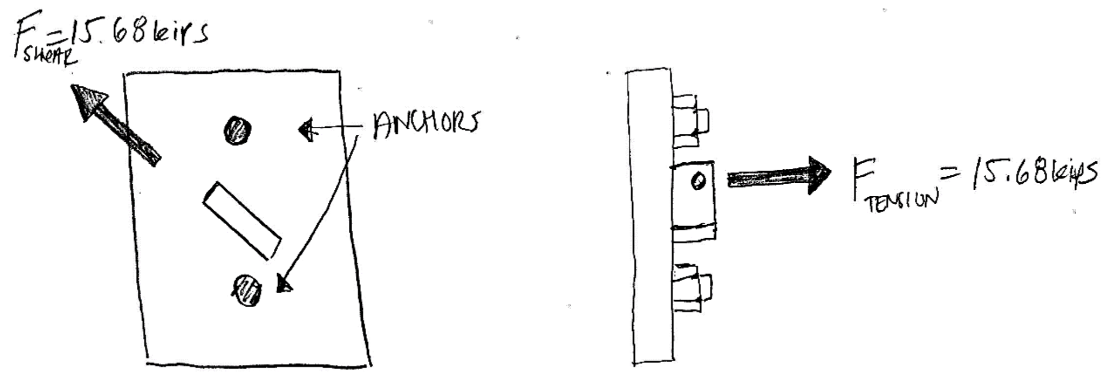

Figure G-4. Cable Bracket Anchorage Design: Anchor Loading

CABLE BRACKET ANCHOR DESIGN

TENSILE LOADING: STEEL STRENGTH

– FROM ANCHOR DESIGN:

$\boxed{\phi N_{sa} = 43.31 \text{ kips}}$

TENSILE LOADING: CONCRETE BREAKOUT

$$\phi N_{cbg} = \phi \frac{A_{NC}}{A_{NCo}} \psi_{ec,N} \psi_{ed,N} \psi_{c,N} \psi_{cp,N} N_b \quad \text{(ACI 17.4.2.1b)}$$

$N_b = 17.67$ kips, FROM ANCHOR DESIGN
A_{NC} = PROJECTED FAILURE AREA OF ANCHOR UNDER GROUP ACTION
$A_{NCo} = 324.0 \text{ in.}^2$, FROM ANCHOR DESIGN
$\psi_{cp,N} = 1.0$ REFER TO ANCHOR DESIGN
$\psi_{ed,N} = 1.0$
$\psi_{c,N} = 1.4$
$\phi = 0.55$
$\psi_{ec,N} = 1.0$, ECCENTRICITY MODIFICATION

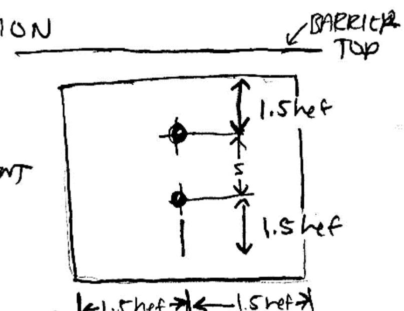

$A_{NC} = (3h_{ef} + s)(3h_{ef})$

$h_{ef} = 6$ in., ANCHOR EMBEDMENT
$s = 9.5$ in., ANCHOR SPACING

$A_{NC} = 495 \text{ in.}^2$

$$\phi N_{cbg} = 0.55\left(\frac{495}{324}\right)(1.0)(1.0)(1.4)(1.0)(17.67 \text{ kips})$$

$\boxed{\phi N_{cbg} = 20.79 \text{ kips}} > 15.65$ kip DEMAND

Figure G-5. Cable Bracket Anchorage Design: Tensile Loading

CABLE BRACKET ANCHOR DESIGN

TENSILE LOADING: BOND STRENGTH

$$\phi N_{ag} = \phi \frac{A_{Na}}{A_{Nao}} \psi_{ec,Na} \psi_{ed,Na} \psi_{cp,Na} N_{ba} \quad \text{(ACI 17.4.5.1b)}$$

$N_{ba} = 29.69$ kips, REFER TO ANCHOR DESIGN
A_{Na} = PROJECTED INFLUENCE OF GROUP OF ANCHORS
$A_{Nao} = 501.14 \text{ in.}^2$, REFER TO ANCHOR DESIGN
$\psi_{ed,Na} = 0.968$,
$\psi_{cp,Na} = 1.0$,
$\psi_{ec,N} = 1.0$, ECCENTRICITY MODIFICATION
$\phi = 0.55$, RESISTANCE FACTOR

$C_{Na} = 11.19$ in. – REFER TO ANCHOR DESIGN

$A_{Na} = (2C_{Na})(C_{a1} + C_{Na} + S)$

$S = 9.5$ in., ANCHOR SPACING

$\boxed{A_{Na} = 686.84 \text{ in.}^2}$

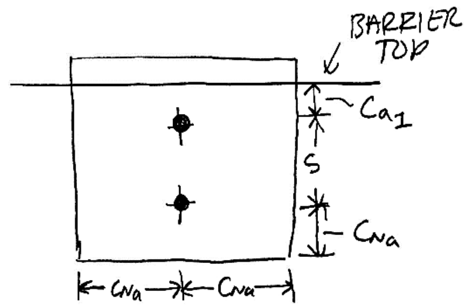

$$\phi N_{ag} = 0.55 \left(\frac{686.84}{501.14}\right)(1)(0.968)(1)(29.69 \text{ kips})$$

$\boxed{\phi N_{ag} = 21.66 \text{ kips}}$ > 15.65 kip DEMAND

Figure G-6. Cable Bracket Anchorage Design: Tensile Loading (Continued)

CABLE BRACKET ANCHOR DESIGN

SHEAR LOADING: STEEL STRENGTH

- REFER TO ANCHOR DESIGN

$$\boxed{\phi V_{sa} = 22.52 \text{ kips}}$$

SHEAR LOADING: BREAKOUT STRENGTH

$$\phi V_{cb} = \phi \frac{A_{vc}}{A_{vco}} \Psi_{ed,N} \Psi_{c,v} \Psi_{h,v} V_b \quad \text{(ACI 17.5.2.1b)}$$

$V_b = 20.12$ kips, REFER TO ANCHOR DESIGN
$A_{vco} = 450$ in.^{2},
$\Psi_{ed,v} = 1.0$,
$\Psi_{c,v} = 1.4$,
$\Psi_{h,v} = 1.33$,
$\phi = 0.55$,
A_{vc}, = PROJECTED AREA OF ANCHOR

$$A_{vc} = 2(1.5 C_{a1}) h_a \quad \text{(CASE 1, FIG. R17.5.2.1b)}$$

$C_{a1} = 10$ in.
$h_a = 8.5$ in., CONCRETE WIDTH AT ANCHOR

$$\boxed{A_{vc} = 255 \text{ in.}^2}$$

$$\phi V_{cbg} = 0.55\left(\frac{255}{450}\right)(1)(1)(1.4)(1.33)(20.12 \text{ kips})(1.5)$$

*NOTE: ACI SPECIFIES THAT V_{cbg} CAN BE DOUBLED FOR FORCE PARALLEL TO BARRIER TOE, FORCE IS @ 45° ANGLE, A FACTOR OF 1.5 WAS ADOPTED

$$\boxed{\phi V_{cbg} = 17.51 \text{ kips}} > \frac{15.68 \text{ kips}}{2} \text{ DEMAND}$$

Figure G-7. Cable Bracket Anchorage Design: Shear Loading

CABLE BRACKET ANCHOR DESIGN

SHEAR LOADING: ANCHOR PRYOUT DESIGN

$\phi V_{cpg} = k_{cp} \phi N_{cpg}$ (ACI 17.5.3.1b)

$k_{cp} = 2.0$, SINCE $h_{ef} \geq 2.5$ in.

$\phi N_{cpg} = 20.79$, LOWER OF BOND & BREAKOUT

$\boxed{\phi V_{cpg} = 41.58 \text{ kips}}$

COMBINED LOADING REQUIREMENT

	TENSION (kips)			SHEAR (kips)		
MODE	STEEL	BREAKOUT	BOND	STEEL	BREAKOUT	PRYOUT
DEMAND	7.84	15.68	15.68	7.84	7.84	15.68
CAPACITY	43.31	20.79	21.66	22.52	17.51	41.58
RATIO	0.181	0.754	0.724	0.348	0.448	0.377

$$\frac{N_{ua}}{\phi N_n} + \frac{V_{ua}}{\phi V_n} \leq 1.2 \quad \text{(ACI 17.6.3)}$$

$N_{ua} = 15.68$ kips, TENSILE LOAD ON ANCHOR GROUP
$\phi N_n = 20.79$ kips, ANCHOR GROUP TENSILE BREAKOUT STRENGTH
$V_{ua} = 7.84$ kips, SHEAR LOAD ON SINGLE ANCHOR
$\phi V_n = 17.51$ kips, BREAKOUT STRENGTH OF SINGLE ANCHOR

$0.754 + 0.448$

$\boxed{1.202 = 1.2}$

Figure G-8. Cable Bracket Anchorage Design: Shear (Continued) and Combined Loading

END OF DOCUMENT